# MECHANISM OF SLIDING CLAMP LOADING BY THE *Escherichia coli* CLAMP LOADER COMPLEXES

By

LAUREN GRACE DOUMA

A DISSERTATION PRESENTED TO THE GRADUATE SCHOOL
OF THE UNIVERSITY OF FLORIDA IN PARTIAL FULFILLMENT
OF THE REQUIREMENTS FOR THE DEGREE OF
DOCTOR OF PHILOSOPHY

UNIVERSITY OF FLORIDA

2016

To my family and friends who support me unconditionally

# ACKNOWLEDGMENTS

First, I would like to thank mentors who have helped guide me through graduate school. Most importantly, I need to thank my chair, Dr. Linda Bloom, who constantly encouraged me to think outside of the box and had an enormous amount of patience as I grew as a researcher. I would like to thank my committee members, Dr. Brian Cain, Dr. Kevin Brown, Dr. Sixue Chen, and Dr. Susan Lovett for their invaluable advice throughout my time at the University of Florida. Additionally, I would like to thank Drs. Brain Cain and Kevin Brown for giving me the opportunity to be the teaching assistant for the undergraduate biochemistry course.

Lastly, I need to thank my family and friends who have supported me throughout graduate school. The past members of the Bloom laboratory were critical to my success in graduate school. I would like to thank them, not only for always being there to discuss scientific ideas, but also for their friendship. I would like to thank my mother, father, sister for always being available when I needed someone to talk to and encouraging me to follow my dreams. Thank you to my fellow graduate student, Dr. Katie O'Shaughnessey, in addition to the rest of the 2010 cohort, for being a source of laughter, smiles, and encouragement throughout the years. Finally, I have to thank Jonathan Adam Watson for being there for me through the good times and the bad. I cannot thank him enough for his support and encouragement throughout my years of graduate school.

TABLE OF CONTENTS

page

LIST OF TABLES

LIST OF FIGURES

## LIST OF ABBREVIATIONS

| | |
|---|---|
| 3’DNA | Primer/template DNA with a 3’ recessed end |
| 5’DNA | Primer/template DNA with a 5’ recessed end |
| AF488 | Alexa Fluor 488 c5 maleimide |
| Amp | Ampicillin |
| ATP | Adenosine 5’triphosphate |
| ATPγS | Adenosine 5’-[γ-thio]triphosphate tetralithium |
| bp | Base pairs |
| Cm | Chloramphenicol |
| DNA | Deoxyribonucleic acid |
| DMSO | Dimethyl sulfoxide |
| dsDNA | Double-stranded DNA |
| DTT | Dithiothreitol |
| EDTA | Ethylenediaminetertraacetic acid |
| FRET | Fluorescence Resonance Energy Transfer |
| IPTG | Isopropyl β-D-1-thiogalactopyranoside |
| Kan | Kanamycin |
| $K_{d,app}$ | Apparent dissociation constant |
| $K_d$ | Dissociation constant |
| $k_{obs}$ | Observed rate constant |
| LB | Luria broth |
| MDCC | 7-diethylamino-3-((((2-maleimidyl)ethyl)amino)carbonyl)coumarin |
| MWCO | Molecular weight cut off |
| nt | Nucleotide |
| PCNA | Proliferating cell nuclear antigen |

| | |
|---|---|
| PBP | Phosphate binding protein |
| $P_i$ | Inorganic phosphate |
| Pol III | DNA Polymerase III |
| p/t | Primer-template junction |
| RFC | Replication factor C |
| RhX | Rhodamine X isothiocyanate |
| RPA | Replication protein A |
| SEC | Size exclusion chromatography |
| SDM | Site directed mutagenesis |
| SDS-PAGE | Sodium dodecyl sulfate polyacrylamide gel electrophoresis |
| SSB | Single stranded binding protein |
| ssDNA | Single stranded DNA |
| SSO | Single stranded overhang |
| Str | Streptomycin |
| TCEP | Tris (2-carboxyethyl) phosphine |
| WT | Wild-type |

Abstract of Dissertation Presented to the Graduate School
of the University of Florida in Partial Fulfillment of the
Requirements for the Degree of Doctor of Philosophy

MECHANISM OF SLIDING CLAMP LOADING BY THE *Escherichia coli* CLAMP LOADER COMPLEXES

By

Lauren Grace Douma

December 2016

Chair: Linda Bloom
Major: Genetics and Genomics

DNA replication is an efficient and precise process which copies genetic information in order to be passed on to daughter cells. DNA polymerase catalyzes the DNA synthesis reaction, but cannot efficiently replicate an organism's genome without the help of other DNA replication proteins. To prevent DNA polymerase from losing contact with DNA during replication, sliding clamps anchor DNA polymerases to the DNA template. Sliding clamps are ring-shaped proteins that are loaded onto the DNA by clamp loader complexes in an ATP dependent manner. Sliding clamps and clamp loaders are found throughout all domains of life and are required for cell viability. In *E. coli*, the clamp loader is the DnaX complex which is named after the gene products of *dnaX,* γ and τ. The DnaX subunits perform the ATP hydrolysis required for clamp loading. Sliding clamps are loaded onto each Okazaki fragment of the lagging strand, corresponding to a clamp being loaded every 2-3 s.

Various aspects of the *E. coli* clamp loading mechanism were studied using fluorescent-based assays and variants of the clamp loaders and clamps. Questions were asked about how the sliding clamp, clamp loaders, and clamp loader-protein interactions all contribute to the regulation of the clamp loading reaction. Chapter 3

examines the sliding clamp role in clamp opening and if the clamp loaders actively open the clamps. Chapter 4 examines the differences of the two DnaX clamp loader subunits, γ and τ. Finally, chapter 5 presents data examining the mechanism of sliding clamp loading regulation by the single-stranded DNA binding protein, SSB. Combined, these studies provide detailed information on the mechanism of clamp loading, an essential reaction for all life to copy their genomic information.

# CHAPTER 1
# INTRODUCTION

## DNA Replication in *Escherichia coli*

Before cells divide, their genetic information is copied in order to be passed down to the daughter cell. Bacteria, like *Escherichia coli*, reproduce through an asexual process called binary fission. In binary fission, the bacteria's genome is duplicated then the cell divides into roughly equal halves with one genome in each cell. The process in which the genomes are replicated is a very precise and quick process. In *Escherichia coli*, DNA replication occurs at approximately 1000 base pairs (bp) per second (1) and makes a mutation approximately 1 in every $10^7$ to $10^8$ base pairs (2, 3). The speed and accuracy of DNA replication are achieved by the coordinated actions many DNA replication and repair proteins inside the cells.

In *Escherichia coli*, DNA replication begins at the origin of replication site, *oriC*. Once the origin of replication is opened by DnaA, the helicase, DnaB, is loaded onto each replication fork (Figure 1-1). DNA helicases are proteins that unwind the DNA at each replication fork making way for the DNA replication machinery. As the DNA is separated, single-stranded DNA is covered in single-stranded binding protein (SSB). The complex that coordinates the replication fork in *E. coli* is the clamp loader complex, τ-complex. The τ-complex binds to the helicase and to (at least) two DNA polymerases (4). DNA polymerase III (pol III) is the protein which performs the actual DNA synthesis in *E. coli*. DNA polymerase alone can only replicate a couple of nucleotides before losing contact with the DNA and falling off. The DNA polymerase binds a doughnut-shaped ring called the sliding clamp (β sliding clamp in *E. coli*) to make the DNA replication process more efficient by increasing the polymerase processivity (5). The

sliding clamp wraps around the DNA and can freely move along the DNA. A polymerase bound to a sliding clamp can replicate thousands of nucleotides in a single binding event, making DNA synthesis more efficient. The sliding clamps are loaded onto DNA by a mechanoenzyme called the clamp loader through an ATP-dependent process. The structure and function of sliding clamps and clamp loaders are highly conserved from prokaryotes to eukaryotes (6).

Once the DNA replication proteins are loaded onto each of the replication forks at the origin, the forks move bidirectionally away from each other in either a clockwise or counterclockwise direction (Figure 1-1). DNA synthesis begins with an RNA primer which is synthesized across from the parental strand by RNA primase. DNA polymerase can extend this RNA primer. The polymerase in *E. coli* is known as DNA polymerase III (pol III) and uses the 3' hydroxyl group on the RNA primer to extend the growing DNA chain. DNA is naturally in an anti-parallel form meaning that one strand of the double-stranded DNA is in the 5' phosphate to 3' hydroxyl group direction, and the other strand is oriented the opposite way (3' hydroxyl to 5' phosphate group). When the replication fork moves, one side of the fork will be moving in the direction of DNA synthesis (5' phosphate to 3' hydroxyl group) and will be continuously synthesized. This strand is called the leading strand of DNA replication. The other side of the replication fork will be moving in the opposite direction of DNA replication (3' hydroxyl to 5' phosphate group) and has to be synthesized discontinuously in fragments called Okazaki fragments (7). In *Escherichia coli*, Okazaki fragments are around 1000 bp long, while only 100-200 base pairs long in eukaryotes. The RNA primase synthesizes a primer for the beginning of each Okazaki fragment. Pol III is ejected from the sliding clamp once it reaches the end

of the previous Okazaki fragment. The τ-complex clamp loader moves the polymerase to the next sliding clamp, which has been loaded onto the new RNA primer by the clamp loader (8). Clamp loaders have to load a sliding clamp onto an Okazaki fragment about every 2 seconds to keep up with the replication fork. Finally, pol III then loads onto the sliding clamp and continues begins to synthesize another Okazaki fragment.

## Proteins of the *Escherichia coli* Holoenzyme

At the heart of DNA replication in all domains of life is the cellular replicase which contains a DNA polymerase, a ring-shaped sliding clamp, and a clamp loader. In *E. coli,* this holoenzyme is composed of polymerase III, the β sliding clamp, and the DnaX complex clamp loader for a total of 10 subunits (9). The holoenzyme coordinates the movements of DNA replication as the replication fork moves at thousands of nucleotides per second (1). The sections below go into more detail about each of these proteins.

### DNA Polymerase III

DNA polymerase is the enzyme that performs the actual DNA synthesis. Arthur Kornberg discovered the first DNA polymerase, DNA polymerase I, in 1956 through the *in vitro* synthesis of DNA using *E. coli* extracts (reviewed in (10)). While Kornberg believed this was the genomic polymerase, but the rate of DNA synthesis was too slow to be the replicative polymerase. In 1969, a viable strain of *E. coli* with a DNA synthesis defective form of pol I (*polA1*) which maintained the exonuclease activity was created. This meant that pol I could not have been the main DNA polymerase. DNA polymerase III was discovered by Kornberg's son, Thomas Kornberg, in 1971 (11). Thomas Kornberg combined the *polA1* mutation with thermosensitive (ts) mutations and tested the enzymatic activity of pol II and pol III. While pol II ts strains were able to grow at the nonpermissive temperatures, the pol III ts strains could not (11). This confirmed that pol

II and pol III were two unique enzymes and that pol III, not pol I, was the genomic DNA polymerase.

DNA polymerase III is made up of 3 different subunits, α, ε and θ, in a 1:1:1 molar ratio. Binding of the subunits occurs in a linear order with α binding to ε and ε binds to θ (12). No interaction between θ and α has been found. The α subunit is encoded by the *dnaE* gene and is the catalytic subunit which adds nucleotides to the growing DNA strand (13). The ε subunit is encoded by the *dnaQ* gene and is the exonuclease subunit. To remove misincorporated nucleotides, ε can remove nucleotides in a 3' to 5' direction (14). Both the α and ε subunits are required for viability (11, 15). The θ subunit is encoded by the *holE* gene and has an unknown function. Strains of *E. coli* in which the θ subunit has been removed are viable and do not have any known obvious phenotypes or growth defects (16). The expression of ε is reduced in the *holE* strain suggesting θ may have a role in stabilizing ε (17). This stabilization role was also suggested by *in vitro* results using thermal inactivation assays (18) and *in vivo* experiments using *dnaQ* mutant strains in a yeast two-hybrid assay (19). In addition, biochemical assays have shown that θ promotes the exonuclease activity of ε (12).

Alone, DNA polymerase III can only add 10-20 nucleotides before losing contact with the DNA (20, 21). This level of processivity, or the number of nucleotides incorporated in a single binding event, is relative low especially considering how fast replication is in *E. coli* (about 1000 base pairs per second) (22). The pol III holoenzyme, however, is highly processive and can incorporate more than 80,000 nt per DNA binding event (22, 23). Recent single molecule studies have measured the holoenzyme

processivity around 80,000 nt (22). High processivity of the holoenzyme is a result of the interaction between the β sliding clamp and DNA polymerase III (5, 24). DNA polymerase III binds the hydrophobic cleft of the sliding clamp through the C-terminal residues of the α subunit (25-27).

**β Sliding Clamp**

*E. coli* contains one known sliding clamp, the β sliding clamp. The β sliding clamp is a doughnut shaped protein that wraps around DNA and tethers the polymerase to DNA so it does not lose contact during replication. The β sliding clamp is composed of two monomers that link to each other is a head-to-tail fashion forming a dimer (28) (Figure 1-2). Each monomer of β contains three domains of near identical structure, yet the primary amino acid sequence is not similar. The sliding clamp has two interfaces at which it can open. These interfaces appear to be very tightly closed and stable (29). When the β sliding clamp is loaded onto circular DNA, the sliding clamp dissociation from the DNA has a half-life of 72 minutes at 37°C (30, 31). The ring in the center of the sliding clamp is 35Å, large enough to encircle duplex DNA (28, 32, 33). The sliding clamp can freely diffuse along the DNA without the need for ATP (5). Crystal structures of β on DNA reveal that the DNA is at a 22° angle as it passes through the sliding clamp, which is thought to be important in the regulation of proteins binding the sliding clamp (32). In addition, the core of the sliding clamp is lined with positively charged residues which have been shown to interact with the negatively charged backbone of DNA (34).

With the long half-life on DNA and being able to move freely along the DNA allows the sliding clamp to act as a platform for many different proteins that function on DNA, like DNA polymerase III. There are distinct faces of the sliding clamp, of which the

C-terminal side contains a hydrophobic pocket where other proteins interact with the sliding clamp (35, 36). The attachment of polymerase III to the sliding-clamp is what gives pol III such a high processivity and also increases the speed of the replication fork by 100-fold (5, 20, 24, 37-39). Seven C-terminal penultimate residues of DNA pol III α interacts with the sliding clamp at the same site that the clamp loader subunit, δ, binds(40). Additionally, β sliding clamp left behind on the lagging strand after replication of an Okazaki fragment interacts with polymerase I, critical in the removal and replacement of RNA primers with DNA, and DNA ligase, which seals the nicks after the replacement of RNA with DNA (41).

The β sliding clamp is also known to interact with proteins involved in DNA repair pathways, like the mismatch repair pathway (MMR) (41-43). Errors that were not corrected by pol III proofreading are targeted by MMR, contributing to the accuracy of DNA replication (44). MutS, a protein in MMR that locates the error, has also been shown to bind to the sliding clamp through a N-terminal domain (41, 42). A C-terminal motif of the MMR protein, MutL, has also been shown to interact with a conserved sequence within the β sliding clamp, which stimulates the endonuclease activity of MutL (45). In addition, a second site on a loop near the ATP-binding domain of MutL has been shown to interact with the hydrophobic pocket of the sliding clamp in the presence of single-stranded DNA (42). The sliding clamp also interacts with translesion DNA synthesis (TLS) polymerases which are activated by the SOS pathway (40, 46). Most proteins that interact with the sliding clamp do so through a conserved sequence (47). It is interesting to note that pol I, II, III, and V all belong to different classes of DNA polymerases, meaning they have divergent primary amino acid sequences, yet they all

interact with the sliding clamp. The diversity of proteins which interact with the sliding clamp demonstrates the importance of the β sliding clamp in many different DNA replication and repair reactions.

**DnaX Clamp Loaders**

Due to the extreme stability of the closed sliding clamp, clamp loaders are required to bind, open, and load the sliding clamp around DNA (48). Clamp loaders are specialized AAA+ (ATPases associated with diverse cellular activities) proteins, which use ATP to power reactions such as loading the sliding clamp onto DNA (Reviewed in (49)). The core of the *E. coli* clamp loader complex is composed of five subunits, δ, δ', and a combination of three DnaX (γ or τ) subunits (Figure 1-3) (50-52). The clamp loader subunits have two domains that contain the conserved AAA+ residues, but the three DnaX subunits are the only ones that bind and hydrolyze ATP (53, 54). A third C-terminal domain is responsible for interlinking the clamp loader subunits, creating a conserved cap structure (52).

The gene *dnaX* encodes both the γ and τ subunits, which perform the ATP binding and hydrolysis during the clamp loading reaction. The τ subunit is the full *dnaX* gene product (71 kDa) while the γ subunit is a truncated form of the full gene product (47 kDa) (55). This shortened γ subunit is produced through a programmed ribosomal frameshift that occurs during translation and causes the ribosome to shift the reading frame by -1 which results in the ribosome reading a premature stop codon (55-57). There is still a debate as to the composition of the clamp loader. Some studies have suggested that the clamp loader contains either three γ or three τ subunits (22, 50, 58, 59). Other studies suggest that the clamp loader is a heterotrimerization of γ and τ, with

two τ and one γ subunit (60, 61). There is a consensus that the clamp loader at the replication fork has at least two τ subunits because two polymerases are required for efficient replication (62).

It was observed that τ, not γ, is required for cell viability (63). Domains I, II, and III of the DnaX subunits, which contain the ATP binding/hydrolysis motifs as well as the residues that interact with the other clamp loader subunits, are present in both τ and γ (64, 65). The C-terminal region of τ, that is not present in γ, has two addition domains, IV and V. Domain IV has been shown to interact with the DnaB helicase and increase the rate of helicase unwinding by more than 10-fold, matching rates of DNA replication *in vivo* (4, 65-67). Helicase binds to primase (DnaG) as well, creating a link between the clamp loader and primase (68-70). Primase synthesizes RNA primers (10-12nt) for pol III at the beginning of the leading strand and the Okazaki fragments of the lagging strand (37). Interestingly, it has been shown that even though τ does not bind primase directly, the presence of τ clamp loader allosterically regulates primer synthesis by DnaG (71). This interaction between τ and the helicase is also important for coupling the leading strand pol III with helicase (4, 66). The C-terminal domain V of τ (not found in γ) has been shown to directly interact with the α subunit (catalytic core) of DNA polymerase III in a 1:1 stoichiometry (66, 72-75). This τ-pol III interaction is important for linking the leading and lagging strand Pol III, coordinating actions at the replication fork (65). When pol III finishes synthesizing an Okazaki fragment on the lagging strand, pol III is moved to the sliding clamp on the following RNA primer by the connected τ subunit in order to begin synthesizing the next Okazaki fragment (76, 77). It has been proposed that the presence of τ at the replication fork also prevents γ from unloading sliding

clamps during DNA replication *in vitro,* providing another possible function for τ *in vivo* (76). Combining all of these important functions of τ can explain why cells without τ are not viable (63). It is still unknown what the exact role of γ is, but has been proposed to be involved in clamp unloading and/or DNA repair (60, 76, 78).

**The clamp loading reaction**

The clamp loading reaction is very dynamic. Many conformational changes occur in the clamp loader and sliding clamp when ATP is bound and hydrolyzed. Each of the three DnaX subunits can bind and hydrolyze one molecule of ATP, driving the clamp loading reaction (79). Before the clamp loader binds ATP, it has a low affinity for DNA and the sliding clamp (35). The low clamp loader affinity for the sliding clamp with no ATP is thought to be the result of steric clashes between the sliding clamp and the clamp loader. Once the ATP is bound, the clamp loader has a high affinity for the sliding clamp (35, 79, 80). When the DnaX subunits bind ATP this causes a conformational change removing steric clashes and allowing the δ subunit to bind one interface of the β sliding clamp (35, 80-83). The energy of the interaction between the δ subunit and the β sliding clamp is what drives the binding reaction (82). The δ subunit interacts with the sliding clamp through the Leu73 and Phe74 residues. (81, 82). ATP causes a conformational change which allows the clamp loader complex to make a more spiral conformation, alleviating the steric clash between the clamp loader and the sliding clamp, and allowing the other clamp loader subunits to bind the clamp loader (Figure 1-4) (35, 79, 83).

When the open clamp-clamp loader complex comes into contact with a primer-template junction (Figure 1-4), this promotes ATP hydrolysis by the DnaX subunits (84). DNA binding by the clamp loader-clamp complex is relatively rapid (85, 86). Without the

DNA-clamp loader interaction, the clamp loader has relatively week ATP hydrolysis (87). When the clamp loader binds DNA, the interactions promote a symmetrical arrangement of the three ATP hydrolysis sites that promotes the reaction (88). In addition, the sliding clamp has also been shown to stimulate the ATP hydrolysis by the clamp loader when bound to DNA (84, 87, 89). ATP hydrolysis by the clamp loader results in a lowered affinity of the clamp loader for the sliding clamp (80, 90). It is hypothesized that the ATP hydrolysis conformational change involves pushing β off the δ subunit by moving the β binding residues back to the proximity of δ', inhibiting binding of another sliding clamp (82). These conformational changes in the clamp loader result in the closing of the sliding clamp around DNA and then the clamp loader releases the sliding clamp allowing other proteins, like DNA pol III, to bind (84, 85, 91). Clamp release has been shown to be relatively slow compared to the rest of the reaction and is thought to be the rate-limiting step (85, 92). The clamp loader will continue to have a low affinity for the sliding clamp until it releases the ADP molecules and replaces them with ATP.

**Clamp loader interactions with DNA and SSB**

Clamp loaders load sliding clamps onto the duplex region of a primer-template junction. When the clamp loader binds the DNA, the duplex region of DNA is flush against the cap of the clamp loader while the single-stranded overhang (SSO) exits out of a channel between the δ and δ' subunits (Figure 1-3) (88). The crystal structure also showed that the positively charged residues of the clamp loader cap interact with the negatively-charged backbone of the template strand of DNA, but not the primer explaining why the clamp loader can load on both DNA and RNA primers (88, 93).

Experiments looking at the effect of mutating different residues of the clamp loader cap have confirmed these interactions (94).

Clamp loaders have been shown to preferentially load clamps onto primer-template regions (86). Specifically, clamp loaders load onto a DNA substrate with a 3' primer-template junction (Figure 1-4). The crystal structure does not give information on why the clamp loaders prefer the 3' primer-template junction, but pol III does require a 3' OH on the primer for DNA elongation reactions showing that the clamp loader prefers DNA substrates needed for DNA replication (95, 96). In addition, the polarity of the ssDNA exiting the clamp loader upon binding does not confer specificity of the clamp loader for 3' primer-template junctions (96).

In addition to the five core subunits, there are two accessory proteins, φ and χ, which are not required for the clamp loading reaction. The φ is the gene product of *holC* which binds to one of the DnaX subunits to help stabilize ATP conformational changes (97). Additionally, the φ subunit is the link between the core clamp loader and the χ subunit (98, 99). The χ subunit is the gene product of the *holD* gene which binds to φ and assists in clamp loader interactions with single-stranded DNA binding protein (SSB) (99-102). Protein-protein interactions between χ and SSB have been shown to increase the replication activity of the pol III holoenzyme and to stimulate clamp loading (100, 101). SSB (single-stranded DNA binding protein) is a homotetramer that binds to single-stranded DNA to prevent secondary structures, nuclease attack, and to coordinate actions of proteins on DNA (Figure 1-1). SSB is very dynamic on DNA and can bind the DNA in various "modes" of different nucleotide lengths (103, 104). The interaction of SSB and the clamp loader has been shown to be critical for the specificity of the clamp

loading to 3’ primer-template junctions and to inhibition of clamp loading on 5’ primer-template junctions (105). The mechanism of clamp loading regulation by SSB is unknown.

## Eukaryotic Replicase

Our lab uses *E. coli* as a model system to determine the steps in the clamp loading cycle and how these proteins contribute to the overall efficiency of the replication fork because of the simplicity of bacteria and the homology of these proteins throughout the domains of life. While the DNA sequences encoding sliding clamps and clamp loaders are quite different between organisms, the structure and function of these proteins are well conserved (Fig 1-2,3) (Reviewed in (93, 106)). In eukaryotes, the replication clamp loader is replication factor C (RFC) and the sliding clamp is proliferating cell nuclear antigen (PCNA). RFC is composed of 5 different subunits (RFC1-5) which organize themselves to resemble a cap-like structure, similar to the core DnaX clamp loader complex (Figure 1-3) (107). PCNA is a homotrimer with each monomer arranged in a head-to-tail fashion (Figure 1-2) (108). Each monomer has two domains resulting in a very similar structure as the *E. coli* β sliding clamp. Like the *E. coli* sliding clamp, PCNA increases the processivity of the DNA polymerase and is required for cell viability (109).

RFC binds five ATP molecules at the RFC1-5 subunits and RFC1-4 are the active ATPase subunits which perform ATP hydrolysis (110). In a similar manner as the DnaX clamp loader, RFC binds and opens PCNA when ATP is bound. RFC shows more of a sequential binding of ATP (110, 111) . Three ATP molecules bind to activate PCNA binding/opening, then another two ATP molecules binds to activate DNA binding. Finally, ATP hydrolysis occurs closing PCNA around the DNA and causing RFC to

release the clamp (110, 112). Like the DnaX clamp loader, RFC also loads clamps onto primer-template junctions and the single-stranded DNA binding protein, RPA, has been shown to regulate loading onto different DNA substrates in a similar manner as SSB in *E. coli* (105, 113).

While the RFC clamp loader is used in DNA replication, the RFC1 (A position) subunit can be exchanged for other proteins to produce alternative clamp loaders, which are required for viability under various conditions. These alternative clamps loaders are conserved throughout all eukaryotes. Elg1 subunit can be incorporated instead of RFC1, producing Elg1-RFC clamp loader which has been shown to unload PCNA from DNA after ligation of Okazaki fragments (114). Another alternative clamp loader is the Rad24-RFC clamp loader, which loads an alternative sliding clamp onto DNA at sites of DNA damage upon which the DNA damage checkpoint pathway is activated (115). A third alternative clamp loader is Ctf18-RFC that assists in the replication of DNA at sites of sister chromatid cohesion. Ctf18-RFC unloads PCNA from DNA at cohesion binding sites allowing the replication machinery to replicate through these regions (116).

## Statement of Problem and Research Design

While the structure of DNA is relatively simple, the process in which it is replicated is complex and involves many different proteins to ensure efficiency and accuracy. DNA replication is a very quick and efficient process, performing synthesis at about 1000nt/s in *E. coli*. The leading strand of replication theoretically only requires the loading of one sliding clamp during the course of DNA synthesis, but the lagging strand requires the loading of a sliding clamp at the beginning of every Okazaki fragment. This requirement means that the clamp loaders need to load a clamp approximately every 2-

3s. To be efficient and precise, sliding clamps must be loaded onto the correct DNA substrate at the right time. In addition, the clamp must be loaded in the correct orientation, as the polymerase only interacts with one face of the clamp. While many studies have examined the different parts of the clamp loading reaction, there are still many questions on how the clamp loading reaction is regulated. Presented here are three studies that looked at the regulation of clamp loading by the sliding clamp, the clamp loaders, and through interactions with other proteins. Various fluorescence-based assays were implemented to study how the clamp loaders load the sliding clamps and how mutations effect this reaction.

In Chapter 3, the role of the sliding clamp in the clamp opening reaction was studied. While the clamp loading mechanism has been studied in detail, there is a still a debate in the field as to whether the clamp loaders actively open the clamp or if clamp loaders stabilize the clamp once the clamp transiently opens. Previous studies have shown that electrostatic interactions at the interface of where the clamp opens and closes are important for the stability of the clamp loader. Electrostatic mutations were introduced to the interface of the clamp and the effect of these mutations on the clamp loading reaction were determined. If the sliding clamp transiently opened and the clamp loader stabilized the open form, then it would be expected that destabilizing the clamps interface would increase the rate of clamp opening.

Experiments in Chapter 4 examined the biochemical difference between two forms of the DnaX *E. coli* clamp loader, γ- and τ-complex. There has been much debate as to the composition of the *in vivo* clamp loaders when it comes to the DnaX subunits. In addition, there has been conflicting views on the role of γ *in vivo* or if γ has any

significant role at all. The studies in this chapter look at the clamp loading reaction of the two different clamps loaders to determine if there are any mechanistic differences in their clamp loading reaction.

Finally, in Chapter 5, the regulation of clamp loading by single-stranded DNA binding protein (SSB) was studied. While the clamp loader has been shown to preferentially load onto DNA substrates that have a 3' primer end at a primer/template junction, it is still unknown why there is this preference. Additionally, the preference is also seen with the eukaryotic clamp loading reaction. The preference for 3' recessed DNA reflects the need of a free 3' OH for the polymerase to bind and catalyze the DNA synthesis. Previous work from our laboratory showed that SSB was stimulating clamp loading on 3' recessed primer/template junctions while inhibiting loading on the wrong polarity DNA, a 5' primer end at a primer/template junction. The studies in this chapter expand on these findings to understand by what mechanism SSB is regulating the clamp loading reaction.

## Medical Relevance

Proteins involved in DNA replication, like the sliding clamp and clamp loader, are highly conserved across all domains of life. While the amino acids sequence itself is not highly conserved, the structure and function of the clamp loader/sliding clamp proteins are very similar from bacteria to eukaryotes. These proteins are fundamental to survival. Cells are unable to survive without clamp loaders or sliding clamps. Mutations in the clamp loader or sliding clamp proteins can lead to abnormal phenotypes. Mutations of the human clamp loader, RFC, have been found in diseases like Hutchinson-Guilford Progeria Syndrome (HGPS). Patients with HGPS have an N-terminal truncation of the RFC1 subunit caused by cytoplasmic proteases gaining access to the nucleus (117).

The truncation of the RFC1 protein has detrimental effects on the clamp loading reaction. Another study examined the effects of microsatellite instability on *RFC3* expression and found that in gastric and colorectal cancers, which a have high amount of microsatellite instability, RFC3 was mutated or truncated leading to a loss of expression(118).

In addition to mutations, abnormal expression levels of the clamp loader proteins have been observed in cancerous cells. The RFC4 subunit of the human clamp loader is known to be aberrantly regulated across different types of cancer. A study found that in colorectal cancer (CRC), the expression of *RFC4* is unregulated and was associated with tumor progression and poor patient outcome (119). By using siRNA to knockdown the RFC4 levels, it was found that the abundance of RFC4 promotes cell cycle progression and DNA replication in the cancer cells. Colorectal cancer is one of the leading causes of cancer-related deaths. By studying the mechanism of clamp loading and the interactions of the clamp loader/sliding clamp with other proteins, more insight can be gained into why the cancer cells upregulate these proteins and possibly find a novel chemotherapeutic target. Interestingly, one study found that decreasing the level of RFC4 in the cancerous cells made them more susceptible to chemotherapies (120). RFC4 is not the only clamp loader protein found to be unregulated in cancers. The RFC2 subunit has been found to be overexpressed in nasopharyngeal carcinoma (121). Also, *RFC3* has been found to be upregulated in esophageal adenocarcinoma (122).

Studying the regulation and mechanisms of the clamp loaders and sliding clamps in *E. coli* can provide insight to the equivalent proteins in higher organisms. Possible antibiotic targets could be discovered, as well as antivirals and chemotherapeutics due

to the conservation of the clamp/clamp loader structures. Laboratories have begun designing small-molecule inhibitors of the sliding clamp for the intention of killing cancerous cells. Small-molecule inhibitors for the human sliding clamp, PCNA, have been discovered that bind to PCNA, reduces the chromatin-associated PCNA, reduces DNA replication and arrest cancer cells in the S and $G_2$/M phases (117). Inhibitors of the sliding clamp are also being screened for antibiotic properties. Strains of antibiotic-resistant bacteria are on the rise, which means new antibiotics to combat these strains is urgently needed. One study designed small-molecule inhibitors that specifically bound to the bacterial sliding clamp at the consensus sequence where other proteins interact with the sliding clamp (123). Blocking the interaction of proteins, like DNA polymerase, with the sliding clamp causes DNA replication to halt and eventually death of the bacterial cells. It has yet to be determined if these inhibitors also interact with the eukaryotic clamp. To be an efficient and safe antibiotic, the inhibitor would have to bind the bacterial proteins without effecting the eukaryotic proteins. Interestingly, the clamp loader is an unexplored drug target even though the clamp loader is essential for DNA replication and cell viability. With multiple ligands and confirmation changes during the clamp loading reaction, there are various mechanisms that inhibition could work by on the clamp loader. By studying the mechanism and regulation of the clamp loaders functions, it will provide more insight into how to design small molecule inhibitor for different uses.

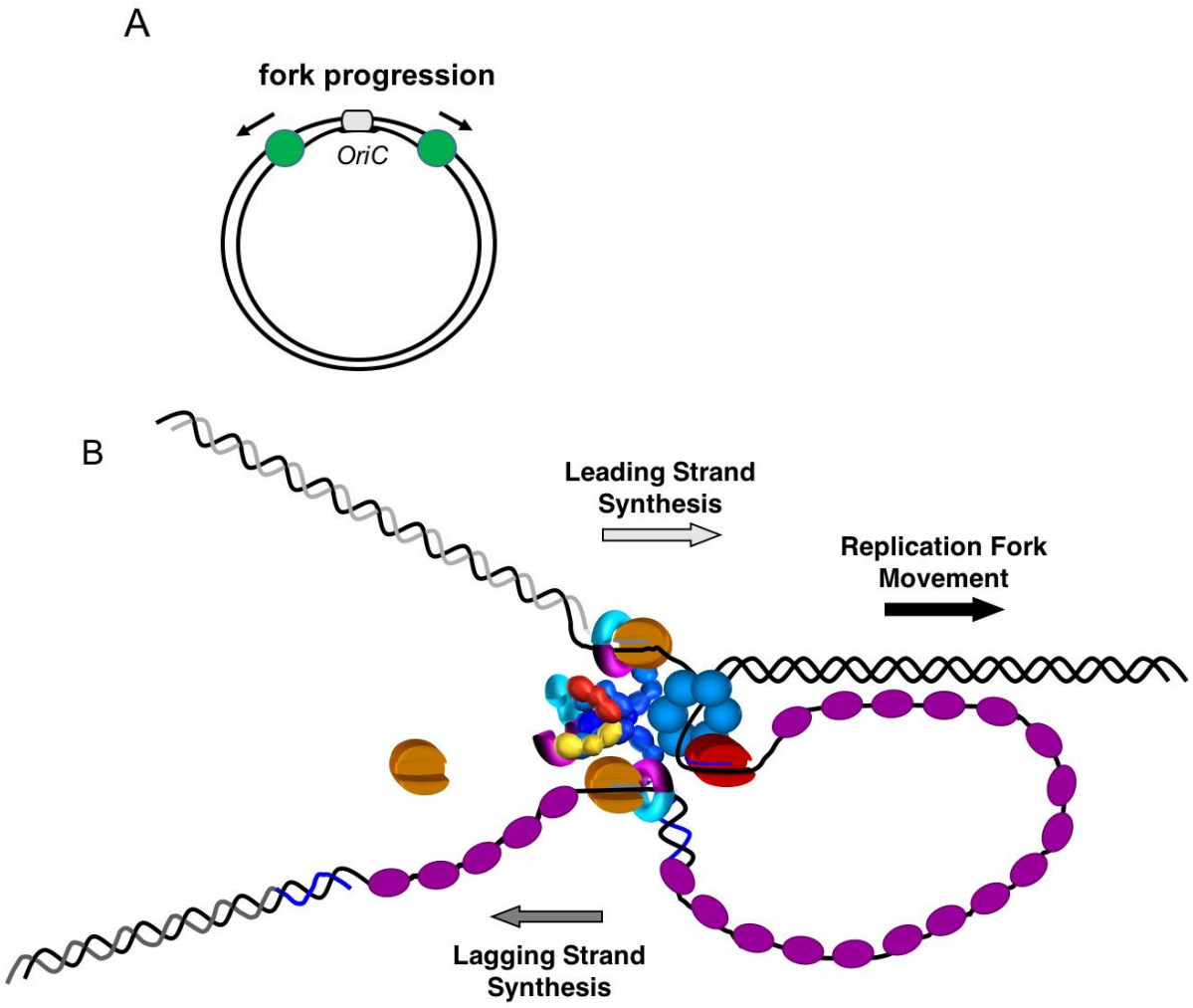


Figure 1-1. A cartoon representation of the *E. coli* replication fork. A shows the direction of replication fork (green circles) progression around the *E. coli* genome. B shows a zoomed in view of the replication fork depicted in A. Helicase is shown in blue spheres, primase in red, DNA polymerase III in orange, SSB in purple, sliding clamp in magenta and cyan, and the clamp loader is the multicolored enzyme in the middle. The blue on the DNA represents the RNA primer. Note that during DNA replication, there is an identical fork on the opposite side as shown in A.

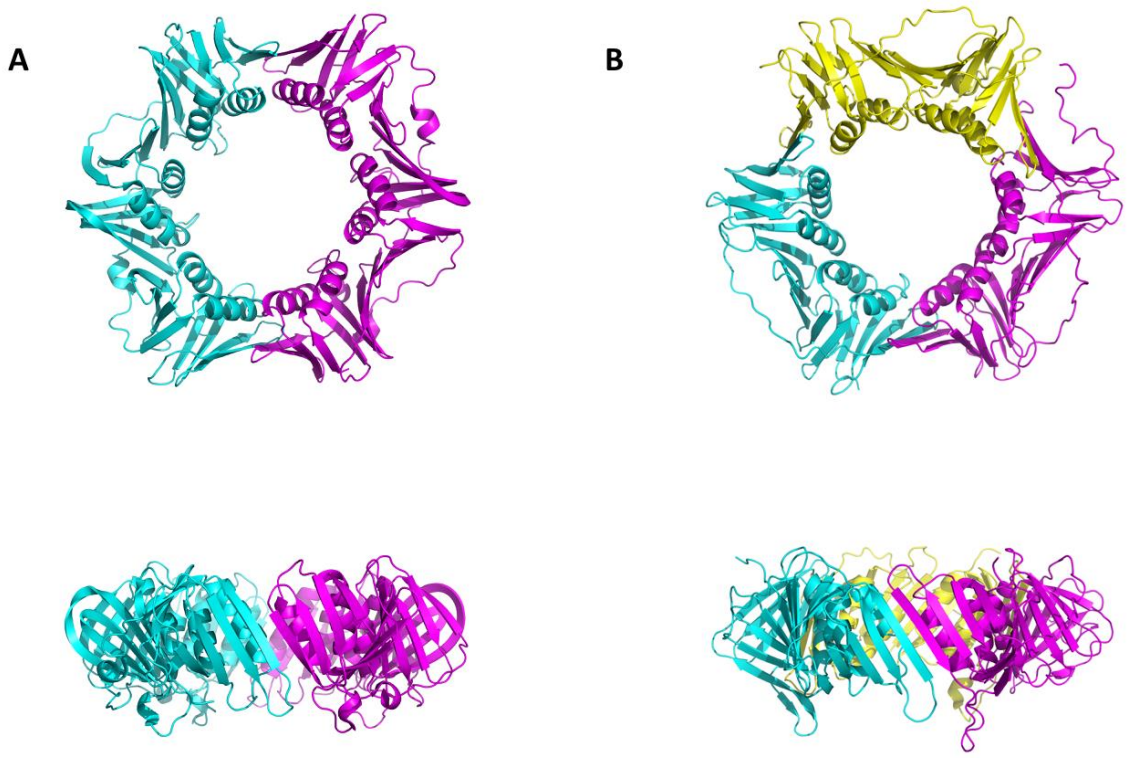


Figure 1-2. Crystal structure of sliding clamps. A) Crystal structure of the *E. coli* β sliding clamp (PDB: 2POL). B) Crystal structure of the eukaryotic (yeast) PCNA sliding clamp (PDB:1SXJ).

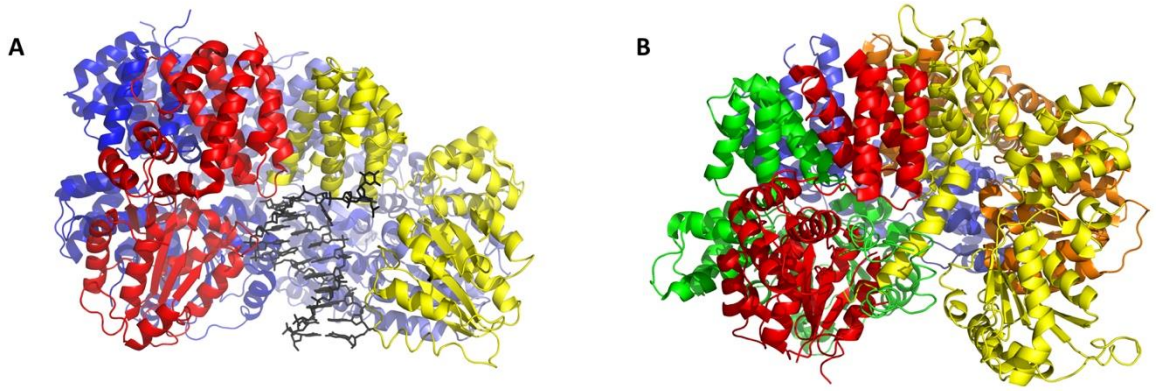


Figure 1-3. Crystal structure of clamp loader complexes. A) *E. coli* γ-complex core clamp loader on a primer-template junction (PDB: 3GLF). The γ subunits are in blue, δ is in yellow, and δ' is in red. The DNA is black and the single-stranded overhang can be seen exiting the gap between the δ and δ'. B) Crystal structure of the yeast eukaryotic clamp loader, RFC (PDB:1SXJ ). RFC1 is yellow, RFC2 in green, RFC3 in blue, RFC4 in orange, and RFC5 in red.

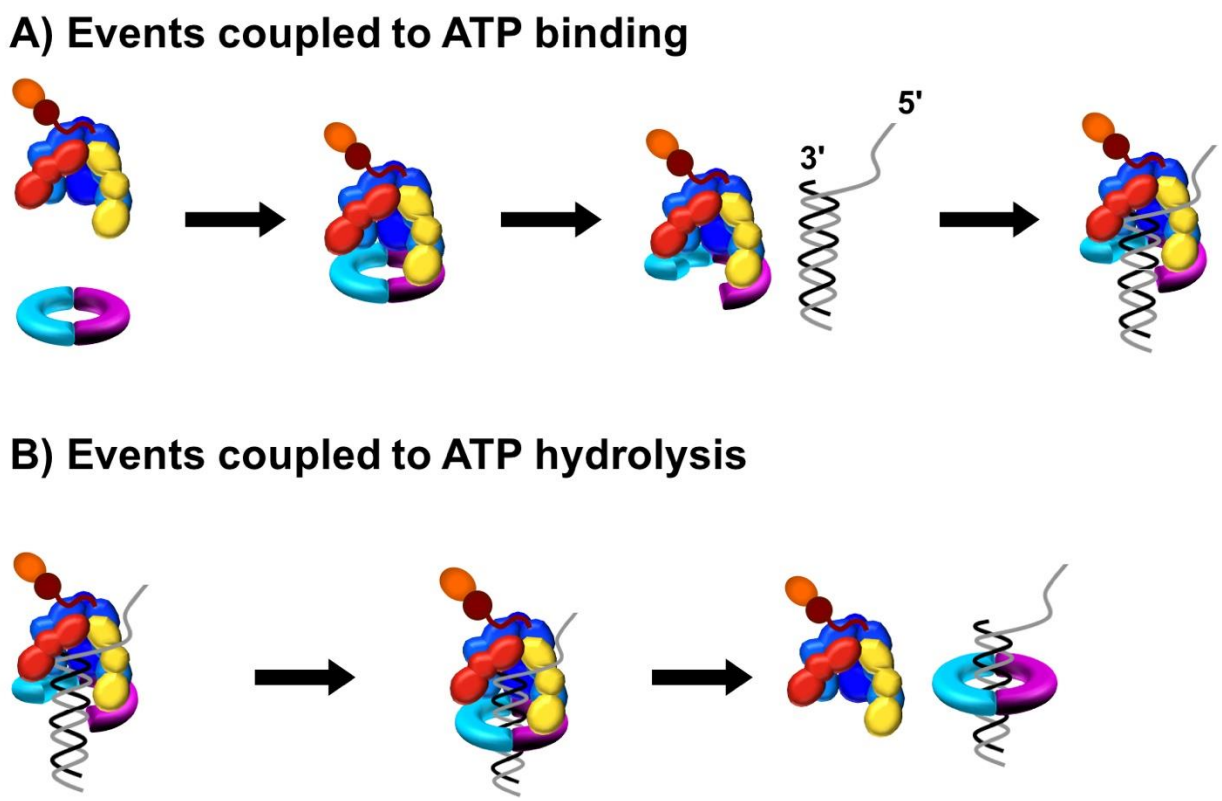


Figure 1-4. Steps of the clamp loading reaction. Based on many studies using mutational and biochemical analysis, the representative steps of the clamp loading reaction can be associated with ATP binding or ATP hydrolysis. A) The steps associated with ATP binding are clamp binding, opening, and binding to a primer/template junction. B) The steps associated with ATP hydrolysis are clamp closing and release of the clamp and DNA.

# CHAPTER 2
# MATERIALS AND METHODS

## Reagents

### Buffers

Clamp loader complexes were stored in a buffer containing 20 mM Tris-HCl pH 7.5, 0.5 mM EDTA, 5 mM DTT, and 30% glycerol. In addition, γ-complex and χ-less γ-complex storage buffer contained 50 mM NaCl, τ-complex contained 100 mM NaCl and holoenzyme contained 200 mM NaCl. DnaX2016 subunits and clamp loader complexes were stored 30 mM HEPES pH 7, 0.5 mM EDTA, 2 mM DTT, 100 mM NaCl, and 10% glycerol.

SSB was stored in the same buffer as the WT clamp loader complexes but with 200 mM NaCl for wild-type SSB, 500 mM NaCl for SSBΔC8, and 200mM NaCl for SSBΔC1. Unlabeled β sliding clamp was stored in 20 mM Tris-HCl pH 7.5, 0.5 mM EDTA, 5 mM DTT, and 10% glycerol, whereas all labeled β was stored in the same buffer but without the addition of DTT. Steady state and pre-steady state assay buffer had a final concentration of 20 mM Tris-HCl pH 7.5, 0.5 mM EDTA, 5 mM DTT, 50 mM NaCl (or 500 mM NaCl if noted), 0.5 mM ATP, 8 mM $MgCl_2$ and 4% glycerol.

### ATP

ATP (Amerisham Biosciences) was diluted in 20 mM Tris pH 7.5. The concentration of the ATP solution was measured by recording the absorbance at 259 nm. Using Beer's law and an extinction coefficient of 15,400 $M^{-1}$ $cm^{-1}$, the concentration was determined.

**Oligonucleotides**

Oligonucleotides used for site-directed mutagenesis (SDM) are listed in Table 2-1. These oligonucleotides were purchased from IDT (Integrated DNA Technology) at 25 nmole scale and dehydrated. TE buffer (10 mM Tris-HCl pH 7.5 and 1 mM EDTA pH 8) was used to dissolve the pellets. The DNA was then diluted to 25 ng/μL with sterile water in preparation for the SDM reactions.

The oligonucleotides used in the assays were purchased from IDT (Integrated DNA Technology) at 1 μmole scale. These oligonucleotides are listed in Table 2-2. For the assays, the full-length oligonucleotides were purified from the incomplete, shorter oligonucleotides by using 10 (>50 nucleotides) -12% (<50 nucleotides) urea polyacrylamide gels. The oligonucleotides were dissolved in NTE (50 mM Tris pH 7.5, 50 mM NaCl and 0.5 mM EDTA) with 50% glycerol and were loaded onto the gels. The gels were run 18-20 hours overnight at 8 watts. UV shadowing was used to visualize the DNA bands, which involves placing the gel on a TLC plate and and then exposing it to UV light. Dark areas appear where the DNA absorbs the UV light. The full length oligonucleotides were excised from the denaturing gel and the gel pieces were placed into a tube of NTE. The tubes were placed on a shaker for 24 hours to extract the oligonucleotides from the gel pieces. After 24 hours, the NTE containing the DNA was removed and dialyzed against 2L of 20 mM Tris pH 7.5 and 50 mM NaCl for 12 hours using 3,500 Da molecular weight cut-off dialysis tubing. Then the tubing was moved into 4L of nanopure water for an additional 24 hours of dialysis. A centrifugal vacuum concentrator was used to concentrate the DNA to about 500 μL. The concentrations of the oligonucleotides were determined by measuring the absorbance at 260 nm and the extinction coefficients provided by IDT. DNA was stored at -20°C.

For the oligonucleotides longer than 100 nucleotides (LD5, Table 2-2), two oligonucleotides were ligated together because IDT could not guarantee the quantity of DNA needed for the assays when the oligonucleotides were longer than 100 nucleotides. To ligate the oligonucleotides, the individual oligonucleotides were purified as described above. After determining the DNA concentration (LD5.1 and LD5.2, Table 2-2), the oligonucleotides were ligated together by annealing a linker oligonucleotide that did not have a 5' phosphate (LD1NoP, Table 2-2) to create a nicked substrate that could be ligated. The annealing reactions contained final concentrations of 13μM DNA (LD5.1, LD5.2, and LD1NoP), 20 mM Tris-HCl pH 7.5, and 50 mM NaCl. The solution was heated to 85°C for 5 minutes and then allowed to cool slowly back to room temperature over about 6 hours. Next, the DNA was dialyzed as above against 2 L of 50 mM Tris-HCl pH 7.5 to remove the NaCl. Ligation reactions were incubated overnight in a 14°C water bath with a final buffer concentration of 50 mM Tris-HCl pH 7.5, 10 mM $MgCl_2$, 5 mM DTT, 1 mM ATP, 50 μg/mL BSA, 9.1 μM DNA, and 10 units of T4 ligase (New England Biolabs). The reactions were stopped by adding EDTA to a final concentration of 25 mM. The oligonucleotides were precipitated by adding 0.3 M sodium acetate and cold 70% ethanol, and was cooled at -80°C overnight. DNA pellets were dissolved in 10mM Tris-HCl pH 7.5, 10mM NaCl, and 0.1mM EDTA and concentrated on a centrifugal vacuum concentrator. Next, formamide was added and the solution was heated for 5 minutes at 95°C to separate the ligated 110 nt oligonucleotide from the linker oligonucleotide. To separate the full length oligonucleotides from the unligated products and the linker, the DNA was run on a 10% urea acrylamide gel as above. DNA

concentration was determined by measuring absorbance at 260 nm and using the sum of the two oligonucleotides extinction coefficients for the unligated oligonucleotides

In preparation for the assays, the desired oligonucleotides were annealed. The oligonucleotides were added to a solution of 50 mM NaCl and 20 mM Tris pH 7.5 to a final DNA concentration of 4 μM. Next, the mixture was heated in a water bath to 85°C for 5 minutes. The heat was turned off and the solution was allowed to cool room temperature overnight. Annealed DNA was prepared fresh the day before each experiment.

## Expression Vectors

### Site-directed Mutagenesis

Site-directed mutations were made using the Quikchange II Site-Directed Mutagenesis kit (Agilent) as per the manufacturer's directions. All oligonucleotides used for SDM are listed in Table 2-1 along with the corresponding gene.

### Cloning *dnaX2016* into pET52b+

Mutations were introduced into the τ and γ forms of the DnaX clamp loader, DanX2016, by introducing 3 missense mutations into the *dnaX* gene which resulted in the amino acid substitutions of G118D, G212D, and A400T (Figure 4-1, Table 4-1). Once *dnaX2016* was prepared by SDM, the genes were subcloned from a pET15b vector (γ) or pBluescript (τ) into a pET52b+ (Novagen) to attach C-terminal histidine-tags which aided in purification and to separate endogenous wild-type clamp loader from the DnaX2016 form. PCR was used to copy the genes from their respective vector and to add a 5' BspHI restriction site and a 3' SacI restriction site as well as 6 nonspecific base pairs to the ends of each to give the restriction enzyme room to bind DNA. The PCR products were then digested with BspHI and SacI while the pET52+

vector was digested with NcoI and SacI. Digestion with BspHI leaves an overhang that is compatible with NcoI. Next, the vector was dephosphorylated using alkaline phosphatase and ligated to the PCR products. For all vectors, a restriction digest was done to confirm insertion of the PCR product and Sanger sequencing performed by UF's ICBR Core confirmed that the gene of interest had been interested without undesired mutations.

**Creating *E. coli* Holoenzyme Duet Vector Expression System**

In order to make our laboratory's clamp loader purification more efficient and to aid in the purification of DnaX2016 clamp loaders, all of the clamp loader genes were subcloned into compatible expression vectors which allow the expression of all clamp loader proteins at the same time, in the same cells. In addition, a third vector was created to express the subunits of polymerase III in order to create holoenzyme. Figure 2-1 to 2-3 shows the final vector system.

The pCOLA Duet Vector (Novagen) contained the *dnaX* and *holA* genes. First, *holA* ($\delta$ subunit) was subcloned into the multiple cloning site (MCS) 2 site. PCR was used to copy *holA* from a pBluescript vector, and to add a 5' NdeI restriction site and a 3' AvrII restriction site, as well as 6 nonspecific base pairs to the ends of each. Primers used for cloning are listed in Table 2-1. After digestion of the PCR products and pCOLA vectors with NdeI and AvrII, the vector was dephosphorylated with alkaline phosphatase and the PCR products were ligated to the vectors. A restriction digest was done to confirm insertion of the PCR product and finally sequencing confirmed the gene of interest had been interested without undesired mutations. Secondly, the γ- or τ-only version of the *dnaX* or *dnaX2016* gene was subcloned into the MCS1 site of pCOLA

duet vector by PCR restriction digestion. PCR was used to copy the genes from their respective vector (wild-type from pET15b and *dnaX2016* from pET52b+, see above) and to add a 5' BspHI restriction site and a 3' SacI restriction site as well as 6 nonspecific base pairs to the ends of each. The PCR products were digested with BspHI and SacI while the pCOLA vector was digested with NcoI and SacI. Digestion with BspHI leaves an overhang that is compatible with NcoI. Next, the vector was dephosphorylated using alkaline phosphatase and ligated to the PCR products. The final vector construct was verified as above.

The pET Duet vector (Novagen) contained either the *holD* ($\psi$) gene only or an operon of *holC* ($\chi$) and *holD,* which was created by a former lab member, in MCS1 and *holB* ($\delta$' subunit) in MCS2. First, the empty pET Duet vector and the Litmus38i (New England Biolabs) vector containing *holB* were both digested with AvrII and NdeI. the vector was dephosphorylated using alkaline phosphatase and ligated to the *holB* digested product. Confirmation of the insert was performed as above. Secondly, *holD* or an operon of *holC* and *holD* was cloned into the MCS1 site. The *holD* only version was created by digesting the pET Duet vector containing *holB* and the pET15b vector containing *holD.* with XbaI and BamHI. Ligation and confirmation of insert were done as described above. The construct with an operon of *holC* and *holD* was created by first digesting the pET Duet vector containing *holB* and the pET15b vector containing *holC* with XbaI and BamHI. Ligation and confirmation of insert was done as described above. Finally, to create the *holC/holD* operon, the pET Duet vector with *holB* and *holC* and the pBluescript vector containing *holD* were digested with BamHI. Ligation and confirmation of insert was done as described above.

The pCDF Duet vector (Novagen) contained the polymerase III subunits, *dnaE* ($\alpha$) in MCS1 and *holE* ($\theta$) in MCS2. First, the empty pCDF Duet vector and the pBluescript (New England Biolabs) vector containing *holE* were both digested with NdeI and AvrII. the vector was dephosphorylated using alkaline phosphatase and ligated to the *holE* digested product. Confirmation of the insert was performed as above. Secondly, *dnaE* was cloned into the MCS1 site by digesting the pCDF Duet vector containing *holE* with NcoI and BamHI and the pBluescript vector containing *dnaE.* with BspHI and BamHI. Ligation and confirmation of insert were done as described above. Two mutations (D12A and E14A) were introduced into the exonuclease subunit, $\varepsilon$, through SDM to make the exonuclease nonfunctional, thus preventing degradation of DNA in future assays. The *dnaQ* ($\varepsilon$) still has to be subcloned into the pCDF Vector, but the subunit that interacts with the clamp loader (α) was the subunit required for the experiments in Chapter 4.

## Proteins

### Purification of DnaX2016 Subunits

For both DnaX2016 $\tau$ and $\gamma$ subunit purification, the his-tagged version in pET52b+ (see above) were used. The vector was transformed into competent BL21(DE3) cells and plated on LB media with agar and ampicillin (100 ng/µl) (Amp) antibiotic. The plates were incubated at 37°C overnight. One colony was used to inoculate 10 mL of LB media with Amp (100ng/µl) which was incubated in a 37°C shaker for 4 hours. This starter culture was stored at 4°C overnight. The next day, the 8 mL of the starter culture was centrifuged at 7000 x g for 5 minutes using and the supernatant was decanted. Cell pellets were resuspended in fresh LB media with Amp

(100ng/µl) and used to inoculate 2 L of LB media with Amp. These cultures were grown up until the $OD_{600}$ was 0.7-0.8. Once the OD was reached, the flasks were put on ice to cool them down to 20°C. Once at 20°C, the flasks were moved to a refrigerated tabletop shaker and expression of the clamp loader subunits was induced with the addition of IPTG to a final concentration of 1 mM. Protein expression continued for 4 hours at 20°C, after which the flasks were placed on ice until they cooled to 4°C. The bacterial cultures were pelleted by centrifugation at 5,200rpm using a Beckman JA 20 rotor for 30 min at 4°C. Liquid media was removed and the pellets were stored at -80°C.

Purification of the His-tagged DnaX2016 proteins began with cellular lysis using a French Press. Lysis buffer was 30 mM HEPES pH 7, 30 mM imidazole, 2 mM DTT, 500 mM NaCl, and 10% glycerol. SigmaFast protease tablets (without EDTA) were also included in τ purification to prevent proteolysis of the C-terminal. Lysis with the French Press was performed 3 times on each sample to ensure full lysis. The lysed cells were centrifuged at 10,000 rpm for 45 minutes at 4°C using a Beckman JLA 10.5 rotor. Supernatant was kept at 4°C and used for the following steps to further purify the clamp loader.

Next, the lysed supernatant was loaded onto two 5 mL HisTrap columns (GE Healthcare). The HisTrap column was prepped for the protein by washing it with 30 mM HEPES pH 7, 30 mM imidazole, 2 mM DTT, 500 mM NaCl, and 10% glycerol for 5 column volumes, then washing it with the same buffer plus 500 mM imidazole for 5 column volumes, then finally washing the column with the same buffer plus 30 mM imidazole. A peristaltic pump (Pharmacia P-1) was used to load the lysed supernatant at 2 mL/min. Once all of the supernatant was loaded, the column was washed with 5

column volumes of buffer matching the lysis buffer at 2 mL/min. The column was relocated to an ÄKTA purification system (GE Healthcare) where the column was washed with lysis buffer until the UV absorbance leveled out at the baseline. The AKTA was programmed to run a gradient from 30 to 500 mM imidazole in lysis buffer over 50 min at a flow rate of 2 mL/min collecting 1 mL fractions. Samples of fractions giving a UV peak were analyzed by 12% SDS-PAGE to identify fractions containing proteins corresponding to the molecular weights of τ (73.6 kDa) or γ (47.5 kDa). The DnaX2016 γ eluted around 170 mM NaCl and DnaX2016 τ eluted around 350 mM NaCl. Fractions to be kept were pooled together and dialyzed twice against 2 L of 30 mM HEPES pH 7, 0.5 mM EDTA, 2 mM DTT, 100 mM NaCl, and 10% glycerol using a 12-14,000 molecular weight cut-off dialysis tubing. Protein was dialyzed overnight for at least 12 hours then the buffer was switched for fresh buffer and dialyzed for another 5 hours.

Quantification of the DnaX2016 subunits was performed by Bio-Rad Bradford assay according to the manufacturer's instructions (124). BSA standards were used to create a standard curve. Final gels of the DnaX2016 subunits are shown in Figure 2-4.

**Purification of DnaX Clamp Loaders and Holoenzyme**

All of the DnaX clamp loaders (γ-, τ-, χ-less γ-complex, and DNA polymerase III holoenzyme) were purified using the same method but with varying NaCl concentrations in the buffers used (see Buffers). In order to express the clamp loaders, the duet vectors for the clamp loaders (Figure 2-1 to 2-3) were transformed into BL21(DE3) cells (Novagen) and plated on LB media with agar and antibiotics. Antibiotics kanamycin (50 ng/μl) (Kan) and ampicillin (100 ng/μl) (Amp) were used to select for the cells that contained both pCOLA and pET Duet vectors (chloramphenicol was added in addition

to Kan and Amp for holoenzyme expression with pCOLA, pET Duet, and pCDF Duet vectors). The plates were incubated at 37°C overnight. One colony was used to inoculate 10 mL of LB media with Amp and Kan which was incubated in a 37°C shaker for 4 hours. This starter culture was stored in 4°C overnight. The next day, the 8 mL of the starter culture was centrifuged at 7000 x g for 5 minutes and the supernatant was decanted. Culture pellets were resuspended in fresh LB media with Amp and Kan and used to inoculate 2 L of LB media with Amp and Kan. These cultures were grown up until the $OD_{600}$ was 0.7-0.8. Expression of the clamp loader subunits was induced with the addition of IPTG to a final concentration of 1 mM. Protein expression continued for 3 hours and the flasks were placed on ice until they cooled to 4°C. The bacterial cultures were pelleted by centrifugation at 5200 rpm for 30 min at 4°C using a Beckman JA 20 rotor. Liquid media was removed and the pellets were stored at -80°C.

Isolation of the clamp loaders began with lysing the cells using a French Press. Lysis buffer for γ-complex was 20 mM Tris pH 7.5, 0.5 mM EDTA, 5 mM DTT, 50 mM NaCl, and 10% glycerol. Lysis buffer for τ-complex and pol III holoenzyme were the same but with 100 mM NaCl or 200 mM NaCl, respectively. SigmaFast protease tablets were also included in τ-complex and pol III holoenzyme purifications to prevent proteolysis of the C-terminal end of τ. Cells were resuspended in 30 mL of lysis buffer and passed through the French press three times to ensure all cells were lysed. The lysed cells were centrifuged at 10,000 rpm for 45 minutes at 4°C using a Beckman JLA 10.5 rotor. Supernatant was kept at 4°C and used for the following steps to further purify the clamp loader.

The clarified lysate supernatant was loaded onto two 5 mL HiTrap Heparin columns (GE Healthcare) that were linked together. The HiTrap Heparin column was prepped for the protein by washing it with 20 mM Tris-HCl pH 7.5, 0.5 mM EDTA, 5 mM DTT, and 10% glycerol for 5 column volumes, then washing it with the same buffer plus 1 M NaCl for 5 column volumes, then finally washing the column with the same buffer plus the NaCl concentration in the corresponding lysis buffer. A peristaltic pump (Pharmacia P-1) was used to load the lysed supernatant at 2 mL/min. Once all of the supernatant was loaded, the column was washed with lysis buffer for 5 column volumes. The heparin column was then moved to an ÄKTA purification system (GE Healthcare) where more lysis buffer was run through the column until the UV absorbance leveled out at the baseline. A protein purification method was created on the ÄKTA chromatography system that started out at the NaCl concentration in the corresponding lysis buffer and over 60 minutes would slowly rise to 500 mM NaCl at 2 mL/min collecting 1.3 mL fractions. Once the program was finished, a 12% SDS-PAGE gel was utilized to visualize the protein in each of the fractions to find the clamp loader complex. The γ-complex clamp loader elutes around 170 mM NaCl, τ-complex elutes around 350 mM NaCl, and holoenzyme elutes around 200 mM NaCl. Fractions to be kept were pooled together and dialyzed against 2 L of 20 mM Tris-HCl pH 7.5, 0.5 mM EDTA, 100 mM NaCl, 5 mM DTT, and 10% glycerol twice using a 12-14,000 molecular weight cut-off dialysis tubing. Protein was dialyzed overnight for at least 12 hours then the buffer was switched for fresh buffer and dialyzed for another 5 hours.

Second, an 8 mL MonoQ column (Pharmacia Biotech) was used to further purify the proteins and to remove any unincorporated subunits. The MonoQ column was

prepped for the protein in the same way the HiTrap Heparin was except that the final buffer on the column was 20 mM Tris-HCl pH 7.5, 0.5 mM EDTA, 5 mM DTT, 10% glycerol, and 100 mM NaCl. Protein from dialysis was loaded onto the column by using the sample pump on the ÄKTA purification system at a rate of 0.5 mL/min. Once all of the protein was loaded onto the column, the column was washed with loading buffer until the UV absorbance returned to the baseline. A protein purification method was created on the ÄKTA machine that started out 100 mM NaCl and over 96 minutes would slowly rise to 500 mM NaCl at 1 mL/min collecting 1mL fractions. Once the program was finished, a 12% SDS-PAGE gel was utilized to visualize the protein in each of the fractions to find the clamp loader complex. The γ-complex clamp loader elutes around 250 mM NaCl, τ-complex elutes around 300 mM NaCl, and holoenzyme elutes around 200 mM NaCl. Fractions to be kept were pooled together and dialyzed against two 2L of the corresponding storage buffer using a 12-14,000 molecular weight cut-off dialysis bag. Protein was dialyzed overnight for at least 12 hours then the buffer was switched for fresh buffer and dialyzed for another 5 hours.

Quantification of the clamp loader complexes was performed by measuring the absorbance at 280 nm in denaturing conditions (6 M guanidine-HCl). Concentration was determined by using Beer's law and the calculated extinction coefficients for the complexes. The extinction coefficient for the γ-complex clamp loader is 220,050 $M^{-1}$ $cm^{-1}$, for χ-less γ-complex is 191,330 $M^{-1}$ $cm^{-1}$, for τ-complex is 302,150 $M^{-1}$ $cm^{-1}$ based on the amino acid sequence (125). For holoenzyme, a Bio-Rad Bradford assay was performed to determine quantification based on the manufacturer's instructions (124). A final gel of the clamp loader complexes in shown in Figure 2-5.

**Size Exclusion Analysis of Clamp Loaders**

To determine the approximate molecular weight of the DnaX2016 subunits, clamp loaders, and wild-type clamp loader complexes, the proteins were run on a 24 mL Superose 12 10/300 GL size exclusion column (GE Healthcare). The column was calibrated by measuring elution volumes for a mixture of protein standards ranging in size from 1.37 to 670 kDa. Standard curves were created by plotting the log of the protein's molecular weights as a function of $K_{av}$, calculated by using Equation 2-1 where where $V_o$ = column void volume, $V_e$ = elution volume, and $V_c$ = geometric column volume.

$$K_{av} = \frac{V_e - V_o}{V_c - V_o} \quad (2\text{-}1)$$

The calculated standard curve is shown in Figure 2-6. Secondly, the clamp loader proteins were run on the column. Based on the volume it took the proteins to elute from the column and the calibration curve, the molecular weights of the proteins could be approximated. The elution profile for τ-complex is shown in Figure 2-6 and the calculated molecular weights for all of the proteins are shown in Table 4-2.

**Purification of SSBΔC8 and SSBΔC1**

Purification of wild-type SSB was performed by a former laboratory member. Purification of SSBΔC8 and SSBΔC1 was performed as previously described with some modifications (126). The pEAW393 vector containing SSBΔC8 was a gift from the laboratory of Dr. Mike Cox and the pET21a vector containing SSBΔC1 was graciously provided by the laboratory of Dr. James Keck.

Expression vectors were transformed into BL21(DE3)pLysS cells (ThermoFisher) and grown overnight at 37°C on LB media plates with Amp to select for the expression

vectors and Cm for selection of the BL21(DE3)pLysS cells. The plates were incubated at 37°C overnight. One colony was used to inoculate 10 mL of LB media with Amp and Cm which was incubated in a 37°C shaker for 4 hours. This starter culture was stored in 4°C overnight. The next day, the 8 mL of the starter culture was centrifuged at 7000 x g for 5 minutes and the supernatant was decanted. Culture pellets were resuspended in fresh LB media with Amp and Cm and used to inoculate 2 L of LB media with Amp and Cm. These cultures were grown up until the $OD_{600}$ was 0.7-0.8. Expression of the SSB was induced with the addition of IPTG to a final concentration of 1 mM. Protein expression continued for 3 hours then the flasks were placed on ice until it cooled to 4°C. The bacterial cultures were pelleted by centrifugation at 5200 rpm for 30 min at 4°C using a Beckman JA 20 rotor. Liquid media was removed and the pellets were stored at -80°C.

Isolation of SSB began with lysing the cells using a French Press. Cells were resuspended in 30 mL lysis buffer (50 mM Tris pH 7.5, 0.5 mM EDTA, 200 mM NaCl, 15 mM spermidine, 10% sucrose, and 1 mM PMSF) and passed through the French press 3 times to ensure complete lysis. The lysed cells were centrifuged at 10000 rpm for 45 minutes at 4°C using a Beckman JLA 10.5 rotor. Supernatant was kept at 4°C and used for the following steps to further purify SSB.

The next step in the purification was ammonium sulfate precipitation. Precipitation of SSB was done by slowly adding 0.24g/mL ammonium sulfate to the cleared lysate over the course of 45 minutes. The ammonium sulfate solution was allowed to precipitate for an additional 90 minutes then was centrifuged at 16,000rpm at 4°C for 30 minutes using a Beckman JLA 10.5 rotor. Then the SSB-containing pellet

was washed by addition buffer with 0.15g/mL ammonium sulfate and mixing for 60 min to remove impurities. The mixture was then centrifuged again as before. Finally, the pellet was washed by adding buffer containing 0.13g/mL and mixed for 60min to remove impurities. The mixture was then centrifuged as before. The final pellet was dissolved in 20mM Tris-HCl pH 7.5, 0.5mM EDTA, 5mM DTT, 200mM NaCl, and 10% glycerol and dialyzed against two 2L of the same buffer using 3,500 MWCO dialysis tubing.

The final sample from the ammonium sulfate precipitation step was loaded onto two 5 mL HiTrap Heparin columns that were joined together. The HiTrap Heparin column was prepped for the protein by washing it with 20 mM Tris-HCl pH 7.5, 0.5 mM EDTA, 5 mM DTT, and 10% glycerol for 5 column volumes, followed by 5 column volumes of the same buffer plus 1M NaCl, and finally washing the column with the same buffer plus 150 mM NaCl. The final sample from the ammonium sulfate step was diluted drop wise with buffer to 150 mM NaCl. A peristaltic pump (Pharmacia P-1) was used to load the lysed supernatant at 2mL/min. Once all of the supernatant was loaded, buffer with 150mM NaCl was run through the column at the same rate for 5 column volumes. The heparin column was then moved to an ÄKTA purification system (GE Healthcare) where more buffer was run through the column until the UV absorbance leveled out at the baseline. A protein purification method was created on the ÄKTA machine that started out at 150mM NaCl and over 60 minutes would rise to 500mM NaCl at 2mL/min collecting 1.3mL fractions. Once the program was finished, a 12% SDS-PAGE gel was utilized to visualize the proteins from fractions corresponding to UV peaks on the chromatogram to find the clamp loader complex. SSB$\Delta$C8 eluted around 380mM NaCl and SSB$\Delta$C1 eluted around 200 mM NaCl. Fractions to be kept were pooled together

and dialyzed against two 2L of 20mM Tris-HCl pH 7.5, 0.5mM EDTA, 200mM NaCl, 5mM DTT, and 10% glycerol using a 3,500 MWCO dialysis bag. Protein was dialyzed overnight for at least 12 hours then the buffer was switched for fresh buffer and dialyzed for another 5 hours.

Lastly, pooled fractions containing SSB were purified by anion exchange chromatography using an 8-mL MonoQ column. The MonoQ column was prepped for the protein in the same way the HiTrap Heparin was. Protein from dialysis was loaded onto the column by using the sample pump on the ÄKTA purification system at a rate of 0.5mL/min. Once all of the protein was loaded onto the column, the column was washed with loading buffer until the UV absorbance returned to the baseline. A protein purification method was created on the ÄKTA machine that started out 150mM NaCl and over 96 minutes would rise to 500mM NaCl at 1mL/min collecting 1mL fractions. Once the program was finished, a 12% SDS-PAGE gel was utilized to visualize the protein corresponding to UV absorbance seen on the chromatogram to find the clamp loader complex. SSBΔC8 eluted around 380mM NaCl and SSBΔC1 eluted around 310 mM NaCl. Fractions to be kept were pooled together and dialyzed twice against 2 L of the corresponding storage buffer using a 12-14,000 MWCO dialysis bag. Protein was dialyzed overnight for at least 12 hours then the buffer was switched for fresh buffer and dialyzed for another 5 hours.

Quantification of all SSB variants was performed using the Bio-Rad Bradford assay according to the manufacturer's instructions (124). BSA standards were used to create a standard curve. SSB was stores in -80°C. A final gel of the SSB mutants in shown in Figure 2-7.

**Purification of β Sliding Clamps**

Purification of the β sliding clamps was performed as previously described with some modifications. The wild-type β gene, *dnaN,* had previously been cloned into pET15b expression vector by a former lab member. SDM was used to create the different mutants (Table 2-1). Purification of all forms of β clamp was performed the same way, which follow a purification method previously described with a few modifications (85, 127).

For expression of β, the pET15b vector was transformed into BL21(DE3) cells and grown overnight at 37°C on LB media plates with Amp antibiotic for selection. One colony was used to inoculate 10mL of LB media with Amp which was incubated in a 37°C shaker for 4 hours. This starter culture was stored at 4°C overnight. The next day, the 4mL of the starter culture was centrifuged at 7000 x g for 5 minutes and the supernatant was decanted. Culture pellets were resuspended in fresh LB media with Amp and used to inoculate 1L of LB media with Amp. The culture was grown up until the $OD_{600}$ was 0.7-0.8. Expression of the sliding clamp was induced by the addition of IPTG to a final concentration of 1mM. Protein expression continued for 3 hours and expression/growth was stopped by cooling to 4°C. The bacterial culture was pelleted by centrifugation at 5,200rpm for 30 min at 4°C using a Beckman JA 20 rotor. Liquid media was removed and the pellets were stored at -80°C.

The first step of the β purification was lysis using a French press 3 times in 30 mL buffer containing 20mM Tris pH 7.5, 0.5mM EDTA, 50mM NaCl, 5mM DTT and 10% glycerol. Cell lysate was clarified by centrifugation at 10,000rpm for 45 minutes at 4°C

using a Beckman JLA 10.5 rotor. Supernatant was kept at 4°C and used for the following steps to further purify the clamp loader.

The next step in the purification was ammonium sulfate precipitation. Precipitation of β was done by slowly adding 0.19g/mL ammonium sulfate to the cleared lysate over the course of 45 minutes followed by mixing for additional 90 minutes and centrifugation at 16,000rpm at 4°C for 30 minutes using a JLA 10.5 rotor. The pellet was discarded and 0.218g/mL ammonium sulfate was added to the supernatant that contained β over 45 minutes and protein was allowed to precipitate for 60 min. The mixture was then centrifuged again as before. The supernatant was discarded and the final pellet containing β was dissolved in 20mM Tris-HCl pH 7.5, 0.5mM EDTA, 5mM DTT, 50mM NaCl, and 10% glycerol and dialyzed twice against 2 L of the same buffer using 12,000-14,000 MWCO dialysis tubing.

Next, the sample from ammonium sulfate precipitation was loaded onto two 5mL HiTrap Q columns that were joined together. The HiTrap Q column was prepped for the protein by washing it with 20 mM Tris-HCl pH 7.5, 0.5 mM EDTA, 5 mM DTT, and 10% glycerol for 5 column volumes, then washing it with the same buffer plus 1 M NaCl for 5 column volumes, then finally washing the column with the same buffer plus 50 mM NaCl. A peristaltic pump (Pharmacia P-1) was used to load the lysed supernatant at 2 mL/min. Once all of the sample from ammonium sulfate precipitation was loaded, buffer with 50 mM NaCl was run through the column at the same rate for 5 column volumes. The HiTrap Q column was then moved to an ÄKTA purification system (GE Healthcare) where the column was washed with the same buffer until the UV absorbance leveled out at the baseline. A protein purification method was created on the ÄKTA machine

that started out at 50mM NaCl and increased to 500 mM NaCl over 60 minutes at 2mL/min collecting 1.3mL fractions. Once the program was finished, a 12% SDS-PAGE gel was utilized to visualize the protein in fractions corresponding to UV absorbance on the chromatogram to find the clamp loader complex. Wild-type and β mutants eluted off the column around 225 mM NaCl. Fractions containing the purest β subunits were pooled together and dialyzed twice against 2 L of 10 mM sodium acetate pH 7.5, and 0.5mM EDTA using 12,000-14,000 MWCO dialysis tubing. Protein was dialyzed overnight for at least 12 hours then the buffer was switched for fresh buffer and dialyzed for another 5 hours.

The dialyzed β solution was loaded onto two 5 mL HiTrap Heparin columns that were linked together. These HiTrap Heparin columns were prepped for the protein by washing it with 10mM sodium acetate pH 7.5, and 0.5 mM EDTA for 5 column volumes, then washing it with the same buffer plus 1 M NaCl for 5 column volumes, then finally washing the column with the same buffer with no NaCl. Protein from dialysis was loaded onto the column by using the sample pump on the ÄKTA purification system at a rate of 0.5 mL/min. At pH 7.5, β does not bind to the column but contaminating proteins do, which are left behind. Once all of β eluted off of the column, the column was washed with buffer until all of the β came off the column, indicated by the UV absorbance returning to baseline. The HiTrap Heparin column was regenerated as before but with 10 mM sodium acetate pH 6, and 0.5 mM EDTA. While the column was regenerating, the β solution pH was changed to pH 6 using 20mM acetic acid at 4°C. A protein purification method was created on the ÄKTA machine that started out at 0mM NaCl and over 60 minutes would slowly rise to 500mM NaCl at 2mL/min collecting 1.3mL

fractions. Once the program was finished, a 12% SDS-PAGE gel was utilized to visualize the protein in each of the fractions to find the sliding clamp. All versions of β eluted off the column around 300mM NaCl. Fractions to be kept were pooled together and dialyzed against two 2L of β storage buffer using a 12,000-14,000 MWCO dialysis bag. Protein was dialyzed overnight for at least 12 hours then the buffer was switched for fresh buffer and dialyzed for another 5 hours.

Quantification of β sliding clamp was performed by measuring absorbance in denaturing conditions at 280nm. The extinction coefficient for the β clamp was calculated to be 14,700 $M^{-1}cm^{-1}$ in 6 M guanidine-HCl (127). A final gel of the β-S109C/Q299C/R103S sliding clamp in shown in Figure 2-8.

**Modified β Sliding Clamp Fluorescence Labeling**

Labeling of the β sliding clamps with fluorophores was performed as previously described with some modifications (128). The sliding clamps were either labeled with tetramethylrhodamine-5-maleimide (TMR) or Alexa Fluor 488 C5 maleimide (AF488) (ThermoFisher). Fluorophores were introduced in site specific manner by changing exposed cysteine residues (C260 and C333) to serine through SDM to prevent unwanted labeling. In addition, mutations were made to residues near each other at the interface (I305/R103 or S109/Q299) in order to change them to cysteines, allowing selective labeling of these sites with the fluorophores.

To begin labeling, 2 mg of β sliding clamp was thawed and dialyzed against 2 L of 50 mM potassium phosphate at pH 7.5 overnight. Dialyzed clamp was treated with fresh 50 mM TCEP and heated at 37°C for 5 minutes to reduce possible disulfide bonds between the interfaces of the clamp. The fluorophores were dissolved in 8% DMSO and

incubated at 37°C for 5 minutes. For the labeling reactions, 20-fold excess of fluorophores per cysteine to be labeled was used. The fluorophores were added drop-wise to the β solution and the labeling reaction was incubated at room temperature for 2 hours covered from the light. The reaction was placed at 4°C overnight. The rest of the purification was carried out at 4°C in the dark.

To remove unincorporated fluorophores, the labeling reaction was loaded onto hand-packed BioRad P6 desalting (6,000 MWCO) resin in an 88 mL flex-column (ThermoFisher). The fluorophore-bound sliding clamps eluted in the void volume of the column, while the excess fluorophores eluted much later. Fractions containing fluorophore-labeled protein were then loaded onto a 1 mL HiTrap Q (GE Healthcare) to further purify the labeled proteins. Regeneration of the column was performed as described in the protein purification section. The final wash of the column left the column in 20 mM Tris-HCl pH 7.5, 0.5 mM EDTA, and 10% glycerol. Labeled β sliding clamp was loaded onto the column at 0.5mL/min followed by 30 mL of 20 mM Tris-HCl pH 7.5, 0.5 mM EDTA, 10% glycerol, and 100 mM NaCl to wash off excess fluorophore. A protein purification method was created on the ÄKTA machine that started out at 100 mM NaCl and over 24 minutes would rise to 500 mM NaCl at 0.5 mL/min collecting 0.3 mL fractions. Often proteins are separated based on the degree of labeling (beta is a homodimer with equivalent sites in each monomer). When the program was finished, the fractions that contained only the protein at the very peak of the chromatogram measured by absorbance at 280 nm was pooled for dialysis. The labeled β sliding clamp was dialyzed twice against 2 L of 20mM Tris-HCl pH 7.5, 0.5mM EDTA, and 10% glycerol.

Quantification of the labeled β sliding clamp was done by performing a Bradford Assay (BioRad) as the manufacturer's instructions detailed (124). Unlabeled β sliding clamp that was quantified by denatured A280 was used to create the standard curve for the Bradford assay. To determine the percentage of the β clamp that had been labeled, an absorbance scan from 650-250nm in 6M guanidine-HCl was performed using a spectrophotometer. The absorbance at the peak of the scan was used in Beer's Law to calculate the concentration of fluorophore. The extinction coefficients of the fluorophores reported by the manufacturer were 74,000 $M^{-1}cm^{-1}$ for AF488 in 50 mM potassium phosphate buffer and 95,000 $M^{-1}cm^{-1}$ for TMR in methanol (ThermoFisher). To calculate a corrected extinction coefficient of the fluorophores in 6 M guanidine, the fluorophore absorbance was measured in 6 M guanidine-HCl and in 50 mM potassium phosphate or methanol, and the ratio of absorbance in guanidine to potassium phosphate/methanol was multiplied by the extinction coefficient reported by the manufacturer. The corrected extinction coefficient for in 6 M guanidine-HCl was calculated to be 77,000 $M^{-1}cm^{-1}$ for AF488 and for 98,000 $M^{-1}cm^{-1}$ TMR. These corrected extinction coefficients were used to calculate the concentration of the fluorophore. The concentration of fluorophore was divided by the concentration cysteine residues to determine the percent labeled. On average, β clamp labeled with AF488 yielded 90-100% labeled and 70% for TMR.

**Fluorescence-Based Equilibrium Assays**

Fluorescence equilibrium measurements were performed using a QuantaMaster QM-1 Spectrofluorometer (Photon Technology International). Reagents were mixed in a

1 cm quartz cuvette (Hellma) to a final volume of 80μL for approximately 30s before readings were taken at room temperature. Data was analyzed using KaleidaGraph.

**β Binding and Opening Assay**

To determine the apparent dissociation constant ($K_{d,app}$) for γ-complex and β sliding clamp, fluorescence emission of β-AF488 was measured at different γ-complex concentrations. Measurements were performed as time-based scans to ensure that the system had reached equilibrium. For these scans, β-AF488 was excited at 495 nm and emission measured at 520 nm using a 3 nm bandpass. Data was collected at 1 s intervals for 2 min for assays in 50 mM NaCl and at 1 s intervals for 4 min in assays with 500 mM NaCl, and the last 30 s were averaged to obtain a value for the fluorescence intensity. Final protein concentrations for the reactions were 10 nM of β-S109C/Q299C-$(AF488)_2$ or β-R103S-$(AF488)_2$ and 0.1 to 1000 nM γ-complex. Each reaction occurred by sequentially adding to the cuvette assay buffer (64 μL) to measure background signal, β-$(AF488)_2$ (8 μL) to measure the signal for unbound β, and γ-complex (8 μL) to measure the signal for complex formation.

To calculate the relative AF488 intensity at each γ-complex concentration, the fluorescence for the β/γ-complex was divided by the fluorescence of unbound β-$(AF488)_2$ (before adding γ-complex). The $K_{d,app}$ was calculated by fitting the data to Equation 2-2, where $\gamma_o$ is the total concentration of γ-complex, $\beta_o$ is the total concentration of β, $I_{max}$ is the maximum intensity, and $I_{min}$ is the minimum intensity.

$$I_{obs}(\gamma_{cx}) = \frac{(\gamma_o + \beta_o + K_{d,app}) - \sqrt{(\gamma_o + \beta_o + K_{d,app})^2 - 4\gamma_o\beta_o}}{2\beta_o}(I_{max} - I_{min}) + I_{min} \quad (2\text{-}2)$$

**Anisotropy DNA Binding Assay**

DNA binding by SSB was measured by anisotropy using the DNA-RhX (Rhodamine X isothiocyanate) sequence in Table 2-2. The DNA-RhX (made by former member of the laboratory) samples were excited at 580nm and emission was measured at 605 nm for 30 seconds with an 8 nm bandpass. Glan-Thompson polarizers were used to polarize both the excitation and emission light in the vertical and horizontal planes. Four different emission measurements were made; a vertical and horizontal emission reading with the excitation light polarized vertically ($I_{VV}$ and $I_{VH}$) and a vertical and horizontal emission reading with the excitation light polarized horizontally ($I_{HV}$ and $I_{HH}$).

To measure polarized intensities and calculate anisotropy changes from SSB binding to DNA, three different emission scans were done. First, an emission scan in all 4 orientations was performed on the assay buffer and ATP. Second, the DNA-RhX was added to the reaction and scans were performed in all 4 orientations. Finally, the SSB was added to the reaction and emission of light polarized vertically were measured. Final reagent concentrations were 50nM DNA-RhX, 500μM ATP, and varying concentrations of SSB.

To calculate the anisotropy values from the data, a correction factor known as the g factor was first calculated using Equation 2-3.

$$g = \frac{I_{HV(DNA)} - I_{HV(buffer)}}{I_{HH(DNA)} - I_{HH(buffer)}} \quad (2\text{-}3)$$

This g factor was then used to calculate the anisotropy (r) for the different SSB concentrations (Equation 2-4).

$$r = \frac{\left(I_{VV} - I_{VV(buffer)}\right) - g\left(I_{VH} - I_{VH(buffer)}\right)}{\left(I_{VV} - I_{VV(buffer)}\right) + 2g\left(I_{VH} - I_{VH(buffer)}\right)} \quad (2\text{-}4)$$

To determine the $K_d$ value, the anisotropy was plotted as a function of SSB concentration. Equation 2-5 was used, where SSB is the total SSB concentration, DNA is the total DNA concentration, $I_{max}$ is the maximum anisotropy, and $I_{min}$ is the minimum anisotropy.

$$I_{obs}(\mathrm{SSB}) = \frac{(SSB + \mathrm{DNA} + K_d) - \sqrt{(SSB + \mathrm{DNA} + K_d)^2 - 4(DNA)(SSB)}}{2\mathrm{DNA}}(I_{max} - I_{min}) + I_{min} \quad (2\text{-}5)$$

**Fluorescence-Based Pre-Steady State Kinetic Assays**

Pre-steady state reactions were measured at 20°C using an Applied Photophysics SX20MV stopped-flow fluorimeter, which quickly mixes reagents together and begins measuring fluorescence intensity on a millisecond timescale. The reactions were performed in either single or sequential mixing mode. In single mixing, reagents in two syringes are mixed together and the fluorescence reading begins immediately. Clamp opening, dissociation, and closing reactions (where noted) were performed as single mix experiments. In sequential mixing, reagents in two syringes are mixed together in a mixing chamber for a 4 s and then that solution is mixed with reagents in a third syringe, where the fluorescence reading begins. Clamp release, clamp closing (where noted), and ATP hydrolysis reactions were performed as sequential mix experiments. Assays were performed in with all room lights turned off to prevent photobleaching of the fluorophores. Data files were converted to ASCII files and KaleidaGraph was used to analyze data and calculate observed rates. Relative intensity was calculated by dividing the observed signal by the starting signal. Data normalized between 0 and 1 was calculated by dividing the maximum intensity minus the minimum

intensity by the observed intensity minus the minimum intensity. For experiments in which the reaction did not complete within the time measured, the data was normalized using the signal of β-AF488$_2$ as the minimum intensity. For concentration dependent experiments, the calculated observed rates were plotted versus the concentration of substrate and the data was fit to a rectangular hyperbola formula (Equation 2-6) to yield the maximum rate ($k_{max}$) and the concentration of substrate to reach half the $k_{max}$ ($K_{0.5}$).

$$v = \frac{k_{max}\,[S]}{K_{0.5} + [S]} \tag{2-6}$$

For the opening, dissociation, and closing reactions, either β-R103C/I305C or β-S109C/Q299C (both with C260S/C333S background mutations) labeled with AF488 or TMR at two sites per monomer was used. These doubly labeled β sliding clamps have low fluorescence when closed due to quenching of the fluorophores by one another. When the clamp loader is added and the clamp opens, the two fluorophores separate and there is an increase in fluorescence. AF488 was excited at 490 nm using a 3.7 nm bandpass and emission was measured using a 515 nm cut-on filter, and steady-state AF488 fluorescence was measured on a millisecond timescale. For experiments with a TMR labeled clamp, TMR was excited at 550 nm using a 3.7 nm bandpass and emission was measured using a 570 nm cut-on filter.

**β Opening Reactions**

Clamp loader-clamp binding/opening was measured in single mix experiments by mixing a solution containing clamp loader and ATP with a solution containing β-R103C/I305C-AF488$_2$ and ATP (Figure 2-9). Final concentrations of clamp loader varied and β was held constant at 20 nM. Fluorescence measurements were made at 1 ms intervals for 10 s. Reaction time courses were initially fit empirically to sums of

exponentials to calculate rates of reactions. Time-dependent changes in intensity for clamp binding/opening reactions were fit to a double exponential increase (Equation 2-7) where $k_{fast}$ and $k_{slow}$ are rates and $a_{fast}$ and $a_{slow}$ are amplitudes of the two reaction phases, t is time, and c is a constant.

$$I(t) = a_{fast}(1 - e^{-k_{fast}t}) + a_{slow}(1 - e^{-k_{slow}t}) + c \quad (2\text{-}7)$$

**β Binding Assay**

Binding of the sliding clamp by the clamp loader was measured using the singly labeled β-S109C-AF488 (with C260S and C333S background mutations). The binding reaction was performed in the same manner as the opening assay. Time-dependent changes in intensity for clamp loader-clamp binding were fit to a double exponential decay (Equation 2-8) where $k_{fast}$ and $k_{slow}$ are rates and $a_{fast}$ and $a_{slow}$ are amplitudes of the two reaction phases, t is time, and c is a constant.

$$I(t) = a_{fast}(e^{-k_{fast}t}) + a_{slow}(e^{-k_{slow}t}) + c \quad (2\text{-}8)$$

**β-Clamp Loader Dissociation Assay**

Clamp loader-clamp dissociation was measured by a mixing a solution of γ complex, β-R103C/I305C-AF488$_2$, and ATP with a solution containing 20-fold excess unlabeled β (Figure 2-10). Final protein concentrations were 40 nM γ-complex, 20 nM β-AF488, and 400 nM unlabeled β. Split time-base measurement was used in which data was collected at 1 ms intervals for the first 10 s and 50 ms intervals for the remaining time (to 500 s). Time-dependent changes in intensity for clamp loader-clamp binding were fit to a double exponential decay formula (Equation 2-8).

### β Closing Reactions

Sliding clamp closing around DNA was measured by addition of a solution containing γ complex, β, and ATP to a solution of DNA, SSB, and excess unlabeled clamp to limit the reaction to one turnover (Figure 2-11). Final protein concentrations were 20 nM γ-complex, 20 nM β-AF488, and 200 nM unlabeled β. Final DNA concentration was varied and 3-fold excess SSB per single-stranded overhang of DNA was used. Measurements were made at 1 ms intervals for 10 s. Time-dependent changes in intensity for clamp loader-clamp dissociation were fit to a double exponential decay formula (Equation 2-8). or a single exponential decay formula (Equation 2-9).

$$I(t) = a(e^{-k_{fast}t}) + c \quad (2\text{-}9)$$

### ATP Hydrolysis Assay

ATP hydrolysis by the clamp loader was measured using 7-diethylamino-3-((((2-maleimidyl)ethyl)amino)carbonyl)coumarin (MDCC, ThermoFisher) labeled phosphate-binding protein (PBP) that had been previously purified and labeled by a former lab member (129). When the clamp loader hydrolyzes ATP into ADP and $P_i$, the $P_i$ binds to PBP causing an increase in the MDCC fluorescence (Figure 2-12). Due to the presence of free $P_i$ which may affect the measurements, the stopped-flow and all solutions used were incubated at room temperature for 45 minutes with 168μM 7-methyl guanosine (MeG, Santa Cruz) and 0.2 U/mL polynucleotide phosphorylase (PNPase, Sigma) before the experiment. PNPase phosphorylates MeG, removing any access $P_i$ in the solutions. During the experiment, MDCC was excited at 425nm and emission was measured with a 455nm cut-on filter. Final protein concentrations were 200nM γ-complex, 200nM β, and 2μM PBP. Final DNA concentration was 400nM and 3-fold

excess SSB per single-stranded overhang of DNA was used when noted. Control reactions that had no ATP were measured to get a signal for unbound MDCC-PBP. Data was converted to the fraction MDCC-PBP bound to Pi by subtracting free MDCC-PBP signal from the observed signal and dividing that by the difference of the completely saturated MDCC-PBP signal and the free MDCC-PBP signal. The fraction MDCC-PBP/$P_i$ was converted to the concentration of MDCC-PBP/$P_i$ by multiplying the fraction MDCC-PBP/$P_i$ bound by the total MDCC-PBP concentration. This was then divided by the total clamp loader concentration to determine the number of Pi release for each clamp loader complex.

### β Release Reactions

To measure the release of the sliding clamp by the clamp loader after closing, purified and labeled β-Q299C-Pyrene (with C260S/C333S background mutations) was used, which was purified by a former lab member. Pyrene was excited at 345 nm and emission was measured with a 365 nm cut-on filter. Final protein concentrations were 20 nM γ-complex, 20 nM β-Q299C-Pyrene, and 200 nM unlabeled β. Final DNA concentration was 40 nM and final ATP concentration was 0.5mM. Time-dependent changes in intensity for clamp loader-clamp dissociation were fit to a double exponential decay formula (Equation 2-8).

## Kinetic Modeling Using Kintek Explorer

Time courses from clamp binding using β-S109C-AF488 and clamp opening using β-R103C/I305C-$(AF488)_2$ were globally fit to kinetic models using KinTek Explorer and rate constants were calculated (Figure 3-10 and 11) (130, 131). For binding reactions, $\gamma_{cx}$ concentrations ranged from 10 to 1280 nM and β-S109C-AF488 was held

constant at 20 nM. For clamp opening reactions, $\gamma_{cx}$ concentrations ranged from 5 to 1800 nM and β-R103C/I305C-$(AF488)_2$ was held constant at 16 nM. For the binding reactions with β-S109C-AF488, three fluorescent states were assumed, one for free/unbound clamps, one for clamp loader-clamp complexes in a closed conformation, and one for all clamp loader-clamp complexes in an open conformation. Low $\gamma_{cx}$ concentration data could be fit using two fluorescent states one for unbound clamps and one for all clamp loader-clamp complexes, but at higher concentrations this two-state model did not fit the data well because the fluorescence decay of the calculated curves tended to be faster than for the data. Relative fluorescence intensities of intermediate states were fit as adjustable parameters but did not change significantly from our initial relative intensity estimates (based on exponential fits) of 1.0 for free clamps, 0.9 for the closed clamp loader-clamp complex and 0.88 for open clamp loader-clamp complexes. For the clamp opening reactions with β-R103C/I305C-$(AF488)_2$, two fluorescent states were assumed, one relative intensity associated with closed clamps and another associated with open clamps. The relative intensities were fit as adjustable parameters but did not vary significantly from our estimates, based on exponential fits of the data, of 1.0 for closed clamps and 2.8 for closed clamps.

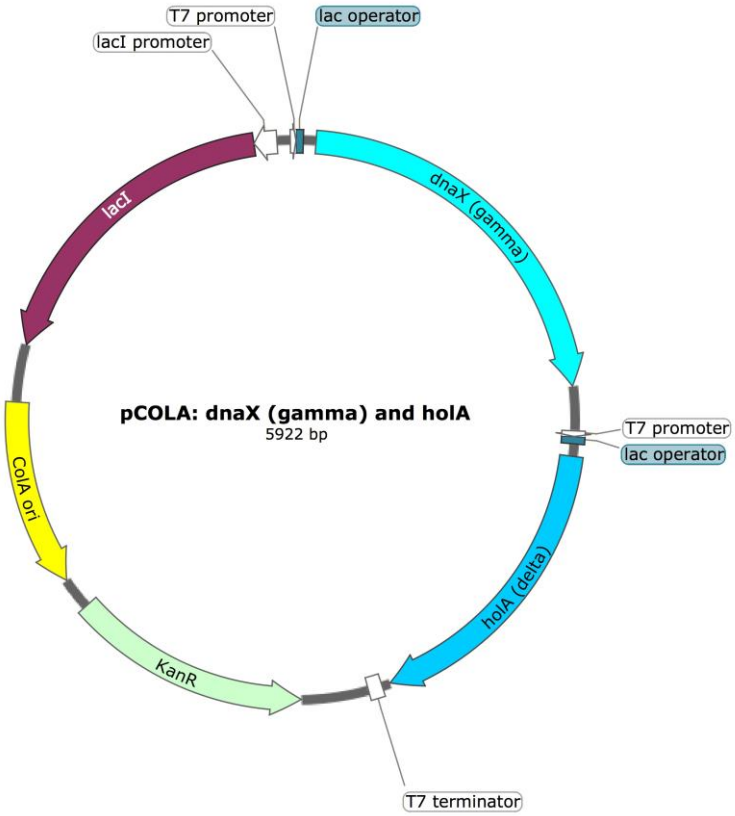


Figure 2-1. A representative map of the pCOLADuet-DnaX-HolA expression vector made using SnapGene. The *dnaX* gene was subcloned into the MCS1 site using NcoI and BamHI restriction sites. The *holA* gene was subcloned into the MCS2 site using NdeI and AvrII. This map is with the γ-only version of *dnaX.* A τ-only version was made as well.

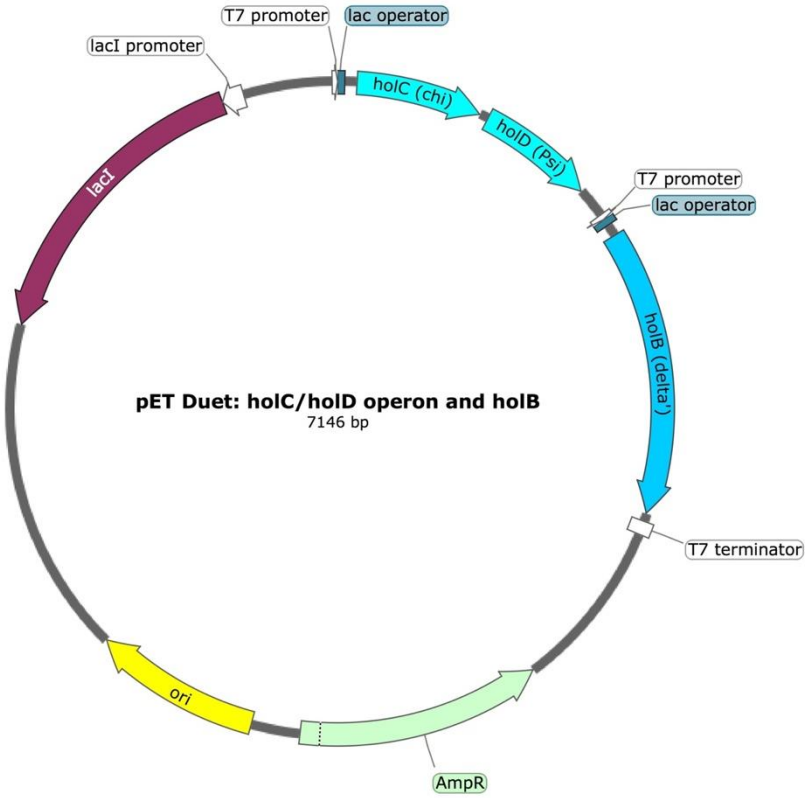


Figure 2-2. Representative map of the pETDuet-HolC-HolD-HolB expression vector made using SnapGene. The *holC/holD* operon or the *holC* only gene was subcloned into the MCS1 site using NcoI and BamHI restriction sites. The *holB* gene was subcloned into the MCS2 site using NdeI and AvrII.

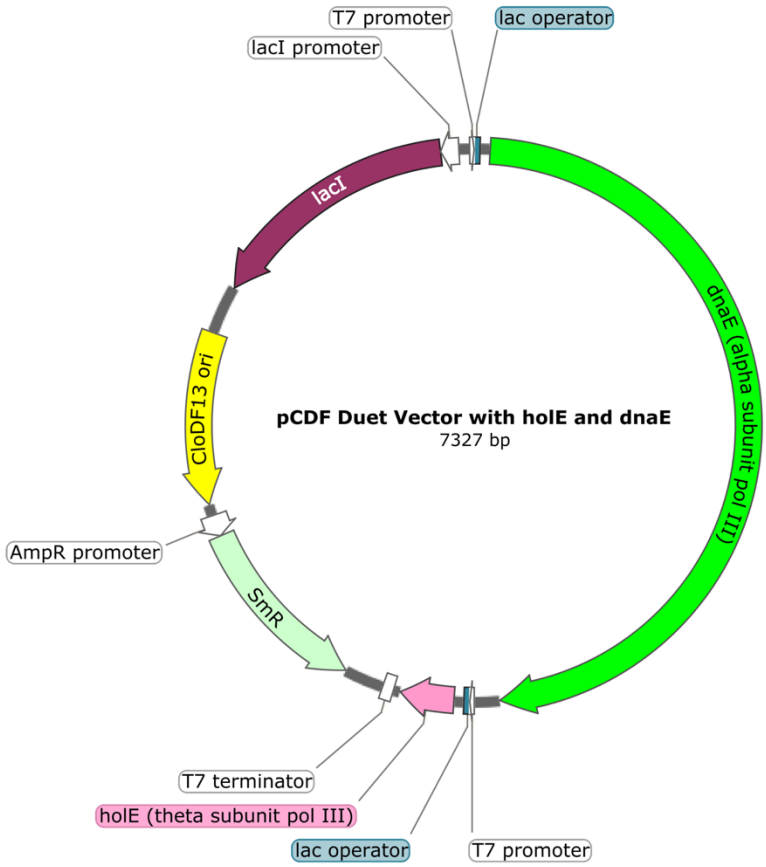


Figure 2-3. Representative map of the pCDF-DnaE-HolE expression vector made using SnapGene. MCS1 contained *dnaE* between NcoI and BamHI MCS2 contained *holE* between NdeI and AvrII..

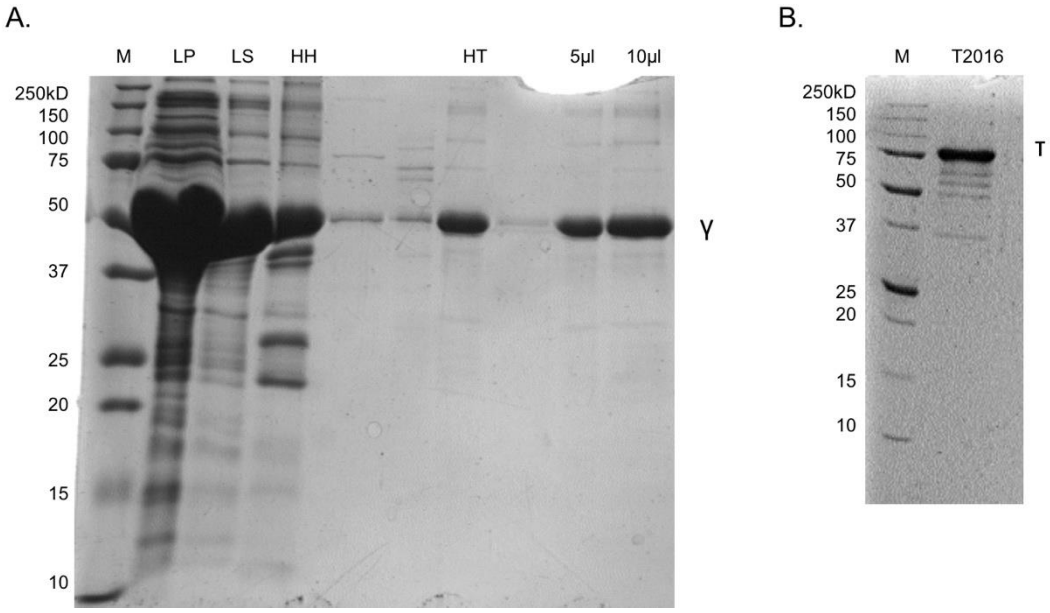


Figure 2-4. DnaX2016 subunit purification. A) SDS-PAGE showing the representative purification steps of the γ DnaX2016. The left lane (M) is the BioRad unstained protein standard marker. The next lanes are the soluble DnaX2016 γ subunit in the lysed supernatant (LS) and the insoluble protein in the lysed pellet (LP) after lysis with French Press. The following lanes are of the γ-complex clamp loader after HiTrap Heparin (HH) and HisTrap (HT) columns, and the final dialyzed product (5µl and 10µl). B) The left lane is the marker, then the final dialyzed DNaX2016 τ subunit (T2016).

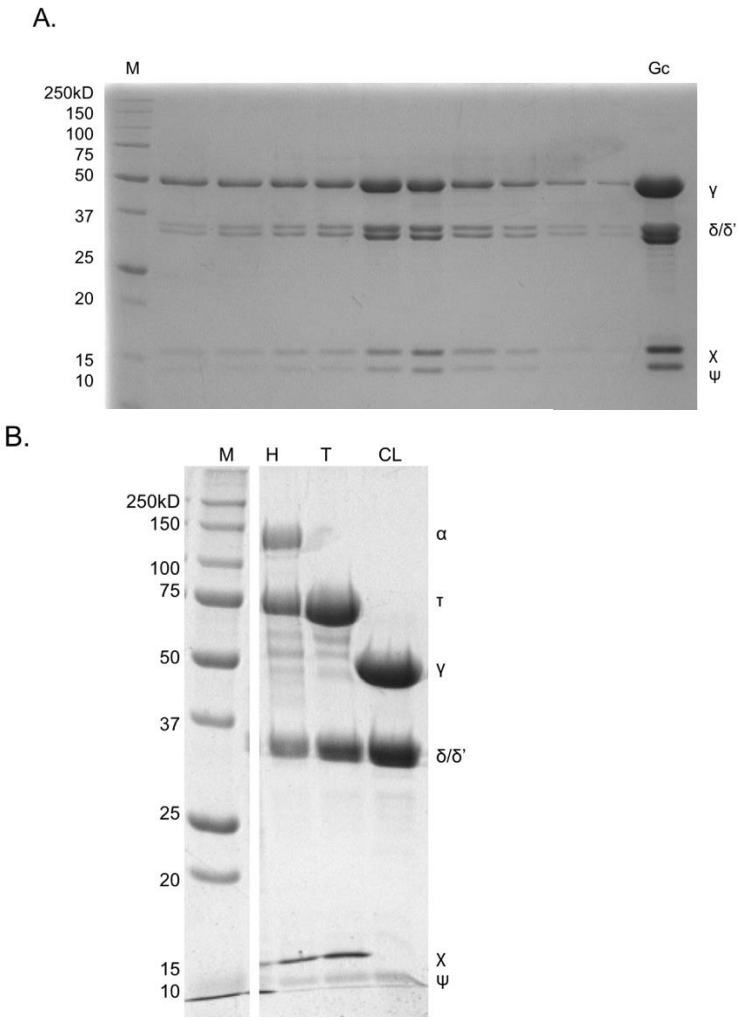


Figure 2-5. SDS Page showing the purification of different clamp loader variants using the Duet vector system. A) SDS-Page of the representative purification steps of the clamp loader using γ-complex clamp loader. The left lane (M) is the BioRad unstained protein standard marker. The next 10 lanes are fractions of γ-complex clamp loader separated by chromatography on a MonoQ column, and the last lane is the final dialyzed product (Gc). B) The left lane is the marker, then the final dialyzed holoenzyme, (H), τ-complex clamp loader (T), and χ-less γ-complex clamp loader (CL). Each subunit of the clamp loaders are marked in the figure.

A.

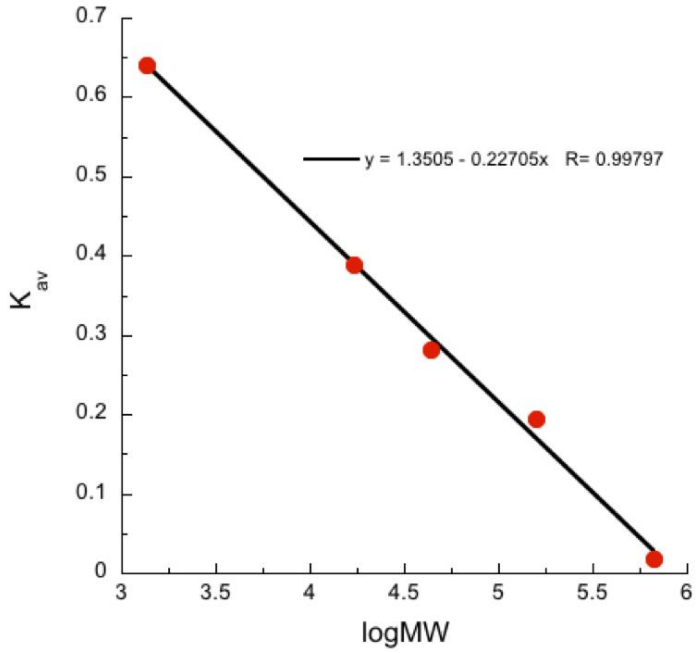


B.

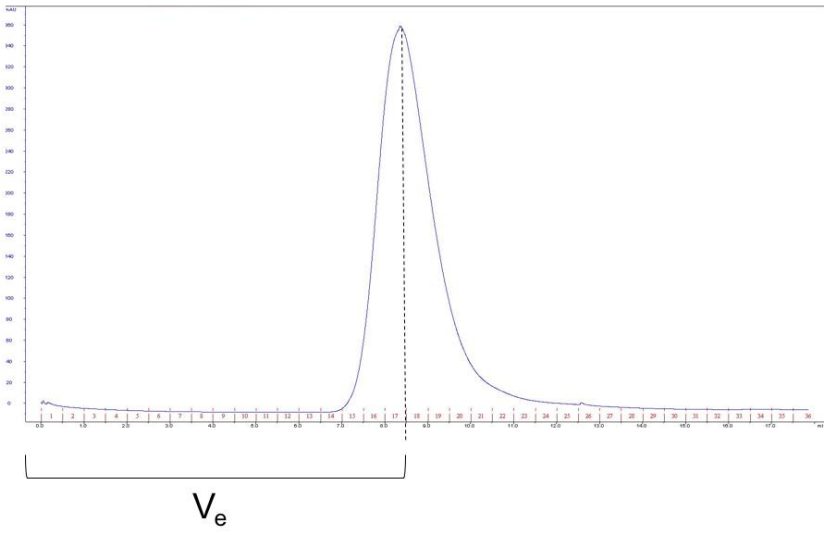


Figure 2-6. Size exclusion analysis of the clamp loaders. A) Size exclusion standard curve created by plotting the log of the BioRad protein standards molecular weight as a function of the $K_{av}$ of the protein determined by running them on a Superose 12 10/300 GL size exclusion column. A linear fit in KaleidaGraph was applied, which gave an equation to determine the size of the clamp loader proteins based off of their elution volume ($V_e$). B) An example run of a protein sample on the size exlcusion column. This is a chromatogram of the DnaX τ clamp loader complex on size exclusion column.

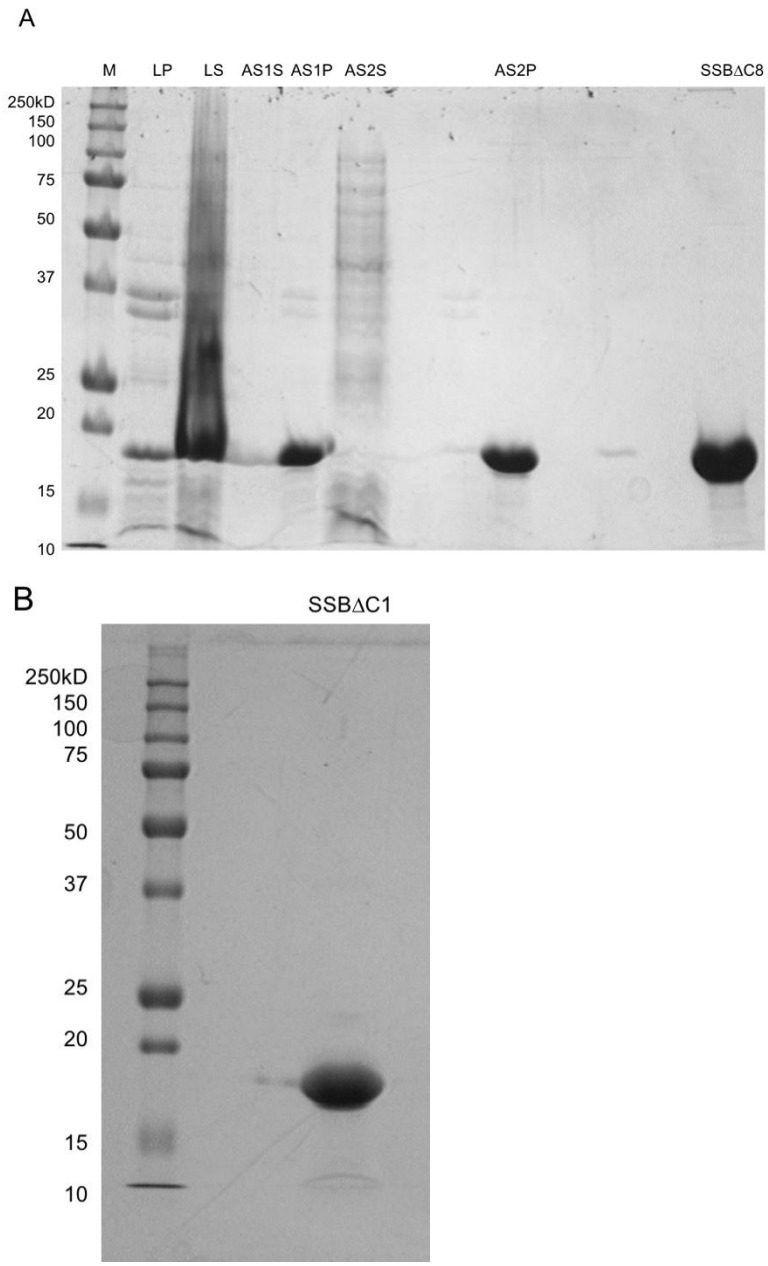


Figure 2-7. SDS PAGE gel of the SSB mutant purification. A) The representative purification steps of SSBΔC8. The left lane (M) is the BioRad unstained protein standard marker. The next lanes are the lysed pellet (LP), lysed supernatant (LS), ammonium sulfate1 supernatant (AS1S), ammonium sulfate 1 pellet (AS1P), ammonium sulfate 2 supernatant (AS2S), ammonium sulfate 2 pellet (AS2P), and the post-HiHeparin and MonoQ purified protein (SSBΔC8). B) The final SDS PAGE of the SSBΔC1 mutant.

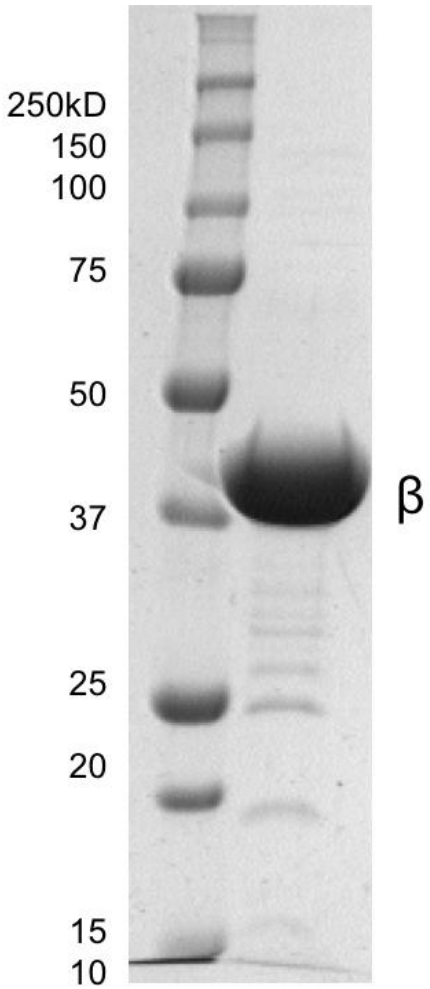


Figure 2-8. SDS-PAGE of final β-S109C/Q299C/R103S. SDS-PAGE gel of the β-S109C/Q299C/R103S sliding clamp before labeling with a fluorophore and passing through 2 additions purification columns.

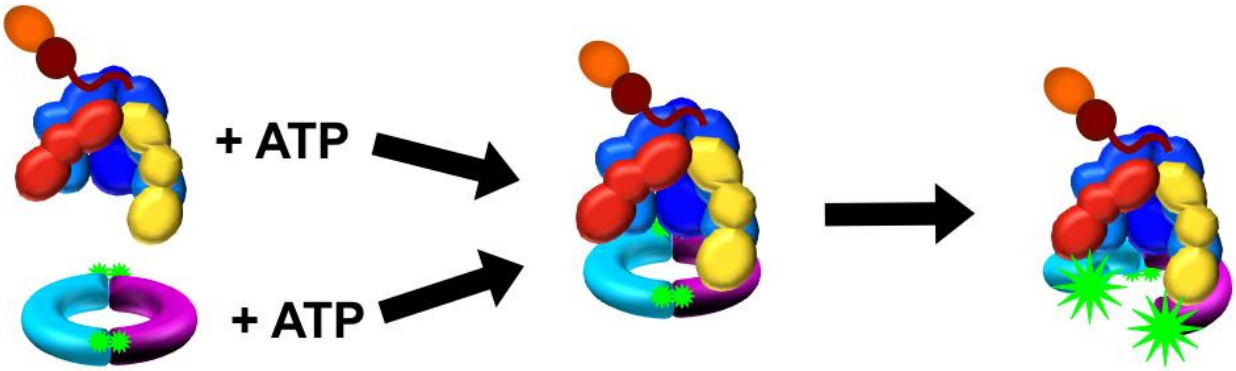


Figure 2-9. Reaction diagram for pre-steady state opening and binding assays in the stopped-flow fluorimeter. Syringe 1 γ-complex clamp loader and ATP. Syringe 2 contains β-AF4882 or TMR2 and additional ATP. When the stopped-flow apparatus mixes the β-AF4882 or TMR2 with the γ-complex, the clamp loader binds and opens the clamp. This opening of the sliding clamp interface causes and relief of the fluorophores quench, and there is a relatively high fluorescence which was measured in real time.

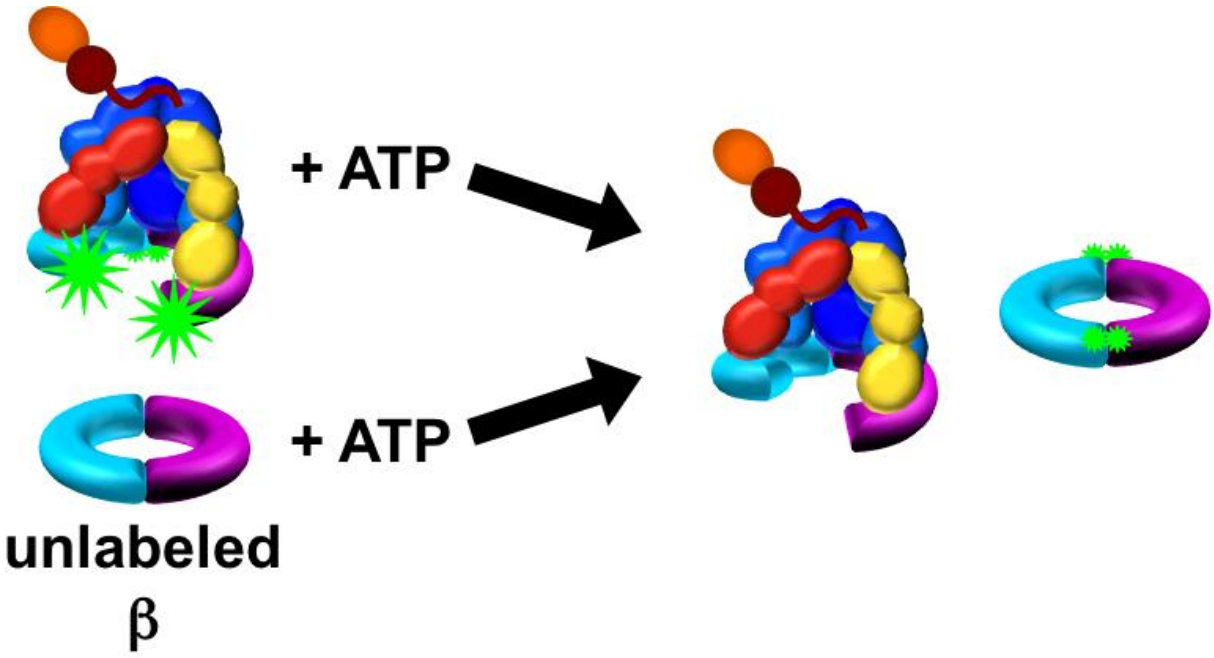


Figure 2-10. Pre-steady state dissociation assay using a stopped-flow apparatus. Syringe 1 contains γ-complex clamp loader, ATP, and β-AF4882. Syringe 2 contains unlabeled β and additional ATP. When the stopped-flow apparatus mixes the open clamp-clamp loader complex with the excess unlabeled clamp, the clamp eventually dissociates with the clamp loader. The clamp loader is then statistically likely to bind to an unlabeled clamp causing a decrease in fluorescence which was measured in real time.

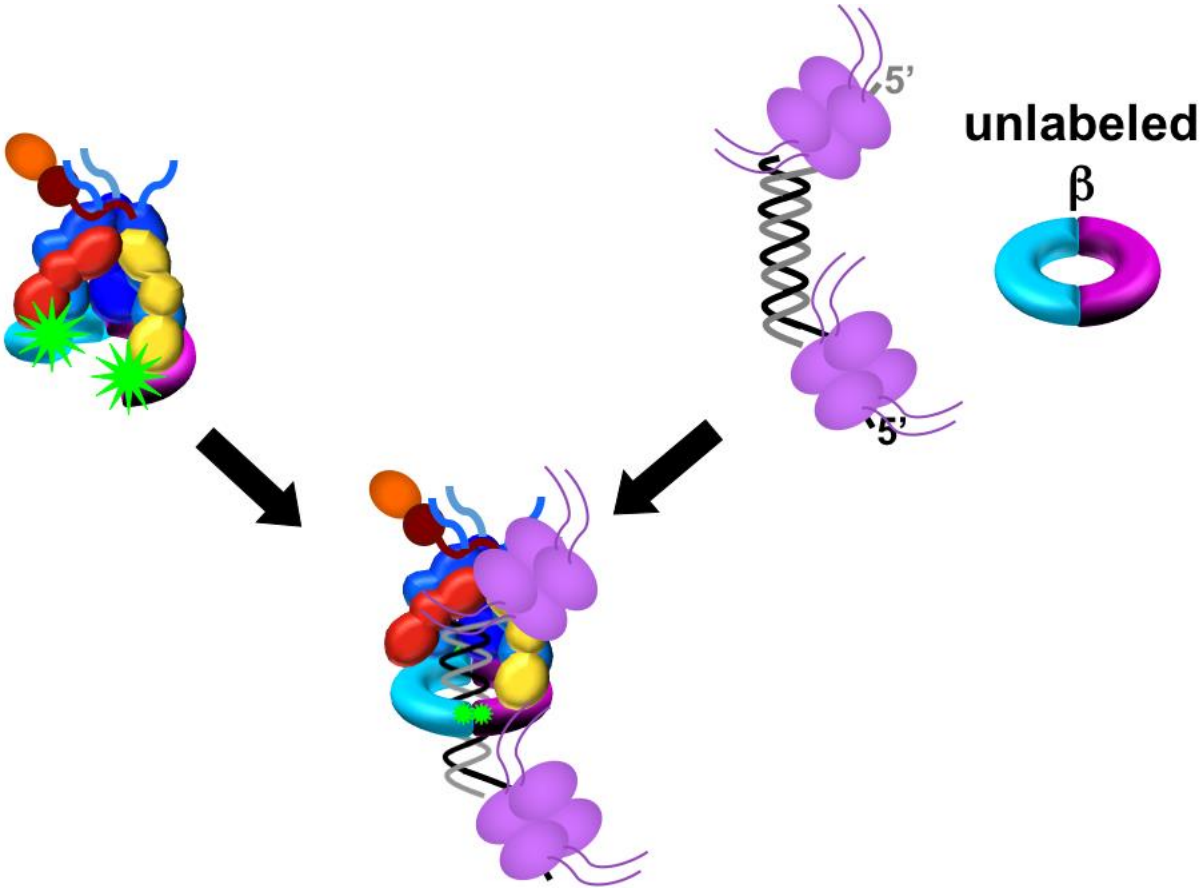


Figure 2-11. Scheme of pre-steady state clamp closing reactions a stopped-flow fluorimeter. Syringe 1 contains γ-complex clamp loader, ATP, and β-AF4882. Syringe 2 contains unlabeled β, DNA, and SSB when needed. When the stopped-flow apparatus mixes the open clamp-clamp loader complex with DNA, the clamp loader closes the clamp around the DNA causing a decrease in fluorescence which was measured in real time.

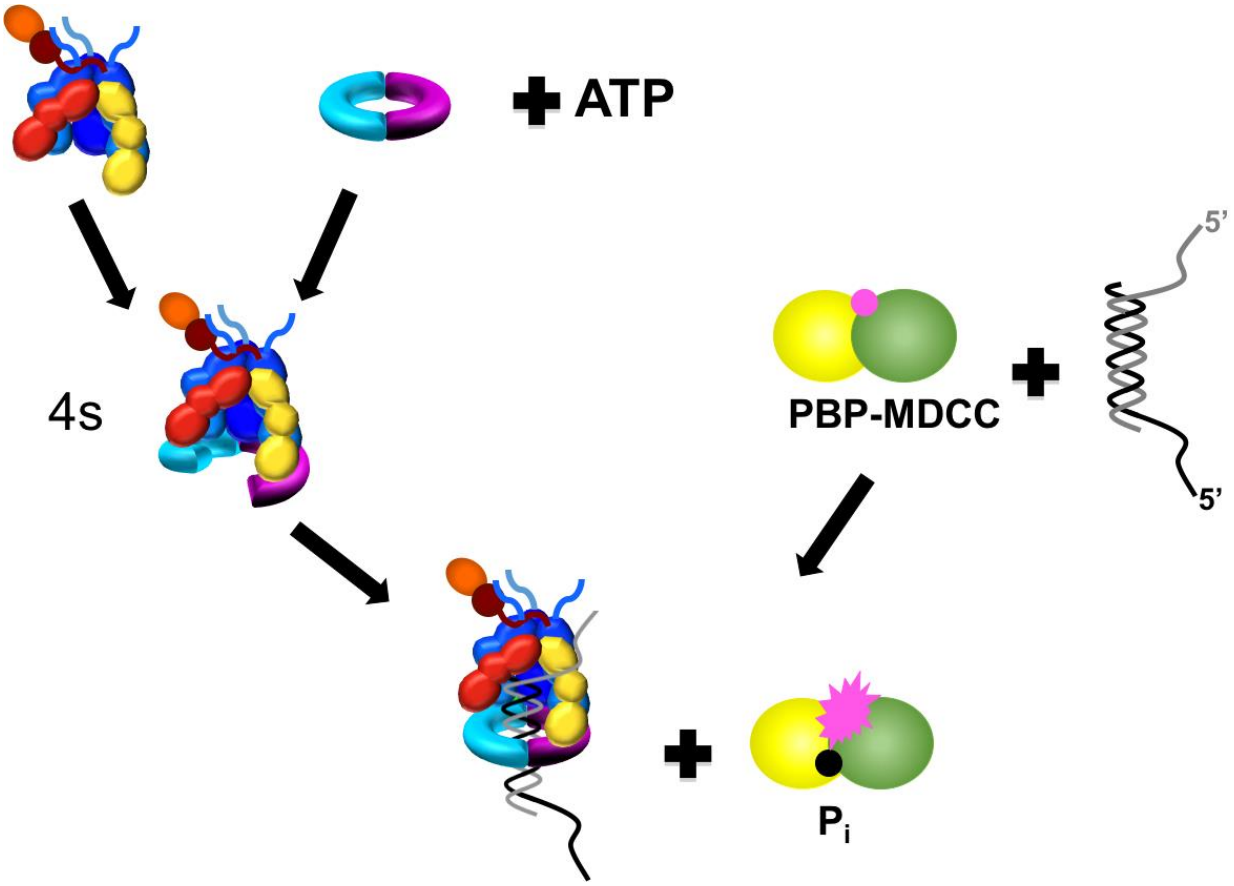


Figure 2-12. Sequential mixing diagram for ATP hydrolysis reactions measured by MDCC fluorescence on phosphate binding protein (PBP). Syringe 1 contains γ-complex clamp loader, which is mixed with syringe 2 containing ATP and β-sliding clamp for 4 seconds. Then this is mixed into a cuvette with syringe 3 containing DNA, PBP-MDCC and SSB when needed. When the stopped-flow apparatus mixes the open clamp-clamp loader complex with DNA, the clamp loader hydrolyses ATP to ADP and Pi. Pi then binds to MDCC and causes an increase in fluorescence which was measured in real time.

Table 2-1. Sequence of the primers used for cloning.

| Procedure | Gene | Forward primer (5' to 3') | Reverse primer (5' to 3') |
|---|---|---|---|
| SDM | *dnaN* | R103S: CGAAAAACGGCTACTCCCGGAGCGTACCAGC | R103S: GCTGGTACGCTCCGGGAGTAGCCGTTTTTCG |
| | *dnaX2016* | G212D: GCGCCGCTGAAGACAGCCTGCGAGA<br>A400T: GCGCCGCAGCAGACGCCGACTGTAC | G212D: TCTCGCAGGCTGTCTTCAGCGGCGC<br>A400T: GTACAGTCGGCGTCTGCTGCGGCGC |
| PCR | *holA* | CTCCTCCATATGATTCGGTTGTACCCGGAACAACTCCG | CTCCTCCCTAGGTCAACCGTCGATAAATACGTCCGCC |
| | *holB* | CTCCTCGATATCCATATGATGAGATGGTATCCATGGTTACGAC | CTCCTCGGATCCCCTAGGTTAAAGATGAGGAACCGGTAGC |
| | *dnaX*γ-only | | CTCCTCGAGCTCTCACTCTTTCTTTGCTTTGGTTGCTCCCTG |
| | *dnaX* τ-only | for all *dnaX:* CTCCTCTCATGAGTTATCAGGTCTTAGCCCGAAAATGGCGCC | CTCCTCGAGCTCTCAAATGGGGCGGATACTTTCTTCATCCAGC |
| | *dnaX* his-tagged | | CTCCTCGAGCTCTTAGTGGTGGTGATGGTGATGATGGTGG |

Table 2-2. Sequence of the primers used for DNA sequencing.

| Gene and Vector | Forward primer (5' to 3') | Reverse primer (5' to 3') |
|---|---|---|
| *dnaN* in pET15b+ | T7 upstream promoter (Novagen) | T7 terminator primer |
| *dnaE* and *holE* in pCDF Duet | ACYCDuetUP1 primer | DuetDOWN1 Primer |
| *dnaQ* in pCDF Duet | DuetUP2 primer | T7 terminator primer |
| *dnaX* in pBAD24 | pBad Forward Primer (ThermoFisher) | pBad Reverse Primer (ThermoFisher) |
| *dnaX* or *dnaQ* in pBluescript | pUC/M13 Forward (Promega) | pUC/M13 Reverse (Promega) |
| *dnaX (all)* in pCOLA Duet | ACYCDuetUP1 primer (Novagen) | DuetDOWN1 Primer (Novagen) |
| *dnaX2016* in pET52b+ | pET Upstream primer (Novagen) | T7 terminator primer (Novagen) |
| *holA* in pCOLA Duet | DuetUP2 primer (Novagen) | T7 terminator primer |
| *holB* in pET Duet | DuetUP2 primer | T7 terminator primer |
| *holC/holD* in pET Duet | pET Upstream primer | DuetDOWN1 Primer |

Table 2-3. Sequence of the primers used for assays.

| Oligo | Sequence (5' to 3') | Use |
|---|---|---|
| JH5 | GTCACACGACCAGTAATAAAAGGGACATTCTGGCC | JH5 and JH6 pair to make a 3' overhang with 5nt ssDNA |
| JH6 | CTGTTGGCCAGAATGTCCCTTTTATTACTGGTCGT | |
| JH9P | ATTATTTACATTGGCAGATTCACCAGTCACACGACCAGTAATAAAAGGGACATTCTGGCC | JH9 and JH10 pair to make 3’DNA overhang with 30nt ssDNA |
| JH10P | CTTTCAGGTCAGAAGGGTTCTATCTCTGTTGGCCAGAATGTCCCTTTTATTACTGGTCGT | |
| JH15P | AACAGAGATAGAACCCTTCTGACCTGAAAGCGTAAGAATACGTGGCACAGACAATAGTCA | JH10 and JH15 pair to make 5’DNA overhang with 30nt ssDNA |
| LD1P | AACAGAGATAGAACCCTTCTGACCTGAAAG | 30nt, anneals to JH10 for 3' overhang 30nt ssDNA with one blunt end, combine with pIIIpI for nicked substrate, also binds to LD5 for 80nt ssDNA substrate. LD1NoP is same sequence without the 5'P |
| LD1NoP | | |
| LD2 | ACAGAGATAGAACCCTTCTGACCTGAAAG | anneals to JH10, combine with pIIIpI for 1nt gap substrate |
| LD3 | ACCCTTCTGACCTGAAAG | 18nt, anneals to JH10, combine with pIIIpI for 12nt gap substrate |
| LD4P | ACGACCAGTAATAAAAGGGACATTCTGGCCAACAGAGATAGAACCCTTCTGACCTGAAAG | 60nt, anneals to JH10 for blunt substrate, reverse complement of JH10 |

Table 2-3. Continued.

| Oligo | Sequence (5' to 3') | Use |
|---|---|---|
| LD5.1 | TAAAGACTAATAGCCATTCAAAAATATTGTC TGTGCCACGTATTCTTACGCTTTCAGGTCA GAA | 64nt, 5' end of LD5, used in ligation reaction |
| LD5.2 | GGGTTCTATCTCTGTTGGCCAGAATGTCCC TTTTATTACTGGTCGT | 46 nt, 5'P, 3' end of LD5, used in ligation reaction |
| LD5 | TAAAGACTAATAGCCATTCAAAAATATTGTC TGTGCCACGTATTCTTACGCTTTCAGGTCA GAAGGGTTCTATCTCTGTTGGCCAGAATGT CCCTTTTATTACTGGTCGT | continuation of JH10 with additional sequence from M13, pIIIpI anneals |
| LD6P | ACAATATTTTTGAATGGCTATTAGTCTTTA | 30nt, anneals to LD5 to create 5' overhang with 30ssDNA |
| pIIIpI | ACGACCAGTAATAAAAGGGACATTCTGGC C | pIIIpI paires with JH10 to make 30nt substrate or along with LD1 for nicked substrate |
| pIIIp2 | ACACGACCAGTAATAAAAGGGACATTCTGG | pIIIp2 pairs with pIIItI-60- RhX to make 3’DNA- RhX structure |
| pIIItI-60-RhX | T*t*CAGGTCAGAAGGGTTCTATCTCTGTTGG C CAGAATGTCCCTTTTATTACTGGTCGTGT | |

*t* denotes a dT with a C6 amino modifier used to label DNA with RhX.

P denotes 5' phosphate

# CHAPTER 3
# CLAMP LOADER-CATALYZED OPENING OF THE β SLIDING CLAMP IS INDEPENDENT OF β DIMER STABILITY

## Background

Sliding clamps were first identified as components of the replisome that increase the processivity of DNA synthesis (132-135). Since their initial discovery as DNA polymerase processivity factors, sliding clamps have been found to bind directly to many different enzymes required for genome maintenance, and function both to increase enzyme residence times on DNA and to coordinate enzyme activities (reviewed in (136-138)). The ring-shaped oligomeric structure of sliding clamps is key to function by allowing sliding clamps to encircle and slide along DNA (5, 28). When a DNA polymerase or another enzyme binds a sliding clamp, the enzyme is effectively anchored to the DNA template (recently reviewed in (139, 140)). Most sliding clamps exist predominantly in closed ring conformations in solution and must open to be assembled around DNA by clamp loading enzymes (recently reviewed in (139, 141)). These clamp loaders chaperone open clamps to DNA and release the clamps at primed template junctions where DNA synthesis will begin. Even clamps that exist predominantly as open rings, or in monomeric form, in solution are chaperoned to DNA by clamp loaders (142-144). Clamp loaders contain five core subunits arranged in a ring that are members of the AAA+ family of ATPases (53, 145, 146). ATP binding and hydrolysis modulate the affinity of clamp loaders for clamps and DNA to promote the assembly of clamps on DNA (80, 84, 89, 112, 143, 147, 148). Clamp loaders may also contain additional subunits (e.g. *E. coli* ψ and χ subunits) or protein domains (e.g. the large subunit of the eukaryotic clamp loader) that mediate protein-protein and/or protein-

DNA interactions at the replication fork. When bound to an open clamp, all five core clamp loader subunits interact with the surface of the clamp (Figure 3-1).

Although many features of the clamp loading reaction have been defined, questions remain about the mechanism of clamp opening by clamp loaders. One question is how opening and closing dynamics of the clamps themselves contribute to the loading process. One possibility is that clamps spontaneously open, even if only transiently, and clamp loaders bind open clamps to stabilize the open conformation. This is the case for the bacteriophage T4 clamp that exists predominantly in an open conformation in solution (142, 143). However, other sliding clamps are inherently more stable than the bacteriophage clamp, and it is not clear whether transient opening events contribute to formation of open clamp loader-clamp complexes for these clamps. For example, the half-lives of the *E. coli* β-clamp and human PCNA-clamp on nicked circular DNA molecules are about 72 and 24 minutes, respectively, at 37°C suggesting that ring-opening (or dissociation into monomers), which would allow the clamp to dissociate from DNA, is a relatively infrequent occurrence (30). In these cases, it is possible that clamp opening dynamics are different when clamps are bound to DNA than when free in solution, or that transient opening occurs, but strong protein-DNA interactions limit dissociation. Both published and unpublished work from the Levitus laboratory at Arizona State University and previous work show that the β-dimer is exceptionally stable when free in solution with a lifetime on the order of 40 h at room temperature (29). Although the *Saccharomyces cerevisiae* sliding clamp is not as stable, the trimer is still long lived with a lifetime of 4.5 h at room temperature. None the less, molecular dynamics simulations suggest that the *Saccharomyces cerevisiae* RFC

clamp loader simply stabilizes the open conformation of the PCNA-clamp rather than destabilizing the closed conformation to actively open the clamp suggesting that the clamp loader depends on spontaneous clamp opening to form an open clamp loader-clamp complex(149). Studies also show that backbone amide protons at the interface between protomers in the *Escherichia coli* β-clamp exchange with deuterium suggesting that the clamp is dynamic (150). Thus, arguments can be made for and against a role for clamp loaders in actively opening sliding clamps.

The study presented here investigates the mechanism of β-clamp opening by the γ complex ($\gamma_3\delta\delta'\psi\chi$ subunits) clamp loader by determining how destabilizing the β dimer interface affects the clamp opening reaction and by defining a minimal kinetic mechanism for clamp opening.

## Results

### Effects of Electrostatic Interactions on Sliding Clamp-Clamp Loader Interactions

#### Mutations to amino acid residues at the β dimer interfaces

Unpublished work from the Levitus laboratory at Arizona State University shows that mutations to charged residues at the β-dimer interface and high salt concentrations destabilize the β-dimer by increasing the rate of dissociation into monomers. The study presented here investigates the effects of destabilization of the β dimer interface on interactions with the clamp loader and steps in the clamp loading reaction. Doubly-labeled β-clamps were made by mutating Ser-109 and Gln-299 to Cys to incorporate two Alexa Fluor 488 (AF488) fluorophores in each β monomer. This doubly-labeled clamp is referred to as β-S109C/Q299C-$(AF488)_2$ (Table 3-1). A mutation shown to destabilize the β-dimer, Arg-103 to Ser (R103S), was incorporated into a second

doubly-labeled clamp and is referred to as β- S109C/Q299C/R103S-(AF488)$_2$. The fluorophores are positioned at both dimer interfaces such that a pair of fluorophores, one on each monomer, interacts across the interface. When the clamp is closed the fluorophores stack and self-quench. Clamp opening separates a pair of fluorophores and increases fluorescence (29).

**Effects of dimer interface destabilization on equilibrium clamp loader-clamp binding/opening**

When bound to ATP, the *E. coli* clamp loader binds the β-clamp with high affinity to form an open clamp loader-clamp complex (79, 80). Equilibrium clamp loader-clamp binding/opening was measured to determine whether the R103S mutation or a high salt (500 mM NaCl) concentration, which destabilize the β dimer interface, promote ring-opening by the clamp loader. If clamp opening by the clamp loader were dependent on clamp dynamics, then destabilization of the interface would be expected to promote opening. The *E. coli* clamp loader, γ complex ($\gamma_{cx}$), containing $\gamma_3\delta\delta'\psi\chi$ subunits, was used in this work. The increase in fluorescence that occurs when $\gamma_{cx}$ binds and opens doubly-labeled clamps was measured for β-S109C/Q299C-(AF488)$_2$ and β-S109C/Q299C/R103S-(AF488)$_2$ in buffer containing 50 mM NaCl. Relative AF488 fluorescence as a function of γ complex concentration is plotted in Figure 3-2A. Because the efficiency of protein labeling differs for different protein preparations, the magnitude of the fluorescence change differs for β-S109C/Q299C-(AF488)$_2$ and β-S109C/Q299C/R103S-(AF488)$_2$. Data were fit to the two-state binding model illustrated in the cartoon using a quadratic equation to calculate apparent dissociation constants, $K_{d,app}$, of 7.0 ± 0.4 nM and 4.2 ± 1.5 nM for β-S109C/Q299C-(AF488)$_2$ and β-

S109C/Q299C/R103S-(AF488)$_2$, respectively. The average $K_{d,app}$ value is about 67% larger for β-S109C/Q299C-(AF488)$_2$ than for β-S109C/Q299C/R103S-(AF488)$_2$, and calculated $K_{d,app}$ values for β-S109C/Q299C-(AF488)$_2$ are consistently greater than for β-S109C/Q299C/R103S-(AF488)$_2$ in each of the three experiments showing that the R103S mutation modestly increases the affinity of the clamp loader for the clamp.

The titration of doubly-labeled clamps with $\gamma_{cx}$ was repeated in assay buffer containing 500 mM NaCl (Figure 3-2B). The decrease in dimer stability for β-S109C/Q299C/R103S-(AF488)$_2$ in 500 mM NaCl was apparent in these experiments. In the absence of $\gamma_{cx}$ and at low $\gamma_{cx}$ concentrations where the majority of the β-clamp is not bound, the fluorescence of β-S109C/Q299C/R103S-(AF488)$_2$, but not β- S109C/Q299C-(AF488)$_2$, increased slowly with time, presumably due to dissociation of the dimer into monomers when diluted 10-fold into the cuvette (Figure 3-3). At high concentrations of $\gamma_{cx}$ where the majority of the β-clamp is bound by $\gamma_{cx}$ and stabilized as open dimers, the fluorescence signal remained constant for both clamps. Due to the instability of β-S109C/Q299C/R103S-(AF488)$_2$ during the course of the titration, the $K_{d,app}$ value for the $\gamma_{cx}$ and the mutant clamp cannot be rigorously determined. But, high salt does not appear to affect the binding/opening equilibrium for the R103S mutant as the calculated $K_{d,app}$ of 5.0 ± 1.2 nM is about the same as in 50 mM NaCl. The average $K_{d,app}$ value for β-S109C/Q299C-(AF488)$_2$ is modestly lower in 500 mM NaCl ($K_{d,app}$ = 5.3 ± 2.4 nM) than in 50 mM NaCl ($K_{d,app}$ = 7.0 ± 0.4 nM), but the difference is within experimental error. Together, these experiments show that the R103S mutation and high salt concentrations have only a modest effect on clamp loader-clamp binding/opening equilibria. This is in contrast to the β monomer-dimer equilibrium where the R103S

mutation and high salt dramatically shift the equilibrium towards the monomer (unpublished data from Levitus laboratory, ASU).

### Dimer interface destabilization does not increase rates of clamp opening reactions

The equilibrium clamp opening reaction consists of at least two steps, clamp binding and clamp opening (128). It is possible that destabilization of the β-dimer interface promotes the clamp opening step, but that a compensatory change in another step reduces the effects of destabilization on the overall binding/opening equilibrium. To test this possibility, pre-steady-state rates of clamp opening were measured to determine whether the R103S mutation or 500 mM NaCl promote the clamp opening step. Clamp opening reactions were initiated by mixing a solution of γ complex and ATP with a solution of β-S109C/Q299C-$(AF488)_2$ or β-S109C/Q299C/R103S-$(AF488)_2$ and ATP. The concentration of $\gamma_{cx}$ was varied from 0.005 to 1.6 μM (representative reaction time courses are shown in Figure 3-4A), and the concentration of β-S109C/Q299C-$(AF488)_2$ or β-S109C/Q299C/R103S-$(AF488)_2$ was held constant. The increase in AF488 fluorescence that occurs when clamps are opened was measured as a function of time in assay buffer containing 50 mM NaCl. The magnitude of increase in fluorescence differs for the two clamps because the labeling efficiency differs, but surprisingly, the time-dependent changes in fluorescence due to opening β-S109C/Q299C-$(AF488)_2$ and β-S109C/Q299C/R103S-$(AF488)_2$ are the same within experimental error. Even though the R103S mutation increases the rate of β dimer dissociation into monomers, this destabilization of the dimer interface does not increase the rate of ring opening by $\gamma_{cx}$. The clamp opening experiment was repeated in assay

buffer containing 500 mM NaCl. Again, time courses for clamp opening for β-S109C/Q299C-$(AF488)_2$ and for β-S109C/Q299C/R103S-$(AF488)_2$ were similar to each other (Figure 3-4B) in contrast to the marked instability of the β-R103S mutant at high salt concentrations (unpublished data from Levitus laboratory, ASU). If clamp opening were dependent on stability of the interface, opening for the R103S mutant would have been faster. If the higher salt concentration were promoting clamp opening, rates for both clamps should have been faster in 500 mM NaCl than in 50 mM NaCl, but at the higher salt concentration, the overall rate of opening was about 2-fold slower. This reduction in rates may be due to effects of increased salt concentration on interactions other than at the dimer interface such as clamp loader-clamp binding or ATP binding. None the less, these kinetic experiments demonstrate clamp opening by the clamp loader is not dependent on clamp stability.

**Dimer interface destabilization modestly increases lifetimes of clamp loader-clamp complexes**

Because the overall association rates of $\gamma_{cx}$ with β-S109C/Q299C-$(AF488)_2$ and β-S109C/Q299C/R103S-$(AF488)_2$ are the same, but $K_{d,app}$ values differ, albeit modestly, the difference in $K_{d,app}$ values should be reflected in differences in dissociation rates. Dissociation of clamps from clamp loader-clamp complexes was measured to test this and to determine whether the R103S mutation or 500 mM NaCl affect the lifetime of clamp loader-clamp complexes. In these experiments, a solution of γ complex, β-$(AF488)_2$ (20 nM final), and ATP (0.5 mM) was added to a solution of unlabeled β (400 nM final) and ATP (0.5 mM). The excess unlabeled β traps clamp loaders that dissociate from AF488-labeled clamps to permit measurement of the decrease in

fluorescence that occurs when γ complex dissociates from β-$(AF488)_2$ and the ring closes. In reactions with 50 mM NaCl, the overall rate of dissociation of β-S109C/Q299C-$(AF488)_2$ is about twice that of β-S109C/Q299C/R103S-$(AF488)_2$ (Figure 3-5A). In other words, the R103S mutation that destabilizes the β-dimer interface increases the lifetime of a clamp loader-clamp complex. Time courses for dissociation of both clamps were biphasic (Table 3-2) indicating that dissociation occurs from two different states at different rates. In reactions with 500 mM NaCl, the overall rate of dissociation for β-S109C/Q299C-$(AF488)_2$ decreased modestly, and the dissociation rate for β- S109C/Q299C/R103S-$(AF488)_2$ increased modestly, such that the difference in overall dissociation rates for the two clamps was smaller (Figure 3-5B). Decreases in fluorescence were also biphasic for both clamps in 500 mM NaCl. In general, the differences dissociation rates can account for the differences in equilibrium dissociation constants.

**The R103S mutation does not affect rates of clamp closing on DNA**

In addition to forming stable open clamp complexes, clamp loaders also chaperone clamps to DNA where the clamps are deposited and closed to encircle DNA (reviewed in (49)). It is possible that destabilization of the β-dimer interface affects the rate at which clamps reform a closed dimer interface. To test this possibility, clamp closing on DNA was measured for β-S109C/Q299C-$(AF488)_2$ and β-S109C/Q299C/R103S-$(AF488)_2$. This experiment used a symmetrical DNA substrate with two ss/ds DNA junctions of the same polarity with 5'-ssDNA overhangs (105). Single-stranded binding protein (SSB) was included in reactions because ssDNA is bound by SSB *in vivo* (100, 101). Clamp loading reactions, in buffer with 50 mM NaCl,

were initiated by adding a solution of clamp loader, β-(AF488)$_2$, and ATP to a solution of DNA, SSB, excess unlabeled β-clamp, and ATP. Excess unlabeled clamp is added to limit the reaction to a single observable cycle of clamp closing. When the clamp closes around DNA, AF488 fluorescence is quenched. The rates of β-S109C/Q299C-(AF488)$_2$ and β-S109C/Q299C/R103S-(AF488)$_2$ onto DNA are similar (Figure 3-6). Together, these results show that the R103S mutation that destabilizes the β-dimer interface has little if any effect on the clamp loading reaction at either the clamp opening step where a dimer interface is broken or at the clamp closing step where a dimer interface reforms.

**Enzymatic Modeling the Clamp Opening Reaction**

**Effects of γ complex binding on the fluorescence of singly-labeled β-clamps**

To further define the clamp opening step of the clamp loading reaction, kinetic data were modeled to define individual kinetic steps. As a control prior to kinetic modeling, singly-labeled clamps were made to determine whether AF488 fluorescence in β-S109C/Q299C-(AF488)$_2$ could be affected by mechanisms other than the unstacking of AF488 dimers that occurs on clamp opening. Clamp binding/opening reactions were measured for singly AF488-labeled clamps that contained either the S109C mutation or Q299C mutation. The fluorescence of AF488 changed when both singly-labeled clamps were bound by $\gamma_{cx}$, but the changes were different. There was a *rapid decrease* in AF488 fluorescence when β-S109C-AF488 was bound by $\gamma_{cx}$ (Figure 3-7A) and a *slower increase* in fluorescence when β-Q299C-AF488 was bound by $\gamma_{cx}$ (Figure3-7B). Because these fluorophores are located on the “top edge” of β (Figure 3-1) at or near sites where $\gamma_{cx}$ contacts the clamp, these changes may be due to environmental effects of fluorophore interactions with $\gamma_{cx}$. The decrease in fluorescence

for β-S109C-AF488 likely reflects the binding of $\gamma_{cx}$ to β because the initial increase in fluorescence is faster than clamp opening, and the time course is a simple exponential function. In contrast, clamp opening time courses (e.g. Figure 3-4A) show a brief lag before a sigmoidal increase in fluorescence that is indicative of a kinetic step (clamp binding) that does not affect fluorescence and occurs before the step (clamp opening) that alters fluorescence. The small increase in AF488 fluorescence that occurs when $\gamma_{cx}$ binds β-Q299C-AF488 is on the same time scale as clamp opening, and most likely results from conformational changes that occur on opening and affect the environment of the fluorophore possibly by increasing interactions with $\gamma_{cx}$. These environmental changes in AF488 for fluorophores attached at residues 109 and 299 complicate the interpretation of fluorescence changes for clamp opening reactions in that the clamp opening reactions cannot be modeled using a simple two quantum-yield-state system where fluorescence changes are solely due to destacking of fluorophores on clamp opening.

**Kinetic modeling of γ complex binding and opening β**

To simplify the system for kinetic modeling, clamp opening kinetics were measured for a doubly-labeled clamp where the fluorophores are located on the "bottom edge" of β (Figure 3-1) away from the $\gamma_{cx}$ binding surface. Arg-103 and Ile-305 were mutated to Cys and labeled with AF488 (β-R103C/I305C-$(AF488)_2$). Note that this clamp contains a destabilizing Arg-103 mutation. Steady-state AF488 fluorescence in the single mutant versions of this clamp are insensitive to clamp loader binding (128). Fluorescence lifetimes measured for β-R103C/I305C-$(TMR)_2$ show that $\gamma_{cx}$ binding to the doubly-labeled clamp does not affect the fluorescence lifetimes. Instead, clamp

loader binding alters the fractional amplitudes associated with the two fluorescence states due stacked and unstacked fluorophores that are measured for β closed and opened conformations, respectively (Unpublished data from the Levitus laboratory at ASU). These lifetime measurements utilized TMR rather than AF488 because the excitation wavelength of TMR was better matched to the laser system used for the measurements. Both these lifetime measurements with the doubly-labeled β-R103C/I305C-$(TMR)_2$ clamp and previous steady-state fluorescence measurements with the singly-lableled clamps support the assumption that the change in fluorescence for fluorophores located on the bottom edge of the clamp is not affected by environmental changes, but only by changes in stacking of a pair fluorophores at the interface. Therefore, we assume that there are only two fluorescence states for β-R103C/I305C-$(AF488)_2$, one for the open clamp where a pair of fluorophores is unstacked and unquenched, and one for the closed clamp where fluorophores are stacked and quenched. Because the fluorescence of AF488 covalently bound to β-R103C/I305C-$(AF488)_2$ is not affected by interactions with the clamp loader, the time course for binding/opening reactions differ in shape from those for β-S109C/Q299C-$(AF488)_2$ (Figure 3-8).

Two data sets for reactions containing 50 mM NaCl were used for kinetic modeling: 1) $\gamma_{cx}$ binding to β-S109C-AF488 (e.g. Figure 3-7C) and 2) $\gamma_{cx}$-catalyzed opening of β-R103C/I305C-$(AF488)_2$ (e.g. Figure 3-9). Clamp binding was measured in reactions containing 10 to 1280 nM $\gamma_{cx}$ and 20 nM β-S109C-AF488, and clamp opening was measured in reaction containing 5 to 1800 nM $\gamma_{cx}$ and 16 nM β-R103C/I305C-$(AF488)_2$. As a starting point, these data were empirically fit to sums of exponentials.

Data for $\gamma_{cx}$ binding β-S109C-AF488 are best fit by a double exponential. Calculated rate constants for the rapid phase are a linear function of $\gamma_{cx}$ concentration as expected for a *binding* reaction (Figure 3-7D). The slope yields an apparent second order rate constant of 3.7 x $10^7$ $M^{-1}s^{-1}$ which is consistent with our previous measurements (2.3 x $10^7$ $M^{-1}s^{-1}$) using another assay (151). Rates of slower phase are in the same range as those for the clamp opening reaction and approach a maximum value of 8 $s^{-1}$. When data for $\gamma_{cx}$ opening β-R103C/I305C-$(AF488)_2$ are fit by a double exponential, the calculated rate constants are not a linear function of $\gamma_{cx}$ but curve approaching limiting values of 11 $s^{-1}$ for the rapid phase and 1.5 $s^{-1}$ for the slow phase (Table 3-3). This is comparable to our previous studies where maximal rates were 9 $s^{-1}$ and 0.8 $s^{-1}$ for the fast and slow phases, respectively (128). Note that time courses for opening reactions are not simple exponentials and contain a short lag phase, but exponential fits were used to estimate rates of change in fluorescence. Both the shape of the opening time course and the change in rate constant with $\gamma_{cx}$ concentration are consistent with a mechanism that contains at least two-steps, binding then opening (128). Dissociation of β-R103C/I305C-$(AF488)_2$ from a clamp loader-clamp complex is biphasic and occurs at a rate similar to that for β-S109C/Q288C/R103S-$(AF488)_2$ (Figure 3-9 and Table 3-2).

Empirical analysis of kinetic data indicates that the clamp opening reaction is at least a two-step reaction consisting of an initial clamp loader-clamp binding step followed by a clamp opening step. However, global fitting of the β-S109C-AF488 and β-R103C/I305C-$(AF488)_2$ binding/opening reactions to this simple kinetic model does not adequately fit the data (Figure 3-10). Recalling that the biphasic dissociation reaction suggests that there are two populations of *open* clamp loader-clamp complexes that

dissociate at different rates, the complexity of the kinetic model was increased by adding an additional open state. The presence of a second open state is also consistent with the biphasic change in fluorescence in clamp opening reactions. Therefore, clamp binding reactions using β-S109C-AF488 and clamp opening reactions using β-R103C/I305C-$(AF488)_2$ were globally fit to a kinetic model in which the clamp loader binds the clamp to form a closed clamp loader-clamp complex, the clamp opens relatively rapidly, and there is a slower conformational rearrangement in the open clamp loader-clamp complex (Figure 3-11). This three-step model fits the data better than the two-step model. We note that these kinetic data could also be fit to a model that includes two parallel two-step binding-opening reactions in which a fraction of the total β is bound and open faster than the rest. This parallel model does not make intuitive sense because it requires that two separate populations of β exist and react at different rates. We favor the first model based on structural data as explained in the Conclusions.

## Conclusions

Although many mechanistic questions about the clamp loading reaction mechanism have been answered, questions regarding the mechanism of clamp opening by the clamp loader remain. Does the clamp loader depend on intrinsic clamp opening and closing dynamics to form an open clamp loader-clamp complex? Or does the clamp loader destabilize and actively open clamps? What are the steps in the clamp opening reaction? Clamp opening reactions catalyzed by the *E. coli* and *S. cerevisiae* clamp loaders are at least two-step reactions consisting of an initial binding step followed by an opening step (152, 153). But, a two-step binding-opening mechanism does not necessarily mean that the clamp loaders actively open clamps; the clamp loaders could

bind closed clamps, which predominate in solution, and “wait” for the clamps to open spontaneously. To address these outstanding questions, the mechanism of the clamp opening reaction was investigated.

Soon to be published data from the Levitus laboratory at ASU establishes conditions that destabilize the dimer interface of the β-clamp and promote dissociation into monomers. Electrostatic interactions between positively charged residues on one side of the dimer interface (N-terminal protein domain) and negatively charged residues on the other (C-terminal domain) can be disrupted by high NaCl concentrations to promote dissociation into monomers. Additionally, a point mutation converting a positively charged Arg residue to a neutral amino acid residue also destabilizes the dimeric form of the clamp. The experiments presented here uses these conditions that destabilize the β-dimer interface to determine whether the clamp loading reaction, and in particular, the clamp opening step is dependent on the stability and dynamics of the β dimer interface. Mutation of Arg-103 substantially destabilizes the dimer interface decreasing the lifetime of the dimeric form of the clamp from 34 h to 5.8 h, and similarly, increasing the NaCl concentration from 50 to 500 mM reduces the lifetime to 9 h (unpublished data from the Levitus laboratory at ASU). The combination of the Arg-103 mutation and high salt leads to even greater destabilization such that the majority of clamps dissociate into monomers within the 20 min it takes to measure the populations of monomers and dimers. Although these conditions substantially destabilize the β-dimer interface, mutation of Arg-103 to Ser does not affect the rate of clamp opening either at a low salt concentration (50 mM NaCl, Figure 3-4A), or a high salt concentration (500 mM NaCl, Figure 3-4B) where the R103S mutant clamp is highly

destabilized. If the clamp opening reaction were dependent on the dynamics and the stability of the β-clamp, the R103S mutation would be expected to increase the rate of clamp opening because the mutation destabilizes the interface. Furthermore, unpublished data from the Levitus laboratory at ASU suggest that spontaneous clamp opening events are infrequent. Destabilizing the clamp interface might also be expected to affect the ease with which the clamp closes, but the R103S mutation did not affect rates of clamp closing on DNA either. This comparison of opening and closing reactions measured under standard and destabilizing conditions is consistent with a mechanism in which the clamp loader destabilizes and actively opens the clamp rather than binding and stabilizing clamps that have spontaneously opened.

The clamp opening mechanism was investigated further by measuring kinetics of the clamp loader-clamp binding (β-S109C-AF488) and opening (β-R103C/I305C-$(AF488)_2$) to define a kinetic mechanism for the reaction. Previous work and empirical fitting of the current data show that the clamp opening reaction is at least a two-step binding-opening reaction, however, this simple model did not adequately fit clamp opening kinetic data (Figure 3-10). The biphasic nature of clamp loader-clamp dissociation and clamp opening kinetics indicate that there is an additional open state. Therefore, kinetic data for clamp binding and clamp opening were fit to a three-step "bind-open-lock" model in which the clamp loader binds a closed clamp, the clamp opens, and the initial open clamp loader-clamp complex undergoes a conformational rearrangement that "locks" the complex in an open state (Figure 3-11). This simple bind-open-lock model fits the data reasonably well, but the reaction likely contains additional kinetic steps. For example, in the bind-open-lock model, the clamp only dissociates from

the closed clamp loader-clamp complex, but the clamp likely dissociates from both of the open complexes also. Clamp loader dissociation kinetics are biphasic, and the rate of the slow phase is the same for all clamps under all conditions, about 0.01 $s^{-1}$. It is interesting to note that this rate is the same as the slow ATP hydrolysis ($k_{cat}$ = 0.012 $s^{-1}$) that occurs in the clamp loader-clamp complex in the absence of DNA (89). We speculate that β may dissociate from the "locked open" complex at a rate that is limited by this slow rate of ATP hydrolysis. There is not enough information in the kinetic data to add or rule out these additional kinetic steps. However, any missing steps are not likely affecting rates or populations of species to a large extent because the minimal bind-open-lock model recapitulates the key features of the kinetic data.

In the bind-open-lock model, the initial clamp opening step does not strongly favor an open conformation of the clamp; the open clamp loader-clamp complex is favored over the closed complex by about 2-to-1. It is the subsequent conformational change step strongly favors the open state with a forward rate that is about 60-fold greater than the reverse rate. The bind-open-lock model can be envisioned in terms of structural data for clamp loader-clamp complexes. When the clamp loader initially binds the closed clamp, the most extensive interactions are likely to be between the δ subunit and the β-clamp. Interactions between the other clamp loader subunits and the clamp are likely to be less extensive to nonexistant as in the *S. cerevisiase* closed clamp loader-clamp complex (Figure 3-1) (83, 107). This complex was trapped in a closed state by mutations to conserved "Arg finger" residues, which have been shown in solution studies to inhibit clamp opening (154, 155). Initial opening of the clamp may not substantially increase contacts between the clamp loader and the clamp, and therefore,

the clamp readily closes. Subsequent conformational rearrangements in the open clamp loader-clamp complex may be required to form a locked open state where *all five* of the core clamp loader subunits interact extensively with the face of the clamp as in the crystal structure of a bacteriophage clamp loader-clamp complex (Figure 3-1) and the EM structures of an archaeal clamp loader-clamp complex (93, 156, 157). The extensive contacts between the clamp loader and clamp may not only stabilize the open state, but also prevent dimeric or trimeric clamps from dissociating into monomers when the rings are open. Oligomer association is highly cooperative for trimeric clamps suggesting that opening one interface would destabilize clamps and favor dissociation into monomers (29, 142, 158).

The proposal that clamp loaders actively open clamps that exist predominantly as closed rings in solution was initially made based on the high stability of the closed ring forms of these clamps (30). The structure the δ subunit of the *E. coli* clamp loader bound to a β monomer suggested that that the δ subunit distorts and destabilizes the β-dimer interface which causes the clamp to open supporting an active role for the clamp loader in clamp opening (83). Results from this work also support a mechanism where the *E. coli* clamp loader actively opens the β-clamp rather than capturing clamps that have spontaneously opened. The bind-open-lock model predicts that clamp opening and closing dynamics ($k_{open}$ = 9 $s^{-1}$ and $k_{close}$ = 4 $s^{-1}$) occur on a time scale and with a frequency that could have been detected by fluorescence correlation spectroscopy if the unbound clamp had similar dynamics (unpublished data from the Levitus laboratory at ASU does not see this). Therefore, we conclude that the clamp loader alters these dynamics. Active β-clamp opening does not contradict results from hydrogen-deuterium

exchange studies showing that the β-dimer interface is dynamic because minor fluctuations in the backbone conformation could allow for hydrogen-deuterium exchange and exchange takes place on a long time scale (≈ 3.5 h) suggesting that opening events are infrequent (150). Nor does an active clamp opening model imply that the clamp loader only destabilizes the clamp to promote opening. The bind-open-lock model suggests that a conformational change occurs the after initial clamp opening event strongly stabilizes an open clamp loader-clamp complex (locked open complex). Together, results showing that clamp opening rates are not affected by destabilization of the β-dimer interface and the bind-open-lock model show that the clamp loader both destabilizes the closed clamp and stabilizes the open clamp. This differs somewhat from molecular dynamics simulations suggesting that the clamp loader does not substantially destabilize the closed clamp, and instead stabilizes the open clamp (149). This difference may simply be due to the differences in the clamp loader-clamps used in the two studies. The molecular dynamics simulations were based on interactions between the eukaryotic clamp loader and trimeric PCNA clamp, and it may be that the eukaryotic clamp loader does not actively open the clamp. The PCNA clamp is less stable than the β-clamp; PCNA dissociates from circular DNA molecules about 3-times faster than β at 37°C and the lifetime of the PCNA trimer is about 10-fold shorter than the lifetime of the β dimer at 20°C (29, 30). This decreased stability of PCNA may lead to more frequent spontaneous opening events and allow the eukaryotic clamp loader to passively capture open PCNA clamps. On the other hand, the molecular dynamics simulations were based on structural data for the Arg finger mutant which is defective in clamp opening, and thus, may not be not be giving the complete picture (Figure 1) (107,

154, 155). Although PCNA is not as stable as the β-clamp, the lifetime of the trimeric PCNA ring (4.5 h) is about the same as the lifetime of the β-R103S mutant (5.8 h) at room temperature which suggests that the clamp loader may also need to destabilize PCNA to form an open complex.

The results in this chapter support a model in which the *E. coli* clamp loader binds a closed clamp and destabilizes the clamp to form an initial open clamp loader-clamp complex. This initial opening event does not strongly favor an open clamp loader-clamp complex. Subsequent conformational changes in the clamp loader-clamp complex strongly stabilize the clamp in an open conformation. This final locked open state likely represents a complex where all five core clamp loader subunits interact extensively with the face of the clamp to stabilize the open conformation. Because breaking one interface in forming an open clamp would likely destabilize clamps, another important function of this final locked open complex is to prevent dissociation of clamps into monomers.

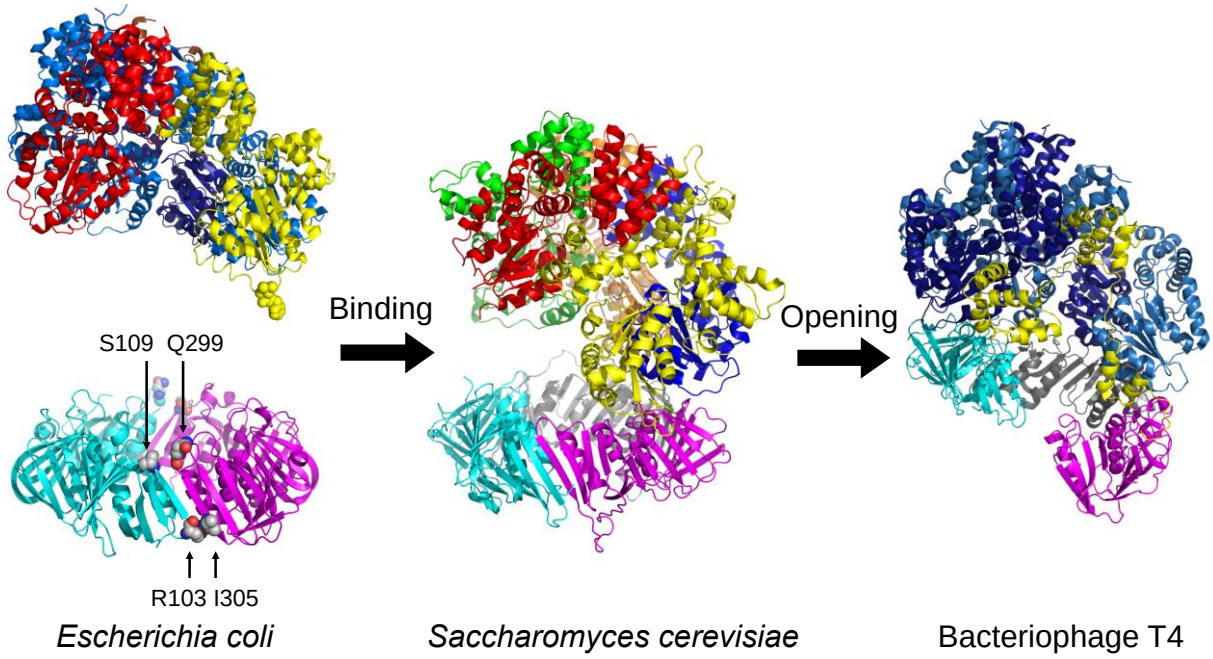


Figure 3-1. Crystal structures of clamp loaders and clamps from different species depicting complexes that are likely to exist in the clamp opening pathway. (*Left panel*) Structures of the *E. coli* $\gamma_3$dd' clamp loader bound to an ATP analog and γ peptide along with the β-clamp illustrate conformations that may exist prior to binding. Residues Leu-73 and Phe-74, part of the clamp interacting peptide on the δ subunit, are shown as spheres. Amino acid residues in β that were mutated to Cys for fluorescent labeling are indicated. (*Center panel*) The clamp loader initially binds β to form a closed complex that may be similar in structure to the closed *S. cerevisiae* RFC-PCNA complex. (*Right panel*) After binding the clamp loader, the clamp either spontaneously opens, or is actively opened by the clamp loader, to form an open clamp loader-clamp complex that may resemble the bacteriophage T4 gp44/62-gp45 clamp loader-clamp complex.

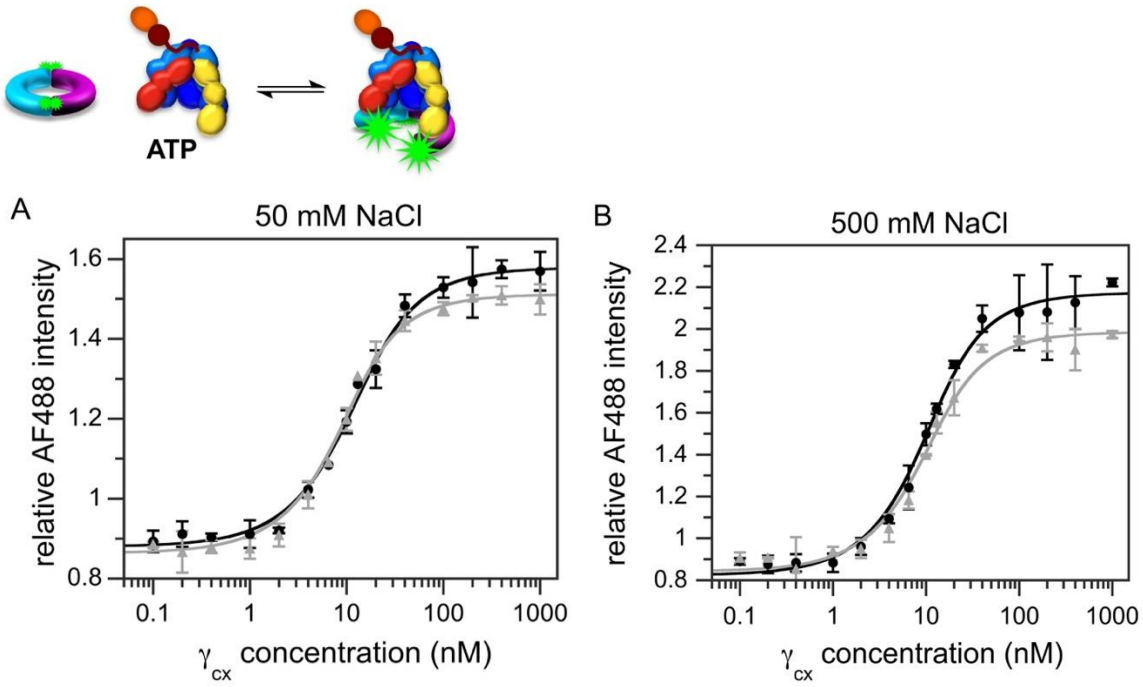


Figure 3-2. Clamp loader-clamp equilibrium binding and clamp opening. Relative AF488 fluorescence is plotted as a function of g complex concentration for solutions of b-S109C/Q299C-$(AF488)_2$ (black circles) and b-S109C/Q299C/R103S-$(AF488)_2$ (gray triangles) in assay buffer containing **A.** 50 mM NaCl or **B.** 500 mM NaCl. Final concentrations of b clamps were 10 nM. Data were fit to a quadratic equation (solid line through data points) assuming a two-state binding model (indicated in the diagram) to calculate apparent dissociation constants, $K_{d,app}$. Assay buffer contained 20 mM Tris-HCl pH 7.5, 8 mM $MgCl_2$, 5 mM DTT, 40 µg/mL BSA, 0.1 mM EDTA, and 4% glycerol. Note that NaCl quenches the fluorescence of AF488 in unbound b-clamps in a concentration-dependent manner so that the magnitude of the signal change is greater in the assay containing 500 mM NaCl. Increased NaCl likely increases the fraction of AF488 molecules that are stacked and quenched.

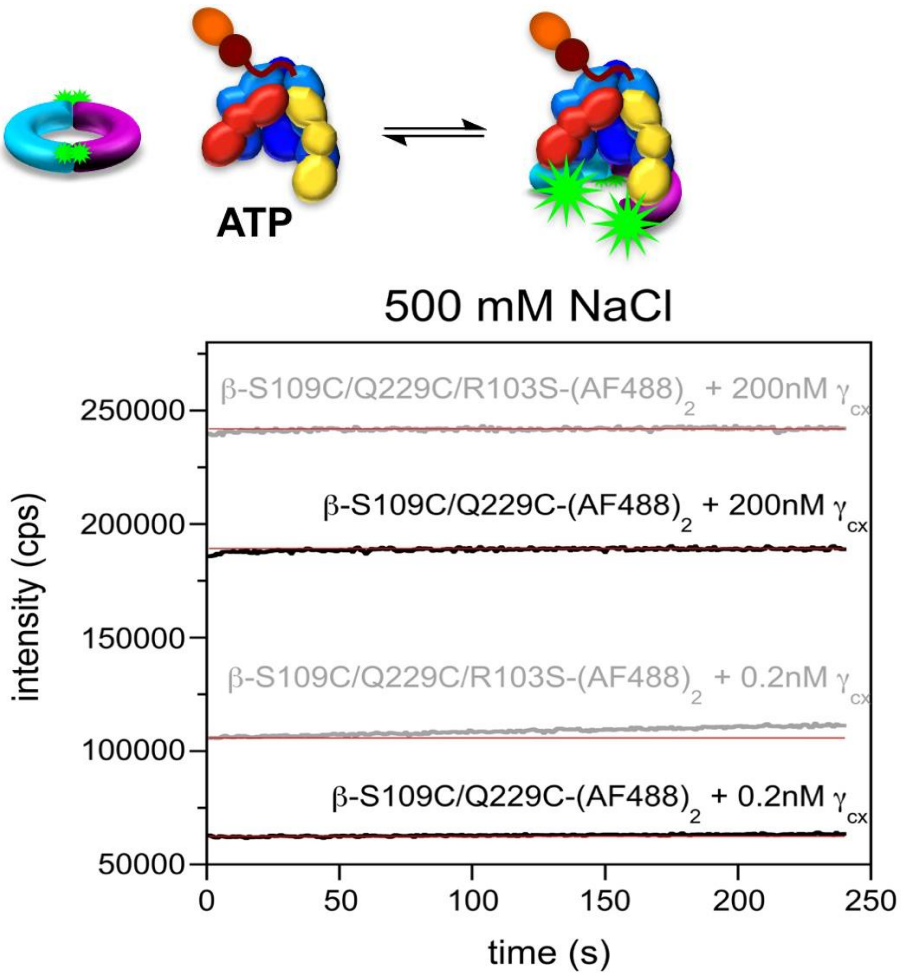


Figure 3-3. Equilibrium binding of $\gamma_{cx}$ and β-$(AF488)_2$ was measured by measuring the increase in AF488 fluorescence that occurs when the clamp loader binds β-$(AF488)_2$ to form an open complex. Varying concentrations of the clamp loader ($\gamma_{cx}$) were added to solutions of β-$(AF488)_2$ (10 nM final concentration) and fluorescence emission was measured at 520 nm for 240 s when exciting at 495 nm. Time-based scans were done to ensure samples had reached equilibrium. Representative traces for β-S109C/Q299C-$(AF488)_2$ (black) and β-S109C/Q299C/R103S-$(AF488)_2$ (grey) at two different $g_{cx}$ concentrations in buffer containing 500 mM NaCl are shown. At low γ clamp loader concentrations (e.g. 0.2 nM $\gamma_{cx}$) where the majority of the clamp is not bound, the fluorescence signal for AF488 in β-S109C/Q299C/R103S-$(AF488)_2$ slowly drifts up with time (compare the experimental grey trace to solid red line representing a constant signal). At high concentrations of $\gamma_{cx}$ where the majority of b-S109C/Q299C/R103S-$(AF488)_2$ was bound (e.g. 200 nM $\gamma_{cx}$), this drift in fluorescence did not occur presumably because the clamp loader held both monomers of the dimer together in the complex even though the interface was destabilized by the R103S mutation and 500 mM NaCl.

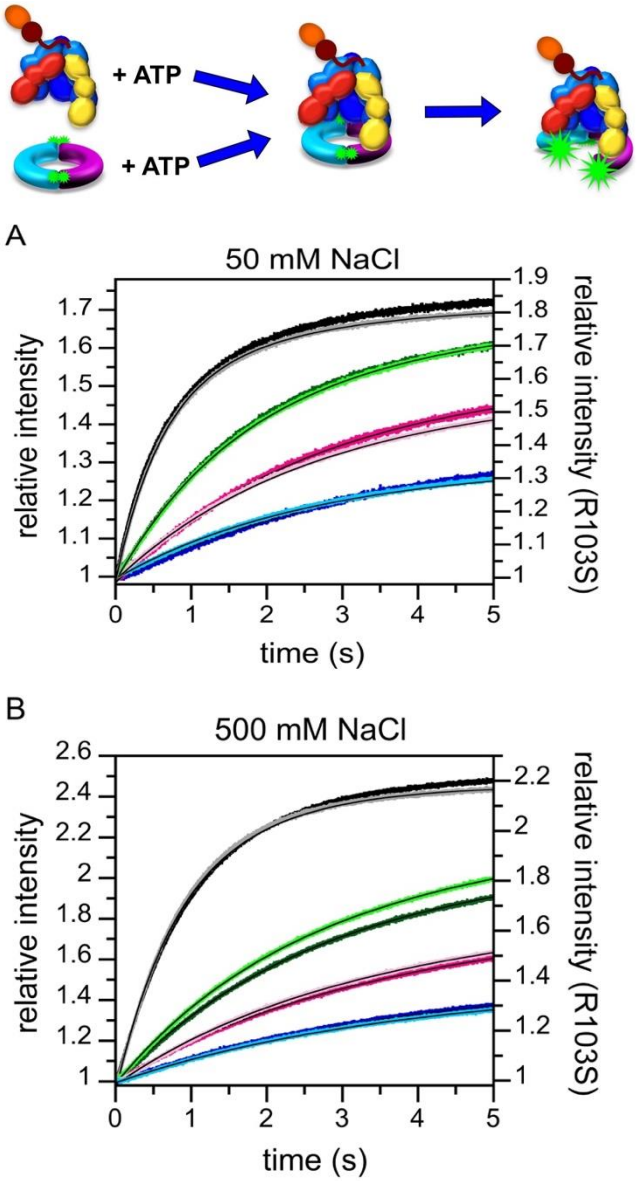


Figure 3-4. Clamp loader-clamp binding/opening reactions at 20°C. The increase in AF488 fluorescence that occurs when $\gamma_{cx}$ binds β-$(AF488)_2$ to form an open complex was measured as a function of time when a solution of γ complex and ATP (0.5 mM) in stopped-flow assay buffer was added to a solution of β-S109C/Q299C-$(AF488)_2$ (dark colors) or β-S109C/Q299C/R103S-$(AF488)_2$ (light colors) and ATP (0.5 mM) in stopped-flow assay buffer. The concentration of $\gamma_{cx}$ was varied and the concentration of β was held constant at 20 nM. Representative reactions are shown that contain 10 nM (blue), 20 nM (magenta), 40 nM (green) or 160 nM (black/gray) $\gamma_{cx}$ and A. 50 mM NaCl or B. 500 mM NaCl

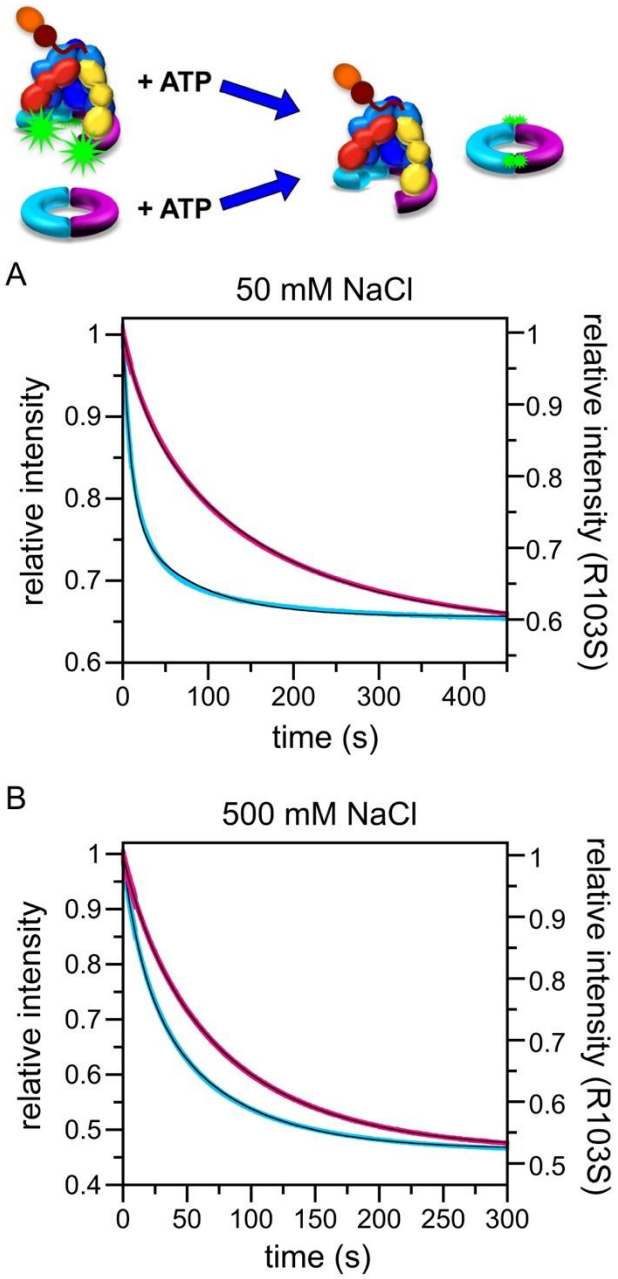


Figure 3-5. Clamp loader-clamp dissociation reactions at 20 °C. The decrease in fluorescence that occurs when β-$(AF488)_2$ dissociates from $\gamma_{cx}$ was measured in assays containing 40 nM $\gamma_{cx}$, 10 nM β-S109C/Q299C-$(AF488)_2$ (cyan) or β-S109C/Q299C/R103S-$(AF488)_2$ (magenta), 400 nM unlabeled β, and 0.5 mM ATP in buffer with A. 50 mM NaCl or B. 500 mM NaCl. Data were fit to the sum of two exponentials (black lines through traces), and rate constants and fractional amplitudes derived from fits are given in Table 3-2.

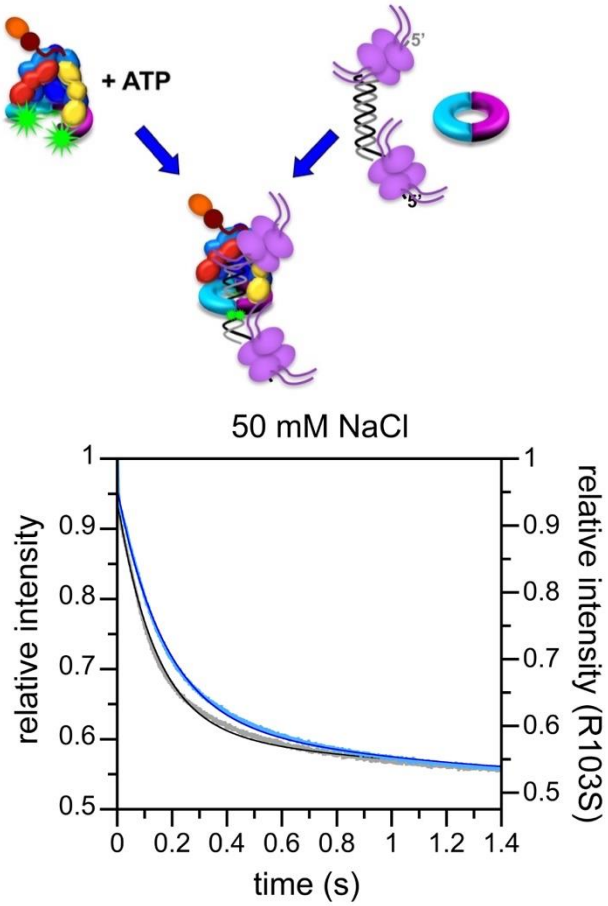


Figure 3-6. Clamp loading on DNA bound by SSB at 20°C. The decrease in AF488 fluorescence that occurs when clamps are closed on DNA was measured in stopped-flow reactions in which a solution of $\gamma_{cx}$, β-$(AF488)_2$, and ATP were mixed with a solution of SSB-bound DNA and excess unlabeled β. DNA is symmetrical, as illustrated, with two 30-nt single-stranded 5' DNA overhangs and a 30-nt duplex. Final concentrations were 20 nM β-S109C/Q299C-$(AF488)_2$ or β-S109C/Q299C/R103S-$(AF488)_2$, 20nM $\gamma_{cx}$, 200 nM unlabeled β, 160 nM DNA, 960 nM SSB, and 0.5 mM ATP in stopped-flow assay buffer containing 50 mM NaCl.

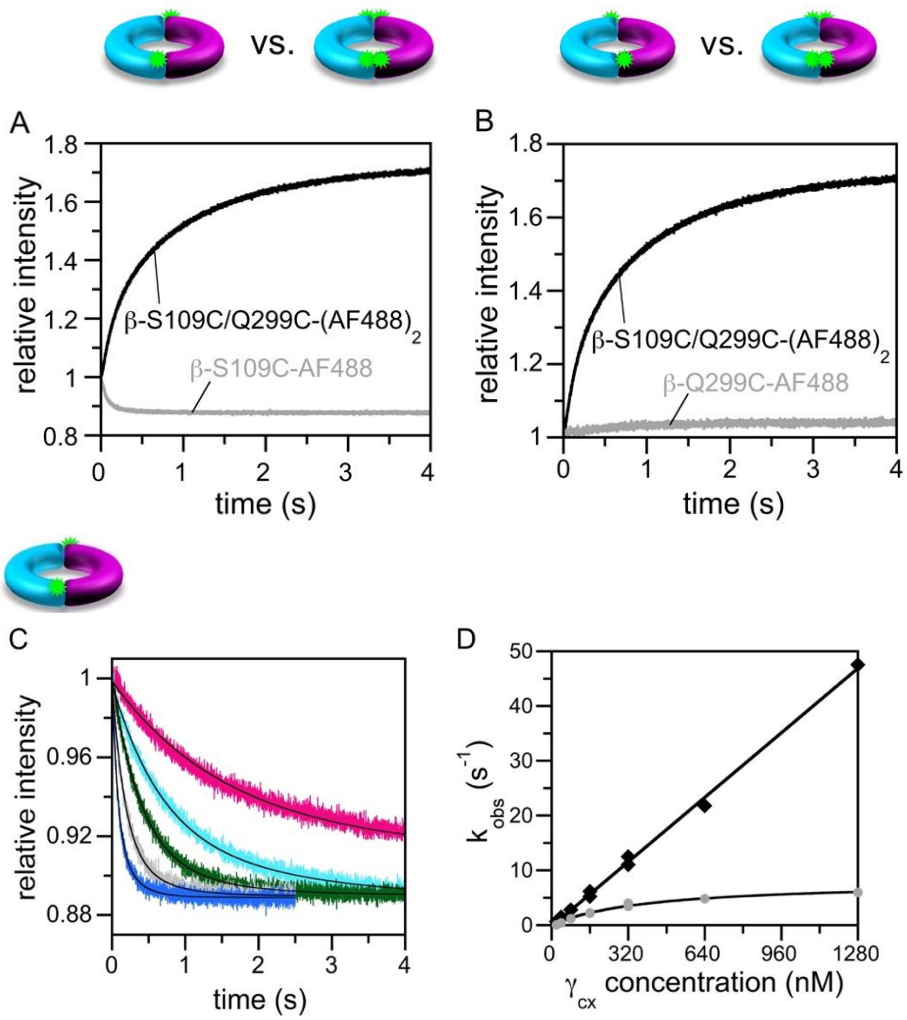


Figure 3-7. $\gamma_{cx}$ binding to singly AF488-labeled clamps affects AF488 fluorescence. Binding reactions were measured side-by-side in stopped-flow experiments for β-S109C/Q299C-$(AF488)_2$, β-S109C-AF488, and β-Q299C-AF488. Fluorescence intensity is plotted relative to the signal for unbound clamp in each case, but note the absolute fluorescence for singly-labeled clamps is greater than for the doubly-labeled clamp because there is no AF488-dimer quenching. **A.** Clamp binding for β-S109C/Q299C-$(AF488)_2$ (black) vs β-S109C-AF488 (grey) is shown. **B.** Clamp binding for β-S109C/Q299C-$(AF488)_2$ (black) vs β-Q299C-AF488 (grey) is shown. **C.** Rates of $\gamma_{cx}$ binding to β-S109C-AF488 was measured in reactions containing 20 nM β-S109C-AF488, 0.5 mM ATP, and 10 (magenta), 20 (light blue), 40 (black), 80 (green), 160 (gray) and 320 (dark blue) nM $\gamma_{cx}$ in stopped-flow assay buffer containing 50 mM NaCl. **D.** Time courses from panel C were fit to double exponentials, and observed rate constants for the rapid (black) and slow (gray) phases obtained from the fit are plotted as a function of $\gamma_{cx}$ concentration.

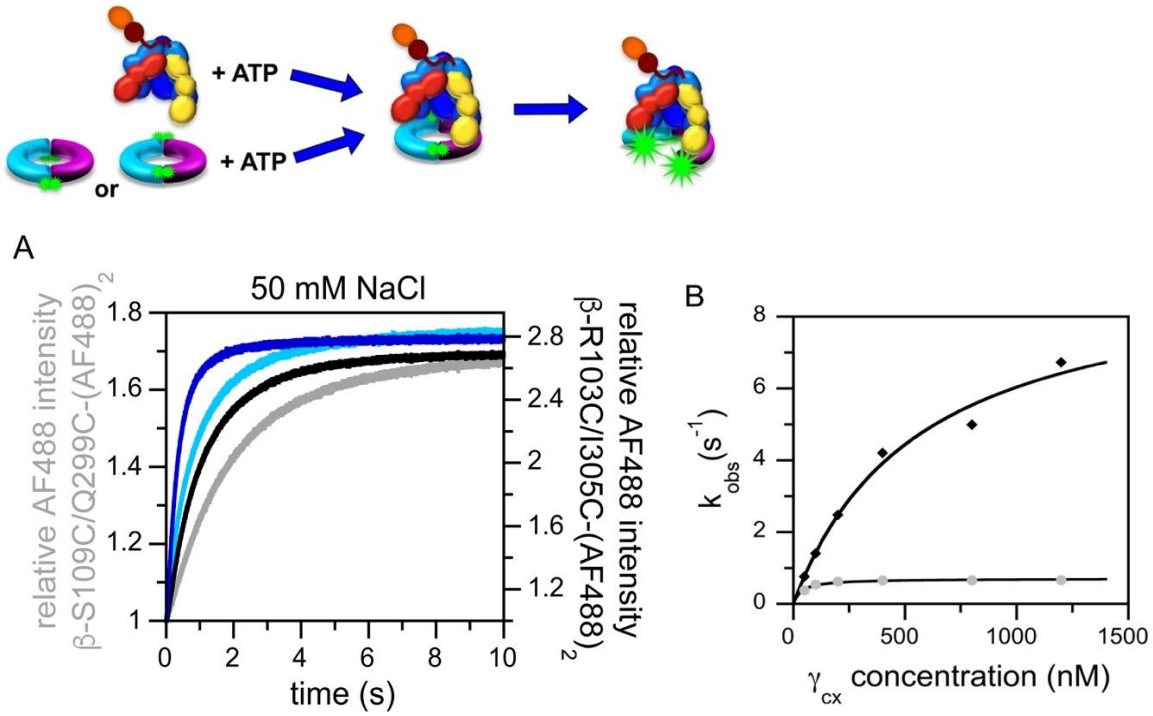


Figure 3-8. Clamp loader-catalyzed opening reactions are shown for β-S109C/Q299C-$(AF488)_2$ and β-R103C/I305C-$(AF488)_2$. Using a stopped-flow fluorimeter, a solution of the clamp loader ($\gamma_{cx}$) and ATP (0.5 mM) was mixed with a solution of β-S109C/Q299C-$(AF488)_2$ or β-R103C/I305C-$(AF488)_2$ (20 nM final concentration) and ATP (0.5 mM) at 20°C. Time-based fluorescence emission was measured at 520 nm for 10 s while exciting at 490 nm. **A.** Representative traces for β-S109C/Q299C-$(AF488)_2$ (light colors) and b-R103C/I305C-$(AF488)_2$ (dark colors) at $\gamma_{cx}$ concentrations of 40 (gray) and 160 nM (blue) are shown. Note that the y-axis scales are different for the two different clamps. The difference in time courses for β-S109C/Q299C-$(AF488)_2$ and β-R103C/I305C-$(AF488)_2$ is due to additional environmental effects on AF488 fluorescence in the β-S109C/Q299C-$(AF488)_2$ construct where the fluorophores are located on the face of the clamp to which the clamp loader binds (Figure 1). The AF488 covalently attached to Cys-109 decreases in fluorescence when the clamp is bound by $\gamma_{cx}$ (Figure 6), and this dampens the rate of increase in fluorescence due to opening the clamp and separating AF488 dimers. **B.** Time courses β-S109C/Q299C-$(AF488)_2$ were fit to a double exponential rise and rate constants ($k_{obs}$) for the rapid and slow phases are plotted as a function of $\gamma_{cx}$ concentration and fit to rectangular hyperbolas to calculate maximal rates.

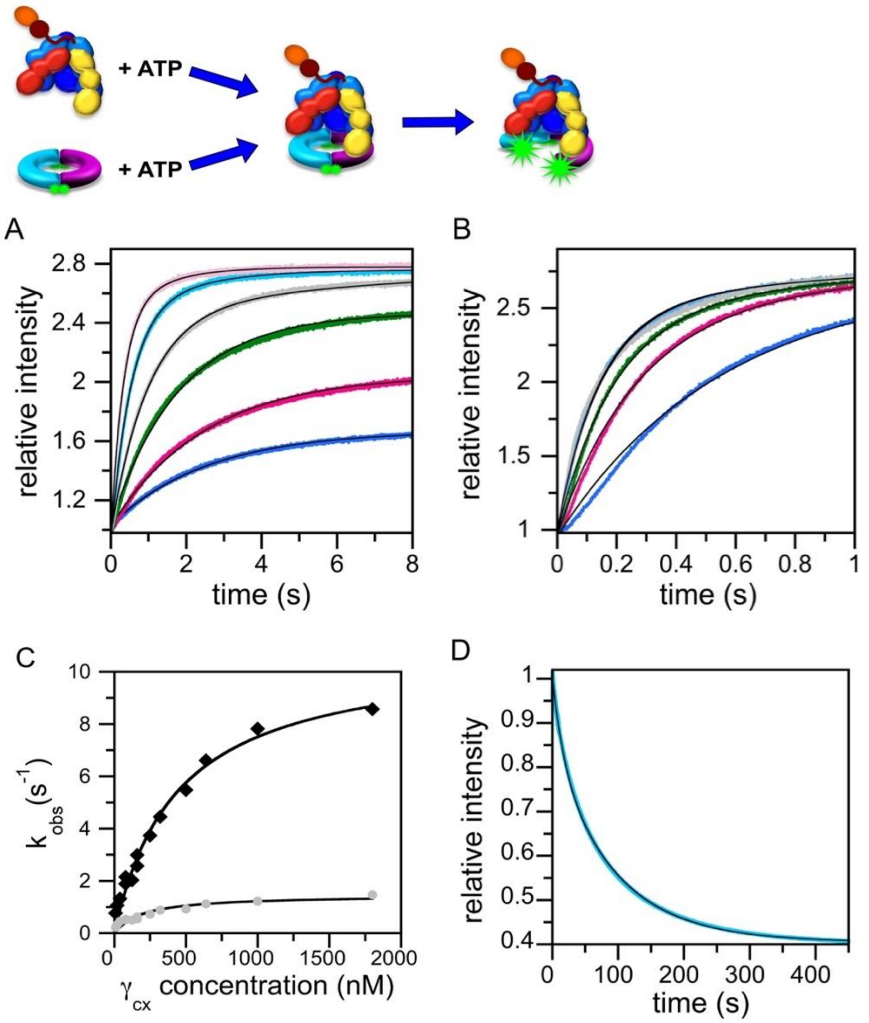


Figure 3-9. Kinetic model for clamp loader-catalyzed clamp opening reactions based on β-R103C/I305C-$(AF488)_2$ opening reactions. Clamp opening reactions were performed in stopped-flow experiments by mixing a solution of $\gamma_{cx}$ and ATP with a solution of β-R103C/I305C-$(AF488)_2$ and ATP. Representative time courses are shown for final $\gamma_{cx}$ concentrations of A) 5 (dark blue), 10 (magenta), 20 (dark green), 40 (grey), 80 (light blue), and 160 (pink) nM and B) 125 (blue), 250 (magenta), 500 (green), 1000 (light blue), and 1800 nM (grey) along with 16 nM β-R103C/I305C-$(AF488)_2$ and 0.5 mM ATP in stopped-flow assay buffer containing 50 mM NaCl. C) Time courses for clamp opening were fit to double exponentials, and observed rate constants for the rapid (black) and slow (gray) phases obtained from the fit are plotted as a function of $\gamma_{cx}$ concentration. Data were fit to a rectangular hyperbola to calculate maximal rates, $k_{max,fast}$ = 11 $s^{-1}$ and $k_{max,slow}$ = 1.5 $s^{-1}$, for the fast and slow phases, respectively. D) Clamp loader-clamp dissociation was measured in assays containing 40nM $\gamma_{cx}$, 20 nM β-R103C/I305C-$(AF488)_2$, 400nM unlabeled β, and 0.5 mM ATP and fit to a double exponential decay.

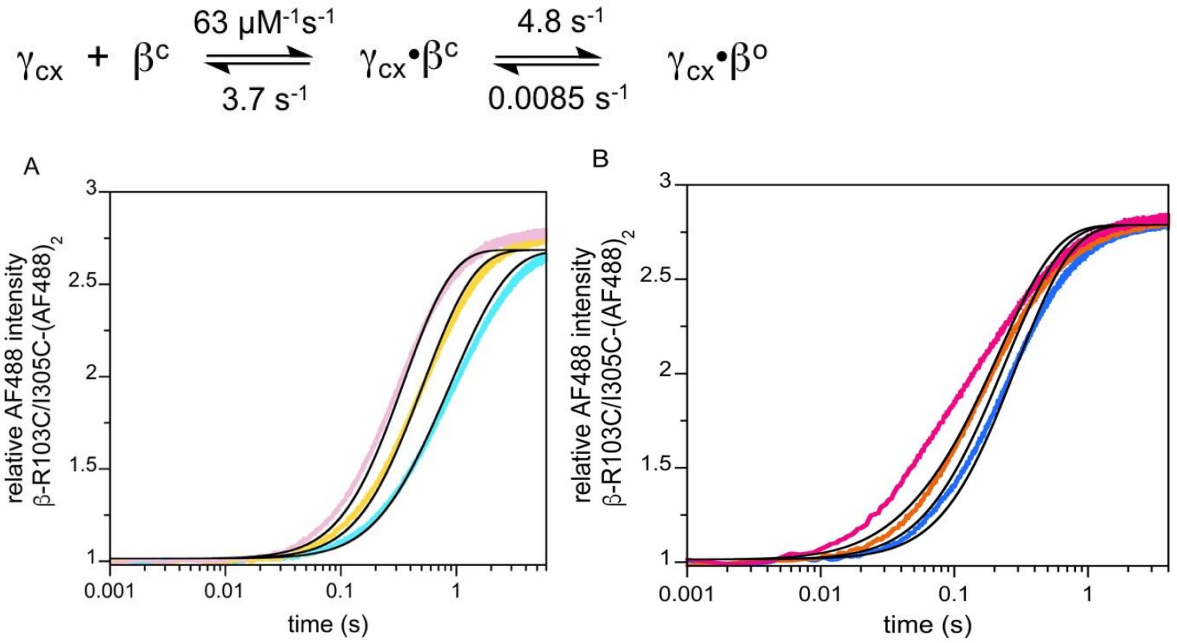


Figure 3-10. Clamp binding reaction time courses and clamp opening time courses were globally fit (using KinTek Explorer) to the two-step binding and opening model shown in the reaction scheme. Representative clamp opening reaction time courses and fits (black lines) are shown for reactions containing A. low concentrations, 40 (cyan), 80 (yellow), and 160 nM (pink) of $\gamma_{cx}$ or B. high concentration 250 (blue), 500 (orange), and 1800 nM of $\gamma_{cx}$ along with 10 nM β-R103C/I305C-$(AF488)_2$ and 0.5 mM ATP. Rate constants calculated from fits are reported in the model scheme. This two-step model does not fit the data well. The fits of the data tend to increase more slowly than the data at early times and faster than the data at longer times. In addition, the second order rate constant calculated for the binding step ($6.3 \times 10^7\ M^{-1}s^{-1}$) is almost twice as the value estimated from a linear fit ($3.7 \times 10^7\ M^{-1}s^{-1}$) of a plot of the observed on-rate as a function of $\gamma_{cx}$ concentration in Figure 7D. Based on the relatively poor fit of the data to the two-step model and the observation that dissociation reactions were biphasic an additional open state was added to the model.

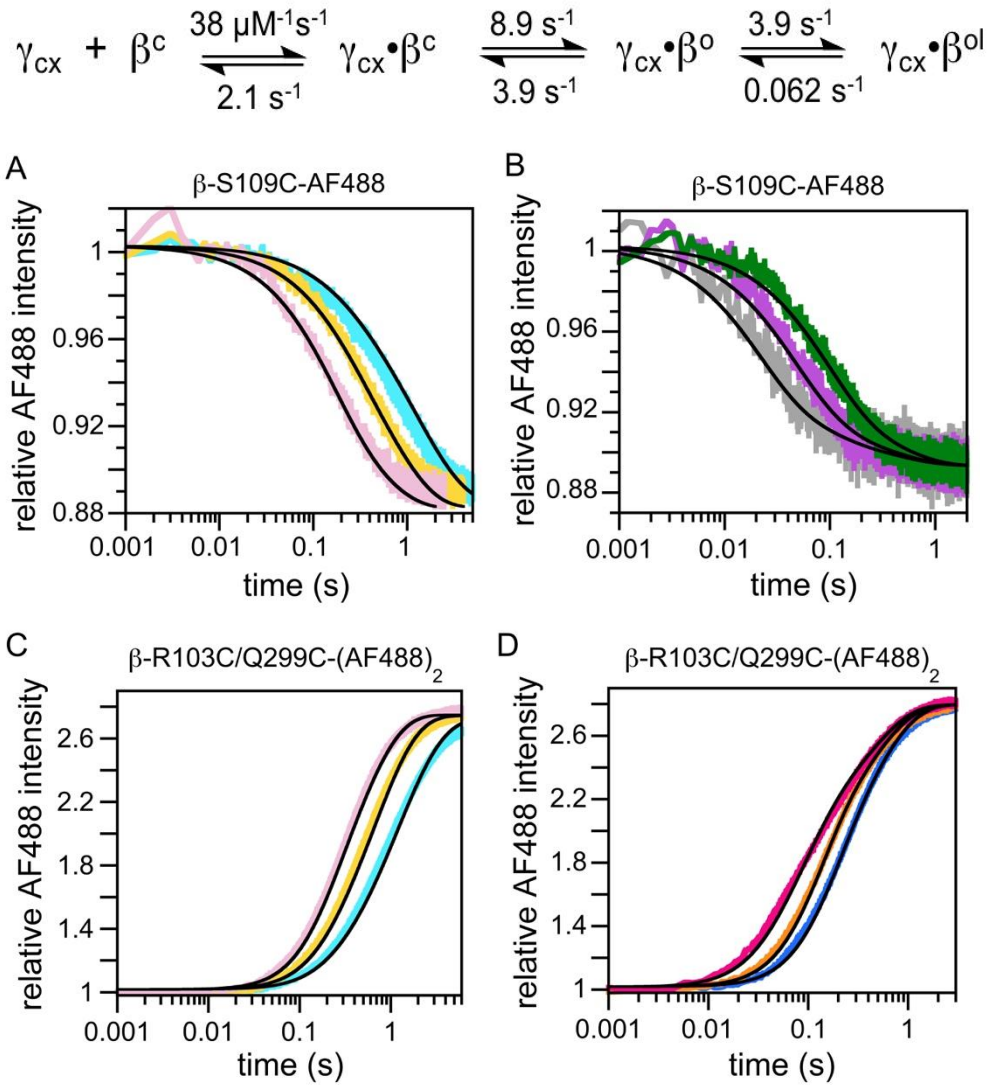


Figure 3-11. Clamp loader binding to β-S109C-AF488 and opening β-R103C/Q299C-(AF488)$_2$ were fit to the model shown in the scheme. *Upper panels* show β-S109C-AF488 binding reactions and *lower panels* show β-R103C/Q299C-(AF488)$_2$ opening reactions at 6 representative concentrations. Black lines through the data are the result of the fit of the model with rate constants shown in the scheme. Clamp binding reactions containing A. 40 (cyan), 80 (gold), and 160 nM $\gamma_{cx}$ or B. 320 (green), 640 (purple), and 1280 nM $\gamma_{cx}$ are shown. Clamp opening reactions containing C. 40 (cyan), 80 (gold), and 160 nM $\gamma_{cx}$ or 250 (blue), 500 (orange), and 1800 nM (red) $\gamma_{cx}$ are shown.

Table 3-1. β mutants and nomenclature.

| β Designation | Mutations |
|---|---|
| β-S109C-AF488[a] | C260S + C333S + S109C |
| β-Q299C-AF488 | C260S + C333S + Q299C |
| β-S109C/Q299C-$(AF488)_2$ | C260S + C333S + S109C + Q299C |
| β-S109C/Q299C/R103S-$(AF488)_2$ | C260S + C333S + S109C + Q299C + R103S |
| β-R103S/I305C-$(AF488)_2$ | C260S + C333S + R103C + I305C |

[a]Cys residues are labeled with Alexa Fluor 488 maleimide (AF488).

Table 3-2. Clamp loader-clamp dissociation rate constants and amplitudes.

| | 50 mM NaCl | | | | 500 mM NaCl | | | |
|---|---|---|---|---|---|---|---|---|
| | $a_f$[a] | $k_f$ ($s^{-1}$)[b] | $a_s$ | $k_s$ ($s^{-1}$) | $a_f$ | $k_f$ ($s^{-1}$) | $a_s$ | $k_s$ ($s^{-1}$) |
| β-S109C/Q299C-$(AF488)_2$ | 0.66 | 0.1 | 0.34 | 0.013 | 0.38 | 0.064 | 0.62 | 0.015 |
| β-S109C/Q299C R103S-$(AF488)_2$ | 0.23 | 0.039 | 0.77 | 0.0098 | 0.18 | 0.046 | 0.82 | 0.012 |
| β-R103S/I305C-$(AF488)_2$ | 0.28 | 0.058 | 0.72 | 0.011 | | | | |

[a]$a_f$ and $a_s$ are fractional amplitudes for fast and slow phases, respectively.
[b]$k_f$ and $k_s$ are rate constants for fast and slow phases, respectively.

Table 3-3. Maximal rates for rapid and slow phases of clamp opening reactions.

| Doubly-labeled clamp | $k_{max,fast}$ ($s^{-1}$) | $k_{max,slow}$ ($s^{-1}$) |
|---|---|---|
| β-S109C/Q299C-$(AF488)_2$ | 8 | 0.7 |
| β-R103C/I305C-$(AF488)_2$[a] | 11 | 1.5 |
| β-R103C/I305C-$(AF488)_2$[b] | 9 | 0.8 |

[a]From Figure 3-9

[b]From Paschall *et al*. (2011)

# CHAPTER 4
# EXAMINING THE FUNCTIONS OF THE TWO *E. COLI* CLAMP LOADERS

## Background

Pol III holoenzyme contains DNA polymerase III, the β-sliding clamp, and a DnaX clamp-loader complex (106). This holoenzyme complex is the core of the replication forks and is the epicenter of DNA replication. The role of the DnaX clamp loader is to load the β-sliding clamp on DNA. *E. coli* DnaX clamp-loader complex is composed of seven subunits, one δ, one δ', one χ, one ψ, and three DnaX subunits (38, 99, 159). In *E. coli*, the gene *dnaX* encodes both the γ and τ subunits. The τ subunit is the full *dnaX* gene product (71 kDa) while the γ subunit is a truncated form of the full gene product (47 kDa) (55). This shortened γ subunit is produced through a programmed ribosomal frameshift that occurs during translation and causes the ribosome to shift the reading frame by -1 which results in the ribosome reading a premature stop codon (55, 56). The two *dnaX* gene products are produced at equal amounts (160). Both products of the *dnaX* gene have the ability to load the sliding clamp onto DNA through an ATP dependent process and to interact with other DnaX subunits, δ, δ', χ and φ (64, 67). The C-terminal region of τ, that is not present in γ, has been shown to interact with the DnaB helicase and the leading and lagging strand Pol III to coordinate actions at the replication fork (161). This coordination is particularly important on the lagging strand of DNA synthesis where clamps are loaded onto the primer at the beginning of an Okazaki fragment and polymerases are recycled from one fragment to the next (4, 162).

There continues to be a debate in the field on which the DnaX subunits comprise the physiological relevant clamp loader in *E. coli*. It is widely accepted that the clamp loader at the heart of the replication fork contains at least two τ subunits each of which

bind to polymerase III (162, 163). The debate lies on whether the third DnaX subunit in the clamp loader contains either another τ subunit attached to a third polymerase, or if the third DnaX subunit is a γ subunit. Evidence for a third τ subunit include *in vivo* fluorescence spectroscopy experiments that used chromosomally expressed fluorescently tagged proteins to show there are approximately three α and three τ subunits at a replication fork (58). In addition, studies have shown that *in vitro* clamp loader complex with three γ or τ subunits is preferentially formed and not a mix of γ and τ (50). To obtain complexes with both γ and τ subunits, a special procedure must be performed which involves a very long incubation period of γ and τ together before any of the other complex subunits are added, which does not occur *in vivo* (59). It has been suggested, though, that the τ subunit may interact with pol III before association with the other clamp loader subunits which could be important for the formation of a clamp loader with two τ and one γ subunit (164). Another study demonstrated through the use of single-molecule studies that a replication fork with the all τ clamp loader with three polymerases had greater processivity and increased lagging-strand synthesis efficiency (22). On the other hand, there has also been evidence for a clamp loader with two τ subunits with one γ complex subunit. Binding studies showed that γ, not τ, interacted with the φ subunit, which is important for SSB interactions and clamp loader stability suggesting that at least one γ subunit must be present at the replication fork (61, 97). More recently, one study isolated clamp loader complexes that contained two τ and one γ subunits from cells which expressed τ from the chromosomal gene and γ with a biotinylated tag from a plasmid suggesting that *in vivo* this is the preferred form of the clamp loader (60).

The one common theme for both of these models is that the role for γ is unknown. If the clamp loader contains three τ subunits, then what is the function of the γ subunit? If the clamp loader contains two τ subunits, then what is the function of the one γ subunit and how is this stoichiometry maintained? It was observed that τ, not γ, is required for cell viability (63). While it could be hypothesized that γ is an evolutionary artifact, γ is found in many organisms besides *E. coli,* including *Thermus thermophiles* (165, 166). These studies suggest that there is a real function for γ within the cells. Only one study has found a sensitivity of the τ only *dnaX* strain towards UV light (60), but the construction of the strains used in this study may have interfered with the expression of *recR,* which plays a role in UV-induced DNA damage repair and has a promoter within the *dnaX* gene (167). Thus, the question of what γ does *in vivo* still remains and is the subject of this chapter.

While examining what happens when the replication fork comes across DNA damage and stalls, Goldfless *et al*. uncovered a possible novel role for γ-complex (78). They were specifically investigating a template-switching pathway that is dependent on DnaK, a heat-shock protein. Template-switching is a mechanism the cell uses to promote error-free replication around a site of DNA damage. During template-switching the nascent daughter DNA strands pair together to allow DNA synthesis past the site of the DNA lesion. After the nascent strand has extended past the site of the DNA damage, the strand is unpaired from the daughter strand and resumes DNA synthesis using the original template strand (78). Post-replication repair may follow to fix the site of DNA damage. One caveat of template-switching is that when there are repeated sequences at the location where the nascent daughter stands pair, the DNA strands

may not align properly and this can cause duplications or deletions of the homologous regions (78). Using this artifact, cells can be screened for enhancement or repression of template-switching by measuring deletion rates in repeated sequences. In the Goldfless *et al*. study they constructed an assay to screen for template-switching. Using this assay they found that a cell line with a mutation in the *dnaX* gene, *dnaX2016*, was deficient in DnaK-dependent template-switching (78). Originally characterized in the 1970's, the cell line *dnaX2016* is temperature sensitive and at non-permissive temperatures (42°C) DNA synthesis is immediately inhibited (168). Inhibition of DNA synthesis in this cell line can be reversed when reducing the temperature to the permissive temperature (30°C), suggesting that the inhibition of DNA synthesis is due to the DnaX protein becoming denatured at the higher temperatures (169). The *dnaX2016* cell line encodes three amino acid substitutions present in both the γ and τ subunits: G118D, G212D, and A400T (170). Cells with a mutation in the *dnaK* gene and the *dnaX2016* mutation were epistatic, suggesting DnaK and DnaX work in the same template-switching pathway. While screening for suppressors of the mutant DnaK phenotype, a suppressor was found that had one copy of wild-type *dnaX* but also had an additional partial copy of the *dnaX* gene that only encoded for γ–complex (170). Cells deficient in template-switching, like *dnaX2016*, are sensitive to exposure of AZT. It was found that exposure to AZT, a nucleotide analog that blocks DNA synthesis, promoted template-switching in E. coli cells (171). To determine if either wild-type γ or τ restores template-switching in *dnaX2016*, AZT was used to screen for complementation. It was found that when a plasmid expressing wild-type γ subunit is introduced to the *dnaX2016* cell line, template-switching repair is restored. When full-length dnaX is expressed in the cell line, the

template-switching repair is not restored (170). This study suggests that γ is required in this template-switching pathway, agreeing with the hypothesis that γ and τ have two different and essential roles in the cell.

The DnaX2016 proteins are particularly interesting because this is an example of a deficient but not dead mutant. The *dnaX2016* cells cannot perform template-switching repair, but must be able to perform DNA replication because these cells are viable at the permissive temperature. Understanding why these mutations cause deficiencies in template-switching but allow, to some extent, DNA synthesis could prove helpful in characterizing the different cellular functions of γ and τ complexes.

Before it was known that the *dnaX2016* gene actually had a total of three mutations it was thought that *dnaX2016* only had one mutation, which corresponded to an amino acid substitution, G118D (63). The DNA sequencing corresponding to the G118D mutation was originally identified through marker rescue, which consisted of taking sections of the wild-type gene and introducing them into the *dnaX2016* cells to determine which sections restore the wild-type phenotype (can grow at the nonpermissive temperature). Depending on which section of the gene was introduced into the cell line that rescued the temperature sensitivity, the approximate location of the mutation was determined and sequencing would be feasible at that point. Through sequencing, it was determined that the region with the mutation encoded for an amino acid substitution of G118D. DNA sequencing of the whole gene was not feasible at the time of this study, so it is unknown if the other two mutations were present in this line or if these mutations developed in this strain at a later point. To investigate what effect the G118D mutation had on the DnaX proteins, γ with the G118D mutation was purified

and characterized by various biochemical assays. Previously, our laboratory created the G118D γ-complex by performing site-directed mutagenesis (SDM) to mutate the glycine at position 118 to aspartic acid (172). The same purification protocol used to purify wild-type DnaX subunit was used for the G118D mutant, expect that expression of the mutant was performed at the permissive temperature of 20°C. It was noted that the mutant behaved quite differently from wild-type DnaX. One step of the wild-type γ-complex purification protocol that was attempted with theDnaX2016 mutant was an ATP agarose step. While wild-type γ-complex tightly binds to the ATP agarose, the mutant did not bind to the column at all. This suggested that there was a deficiency in ATP binding. To test ATP binding more directly, a fluorescence-based assay was performed using TNP-ATP (2',3'-O-(2,4,6-trinitrophenyl) adenosine-5'-triphosphate), which is a fluorescent analog of ATP. Various amounts of γ-complex were titrated into TNP-ATP and the change in fluorescence was measured by a fluorimeter. When γ-complex binds the TNP-ATP, the fluorimeter would read an increase in fluorescence due to the change of the fluorophores' environment. When this experiment was performed with DnaX2016 γ-complex the mutant complex was deficient in ATP binding when compared to wild-type γ-complex. This result was interesting because ATP binding is necessary for the clamp loader to perform the clamp loading reaction. Without the ability to perform ATP binding, it would be expected that dnaX2016 cells are not viable because τ would not be able to do its required role in the cell for viability. This would suggest that either we are missing something, or the activity of the τ complex differs

from γ complex such that the requirements for ATP differ for the τ complex or the mutation does not have the same effect on the τ complex.

Recently, when sequencing of the whole *dnaX2016* gene was completed, not one, but four mutations were found (170). The *dnaX2016* cell line encodes three amino acid substitutions present in both the γ and τ subunits: G118D, G212D, and A400T (Figure 4-1) (170). Originally, through marker rescue of the temperature sensitivity, only the G118D mutation was found (63). It may be that the G118D mutation is largely responsible for the temperature sensitivity and the other mutations induce other defects of this mutant, like the inability to perform template-switching. This could explain why the marker rescue only identified the G118D mutation. Because the *dnaX2016* cells are viable, just deficient in template-switching repair, it is hypothesized that these clamp loaders should have some clamp loading ability unlike the single G118D mutant which, according to the results of the preliminary studies, cannot perform clamp loading.

## Results

### DnaX2016 Subunits Aggregate and are Unable to Form Clamp Loader Complexes

The results with the G118D mutation were surprising because the *dnaX2016* cells are temperature sensitive yet viable, but according to our laboratory's biochemical assays the G118D γ-complex was not efficient in any of the clamp loading reactions. Knowing now that there are two additional mutations (G212D and A400T) (Figure 4-1), these mutations may restore some clamp loading ability to the G118D mutant. To understand what effects the DnaX2016 (G118D, G212D, and A400T) mutations have on the clamp loaders, the DnaX2016 γ and τ proteins were purified to characterize them using *in vitro* assays (Chapter 2). The template that was used to create the DnaX2016 encoding gene was the *dnaX* gene that had been cloned into a pBS-SK(+) vector from

chromosomal DNA. In order to produce only γ, the 3' end of the *dnaX* gene was removed and one codon was added. To produce τ only, the poly-A region of the frameshift was interrupted through SDM to AAG AAA, preventing the frameshift that produces γ, but keeping the amino acid sequence of τ intact. To produce either DnaX2016 γ or τ, these genes were mutated through the use of SDM to produce the amino acid substitutions G118D, G212D, and A400T. These γ or τ only genes were cloned into pET52b-(+) vectors (Novagen) between the NcoI and SacI sites. The pET52b-(+) vectors have a C-terminal His-tag that was utilized for purification purposes, to allow selection of the DnaX2016 subunits and preventing wild-type contamination. This plasmid was then transformed into BL21(DE3) competent *E. coli* cells, which are ideal for bulk protein expression. The temperature of the incubator during expression was kept at 20°C for the period because functional DnaX2016 proteins could not be made at non-permissive temperatures (169).

For further purification and to determine the molecular weight of DnaX2016-γ or-τ, after purification with a HisTrap Column (GE Helathcare) the proteins were loaded onto a Superose 12 10/300 size exclusion column. In size exclusion columns, large proteins elute before smaller proteins. By running BioRad Gel Filtration standards on the size exclusion column and creating a standard curve of the molecular weight versus elution volume, the molecular weights of the DnaX2016 proteins were calculated. Wild-type γ and τ have been shown to form tetramers in solution (163). Wild-type γ eluted from the superose column in a volume corresponding to the size of a tetramer (about 190 kDa) (Table 4-2). With the DnaX2016 γ and τ proteins though, the subunits eluted from the size exclusion column in a volume corresponding to the equivalent of 16 (about

760 kDa) and 13 subunits (about 930 kDa), respectively. These elution volumes were at the edge of the void volume, meaning the molecular weights could not be determined accurately and are just estimates. Addition of high salt concentrations or nonionic detergents did not affect the oligomeric state of the DnaX2016 proteins. Due to the fact that wild-type DnaX subunits do not form these high-ordered oligomers, it was concluded that one or more of the DnaX2016 mutations are causing this large oligomerization. This observation is quite interesting because a mutation in the heat-shock protein, DnaK, and the mutations in the *dnaX2016* gene are epistatic (78).

From the preliminary data with the G118D mutant, it was known that the G118D mutation affected the ability of the clamp loader to bind ATP. For an indirect analysis of ATP binding with the DnaX2016 mutants, during the protein purification, a fraction of the protein was loaded onto an ATP agarose column to determine if this mutant would bind to the column. When DnaX2016 γ was loaded onto the column, the protein washed through the column without binding suggesting a defect in ATP binding. But, when high salt was introduced to the column to elute any remaining protein, some of the DnaX2016 γ also eluted here. These results would suggest that there is a deficiency but there is still some ATP binding, unlike clamp loaders with only G118D. This is expected since the dnaX2016 cells are viable and ATP binding is required for the clamp loading reaction. This data is very much still preliminary since the high-ordered oligomerization of the DnaX2016 subunits could be affecting the ability to bind ATP agarose. Once the DnaX2016 subunits are reconstituted into clamp loader

complex, direct analysis of ATP binding can be performed to determine if the DnaX2016 mutants differ from the G118D mutants.

The purified DnaX2016 subunits were used in a reconstitution reaction to determine if the subunits could form clamp loader complexes. The reconstitution reaction is described in detail in Chapter 2, but briefly, all of the clamp loader subunits (DnaX2016 τ or γ, δ, δ', χ, and φ) are sequentially mixed together to form clamp loader complex then purified from unincorporated subunits by anion-exchange chromatography on a MonoQ (GE Healthcare) column. When either of the DnaX2016 clamp loaders were used in the reaction, the proteins precipitated out of solution. Multiple buffer conditions were tested, but every time the DnaX2016 subunits were used in the reconstitution the proteins precipitated before analysis could be performed.

**Expression of Pol III****In Vivo***

Due to the extreme aggregation of the DnaX2016 subunits *in vitro,* an *in vivo* clamp loader expression system was constructed using Duet Vectors from Novagen. The hypothesis was that if all of the clamp loader subunits are expressed at once it may help with the DnaX2016 aggregation. Cells with only the DnaX2016 clamp loaders are viable at permissive temperatures, so there must be some clamp loader function within the cells because cells without the τ version of the clamp loader are not viable (63). Three different Duet Vectors were used; pET Duet, pCOLA Duet, and pCDF Duet Vectors. Each of these vectors have a unique origin of replication and an antibiotic resistance marker allowing all three vectors to be selectively expressed within the same cell. In addition, each Duet Vector contains two multiple cloning sites under the control of the *Lac* promoter. Figures 2-1,2, and 3 show the final vector maps. The pCOLA Duet Vector contained either the γ or the τ version of *dnaX* and *holA* (δ). The pET Duet

Vector contained *holB* (δ') and either *holD* (φ) alone or in an operon with *holC* (χ). Transforming these two vectors into BL21(DE3) cells allows expression of γ-complex, τ-complex, and even χ-less versions of the clamp loaders (used in Chapter 5). In addition, the pCDF Duet Vector contained the genes for Polymerase III; *DnaE* (α, the catalytic subunit) and *holE* (θ). Two amino acid substitutions (D12A and E14A) were introduced into the exonuclease subunit to remove the exonuclease activity through SDM (15), but still needs to be subcloned into the pCDF vector. Expression of the pCDF vector along with the other two vectors allows for the expression and purification of the Pol III* complex (3 τ clamp loader plus Polymerase III).

Before expressing DnaX2016 with the Duet Vector expression system, conditions of expression and purification were optimized with the wild-type clamp loaders. Previously, clamp loaders in our laboratory have been assembled via a reconstitution reaction (as explained in the above section on DnaX2016) after purification of the individual subunits separately. With this new *in vivo* expression system, purification of the entire clamp loader can be performed in a fraction of the time and with a fraction of the materials. In addition, the Duet Vector system makes it easy to create alterations to the genes for study, like the ability to make χ-less clamp loaders or the DnaX2016 clamp loaders. A previous study created a vector with the five clamp loader subunits for *in vivo* expression (173), but it would be very difficult to create different variants of the clamp loader with this system and it does not allow the expression of Polymerase III in the same cell as the Duet Vector system does. Chapter 2 describes in detail the purification procedure and Figure 2-5 shows a SDS-PAGE with the final complexes.

The wild-type clamp loader complexes were biochemically compared to clamp loaders that were reconstituted through the older method to determine if the clamp loaders functioned the same. Figure 4-2 shows the results of a clamp closing assay using γ-complex made through the old reconstitution method and γ-complex made using the Duet Vector system. The clamp loading assay is the same used in Figure 3-6. Clamp loading was tested on 5'DNA with and without SSB. As will be discussed in Chapter 5, clamp loaders load onto either 3' or 5'DNA, but SSB inhibits loading onto 5'DNA. Due to time and sample limitations, clamp closing on 3'DNA has yet to be performed. The clamp closing on the 5'DNA was measured first to determine if SSB regulates the clamp loading with pol III the same way it regulates the clamp loader alone. Pol III requires a 3' OH to extend the growing DNA strand, so it is expected that clamp closing on the correct DNA substrate, 3'DNA, will occur at a similar or possibly faster rate than the clamp loader alone. As seen in Figure 4-2, both of the clamp loader complexes load clamps onto the DNA substrate at the same rates both with and without SSB. In addition, in the following section, all of the assays were performed at least once with a clamp loader made through the reconstitution method and once with a clamp loader made through the Duet Vector system method to ensure the clamp loaders function exactly the same.

A sample of pol III* (τ-complex bound to pol III) made through the Duet Vector system was sent to the laboratory of Dr. Myron Goodman, whom graciously performed a primer extension assay to determine the activity of the protein complex (21). Figure 4-3 shows a denaturing polyacrylamide gel electrophoresis of reactions without polymerase (first two lanes), extension after 3 minutes (middle three lanes), and

extension after 10 minutes (last three lanes). As seen in the figure, pol III* extends the product to the full length already by the 3 min reaction. Polymerase IV, an SOS-induced error-prone DNA polymerase, was used as a control for the assays. Pol IV is not as processive and should lead to shorter extension products, as seen in the figure. The primer extension assay shows that the pol III* complex formed using the Duet Vector system is active.

**Biochemical Behavior of the Different *E. coli* Clamp Loader Variants**

Before examining the DnaX2016 clamp loaders, various fluorescence-based assays were used to compare wild-type γ and τ. While the role of the τ subunit as the replication fork organizer has been well established, the role of γ in the cell is unknown. Yet, in most clamp loader studies clamp loaders containing only γ is used as a model for both clamp loaders. For the research presented here, clamp loaders with the stoichiometry $\gamma_3\delta\delta'\chi\psi$ will be called γ–complex and clamp loaders with $\tau_3\delta\delta'\chi\psi$ will be called τ-complex. Purified clamp loader complexes are shown in Figure 2-5. A direct comparison of the clamp loaders kinetics has never been performed to determine if these two clamp loaders do indeed behave biochemically the same.

**The two DnaX clamp loaders have the same affinity for β**

Both γ- and τ-complex bind ATP which creates a high affinity for the sliding clamp (79, 80). Equilibrium clamp loader-clamp binding/opening was measured to determine whether γ- and τ-complex have similar or different affinities for the sliding clamp. For this assay, a doubly-labeled fluorescent clamp, β-R103C/I305C-$(AF488)_2$, was used. Briefly, β-R103C/I305C-$(AF488)_2$ has two AF488 fluorophores at the interface of where the clamp opens and closes, and when the clamp is closed there is relatively low fluorescence. When the clamp loader opens the sliding clamp, there is a relief of the

quench and the fluorescence increases (128). Each reaction occurred by sequentially adding to the cuvette assay buffer containing ATP to measure background signal, β-R103C/I305C-(AF488)$_2$ to measure the signal for unbound β, and then clamp loader to measure the signal for complex formation. Relative AF488 fluorescence was plotted as a function of clamp loader concentration (Figure 4-4). Data were fit to the two-state binding model (Figure 3-2) using a quadratic equation (Equation 2-2) to calculate apparent dissociation constants, $K_{d,app}$, of 9.4 and 8.0 nM γ- and τ-complex, respectively. More replicates with τ-complex will be needed for error analysis, but this preliminary assay shows that γ- and τ-complex have a similar affinity for the sliding clamp, with γ-complex having a slightly higher $K_{d,app}$.

**Pre-steady state clamp opening and loading kinetics are the same for γ- and τ-complex**

Even though the $K_{d,app}$ suggests that γ- and τ-complex have the same affinity for the sliding clamp, the kinetics of this reaction could be different. Fluorescence-based pre-steady state assays designed to measure the main steps in the clamp loading reaction were used to determine if γ- and τ-complex preform the whole clamp loading reaction kinetically the same. The main steps associated with ATP binding and hydrolysis are shown in Figure 1-4. First, clamp opening, which occurs once the clamp loader binds ATP, was measured in real time for reactions with γ- or τ-complex. For the clamp opening assay, the β-R103C/I305C-(AF488)$_2$ sliding clamp variant was used. The β-R103C/I305C-(AF488)$_2$ sliding clamp contains two AlexaFluor488 molecules at the interface of the two β monomers. When the clamp is closed, there is little fluorescence. As γ- or τ-complex is added to the reaction, the clamp loader with ATP bound then binds the sliding clamp and opens the sliding clamp causing an increase in

fluorescence. The change in fluorescence was monitored in real-time by a stopped-flow fluorimeter. A single mix reaction was used where clamp loader and ATP were mixed with a solution of β-R103C/I305C-$(AF488)_2$ and ATP, and the reaction was monitored over 10 seconds while collecting 1 point per millisecond. Final concentrations in the reactions were 20 nM γ-complex, 20 nM β-R103C/I305C-$(AF488)_2$, and 0.5 mM ATP. Figure 4-5 is a plot of the relative fluorescence over time for γ- and τ-complex. As seen in Figure 4-5, the clamp opening reaction kinetics is the same for γ- and τ-complex. This data combined with steady-state data shows that both γ- and τ-complex have the same affinity for the sliding clamp and opens the clamp at the same rate.

Secondly, ATP hydrolysis was measured for both γ- and τ-complex. When the clamp loader complex loads the open clamp onto a primer-template junction, the ATP bound to the DnaX subunits is hydrolyzed and then the clamp closes around the DNA. The site of ATP hydrolysis in the γ and τ DnaX subunits is within the region that is shared between the two DnaX products (174, 175). To determine if ATP hydrolysis occurs at similar rates for the two clamp loaders, an ATP hydrolysis assay was performed as described in Chapter 2. Briefly, when the clamp loader hydrolyzes and releases a $P_i$ molecule, MDCC-labeled phosphate binding protein (PBP) will bind the $P_i$ which causes an increase in fluorescence. Figure 4-6 shows representative ATP hydrolysis traces for assays with γ- (blue) or τ-complex (orange). Fluorescence data was converted into ATP hydrolyzed per clamp loader. As seen in the figure, there is a quick burst of ATP hydrolysis for the first 0.1s then the reaction moves into a steady-state cycle, as previously reported (84, 85, 89, 91). The γ- and τ-complex have the same burst and approximately the same steady-state rate, showing that ATP hydrolysis

kinetics are the same in clamp loading reactions with γ- or τ-complex. The τ-complex has a slightly slower steady-state rate, but this may but due to differences in the activity of the protein preparations.

After ATP hydrolysis, the clamp loader closes the siding clamp around the duplex portion of the primer-template junction (92). This clamp closing has been shown to be directed to the correct polarity DNA and inhibited on the incorrect polarity DNA by the single-stranded DNA binding protein, SSB (105). SSB is found on single-stranded DNA, primarily on the lagging strand of DNA replication where the DNA is synthesized in Okazaki fragments (see Chapter 1). DNA polymerase III requires a DNA or RNA primer with a 3' hydroxyl group to extend the DNA strand. SSB directs the clamp loader to primer-template junctions that have a free 3' hydroxyl group and inhibits the loading on primer-template junctions with 5' phosphate groups (105). The C-terminal tail of the τ subunit that is absent in γ has been shown to not only interact with the pol III catalytic subunit α, but also with helicase (75, 176). There could be potentially be additional interactions between SSB and τ-complex that enhance the regulation of clamp loading by SSB, which would be absent in γ-complex. To test this hypothesis, clamp closing of γ- and τ-complex was measured using the same β-R103C/I305C-$(AF488)_2$ sliding clamp used in the opening assay (Figure 4-5) and was performed as in Figure 4-3. A cartoon representation of the symmetrical DNA substrates used are shown in Figure 4-7. The DNA substrates have a 30nt duplex region with 30nt SSO on each end. The primer-template junction of the DNA substrates either contained a 3' hydroxyl group (3'DNA, correct polarity) or a 5' phosphate (5'DNA, incorrect polarity). As seen in Figure 4-7, the clamp closing reaction for both γ- and τ-complex on the 3' and 5' DNA substrates with

SSB are the same. This means that the regulation of clamp loading by SSB is directed through regions in common with both γ- or τ-complex (the focus of Chapter 5), which matches previous data showing that the stimulation of clamp loading on the correct polarity DNA is regulated by the interaction of SSB with the χ subunit (105).

While γ- and τ-complex are regulated in the same manner by SSB, *in vivo* the τ-complex is bound to at least two molecules on polymerase III (4, 163). It is possible that with polymerase III being in such close proximity to the sliding clamp during loading that it could change the kinetics of the clamp loading reaction. To determine if the presence of polymerase III has any effect on the clamp loading reaction, clamp loading of τ-complex bound to the α subunit of polymerase III produced through the Duet Vector expression system was compared to clamp closing with τ-complex alone. The same 5'DNA substrate as in Figure 4-7B was used with and without SSB. Previously, it has been shown that the clamp loader can load onto 5'DNA at a similar rate a 3'DNA unless SSB is present, in which SSB inhibits clamp loading. Results from the clamp loading assay are present in Figure 4-8. As seen in the figure, the clamp loading of τ-complex with and without polymerase III is the same whether SSB is present or not. Not only does this show that clamp loading is unaffected by the presence of polymerase III, but it also shows that SSB regulation of clamp loading holds true for τ-complex bound to polymerase III, the physiological relevant form of the clamp loader. Clamp loading with τ-complex bound to the α subunit of polymerase III still needs to be measured on 3'DNA (correct polarity) to determine if the presence of the α subunit has an effect on the clamp loading reaction.

Finally, the release of the sliding clamp by γ- and τ-complex was measured. After the clamp loader hydrolyzes the bound ATP and closes the clamp, the clamp loader has a low affinity for the sliding clamp and releases the sliding clamp, leaving it on the DNA (92). Clamp release was measured using a previously designed sliding clamp that is labeled with pyrene (PY) on the surface of β where the clamp loader binds (151). When the clamp loader is bound to β-Q299C-PY, the environment around PY causes it to fluoresce and when the clamp loader releases there is a decrease in fluorescence. Reactions were performed in a stopped-flow fluorimeter and were initiated by adding clamp loader complex, β-Q299C-PY, and ATP to a solution of DNA, ATP, and 10-fold excess unlabeled, which limited the observable reactions to a single-turnover. As seen in Figure 4-9, the rate of clamp release is the same for γ- and τ-complex. The results of the release assay combined with all of the other results presented here show that there is no difference in the kinetics of clamp loading between γ- and τ-complex. It would be interesting to compare rates of release from the clamp by the τ-complex with and without polymerase III. During DNA replication, once a sliding clamp is loaded, polymerase III replaces the bound clamp loader by binding to a hydrophobic pocket on the same side the clamp loader binds. The affinity of polymerase III for the sliding clamp may increase rates of release by the clamp loader, assisting with the efficiency especially on the lagging strand where Okazaki fragments are produce every 1-2s.

## Discussion

Multiple studies have previously examined whether the *in vivo* clamp loader contains a mixture of three DnaX subunits (two τ and one γ subunits) or if the clamp loaders contain a homotrimer of the DnaX subunits (three τ or three γ subunits). The debate on the composition of the clamp loader stems from the unknown function of the

γ subunit and whether the two τ one γ clamp loader is an artifact of proteolysis on isolation. *E. coli* strains without the τ subunit are not viable, reflecting the need for the τ subunit during DNA replication, while *E. coli* strains without the γ subunit are viable and have no abnormal phenotype detected (63). Only one study has found a sensitivity of the τ only *dnaX* strain towards UV light (60), but the construction of the strains used in this study may have interfered with the expression of *recR,* which plays a role in UV-induced DNA damage repair and has a promoter within the *dnaX* gene (167). The studies reported here attempt to give insight into the role of the γ subunit by studying the DnaX2016 clamp loader and by comparing the clamp loading reactions of wild-type γ/τ-complexes.

**DnaX2016 Subunits Cannot Form Complex *In Vitro***

Temperature sensitive *E. coli* strains *dnaX2016* have been shown to be deficient in the DNA repair template-switching pathway (78). Previously, it was thought that the *dnaX2016* gene contained one mutation which led to the amino acid substitution G118D (63). Previous work from our laboratory demonstrated that γ-complex with G118D results in a nonfunctional γ-complex that cannot bind ATP (172). With improved sequencing technology, it was determined that *dnaX2016* actually contains four mutations resulting in G118D, G212D, A400T amino acid substitutions and one silent mutation (170). Purification of this form of DnaX2016, described in this Chapter, resulted in a DnaX subunit that formed a high-ordered oligomer not seen with the wild-type DnaX. Both the γ and τ forms of DnaX2016 demonstrated this aggregation, independent of NaCl and detergent concentration. Additionally, when introduced to the other clamp loader subunits, both DnaX2016 γ and τ precipitated from solution and would not form clamp loader complex. This high-ordered oligomerization could influence

how γ and τ form complex with the other subunits. The lack of template-switching and the restoration of this repair pathway with the expression of wild-type γ may be related to the aggregation seen in the purification. In the cell, τ is bound to pol III α and has been hypothesized to bind to pol III before the additional clamp loader subunits meaning that the pathway for formation of the pol III holoenzyme may be different than that for forming clamp loaders without pol III (164). This clamp loader-polymerase interaction may sequester τ in a complex with pol III to inhibit aggregation of the τ allowing DnaX2016 clamp loader to form and perform essential roles. The polymerase-clamp loader interaction is absent in γ, so the aggregation may be preventing γ from being incorporated into the clamp loader complex and from performing the unknown role in template-switching repair, which would explain why wild-type γ expression restores template-switching (170).

In addition, the preliminary data suggests that the mutations may affect DnaX2016 clamp loader interaction with ATP. Interestingly, previous studies have shown that ATP hydrolysis by the DnaX clamp loader enhances loading of the sliding clamp, but it is not absolutely required in a mechanistic sense for formation of functional replication initiation complexes (177). The leading and lagging strand DNA replication coordination by τ is critical for complete and efficient replication. Even with the possible ATP binding/hydrolysis defects, clamp loaders with τ may be able to still form functional replication initiation complexes because the domain of τ that interacts with the helicase and pol III to coordinate the actions at the replication fork does not depend on ATP. It may be the case that clamp loaders with γ may involve loading and unloading of sliding clamps outside of the replication fork and these functions would be impaired if the

mutations affect the use of ATP by the clamp loader. This rationale may be able to explain why there is a lack of template-switching repair in cells with the *dnaX2016* mutation, but still retain the ability to perform replication at the permissive temperature. It is still unknown what the function of the clamp loader is in the template-switching pathway.

Further experiments will be performed with the DnaX2016 γ and τ subunits to determine if the aggregation state of these subunits affects its ability to form clamp loader complex with the other subunits (δ,δ', χ, ψ). An *in vivo* DnaX2016 clamp loader expression system was created using Duet Vectors. This expression system will allow expression of all clamp loader subunits in the same cells. Additionally, polymerase III can be expressed in the same cells expressing clamp loaders with τ. These expression vectors will be used to determine if clamp loaders with DnaX2016 γ and/or τ can be purified. Since τ has been shown to be essential for viability and *dnaX2016* cells are viable at the permissive temperature, it would be expected that τ can be incorporated into clamp loader complex when pol III is present. It is hypothesized that DnaX2016 γ, missing the interaction with pol III, will still aggregate *in vivo* and will not be incorporated into clamp loader complexes, explaining why expression of wild-type γ restores template-switching repair in *dnaX2016* cells. If the DnaX2016 subunits can form complex with the other clamp loader subunits, then clamp loaders with DnaX2016 γ and τ will be compared to wild-type DnaX-complex to determine which step of the clamp loading reaction is deficient in these mutants.

**Duet Vector System used to Aid in Clamp Loader Purification**

A Duet Vector system was created to allow expression of all clamp loader and pol III subunits within one cell, aiding with purification of DnaX2016 and wild-type clamp

loader. This new system reduces the workload of purifying the clamp loader and provides ample material for our biochemical assays which use a significant amount of protein. In addition, these Duet Vectors have already been used for structural analysis because these studies require a large amount of protein (178). New and exciting techniques in structural analysis, like SAXS used in the previously mentioned study, allow for in solution analysis of proteins with the potential for determining the structure of flexible regions. The C-terminal end of the τ subunit has not been visualized with the use of a structural method because of the flexibility of this region. The Duet Vector system presented here is able to produce milligram quantities of clamp loaders with τ with or without the pol III enzyme. This gives the potential of screening different conditions for structural analysis of the τ subunit which would provide information on how the τ subunit interacts with other proteins while being a part of the clamp loader complex.

Note that there are other protein bands in the final protein samples (Figure 2-4B). These impurities are much less concentrated than our clamp loader samples, but it is interesting to note that the molecular weight of these products match those found to be produce through proteolysis of τ into γ (179). Previous studies have shown that the cell surface protease OmpT can perform proteolysis on τ creating γ (66, 173). This proteolysis of the C-terminal tail of τ-complex complicates the analysis of the composition of *in vivo* clamp loaders. More recent studies have performed purification of τ using *ompT*$^{-}$ strains and saw a reduction of the proteolysis products (173). Even though there was a reduction of the proteolysis products in the *ompT*$^{-}$ strains, there was still visible impurities that corresponded to the γ molecular weight. Very similar

impurities are seen with the Duet Vector system, even though BL21(DE3) expression cells are used which are supposed to be *ompT*$^{-}$. To verify that these impurities are actually proteolysis products and not another protein, mass spectrometry could be performed. If these impurities are γ then conditions where proteolysis does not occur should be determined in order to get a homogeneous solution of clamp loader. These conditions could later be used for determining the composition of *in vivo* expressed clamp loaders from the wild-type *dnaX.* For the experiments described in this chapter, only γ or τ was expressed from the Duet Vector. By inserting the wild-type *dnaX* gene into the Duet Vector system, composition of the clamp loaders expression from the wild-type gene could be determined. While the Duet Vector system over expresses protein, it would be interesting to see what variations of the clamp loader are formed with and without the expression of pol III.

There is still a debate in the field as to the composition of the clamp loader *in vivo.* Most agree that the *in vivo* form of the clamp loader at the replication fork has at least two τ subunits that are bound to two pol III complexes, one for leading strand replication and one for lagging strand replication. The debate stems around the unknown role of γ. Some studies have suggested that the clamp loader contains two τ and one γ subunits, while others have suggested that there are two different clamp loaders, one made of all τ subunits and another made of all γ subunits. Currently, all chromosomally expressed and isolated clamp loaders have contained a mixture of τ and γ subunits (60, 180). Another recent study using single-molecule analysis of fluorescently labeled τ and pol III expressed from the chromosome found that there was an average of 3 pol III and 3 τ subunits at the replication fork (58). The problem was that

the error in the study was around 1, meaning that there could possibly be only 2 of each pol III and τ at the replication fork. This year, a study was published which used a biotinylated-tagged γ expressed from a plasmid and τ expressed from the chromosome through a τ-only *dnaX* gene (60). The biotinylated tag would insure that purified clamp loader was not the result of OmpT digestion. They found that the clamp loader contained two τ and one γ subunits. These studies combined suggest that the clamp loader does in fact contain two τ and one γ subunits, but the function of the γ subunit is still unknown.

**γ- and τ-Complex Load Clamps at the Same Rate**

It has been assumed that the clamp loading reactions of wild-type γ- and τ-complex are the same because both complexes can load clamps (52, 62, 181), but a direct comparison of the clamp loading reactions in real-time has never been reported to prove that the two clamp loaders load clamps using the same mechanism (182). Using previously optimized fluorescence-based assays, the clamp loading reactions of the γ- and τ-complex were compared. Steady-state equilibrium reactions used to calculate the $K_{d,app}$ reveled that γ and τ clamp loaders have the same affinity for the sliding clamp. Additionally, pre-steady state reactions were used to measure the rates of different steps in the clamp loader reaction. Clamp opening, ATP hydrolysis, clamp closing, and clamp release calculated rates were all the same for both γ- and τ-complex. The results presented here suggest that there is no difference in the clamp loading reaction of τ- and γ-complex. These results match previous results showing that both τ- and γ-complex can perform clamp loading (177, 181). The fact there is no difference between the clamp loading reactions matches hypothesis that the difference between the

function of γ and τ is ability of τ to give polymerase III preferential access to the sliding clamp (164, 183).

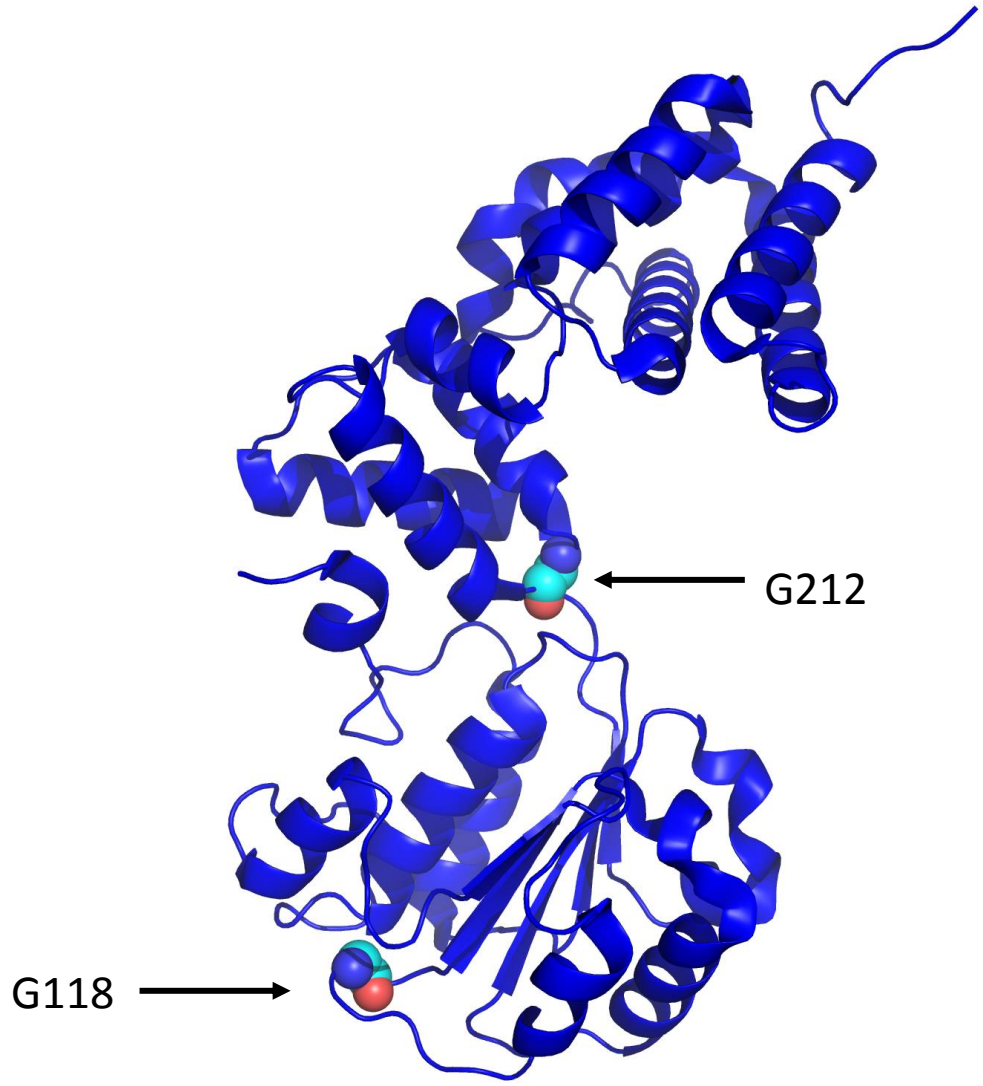


Figure 4-1 Crystal structure of a DnaX γ subunit showing the locations of G118 and G212. The PDB file 1JR3 was used in PyMOL to create the image with the G118 and G212 amino acids shown as spheres. The location of the A400 amino acid is in the C-terminal unstructured region of the clamp loader that was not included in the published crystal structure.

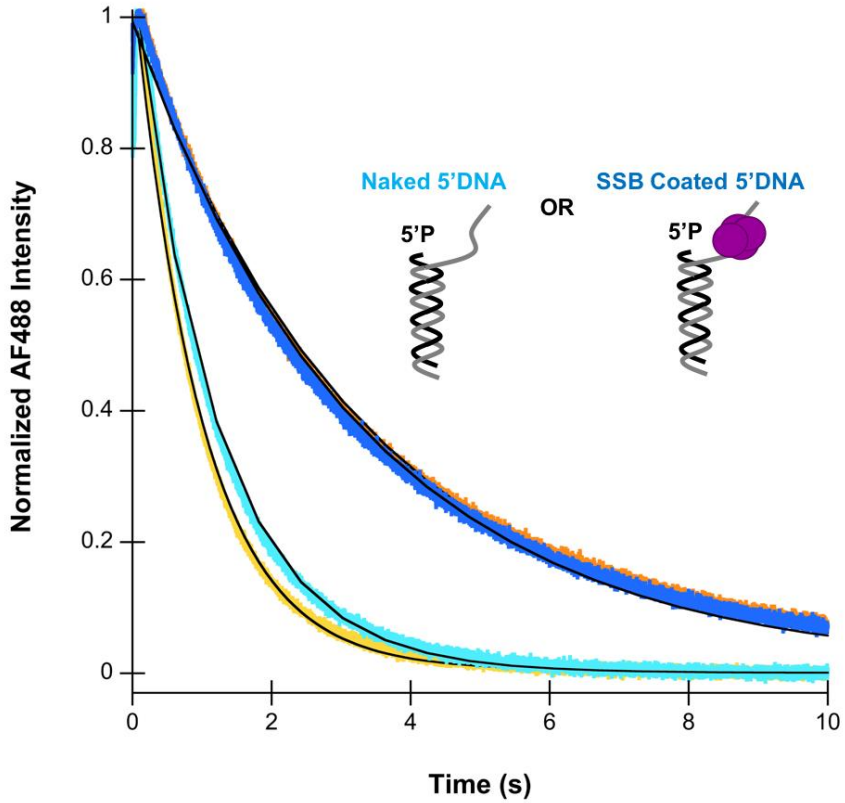


Figure 4-2 Clamp closing of *in vitro* reconstituted γ-complex and γ-complex made using the Duet Vector system to co-express proteins *in vivo*. Clamp closing was performed using an asymmetrical recessed 5' DNA substrate without (light) or with SSB (dark). Clamp closing on DNA by reconstituted γ-complex is shown in blue and γ-complex made from the Duet system is in orange. All traces were fit to a single exponential decay formula and the fit is shown (black line). Final reactant concentrations for the closing reactions were 20nM γ-complex, 20nM β-R103S/I305C-$(AF488)_2$, 200nM unlabeled β, 40nM DNA, and 0.5mM ATP.

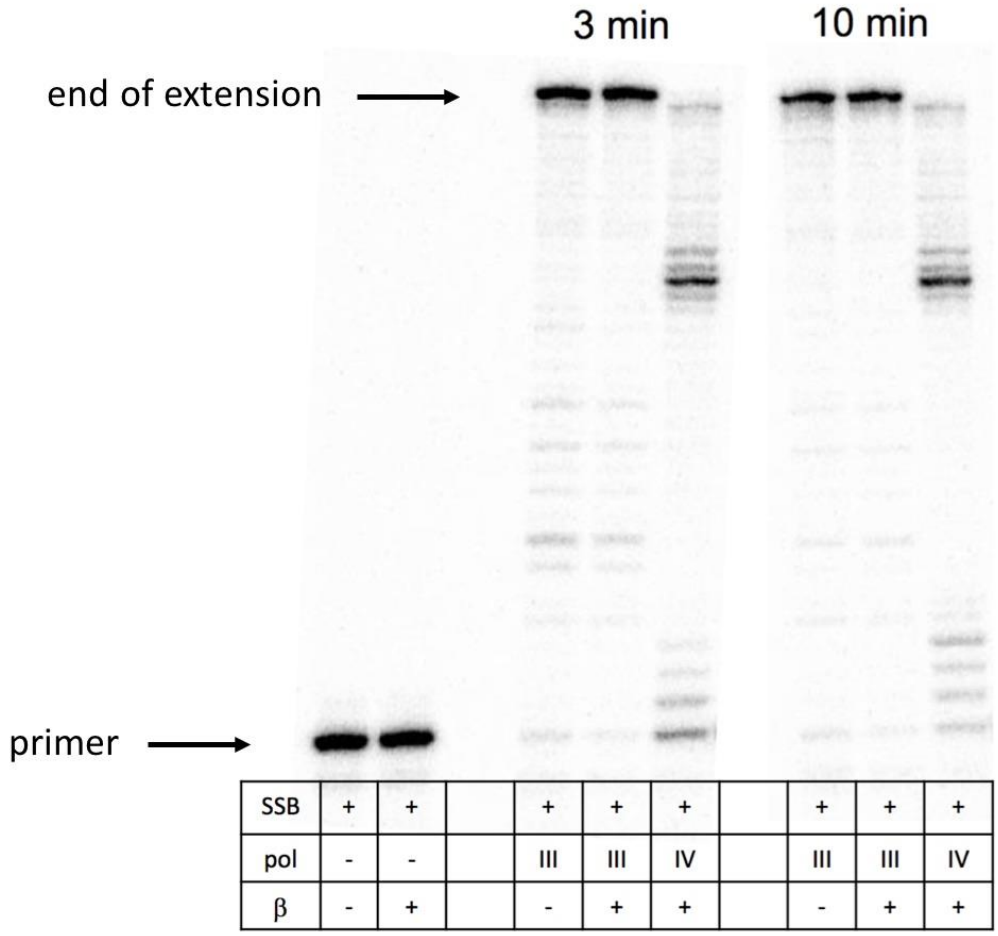


Figure 4-3. Pol III* produced through Duet Vector System has processive DNA synthesis activity. This primer extension assay was performed by the Myron Goodman laboratory using the purified Pol III*. Final reactant concentration were 5 nM p/t (30nt primer annealed in the middle of a 100nt template), 5 nM pol III* or pol IV, 167 uM ATP, 133 uM each dNTP, 80 nM β, and 320 nM SSB. Pol IV was used as a control reaction, which was expected to be not as processive as Pol III*. Reactions were stopped at 3 min and 10 min using EDTA and formamide. Reactions were analyzed by denaturing (8 M urea) polyacrylamide gel electrophoresis.

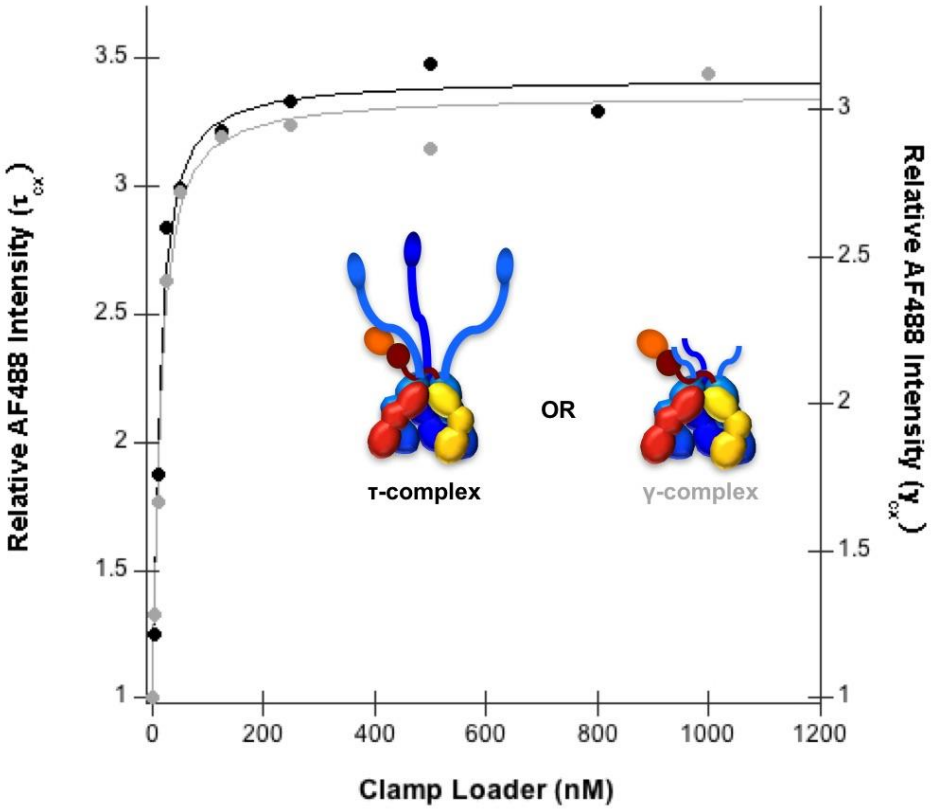


Figure 4-4. Clamp loader-clamp equilibrium binding and clamp opening. Relative AF488 fluorescence is plotted as a function of τ-complex (black) or γ-complex (gray) concentrations. Final concentrations of β clamps were 10 nM. Data were fit to a quadratic equation (solid line) assuming a two-state binding model to calculate apparent dissociation constants, $K_{d,app}$. Assay buffer contained 20 mM Tris-HCl pH 7.5, 8 mM $MgCl_2$, 2 mM DTT, 0.1 mM EDTA, and 4% glycerol.

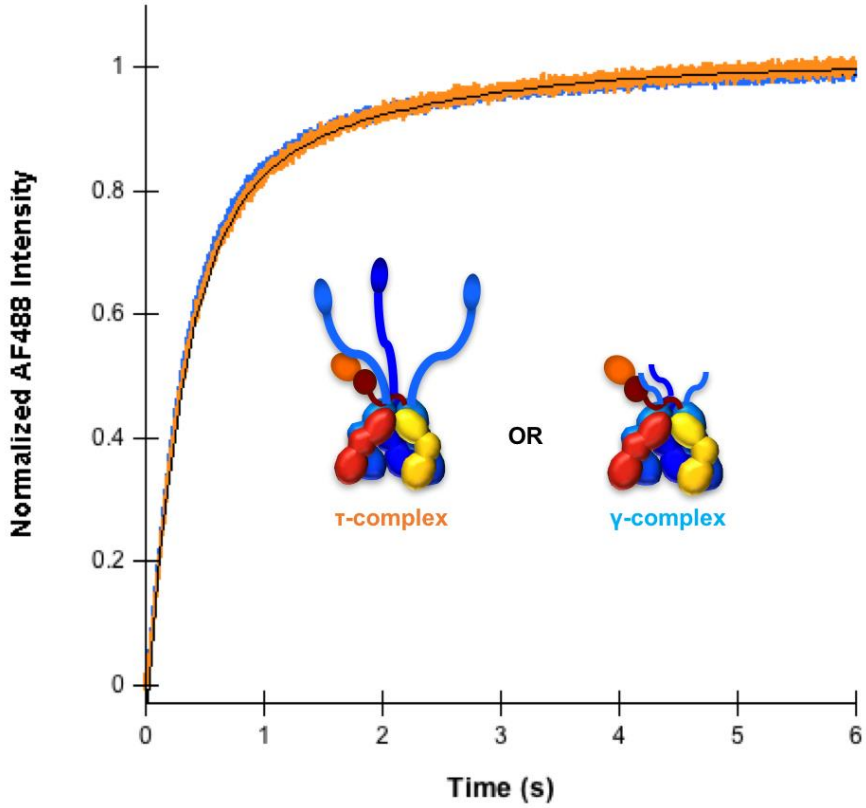


Figure 4-5. Pre-steady state clamp opening by γ-and τ-complex. The increase in AF488 fluorescence that occurs when γ-complex (blue) or τ-complex (orange) binds β-$(AF488)_2$ to form an open complex was measured as a function of time. Reactions began when a solution of clamp loader and ATP (0.5 mM) was added to a solution of β-R103C/I305C-$(AF488)_2$ and ATP (0.5 mM). The final concentration of clamp loader was 40 nM and the final concentration of β was 20 nM.

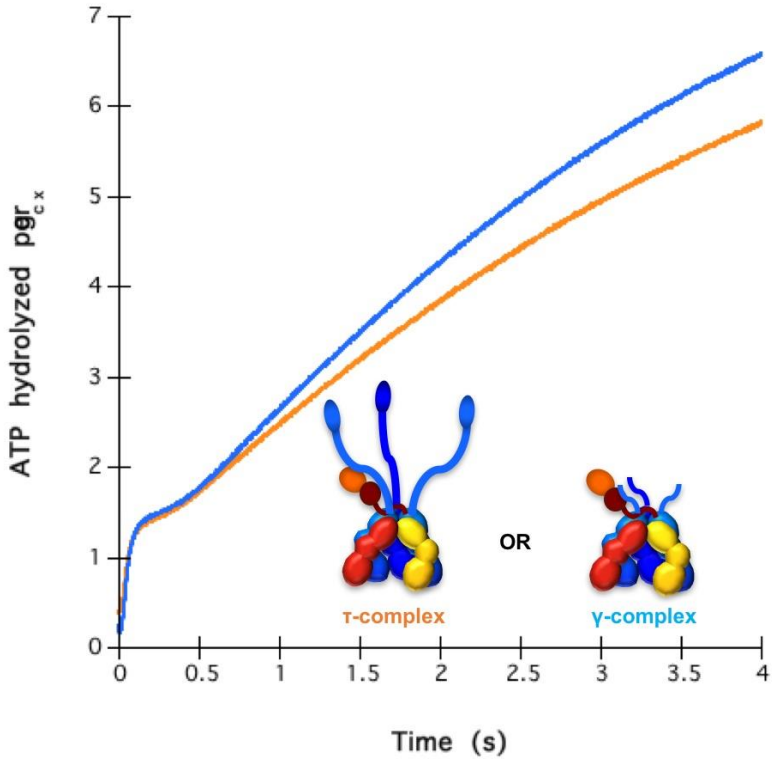


Figure 4-6. Pre-steady ATP hydrolysis by γ-and τ-complex. Release of inorganic phosphate following ATP hydrolysis by the either the τ-complex (orange) or the γ-complex (blue). ATP hydrolysis reactions contained 200 nM γ complex, 200 nM β, 400 nM DNA, 0.2 mM ATP and 2 μM ATPγS and 2 μM PBP-MDCC.

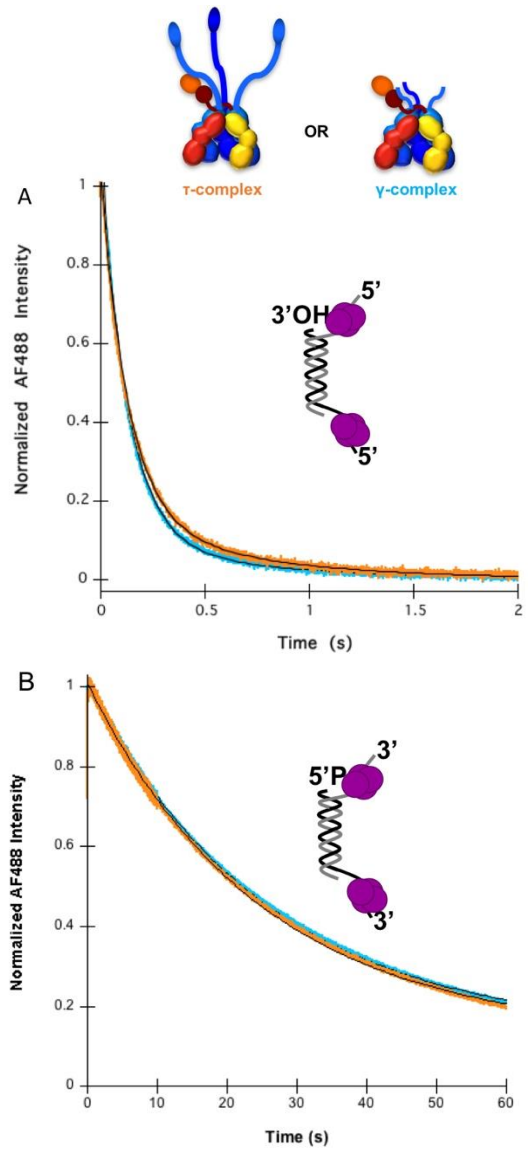


Figure 4-7. Pre-steady state clamp closing by γ-and τ-complex. A) Clamp closing traces on symmetrical SSB-coated 3'DNA with 30nt SSO. All traces were fit to a double exponential decay formula and the fit is shown (black line) in the figure. Final reactant concentrations for the closing reactions were 20nM γ-complex (blue) or τ-complex (orange), 20nM β-R103S/I305C-$(AF488)_2$, 200nM unlabeled β, 40nM DNA, and 0.5mM ATP. B) Clamp closing traces on symmetrical SSB-coated 5'DNA with 30nt SSO. Traces were fit to a single exponential decay formula to determine the rate and the fit is shown (black line).

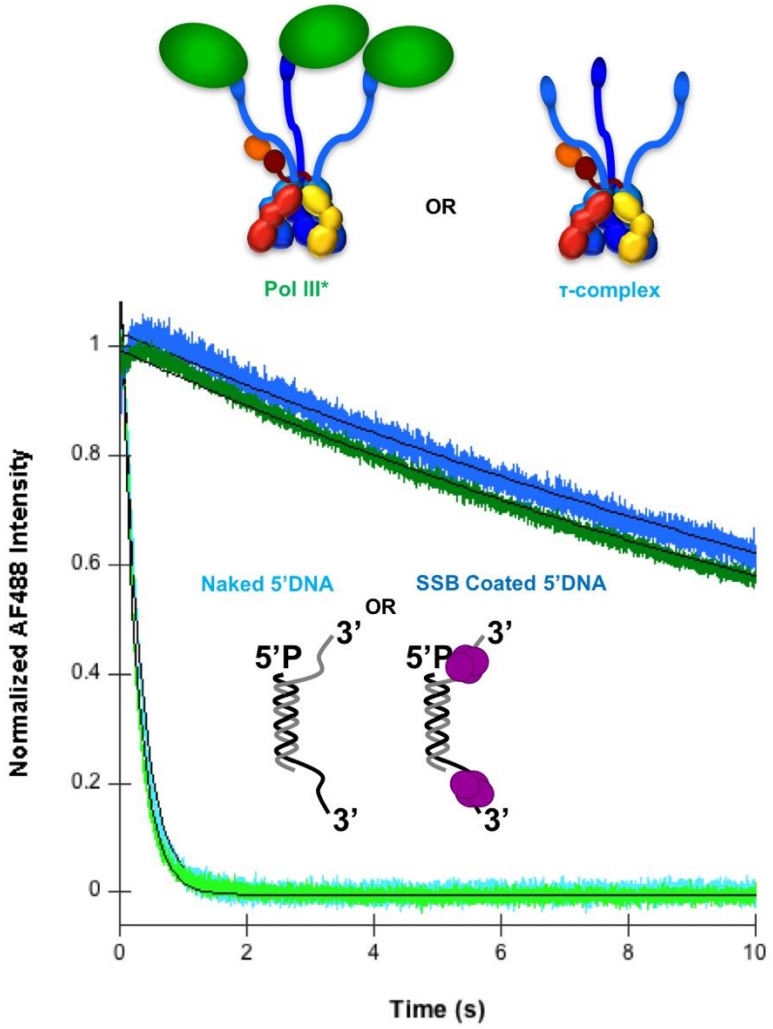


Figure 4-8. Clamp loading by τ-complex with and without the Pol III catalytic subunit, α. Clamp closing traces on symmetrical naked 5'DNA (light colors) with 30nt SSO or symmetrical SSB-coated 5'DNA with 30nt SSO (dark colors). All traces were fit to a double exponential decay formula and the fit is shown (black line) in the figure. Final reactant concentrations for the closing reactions were 20 nM τ-complex (blue) or τ-complex bound to α (green), 20 nM β-R103S/I305C-$(AF488)_2$, 200 nM unlabeled β, 40 nM DNA, and 0.5 mM ATP.

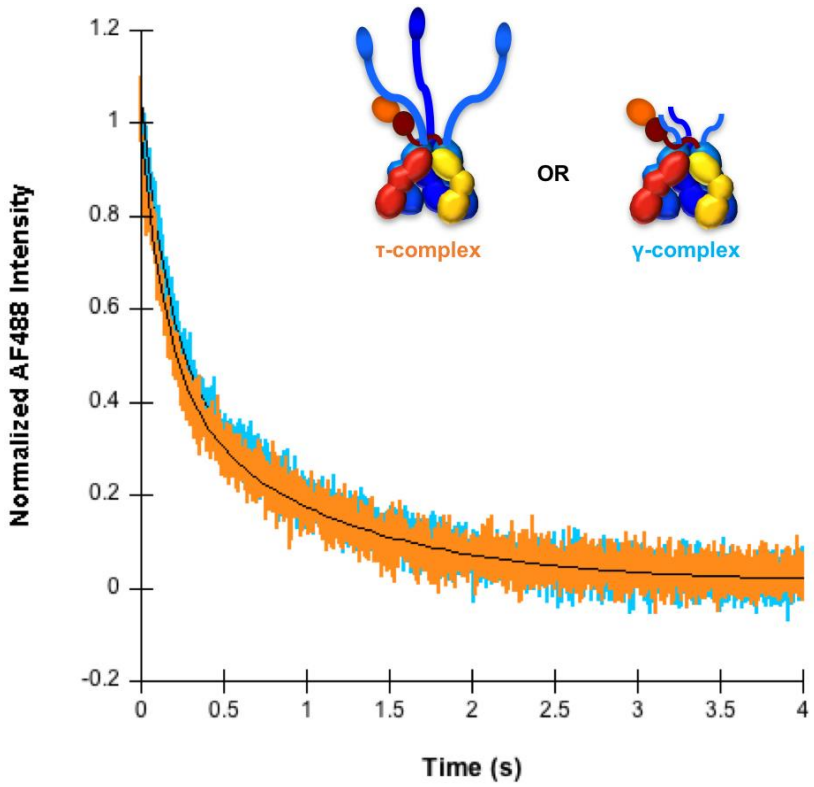


Figure 4-9. Pre-steady state clamp release by γ-and τ-complex. Clamp release traces with γ-complex (blue) or τ-complex (orange). All traces were fit to a double exponential decay formula and the fit is shown (black line). Final reactant concentrations for the closing reactions were 20 nM γ-complex (blue) or τ-complex (orange), 20 nM β-Q299C-(PY), 200 nM unlabeled β, 40 nM DNA, and 0.5 mM ATP.

Table 4-1. Four DNA mutations in the dnaX2016 gene

| Mutation within *dnaX* Gene | Corresponding Amino Acid Mutation |
|---|---|
| 353 G to A | G118D |
| 635 G to A | G212D |
| 660 G to A | L220L |
| 1198 G to A | A400T |

Table 4-2. Molecular weights of purified clamp loaders determined by size exclusion.

| Protein | Elution Volume (Ve) | Calculated molecular weight (Da) | Theoritical molecular weight (Da) |
|---|---|---|---|
| DnaX γ subunit | 9.1mL | 220,000 | 190000 (tetramer) |
| DnaX2016 γ subunit | 6.9mL | 797,000 | 190000 (tetramer) |
| DnaX γ clamp loader | 8.8mL | 275,000 | 249,900 |
| DnaX2016 τ subunit | 6.9mL | 929,000 | 294400 (tetramer) |
| DnaX τ clamp loader | 8.4mL | 384,000 | 320,700 |

# CHAPTER 5
# REGULATION OF THE CLAMP LOADING REACTION BY INTERACTIONS WITH SSB

## Background

DNA replication and repair are very quick and efficient cellular processes with many different proteins involved. The coordination of these proteins is critically important to the integrity of the genome. Certain DNA replication and repair proteins must be loaded onto the correct substrate without unproductive loading at incorrect substrates. If the DNA replication and repair proteins do not recognize the correct DNA substrates, it could be detrimental to the survival of the cell. While there have many studies examining the functions of the DNA replication and repair proteins, there is a gap in the field of how these proteins detect the correct substrate for their function and how the proteins get to these substrates in time for their needed catalysis. One protein that has been shown to be important in the coordination of enzymes in many organisms is the family of single-stranded DNA binding proteins (SSB) (reviewed in (184)). To investigate a possible mechanism SSB uses to regulate DNA replication and repair proteins, clamp loading regulation by SSB was used as a model.

During DNA replication, the clamp loader must to load the sliding clamp onto DNA with a 3'OH ("correct" polarity DNA) because DNA polymerase requires a 3'OH to catalyze the DNA synthesis reaction. If the clamp loader loads sliding clamps onto the wrong polarity DNA (DNA with a 5'P), the DNA polymerase will not be able to replicate the DNA possibly causing replication fork collapse and genome instability. Crystal structures of the *E. coli* clamp loader bound to DNA suggests that the clamp loader interacts with the duplex portion of a primer-template junction through interaction of positively charged residues in the cap of the clamp loader with the negatively charged

phosphate backbone of the template DNA (88). The single-stranded overhang (SSO) at the primer-template junction where the clamp loader binds was observed in the crystal structure to exit the clamp loader through an opening between the δ and δ' subunits (Figure 1-3A). While the crystal structure provides information on how the clamp loader binds to DNA, there is no information that suggests how the clamp loader prefers the correct polarity DNA over the incorrect polarity DNA. One study even modeled the opposite polarity DNA of that used in the crystal structure and demonstrated that the same contacts existed between the clamp loader and the DNA (96).

The clamp loader has been shown to have a preference for the correct polarity over the incorrect polarity, but what dictates this preference is unknown (96, 185). The clamp loader preference is not strong enough to prevent significant loading on the incorrect polarity. Studies from our laboratory have demonstrated that SSB tightly regulates the loading of the sliding clamp (105). In addition, the eukaryotic single-stranded binding protein RPA has been shown to direct replication and repair proteins to their specific DNA substrate (113, 186). The *E. coli* SSB was found to stimulate clamp loading on the correct polarity DNA and inhibit the clamp loading on the incorrect polarity (105). The stimulation of clamp loading on the correct polarity was suggested to be regulated by the interaction between the clamp loader and SSB. On the other hand, the inhibition of clamp loading on the incorrect polarity DNA was observed to be independent of known clamp loader-SSB interactions. The mechanism of the regulation of clamp loading by SSB is still not understood and the studies in this chapter were performed to give insight into the mechanism of SSB regulation. Interestingly, while SSB and RPA have different structures, they both demonstrated this regulation of clamp

loading (92, 113, 186). By understanding the mechanism of this regulation, it can be better understood how two proteins with very divergent structures can accomplish the same tasks.

To further investigate the regulation of clamp loading by SSB, multiple variants of clamp loaders and SSB mutant proteins were used (purified as described in Chapter 2) in fluorescence-based assays. The goal of this work was to provide insight into the mechanism by which SSB directs the clamp loader to load sliding clamps onto the correct polarity DNA. Previously studies examining the role of the SSB-pol III holoenzyme interactions have focused on the effect of this interaction on DNA synthesis, which occurs after the sliding clamps have been loaded onto the DNA. Using the clamp loader as a model, information on the mechanism of how SSB targets DNA replication and repair proteins to DNA substrates can be obtained.

## Results

### Stimulation of Clamp Loading by SSB on 3'DNA

#### SSB increases the clamp loader-clamp complex affinity for DNA

During clamp loading, the presence of DNA stimulates the ATP hydrolysis of the clamp loader (Chapter 1), which closes the clamp around the DNA and causes the clamp loader to release the clamp (92). SSB has been shown to stimulate clamp loading on primer-template structures with a 3' recessed end, but the mechanism of defining DNA specificity by SSB is unknown. For the research presented here, the "correct" polarity DNA substrate that contains a single stranded-double stranded DNA junction with 3'-recessed ends (Figure 5-1) are called 3'DNA.

Pre-steady state rates of clamp loading on 3'DNA DNA was measured with and without SSB at various DNA concentrations. The DNA substrate used contained a

symmetrical 3' recessed primer-template junction with 30nt SSO (JH10/JH9, Table 2-2). To measure closing of the clamp around DNA, a fluorescently labeled clamp, β-R103C/I305C-$(AF488)_2$, was utilized. Briefly, β-R103C/I305C-$(AF488)_2$ has two AF488 fluorophores at the interface of where the clamp opens and closes, and when the clamp is closed these fluorophores quench each other and have relatively low fluorescence. When the clamp loader and the sliding clamp opens, there is a relief of the quench and relatively high fluorescence (128). The change in fluorescence was monitored in real-time by a stopped-flow fluorimeter. A sequential mix reaction was used where clamp loader and ATP were mixed with β-R103C/I305C-$(AF488)_2$ and allowed to incubate for 4 seconds to give the clamp loader time to bind and open the sliding clamp. Then, DNA (with or without SSB), ATP, and excess unlabeled β (to limit the reaction to one observable turn-over), were mixed with the open clamp-clamp loader complex and fluorescence was measured over 10 seconds (unless otherwise noted) while collecting 1 point per millisecond. Final concentrations in the reactions were 20 nM clamp loader (γ-complex), 20 nM β-R103C/I305C-$(AF488)_2$, 200 nM unlabeled β, 0.5 mM ATP, 3x SSB per single-stranded overhang of DNA, and varying concentrations of DNA. For clamp loading experiments without SSB, DNA concentrations ranged from 40-280nM and for experiments with SSB the DNA concentrations from 40-160nM were measured. The concentration of SSB used was determined by titrating increasing amounts of SSB into the closing reaction to ensure all SSO were bound. This saturated amount of SSB was used throughout these experiments to make sure DNA was saturated with SSB (3x SSB per SSO). Each trace represents the average of at least three measurements.

Figure 5-1 shows representative traces of sliding clamp closing on naked 3'DNA (A) or SSB covered 3'DNA (B). For naked 3'DNA, traces corresponding to 40, 80, 160, and 280nM DNA (light to dark pink, respectively) are shown. For SSB coated 3' DNA, traces corresponding to 40, 80, and 160nM DNA (light to dark green, respectively) are shown. All traces were fit to a double exponential decrease formula (Equation 2-7) to estimate clamp closing rates. While data could fit a single exponential decrease, as shown in Figure 5-2, the double exponential decrease formula improved the fit as demonstrated by the change in the residuals pattern. A triple exponential decay did not further improve the fit. While a double exponential decay formula is used to determine approximate rates, the closing curves are actually more sigmoidal in shape due to reaction steps (DNA binding and ATP hydrolysis) that occur before clamp closing and do not change the fluorescence.

Fitting the data to a double exponential decay give two rate constants, one corresponding to a fast phase ($k_{fast}$) and one corresponding to a slow phase ($k_{slow}$). While the $k_{fast}$ most likely corresponds to the closing of the clamp interface, the $k_{slow}$ could correspond to an intermediate fluorescence state due to conformational changes during the clamp loading reaction or possibly a fraction of clamp-clamp loader complexes that are not as active. There is not enough data currently to determine what the slow phase corresponds to. Closing rates corresponding to the fast and slow phases were plotted against the concentration of DNA and individually fit to a rectangular hyperbola (Equation 2-9) (Figure 5-1 C-D). Both of the clamp loading rates are concentration dependent as the observed closing rates increase as DNA concentrations increase until the maximum velocity ($k_{max}$) is reached. Fitting the data of $k_{fast}$ or $k_{slow}$

rates versus the DNA concentration to Equation 2-9 results in two constants, $k_{max}$, or the maximum reaction rate at which DNA binding is longer rate limiting, and $K_{0.5}$, or the concentration of DNA at which the rate is ½ $k_{max}$ (Table 5-1). As seen in Table 5-1, the $k_{max}$ for both the fast and slow phases are approximately the same with and without SSB. On the other hand, $K_{0.5}$ for both the fast and slow phases are significantly reduced in reactions with SSB when compared to reactions on naked DNA. The reduced $K_{0.5}$ means less DNA is required to reach the maximum velocity in the reactions with SSB. In order to get a more accurate estimate of the constants for the SSB-coated DNA, reactions with DNA concentrations lower than 40 nM will need to be performed. These results suggest that with SSB, the reaction becomes less dependent on the DNA concentration and that SSB increases the affinity of the clamp loader for the correct polarity DNA.

**SSB does not affect the ATP hydrolysis step of the clamp loading reaction**

The clamp loading process is a multiple step enzymatic reaction with multiple conformation changes. Before clamp closing around DNA, the clamp loader first hydrolyzes the ATP (reviewed in Chapter 1). To determine if SSB is effecting the ATP hydrolysis step that comes before clamp closing to stimulate closing on 3'DNA, a fluorescence-based ATP hydrolysis assay was performed. The details of how this assay was performed are listed in Chapter 2, but briefly, when the clamp loader hydrolyses and releases a $P_i$ molecule, MDCC-labeled phosphate binding protein (PBP) will bind the $P_i$ which causes an increase in fluorescence. Figure 5-3 shows representative ATP hydrolysis traces for assays without SSB and with SSB. As seen in the figure, there is a quick burst of ATP hydrolysis for the first 0.1s then the reaction moves into a steady-state cycle, as previously reported (84, 85, 89). The steady-state rates (linear portion

after lag) of ATP hydrolysis are approximately the same with and without SSB. In addition, the bursts at the beginning of the reactions give the approximate same number of ATP molecules hydrolyzed per γ-complex, about 1.5-1.7ATPs. The γ-complex contains 3 DnaX subunits, which are all capable of hydrolyzing DNA (84, 85, 91). It is unknown why this ATP hydrolysis assay is not showing all 3 ATPs being hydrolyzed. One possibility for not seeing all 3 ATP hydrolyzed is that the incubation of the sliding clamp with the clamp loader needs to be longer than 4 s. Based on opening assays in Chapter 3, the clamp opening reaction is not completely finished until after 10 s. With an incubation time of only 4 s, not all of the clamps are opened yet which could be the reason why only 2 ATPs are seen hydrolyzed in the assays. These experiments should be repeated with a longer incubation time to ensure all clamps are opened before ATP hydrolysis is measured.

One interesting observation is that the burst at the beginning of reaction is normally followed by a lag, as seen in the trace without SSB, but with SSB this lag almost completely disappears. The lag following the first round of hydrolysis is the time required for the subunits to release ADP, bind new ATP, bind the clamp, and to interact with the DNA substrate before the next round of ATP hydrolysis. It is unknown why the SSB traces have a much less predominate lag, but possibly SSB is stimulating one of these steps, like DNA binding, to reduce the lag time. The main takeaway from these experiments is that the number of ATPs hydrolyzed in the burst and the steady-state rate of the ATP hydrolysis is approximately the same with and without SSB suggesting that SSB does not directly affect the ATP hydrolysis step.

**Stimulation by SSB is not due to removal of secondary structures**

Based on the values calculated from the fits, SSB has a stimulatory effect on the DNA binding of the clamp loading. While SSB does not change the overall $k_{max}$ of the reaction, the presence of SSB decreases the concentration of DNA required to reach ½ $k_{max}$. A decrease in $K_{0.5}$ is an indication that the SSB might be stimulating DNA binding by the clamp loader. SSB is known for its important role in removal of secondary structures from DNA (reviewed in (103). The increased DNA binding of the clamp loader when SSB is present may be due to the fact that SSB removes secondary structure from the DNA substrates. To determine if SSB is simply removing secondary structures or if SSB has some other stimulatory action, sliding clamp loading on SSB coated 3'DNA with 30 nt SSO was compared to loading on DNA with a 5 nt SSO. Previously, clamp closing was measured on DNA with varying SSO lengths. It was found that 5 nt of SSO was enough to have efficient clamp loading and did not differ from closing reactions with 30 nt SSO. In addition, the crystal structure of the clamp loader on DNA showed that 4 nt of SSO were held in a rigid position by the clamp loader, suggesting 4 nt are minimally required for binding (88). It would be expected that if SSB increases the clamp loader affinity for DNA by only removing secondary structures, then clamp loading on a 5 nt SSO should mimic that of DNA with SSB since the 5 nt SSO structure would not have any secondary structures to remove.

Clamp closing assays were performed as explained above with a different DNA substrate, JH5/JH6, which is a symmetrical substrate with 3' recessed ends and 5 nt SSO overhangs (Table 2-2). DNA concentrations ranged from 25-400 nM DNA and representative traces of are shown in Figure 5-4A. The clamp closing reactions demonstrated biphasic kinetics as reactions on the 30 nt SSO substrates and were fit to

a double exponential decrease formula (Equation 2-7). Closing rates corresponding to the fast and slow phases were plotted against the concentration of DNA and individually fit to a rectangular hyperbola (Equation 2-9) (Figure 5-1 C-D). The $k_{max}$ of the fast phase was calculated to be 17 $s^{-1}$ and the $K_{0.5}$ was 92 nM DNA. The $k_{max}$ of the slow phase was calculated to be 3.3 $s^{-1}$ and the $K_{0.5}$ was 115 nM DNA. Comparing the 5 nt SSO and the 30 nt SSO constants with and without SSB, the 5 nt SSO substrate has a relatively higher $K_{0.5}$, similar to that of the naked 30 nt SSO (Table 5-1). This suggests that the stimulation effect SSB has on the clamp closing reaction is not due to removal of the secondary structure by SSB, but by some interaction between the clamp loader and SSB that reduced $K_{0.5}$.

**Stimulation of clamp loading on 3'DNA is dependent on the χ-SSB interaction**

SSB is known to interact with the *E. coli* clamp loader through the χ subunit (100, 101) (reviewed in Chapter 1). The SSB-x interaction has been shown to increase the stability of the DNA polymerase III holoenzyme, to coordinate the transition of pol III onto RNA primers made by primase, and to increase the efficiency of DNA synthesis on the leading strand (100, 102, 187). Preliminary experiments suggested that this interaction is required for the stimulation of clamp loading by SSB on the correct polarity DNA structure (105). To investigate this further, clamp closing reactions with a χ-less form of the clamp loader were performed at different DNA concentrations. Clamp closing without the χ subunit on naked DNA is similar to that of WT clamp loader (Figure 5-5). Representative traces of clamp loader closing with WT and χ-less clamp loaders are shown in Figure 5-5A. As in wild-type clamp closing experiments, the χ-less clamp loader reactions fit to a double exponential decay formula but only at higher substrate concentrations (>100nM DNA+SSB), at lower concentration the data was fit with a

single exponential decay formula. In addition, the rates of closing for the χ-less clamp loader are very dependent on DNA concentration. As the DNA concentration goes up, so does the rate of clamp closing. When the rates are plotted against the DNA concentration and fitted to Equation 2-9, a $k_{max}$ of 7.1 $s^{-1}$ and a $K_{0.5}$ of 260 nM DNA for the fast rate is obtained (Table 5-1). Clamp closing assays at higher DNA concentrations with the χ-less form of the clamp loader will be needed to get a more accurate measurement of these constants. It is possible that with enough DNA, the rate of clamp closing with the χ-less clamp loader could match that of WT. The increased $K_{0.5}$ of the closing reactions with χ-less clamp loader and SSB means that a higher DNA concentration is required to reach the $k_{max}$. Additionally, $k_{max}$ is at least 2-fold slower than reactions with WT clamp loader. This suggests that the interaction of SSB and χ is required for stimulation of clamp loading on the correct polarity DNA when SSB is present. Without the χ-SSB interaction DNA binding of the clamp loader inhibited, but the clamp loader can still load clamps onto the SSB coated DNA.

If clamp loading on the correct polarity DNA with SSB is dependent on the SSB-χ interaction, then a SSB mutant that cannot interact with other proteins should exhibit the same kinetics as the χ-less form of the clamp loader. The acidic C-terminal tail of SSB is known to be the main site of interaction with other proteins (101). A previously created SSB mutant, SSBΔC8, has a deletion of the last 8 amino acids and has been shown to be defective in protein-protein interactions (188, 189). Clamp closing was repeated as WT SSB reactions except with SSBΔC8 coated 3'DNA containing symmetrical 30nt SSO. Figure 5-6A shows representative traces of clamp closing on SSBΔC8 coated 3'DNA compared to WT SSB coated 3'DNA. Interestingly, SSBΔC8 seems to inhibit

clamp closing activity more than the χ-less clamp loader. The clamp closing traces on DNA with SSBΔC8 fit were to single exponential decay formula (Equation 2-8). When the rates were plotted against DNA concentration and fit to Equation 2-9, a $k_{max}$ of 1.1 $s^{-1}$ and a $K_m$ of 225 nM DNA for the fast rate is obtained (Table 2-1). This suggests, that as in the χ-less clamp loader reactions, removal of the interaction between SSB and the clamp loader slows the clamp closing reaction, possibly due to inhibition of DNA binding by the clamp loader. This agrees with the hypothesis that the interaction between SSB and the clamp loader is required for stimulation of clamp loading on the correct polarity DNA. The $k_{max}$ for SSBΔC8 is about 7x smaller than for the reactions with the χ-less clamp loader, which suggests that SSBΔC8 has additional inhibitory actions that are not present in the χ-less reactions.

Clamp closing was performed with the χ-less clamp loader and SSBΔC8 coated DNA to see if there was any additive effect. Figure5-5B shows representative χ-less clamp closing traces (40-160 nM DNA) as well as the 160 nM DNA χ-less clamp loader trace with WT SSB for reference. The rates of closing with the χ-less clamp loader and SSBΔC8 coated DNA are similar to those with WT clamp loader and SSBΔC8 (Table 5-1). Taken together, the experiments with SSBΔC8 match the hypothesis that clamp loader-SSB interactions are required for stimulation on 3'DNA.

Previous studies have shown that removal of the acidic C-terminal tail of SSB (last 10 amino acids) slightly increases the affinity of the SSB for the DNA by approximately 2-fold (188). To determine if this enhanced DNA binding by SSB is present in our reactions with SSBΔC8, a DNA binding assay using fluorescence anisotropy was performed. DNA binding by anisotropy is explained in detail in Chapter

2, but briefly, a 3'DNA substrate is used which is labeled with a Rhodamine X isothiocyanate fluorophore on the template DNA strand (pIIIp2/pIIItI-60-Rhx, Table 2-2). When the DNA is alone in solution, the DNA tumbles very quickly which depolarizes the light and leads to a low anisotropy. When a protein is added that binds the DNA, like SSB, the protein/DNA complex tumbles more slowly leading to less depolarization and a high anisotropy. Final concentrations in the experiment were 50 nM DNA-RhX, 500 μM ATP, and 0-250 nM SSBΔC8 or 0-500 nM WT SSB. Anisotropy values were calculated using Equation 2-3 and the $K_d$ values were calculated using Equation 2-5. This assay was performed two times. Anisotropy titration curves and fits are shown in Figure 5-7. Both the anisotropy values for WT SSB and SSBΔC8 plateau around 0.34. The calculated $K_d$ value for SSBΔC8 was 20 nM and for WT SSB was 70 nM. A lower $K_d$ means a higher affinity of SSB for DNA, so SSBΔC8 mutant binds the DNA substrate more tightly than the WT SSB. While our assay suggests that SSBΔC8 binds 3.5-fold more tightly than WT SSB, addition of another replicate and errors bars may show that the difference is not that extreme.

To investigate the interaction of the clamp loader with SSB and the effect on clamp loading without the artifact of tighter DNA binding by SSB, the mutant SSBΔC1 was used. This SSB variant has the C-terminal phenylalanine removed. The C-terminal phenylalanine is highly conserved among bacteria and is important in the protein-protein interactions, including the clamp loader (103, 190). By not removing the acidic 8 amino acid C-terminal region and just the 1 C-terminal phenylalanine, the DNA binding should not be effected. This still needs to be tested through the anisotropy DNA binding assay as with SSBΔC8 as there is no previous data on the DNA affinity of SSBΔC1. Clamp

closing was performed with the 3'DNA 30 SSO substrate. A DNA concentration series has yet to be performed on this mutant, but clamp closing was measure with 160nM DNA. Figure 5-8A shows clamp closing traces for reactions on DNA coated with SSBΔC1 (purple) and WT SSB (green). Closing with SSBΔC1 was fit to a single exponential decay formula (Equation 2-8) and the rate obtained was $0.7s^{-1}$ which is the same as reactions with SSBΔC8 and 160nM DNA (Table 5-2). This is very interesting, because without the tighter DNA binding effect as seen in the SSBΔC8 reactions, it would be expected that the SSBΔC1 closing reactions would be similar to that with WT SSB and the χ-less clamp loader. The rate with WT SSB and the χ-less clamp loader is almost 4 times faster than reactions with SSBΔC1 (Table 5-2). These results suggest that SSB may be able to interact with the clamp loader at a different position other than χ in order to allow the clamp loader to bind to the DNA, albeit at a much slower rate than WT SSB. Only one assay was performed SSBΔC1 and more replicates will be needed to confirm this observation.

**Inhibition of Clamp Loading on the Wrong Polarity DNA by SSB**

**SSB inhibition of clamp loading on 5'DNA is independent of DNA concentration**

Previous work from our laboratory has demonstrated that on the incorrect polarity DNA SSB inhibits clamp loading to the same rates as reactions with no DNA (105). For the research presented here, the "incorrect" polarity DNA substrate that contains a single stranded-double stranded DNA junction with 5'-recessed ends (Figure 5-9A) are called 5'DNA. To determine if this inhibition is dependent on the DNA concentration, clamp closing assays were performed the same as in reactions with 3'DNA except the DNA used was a 5'DNA substrate that contains symmetrical 30 nt SSO (JH15/JH10, Table 2-2). The data was fit to a single exponential decay formula (Equation 2-8) which

yields $k_{obs}$ of 0.05$s^{-1}$ for all DNA concentrations, which is equivalent to the rate of dissociation as measured by assays with no DNA (105). As seen in the Figure 5-9A, the rate of clamp closing on the incorrect polarity DNA with SSB is independent of DNA concentration, unlike the reactions with 3'DNA. The fact that the rates are independent of DNA concentration suggests that SSB is completely blocking the clamp loader's access to the 5'DNA primer-template junction or that the reactions are already at $k_{max}$ at these DNA concentrations. A previous study using a pull-down assay showed that the clamp loader does bind 5'DNA when SSB is present, but at a much lower efficiency than on 3'DNA (96). The results combine suggest that SSB does not completely inhibit DNA binding by the clamp loader, but that the clamp loader binds in an unproductive complex that prevents clamp closing. Rates of clamp closing on 5'DNA are similar to dissociation rate of the clamp-clamp loader complex, suggesting that the only way the clamp loader can close the clamp is through dissociation in these reactions.

**Clamp loader prefers blunt DNA to 5'DNA with SSB**

Previously, clamp closing on different DNA substrates with varying SSO overhangs were measured and clamp closing on blunt DNA (no SSO) yielded a $k_{max}$ of 7.9$s^{-1}$ but required much higher DNA concentrations to reach (191). Structural studies have shown that the SSO makes important contacts with the clamp loader in an opening between the δ and δ' subunits (88). Removal of the SSO could has a negative effect on the ability of the clamp loader to bind to the DNA. Interestingly, clamp loading on 5'DNA with SSB is even worse than loading on blunt DNA (Figure 5-9B). A DNA substrate with one blunt end and one 5'DNA end with 30nt of SSO (LD1/JH10; Table 2-2) or one 3'DNA end with 30nt of SSO (pIIIpI/JH10; Table 2-2) was created and used to measure clamp closing compared to blunt DNA. Figure 5-9B shows representative

traces. Clamp closing on the blunt/3'DNA structure was fit to a double exponential decay formula while the blunt DNA and blunt/5'DNA structure was fit to a single exponential decay formula. As seen in Figure5-9B, clamp loading on blunt/5'DNA with SSB in slower than blunt DNA, demonstrating how inhibitory SSB is on clamp loading on 5'DNA. In addition, when the blunt/5'DNA trace is fit to a single exponential decay formula it yields a rate of 0.3 $s^{-1}$, a difference of almost 10 fold from the symmetrical 5'DNA substrate rate of 0.05 $s^{-1}$. The rate is more similar to the rate of blunt DNA (at the same concentration the rate is 0.76 $s^{-1}$). This suggests that the clamp loader loads clamps on blunt DNA faster than on 5'DNA when SSB is present. These results demonstrate how inhibitory SSB is on clamp loading with 5'DNA.

**SSB inhibition of clamp loading on 5'DNA is independent of χ-SSB interactions**

Previous work from the laboratory has shown that the inhibition on 5'DNA by SSB is independent of the clamp loader χ subunit-SSB interaction (105). Clamp closing assays performed with the χ-less form of the clamp loader on 5'DNA with or without SSB are shown in Figure 5-5B. Clamp closing of χ-less form of the clamp loader on naked 5'DNA was 0.2 $s^{-1}$ while with SSB was 0.04 $s^{-1}$. In addition, the closing rate on 5'DNA-SSB was not DNA concentration dependent, like in reactions with wild-type clamp loader. This agrees with previous observations that the χ subunit was not required for the 5'DNA clamp loading inhibition by SSB. Unless SSB is interacting with the clamp loader through another subunit besides the χ subunit, then these results suggest that the inhibition of clamp loading on the 5'DNA is due to a SSB/DNA interaction.

To determine if inhibition of clamp loading by SSB on 5'DNA is independent of all clamp loader interactions, whether through the χ subunit or not, the SSBΔC8 variant

was used in clamp closing assays on 5'DNA. Figure 5-6C shows representative traces of clamp closing on 5'DNA with WT SSB or SSBΔC8. As seen in the figure, even without the SSB protein-protein interacting C-terminal tail, the SSBΔC8 still inhibited clamp loading to rates of dissociation with no DNA (0.04 $s^{-1}$) (Table 5-3). This matches the hypothesis that the protein-protein interactions are not required for inhibition by SSB.

As mentioned above in the section on 3'DNA, SSBΔC8 has a higher affinity for DNA than WT SSB. In order to confirm that the results with SSBΔC8 are not due to increased DNA binding by SSBΔC8, the variant SSBΔC1 was used in clamp closing assay on 5'DNA with 30 SSO. Figure 5-8B shows representative clamp closing on 160 nM 5'DNA with WT SSB (green) or SSBΔC1 (purple). Both traces were fit to a single exponential decay formula (Equation 2-8). The same results are seen for SSBΔC1 as WT and SSBΔC8, the presence of the SSB completely inhibits the clamp loading reaction (Table 5-3). Clamp closing rates were also independent of the DNA concentration. Taken together, this evidence suggest that SSB inhibits clamp loading on 5'DNA via SSB-DNA interactions which blocks loading clamps onto the DNA.

**The 5'P is not the signal for SSB inhibition**

The previous experiments suggest that the inhibition of clamp loading by SSB on 5'DNA is due to a SSB-DNA interaction. On 3'DNA, there is a 3' hydroxyl group (-OH) while on 5'DNA there is a 5' phosphate group. It is possible that the SSB-DNA interaction is mediated by these groups. Previous work from our laboratory showed that DNA substrates with a phosphate on the 5' end inhibited clamp loading on 5'DNA more than substrates without the phosphate, an observation that is more obvious with the χ-less version of the clamp loader (105). To determine if the 5' phosphate is the signal for

SSB inhibition, a 3' DNA 30nt SSO symmetrical substrate with a 3' phosphate group was used (sequence is the same as JH9/JH10, Table 2-2). If the 5' phosphate group required for inhibition of clamp loading by SSB, then adding a phosphate group to the 3' side should reduce clamp closing on this substrate. As seen in Figure 5-10, the 3'P has no effect of clamp closing with WT clamp loader. There is a slight decrease in the rate of clamp closing with the χ-less clamp loader on 3'P, but the effect is not significant. These results show that 5'P is not important for SSB inhibition of clamp loading on 5'DNA.

**SSB can be moved away from the 5' primer-template by the clamp loader**

As a preliminary experiment to determine if SSB is physically "stuck" to the 5'DNA or if the SSB could be moved, a DNA substrate containing an internal 14nt oligonucleotide "primer" was created that had one 5'DNA primer-template junction (with 48nt of SSO) and one 3'DNA primer-template junction (with 43nt of SSO) (Table 2-2). The footprint of the clamp loader-sliding clamp on ds DNA is at least 30nt, so in order for clamps to load on this DNA substrate the SSB on the 5' end would have to move even if the clamp was loaded on the 3' side (95, 192). If clamp loading occurs, then the SSB on the 5' end is not physically stuck to the 5' end. In Figure 5-11, the clamp closing reactions with and without SSB are plotted. Clamp closing reactions were performed as described above with 160 nM DNA. The trace with no SSB can be fit to a double exponential decrease formula with a $k_{fast}$ of 4 $s^{-1}$ and $k_{slow}$ of 0.7 $s^{-1}$ which is about the same as the 3'DNA symmetrical substrate with no SSB, so the DNA substrate itself has no effect on the clamp closing activity (Table 5-4). With SSB, the internal 14-mer substrate yields slower clamp closing which was fit to a single exponential curve yielding a rate of 0.72 $s^{-1}$. This is a rate similar to that of χ less clamp loader clamp

closing on 3'DNA with SSB. There was clamp closing detected in these reactions which means that the SSB on the 5'DNA side had to of moved in order to make room for the clamp-clamp loader complex which has a footprint of at least 30 nt on the double-stranded DNA (192). This result suggests that SSB is not physically bound to the 5' recessed end and can move away from the primer-template junction.

**Effect of SSO Length On Clamp Loading Regulation by SSB**

SSB has multiple binding modes seen *in vitro*, reviewed in Chapter 1 (reviewed in (103). To see the effects of different binding modes of SSB on the regulation of clamp loading, DNA substrates of varying length were created. DNA substrates with 30 nt, 50 nt, and 80 nt SSO were compared using the clamp closing assay. While 30 nt is enough to bind 1 tetramer of SSB, 50 nt would possibly allow movement of the SSB, and 80 nt would allow a lot of movement by SSB, allow it to bind in the 65nt binding mode, or possibly would have 2 SSB tetramers bind. Clamp closing assays were performed as above on these 3 different substrates. Figure 5-12A shows representative traces of the clamp closing assays for the three different DNA substrates. All reaction traces fit to a double exponential decrease formula and the fits are shown in the figure. The rates of clamp closing on the 30 nt and 80 nt SSO substrates with SSB are the same, but the 50 nt SSO trace gives a different result (Table 5-5). For the 50 nt SSO substrate, the double exponential decrease fit leads to a slightly faster $k_{fast}$ than the 30 nt and 80 nt SSO substrate and a $k_{slow}$ that is the same as the 80 nt substrate, but about half of the 30 nt SSO substrate. In addition, fractional amplitudes of these rates is different. In the 30 nt and 80 nt SSO reactions, the fast phase comprises about 80% of the reaction and the slow phase comprises of about 20% of the reaction. In the 50 nt SSO reactions, the fast phase comprises about 60% of the reaction and the slow phase comprises of about

40% of the reaction. The cause of this difference is unknown; the difference could be due to the ability of SSB to move along this DNA substrate or maybe SSB binds in a different binding mode, or it could be sequence differences. More experiments will need to be performed to determine what the difference of the 50 nt SSO is, but overall, the rates for all 3 DNA substrates are similar.

Additionally, clamp closing experiments were performed on 5'DNA with 80 nt SSO to determine if the DNA length had any effect in the inhibition. Figure 5-12B shows a representative traces of clamp closing on 5'DNA with 80 nt SSO and WT SSB. The data was fit to a single exponential decay formula and the rate calculated was 0.4 $s^{-1}$. The 80 nt SSO substrate is an asymmetrical one in which one end is blunt and the other end is the recessed 5' primer-template junction with the 80 nt SSO. As shown in Figure 5-9B, the minimum rate on the asymmetrical substrates with SSB is around 0.3 $s^{-1}$ because the clamp loader prefers to loads faster on the blunt end compared to the 5' end with SSB. This results suggests that the length of the SSO does not affect the SSB regulation of clamp loading on the incorrect polarity DNA (5'DNA).

## Discussion

Sliding clamps are used as platforms for multiple different DNA replication and repair proteins including the main replication polymerase, DNA polymerase III. During DNA replication, a sliding clamp needs to be loaded onto every Okazaki fragment before the polymerase binds for processive replication. This means a sliding clamp must be loaded every 2-3 seconds. In order for the clamp loader to deliver a sliding clamp when it is needed, the clamp loader must have specificity for the correct substrate. There are many different DNA substrates that contain both 5' and 3' ends, including primed templates, ssDNA gaps, and other DNA replication and repair

intermediates. During DNA replication, the single-stranded DNA on the lagging strand is covered in SSB to prevent secondary structures and to interact with replication and repair proteins. The clamp loader is one of the proteins that interact with SSB. While there have been numerous studies demonstrating the interaction and the ability of SSB to stimulate the activity of different proteins, the mechanism of how SSB gives the clamp loader specificity for the correct polarity DNA is unknown. SSB has been shown to stimulate the clamp loading reaction on the correct polarity DNA (3'DNA) and inhibits on the incorrect polarity (5'DNA) (105). The experiments presented here were done to expand on the study of the SSB-clamp loader interaction and to determine the mechanism of the regulation of clamp loading by SSB.

**Clamp Loading on Correct Polarity DNA**

DNA polymerase requires a primer with a 3'OH to extend the growing DNA chain. SSB has been shown to stimulate clamp loading on the correct polarity DNA. By titrating in DNA to the clamp closing assays, the $K_{0,5}$ and $k_{max}$ were determined for reactions with and without SSB. While the $k_{max}$ is the same for both, the $K_{0.5}$ is lowered in reactions with SSB suggesting that the stimulation of clamp loading by SSB is due to SSB increasing clamp loader contacts with the DNA. One reason SSB could be increasing the clamp loader's affinity for DNA could be due to removal of secondary structures, but clamp loading onto DNA without secondary structures has similar $K_{0,5}$ and $k_{max}$ to naked DNA. This result combined with the fact that in reactions with SSB the clamp closing rates become less dependent on DNA concentration suggests that SSB is increasing DNA binding to 3'DNA by the clamp loader. In addition, ATP hydrolysis was not affected by the addition of SSB. ATP hydrolysis occurs when the clamp loader comes in contact with DNA which causes the clamp loader to close the clamp around

the DNA and release it. SSB did not affect the rate of ATP hydrolysis or the number of ATP's hydrolyzed per clamp loader complex. This suggests that the stimulation of clamp loading by SSB is not at the ATP hydrolysis step. Again, this result matches the hypothesis that SSB is stimulating clamp loading onto DNA by increasing the clamp loader's affinity for the correct polarity DNA.

SSB and the clamp loaders interact through the χ subunit of the clamp loader. The χ-less version of the clamp loader is capable of loading clamps in a similar manner to WT clamp loader when there is no SSB on DNA. When SSB is on DNA though, the clamp loading by χ-less clamp loader is reduced significantly. The clamp loading by the χ-less clamp loader is dependent on DNA concentration and has a much higher $K_{0.5}$ than WT clamp loader suggesting that without χ the DNA binding by the clamp loader on SSB coated DNA is significantly reduced. With χ, the clamp loader-SSB interaction allows the clamp loader to gain access to the primer-template junction. Without χ, SSB and the clamp loaders both compete for access to the DNA. Even though SSB binds DNA very tightly, SSB is a very dynamic protein and diffuses along the DNA (104, 193). Based on the data presented here, it is hypothesized that the χ-less clamp loader can load clamps onto the primer-template junction once the SSB moves away from the 3' end. The lowered clamp closing rate with the x-less clamp loader is a reflection of the clamp loader having to wait for SSB to move away from the primer-template junction before loading the sliding clamp.

In addition, the SSB mutants, SSBΔC8 and SSBΔC1, both significantly reduced the rate of clamp loading by the WT clamp loader onto the correct polarity DNA. While the SSBΔC8 mutant has been shown to have increased DNA binding, the SSBΔC1

mutant (which is expect to not have a DNA binding effect) reduced clamp loading to the same levels as SSBΔC8. This is very interesting because the C-terminal tail is the only known way that the clamp loader interacts with SSB (101, 187). If the stimulation of clamp loading by SSB on correct polarity DNA is regulated only by the SSB-χ interaction, then it would be expected that the clamp loading reactions with the χ-less clamp loader and the SSB mutants would be similar. The reactions with the SSB mutants are about 4-fold slower than reactions with χ-less clamp loader and WT SSB (Table 5-3). This suggests that there may be an additional interaction between the clamp loader and SSB besides through the χ subunit. Interestingly, a previous study looking at initiation complex formation found that assembly onto SSB coated DNA required the C-terminal tail of SSB, but not the χ subunit, suggesting another interaction between SSB and the clamp loader (183).

When the clamp loader loads the sliding clamp, the clamp loader binds the dsDNA region of the primer-template junction as well as at least 4 nt of ssDNA (88, 192). The data presented here leads to the hypothesis that SSB and the clamp loader compete for DNA binding at the primer-template junction and that the χ-SSB interaction allows the clamp loader to remodel the SSB-DNA structure in order to gain access to the primer-template junction. This mechanism may be similar to that of PriA-SSB interactions during replication restart. PriA has been shown to interact with SSB on the lagging strand of replication (194). This interaction causes a remodeling of SSB-DNA, revealing ssDNA to which PriA can bind to (195). PriA then keeps this ssDNA open to allow the DnaB helicase to bind for reformation of the replication fork.

**Clamp Loading on Incorrect Polarity DNA**

Clamp loading reactions were also performed with the incorrect polarity (5'DNA) to give insight into the mechanism of clamp closing inhibition on 5'DNA. SSB has been shown to inhibit the clamp loading reaction on the incorrect polarity DNA (105). When DNA was titrated into the clamp loading reaction, it was observed that the inhibition by SSB was not dependent on the DNA concentration. The lack of DNA dependence suggests that either SSB completely inhibits all DNA binding or that the reaction had already reached the $k_{max}$ at these DNA concentrations. A study using a pull-down assay demonstrated that the clamp loader does bind to 5'DNA-SSB, just with less efficiently than on 3'DNA-SSB, suggesting DNA binding is not completely inhibited on 5'DNA (96). The clamp loader-clamp complex most likely forms a type of unproductive complex that cannot perform ATP hydrolysis and clamp closing. ATPase activity has shown to be reduced on 5'DNA-SSB substrates (96). The rate of clamp closing for all reactions with 5'DNA-SSB was calculated to be about 0.05 $s^{-1}$ which is equivalent to reactions with no DNA representing dissociation of the clamp from the clamp loader. Based on these results, it is hypothesized that the clamp loader binds 5'DNA-SSB that results in an unproductive complex and the only way the clamp can be released is through passive dissociation.

To determine if this inhibition is due to a SSB-clamp loader interaction or a SSB-DNA interaction, clamp loading was measured using χ-less clamp loader and SSB C-terminal deletion mutants, SSBΔC8 and SSBΔC1. Interestingly, all of the mutants behaved exactly like their wild-type counterparts. The inhibition of clamp loading by SSB was independent of all known protein-protein interactions. This results suggests that the SSB-DNA dynamics are important in the inhibition of clamp loading on 5'DNA. There

may also be a novel clamp loader-clamp complex interaction with SSB that is assisting in this regulation. A novel SSB-clamp loader interaction has previously been hypothesized (183). Additionally, both the sliding clamp and the subunits of the clamp loader complex have been shown to have roles in binding to DNA and defining primer-template junctions (96, 196).

Previous studies have shown that SSB can move freely along both 5’ and 3’DNA suggesting that SSB is not tightly bound to the primer-template junction (193, 197). To determine if SSB is physically bound to the 5’DNA end, clamp closing was measured on an DNA structure with an internal primer of 14 nucleotides with SSB. The footprint of the clamp loader-clamp complex is at least 20 nucleotides long (192) and the clamp loader is known to load the sliding clamp onto the duplex part of the primer-template junction. In order for clamp loading to occur on a DNA substrate with an internal 14 nt primer, SSB on the 5’DNA end would have to be relocated in order for the sliding clamp to load. Clamp closing on the internal 14 nt primer occurred at a rate almost 10x fast than on 5’DNA with SSB. Since clamp loading is occurring, SSB on the 5’ side of the internal oligonucleotide substrate must move when clamp loader loads the clamp on the 3’DNA side. Clamp loading on this substrate requires the clamp loader-clamp complex must either wait for SSB on the 5’ end to remodel, or the clamp loader-clamp complex must push SSB away from the 5’ end.

Based on the results presented here, inhibition of clamp loading by SSB on 5’DNA seems to be dependent on a difference in the SSB-DNA dynamics on 5’ versus 3’DNA. SSB is a dynamic protein meaning that it is unlikely SSB is “stuck” to the 5’end, as confirmed with clamp loading on a 14 nt primer. The χ subunit can remodel SSB on

3’DNA to allow clamp loading, but χ cannot remodel the 5’DNA-SSB complex. Inhibition of clamp loading on 5’DNA-SSB could be due to a difference in the direction the clamp loader approaches the DNA-SSB complex. While SSB has been shown to freely move along ssDNA in either direction, when there is a primer-template junction, this movement may be polarity specific. The DNA binding core of SSB may translate this polarity dependence to the clamp loader-clamp complex. SSB binding to ssDNA has been thoroughly investigated, but there is a lack of knowledge of the movement of SSB on ss/dsDNA structures. On a ss/dsDNA structure, the clamp loader may be able to remodel the DNA-SSB complex when coming from the 3’DNA side, but may not be able to remodel the DNA-SSB interaction when approaching from the 5’DNA side. A SSB rearrangement by the clamp loader to load clamps and allow polymerase to bind has been previously proposed (183) and match the hypothesis that the rearrangement of SSB by the clamp loader is polarity dependent. This model is similar to the model of DNA replication termination in *E. coli.* When the DnaB helicase approaches Tus-Ter sites the helicase will either pass through the sites or will stop depending on which direction the helicase approaches the sites (198, 199). The SSB-DNA interactions could function in a similar manner as the Tus-Ter sites by only allowing the clamp loader-clamp complex to gain access to a primer-template junction only when it approaches the 3’DNA.

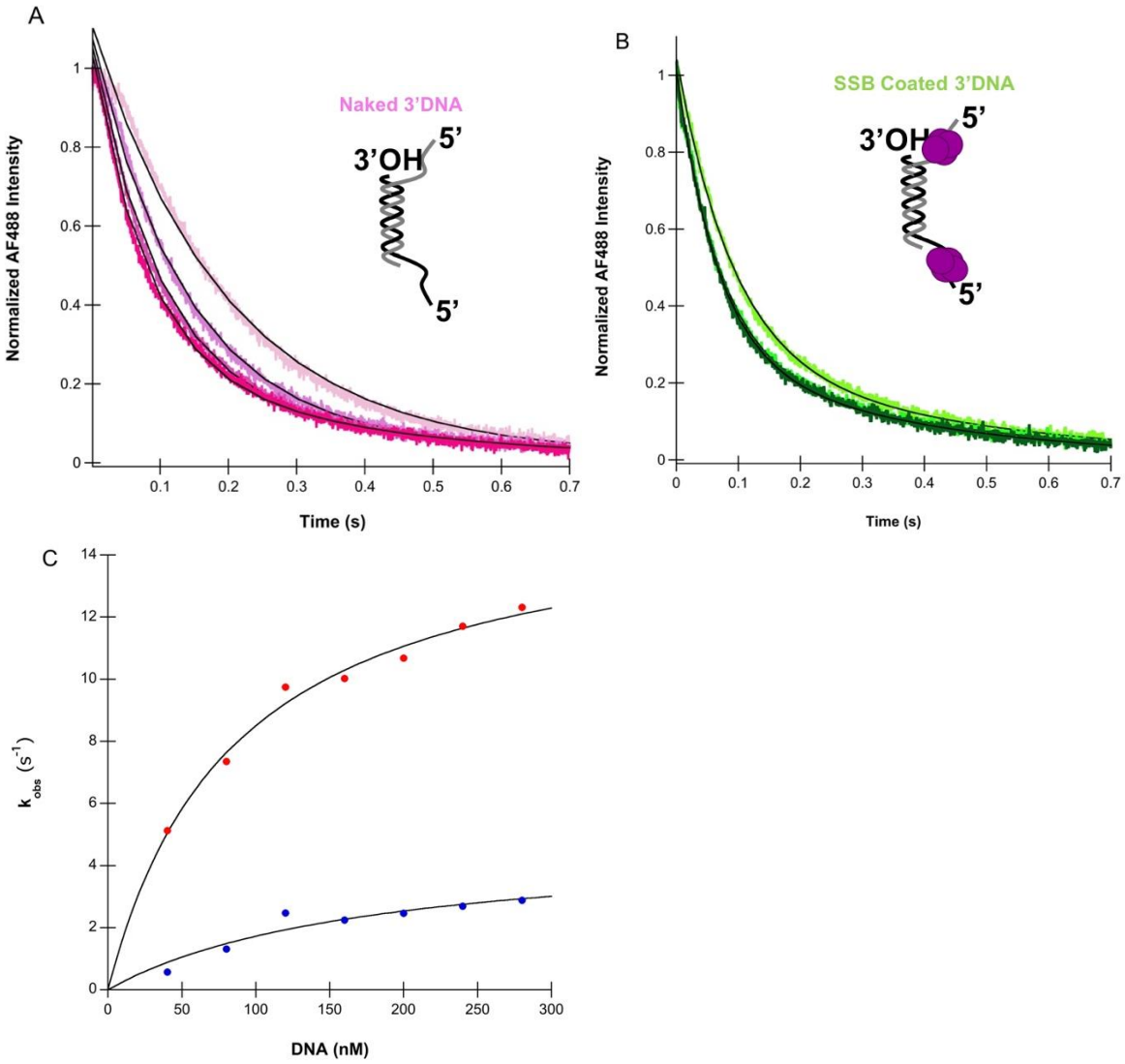


Figure 5-1. Representative reaction traces of clamp closing on correct polarity DNA with and without SSB. A) Closing assays on symmetrical naked 3'DNA with 30nt SSO. Assays were performed with 40-280nM DNA and representative reactions are shown at 40nM (lightest pink), 80nM, 160nM, and 280nM (darkest pink). All traces were fit to a double exponential decay formula to calculate $k_{fast}$ and $k_{slow}$ closing rates and the fit is shown (black line). Final concentrations for reactions were 20nM γ-complex, 20nM β-R103S/I305C-$(AF488)_2$, 200nM unlabeled β, and 0.5mM ATP. B) Clamp closing assay on symmetrical SSB-coated 3'DNA with 30nt SSO. Assays were performed with 40-160nM DNA and representative reactions are shown at the DNA concentrations are 40nM (lightest green), 80nM, and 160nM (darkest green). Traces were fit as above and concentrations were the same except with 3x SSB per SSO. C) To obtain $k_{max}$ and $K_{0.5}$ values, the $k_{fast}$ (red) and $k_{slow}$ (blue) values are plotted against DNA concentration and fit to Equation 2-6. The example shown is of the naked 3'DNA reactions.

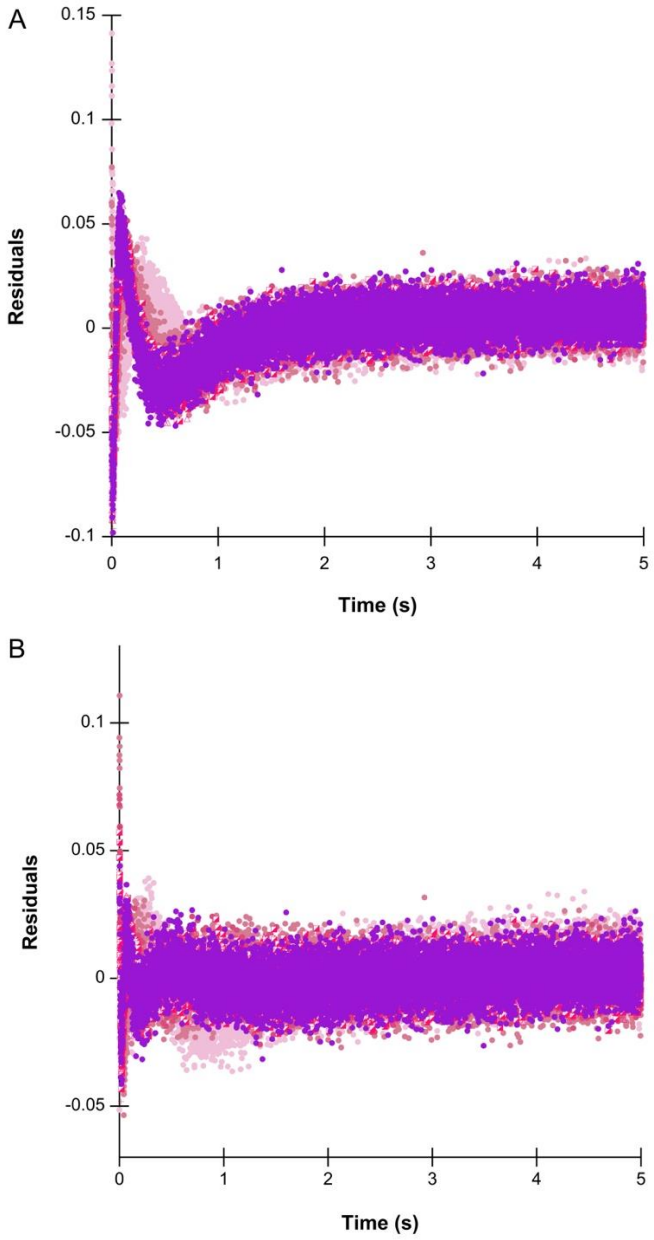


Figure 5-2. Residuals from fitting data with a single or double exponential decay formula. Data from Figure 5-1 was fit with either A) a single exponential decay formula or B) a double exponential decay formula using KaleidaGraph. The residuals represent the difference between the observed value and the predicted value from the fit. A random pattern of points around 0 represents a good fit of the data.

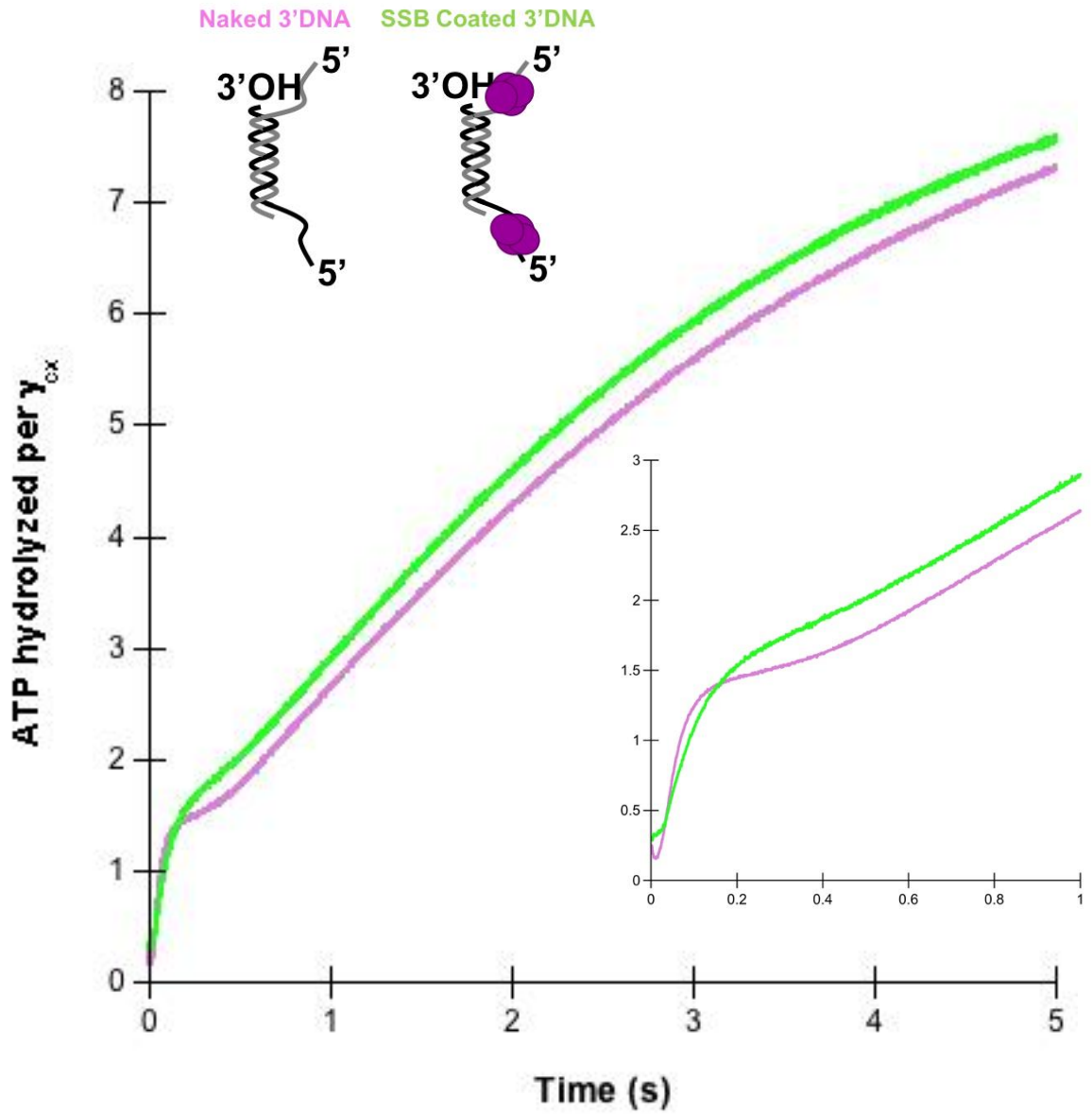


Figure 5-3. Effect of SSB on ATP hydrolysis by γ-complex. Representative traces for release of inorganic phosphate following ATP hydrolysis by the clamp loader in reactions without SSB (pink) or with SSB (green). ATP hydrolysis reactions contained 200nM γ complex, 200nM β, 400nM DNA, 0.2 M ATP and 2μM ATPγS and 2μM PBP-MDCC. The insert contains the same graph but zoomed into the burst phase.

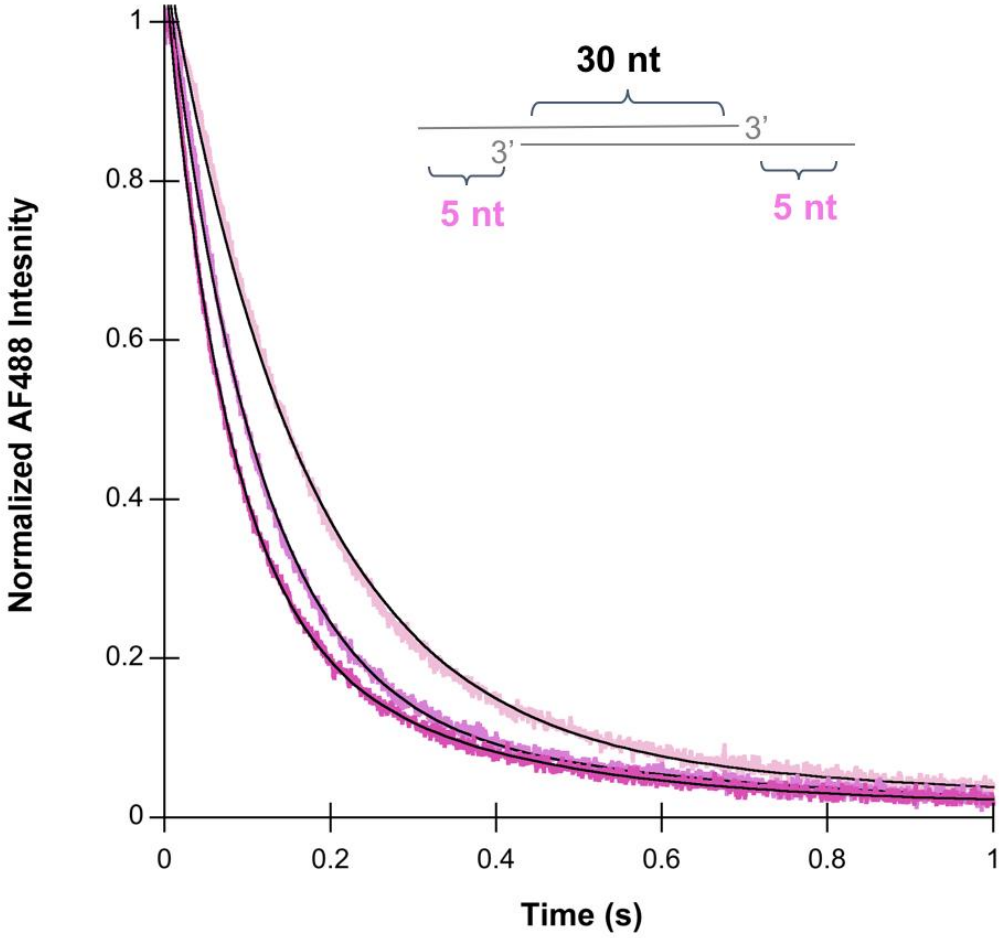


Figure 5-4. DNA titration of clamp closing on 5 nt SSO symmetrical substrate. All traces were fit to a double exponential decay formula and the fit is shown (black lines) in the figure. Final protein and ATP concentrations for the closing reactions were 20 nM γ-complex, 20 nM β-R103S/I305C-$(AF488)_2$, 200 nM unlabeled β, and 0.5 mM ATP. DNA concentrations shown are 50 nM (lightest pink), 100 nM, and 200 nM (darkest pink).

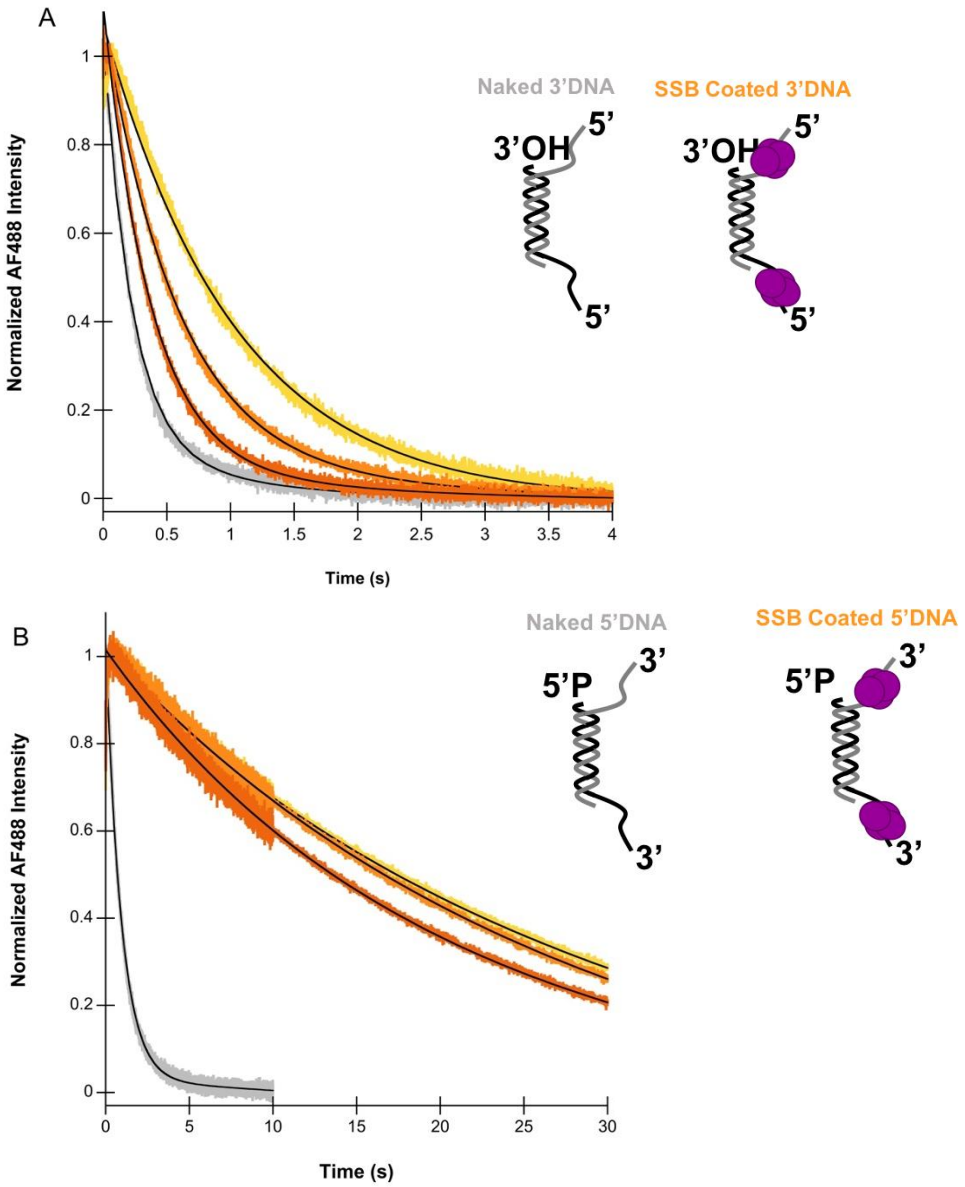


Figure 5-5. Representative reaction traces of clamp closing DNA by χ-less clamp loader. A) Representative clamp closing traces on symmetrical 3'DNA with 30nt SSO either without (gray) or with SSB (orange). The DNA concentrations are 40nM (lightest orange and gray), 80nM, 160nM (darkest orange). All traces were fit to a double exponential decay formula and the fit is shown in the figure. Final protein and ATP concentrations for the closing reactions were 20nM γ-complex, 20nM β-R103S/I305C-$(AF488)_2$, 200nM unlabeled β, and 0.5mM ATP. B) Representative clamp closing traces on symmetrical 5'DNA with 30nt SSO either without (gray) or with SSB (orange). The DNA concentrations are 40nM (lightest orange and gray), 80nM, 160nM (darkest orange). Traces were fit to a single exponential decay and concentrations were the same as in A.

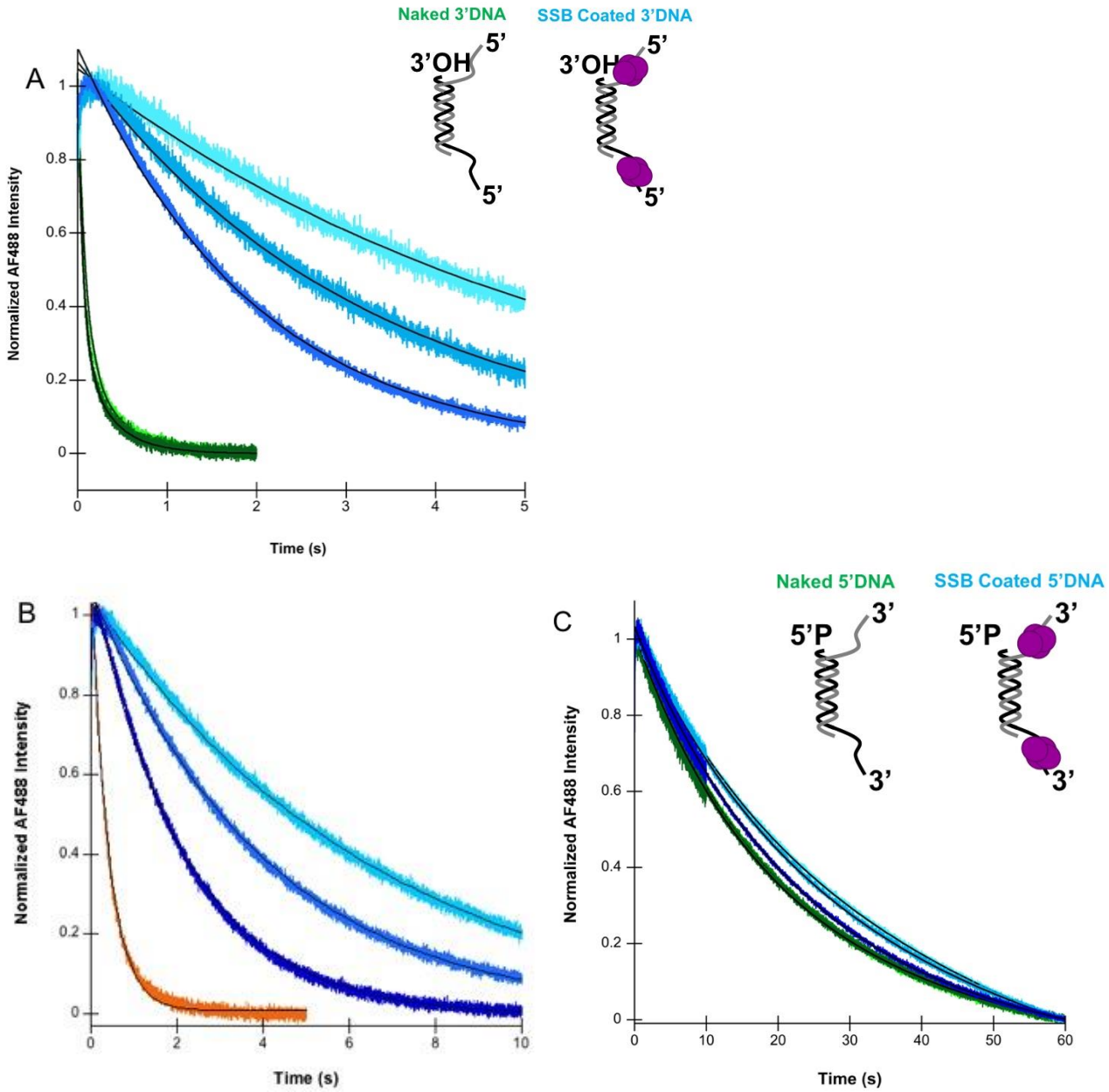


Figure 5-6. Representative reaction traces of clamp closing on DNA with and without SSBΔC8. A) Representative clamp closing traces on symmetrical naked 3'DNA with 30nt SSO. Reactions contained WT SSB (green) or SSBΔC8 (blue) The DNA concentrations are 40nM (lightest blue), 80nM, 160nM (darkest blue). All SSBΔC8 traces were fit to a single exponential decay formula and the fit is shown in the figure. Final protein and ATP concentrations for the closing reactions were 20nM γ-complex, 20nM β-R103S/I305C-$(AF488)_2$, 200nM unlabeled β, and 0.5mM ATP. B) Representative clamp closing as in A but with χ-less γ-complex. WT SSB is shown (orange) for comparison to closing with SSBΔC8. C) Representative clamp closing as in A but with symmetrical naked 5'DNA with 30nt SSO.

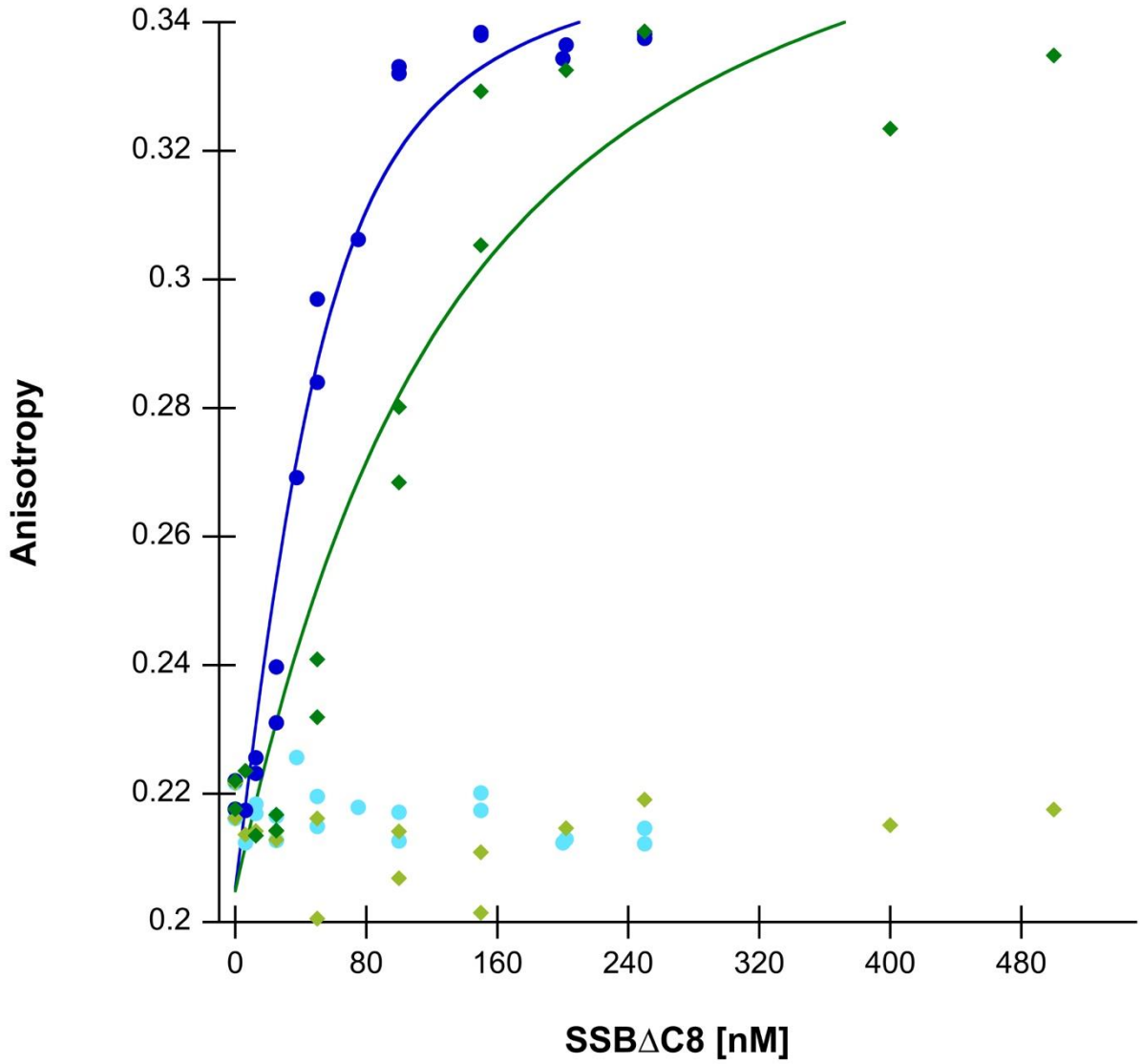


Figure 5-7. DNA-Rhx binding by WT SSB and SSBΔC8 . Anisotropy of free DNA for WT SSB (light green diamonds) and SSBΔC8 (light blue circles) are plotted. Anisotropy of WT SSB bound to DNA-Rhx (dark green diamonds) and SSBΔC8 bound to DNA-Rhx (dark blue circles) are plotted along with the *Kd* fit for each SSB determined by Equation 2-5. Final reagent concentrations were 50nM DNA-RhX, 500μM ATP, and varying concentrations of SSB.

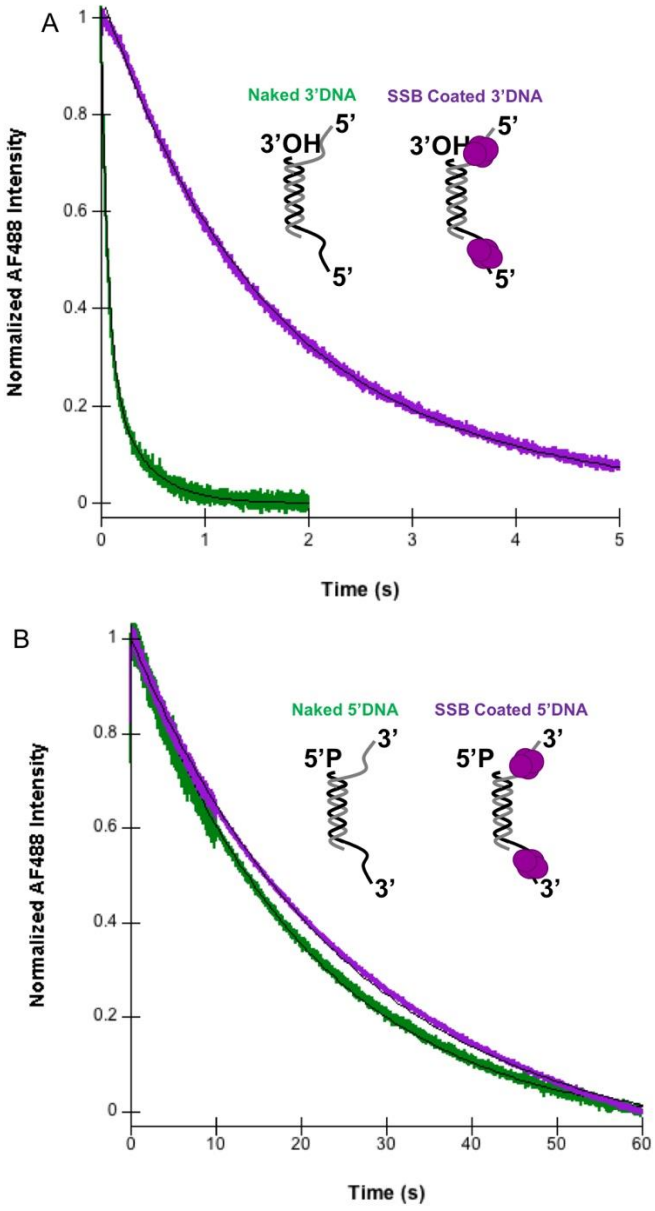


Figure 5-8. Representative reaction traces of clamp closing on DNA with and without SSBΔC1. A) Representative clamp closing traces on symmetrical naked 3'DNA with 30nt SSO. Reactions contained WT SSB (green) or SSBΔC1 (purple) and 160nM DNA. All SSBΔC1 traces were fit to a single exponential decay formula and the fit is shown in the figure. Final protein and ATP concentrations for the closing reactions were 20nM γ-complex, 20nM β-R103S/I305C-$(AF488)_2$, 200nM unlabeled β, and 0.5mM ATP. B) Representative clamp closing as in A but with symmetrical 5'DNA with 30nt SSO.

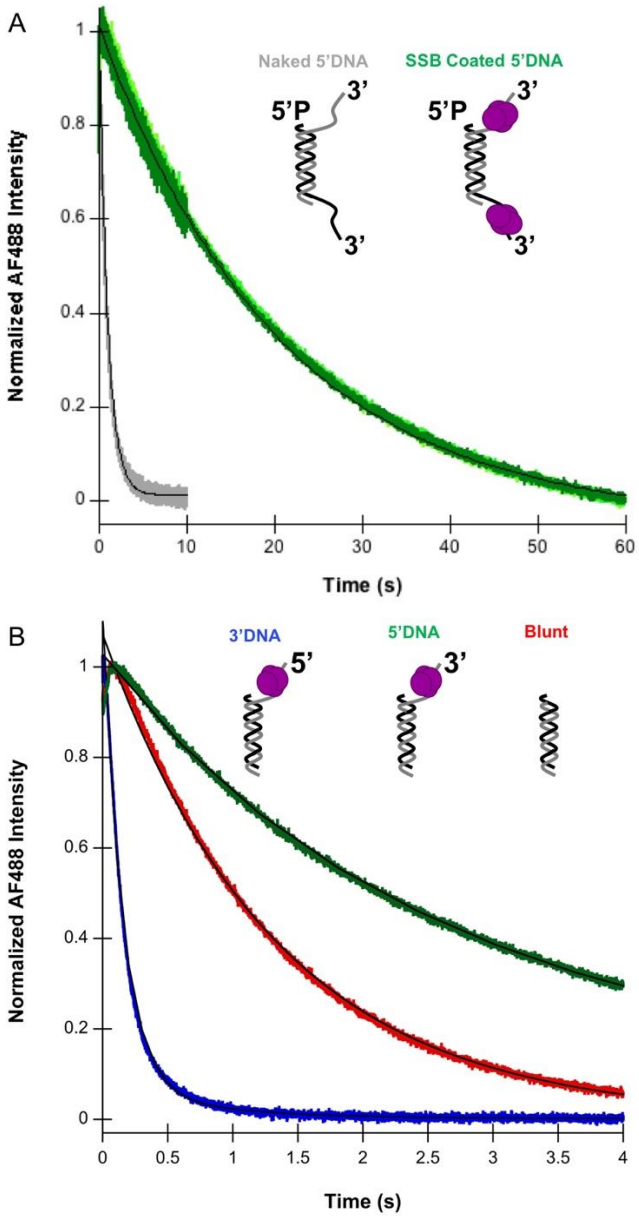


Figure 5-9. Effect of SSB on clamp loading with various DNA substrates. A) Representative clamp closing traces on symmetrical 5'DNA with 30nt SSO either with (green) or without SSB (gray). The DNA concentrations are 40nM (lightest green), 80nM, and 160nM (darkest green). The no SSB trace has a DNA concentration of 40nM. All traces were fit to a single exponential decay formula and the fit is shown in the figure. Final protein and ATP concentrations for the closing reactions were 20nM γ-complex, 20nM β-R103S/I305C-$(AF488)_2$, 200nM unlabeled β, and 0.5mM ATP. B) Representative clamp closing reactions performed as above but with an asymmetrical DNA substrate that has one blunt end and the other end is 3'DNA (blue), 5'DNA (green), or blunt (red).

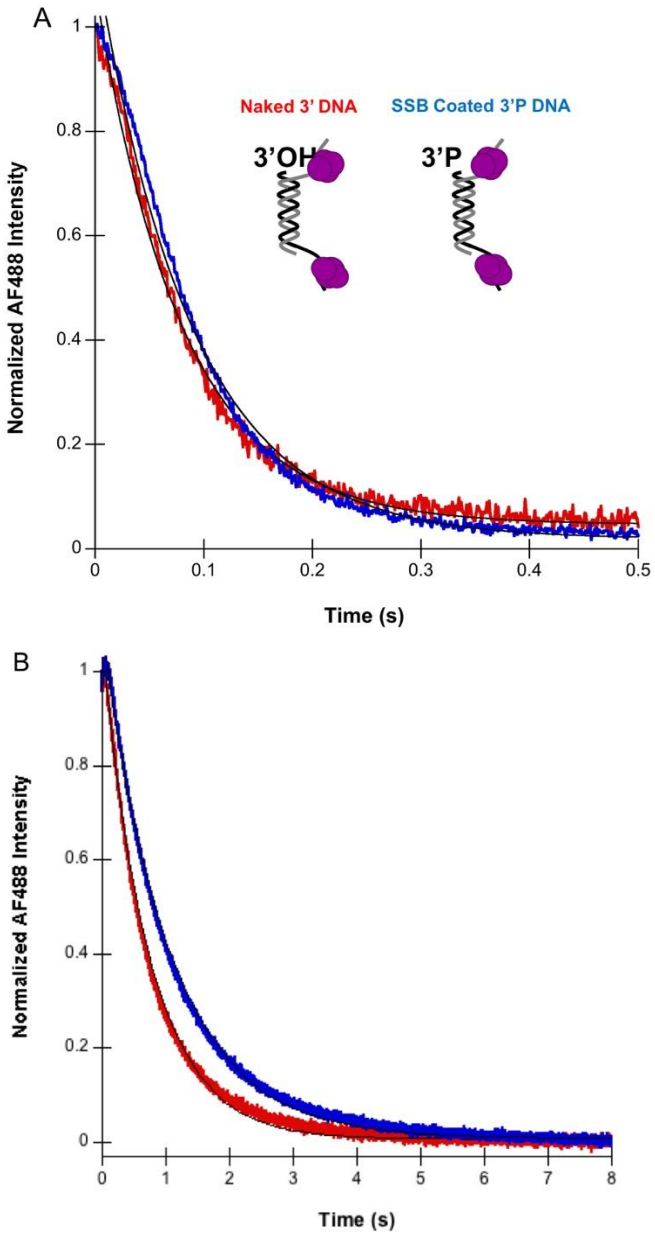


Figure 5-10. Clamp closing on 3'DNA with a 3' phosphate group. A) Representative WT clamp closing traces on symmetrical naked 3'DNA with 30nt SSO and either a 3' OH group (red) or a 3'P group (blue). The traces were fit to a double exponential decay formula and the fit is shown in the figure. Final protein and ATP concentrations for the closing reactions were 20nM γ-complex, 20nM β-R103S/I305C-$(AF488)_2$, 200nM unlabeled β, 480nM SSB, and 0.5mM ATP. B) Clamp closing performed as in A but χ-less clamp loader complex.

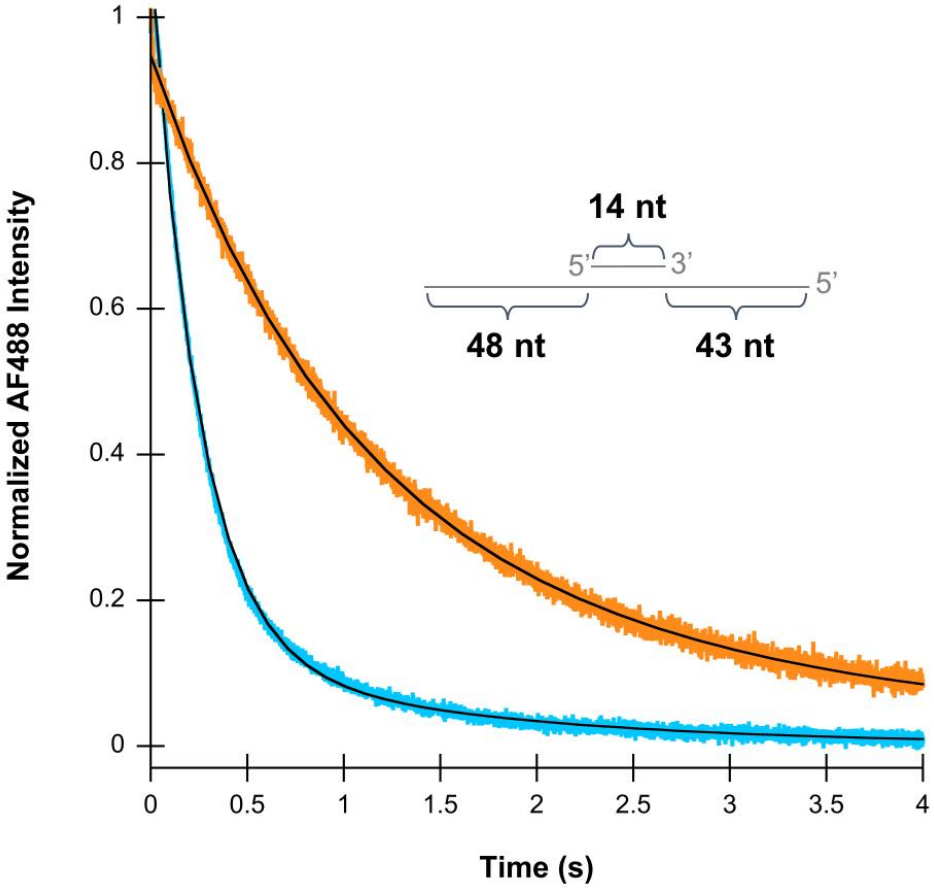


Figure 5-11. Clamp closing on an internal 14nt primer. A structure of the DNA substrate used in this assay is shown. These reactions were performed with no SSB (blue) or with WT SSB (orange). All traces were fit to a single exponential decay formula and the fit is shown in the figure. Final reactant concentrations for the closing reactions were 20nM γ-complex, 20nM β-R103S/I305C-$(AF488)_2$, 200nM unlabeled β, 0.5mM ATP, and 160nM DNA.

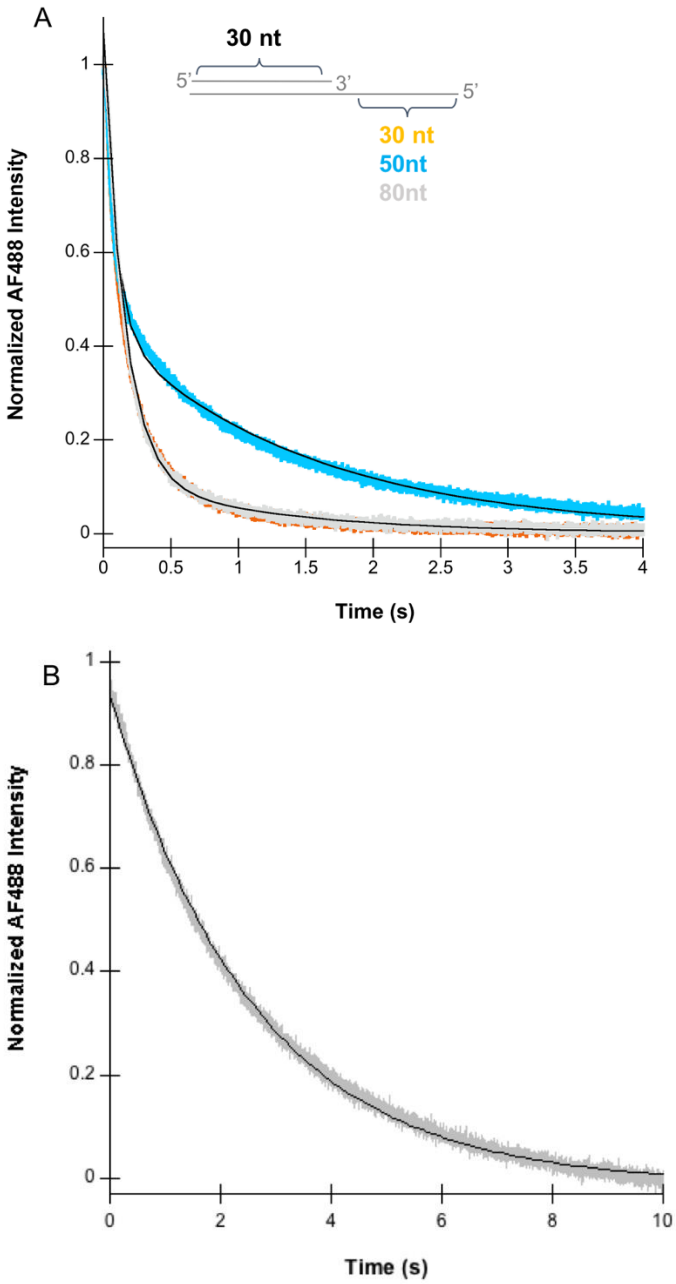


Figure 5-12. Clamp closing on 30nt, 50nt, and 80nt SSO symmetrical substrates. A) Reactions performed with DNA substrates that had 3'DNA with a 30nt SSO (orange), a 50nt SSO (blue), a 80nt SSO (gray) are shown. All traces were fit to a double exponential decay formula and the fit is shown in the figure. Final reactant concentrations for the closing reactions were 20nM γ-complex, 20nM β-R103S/I305C-$(AF488)_2$, 200nM unlabeled β, 0.5mM ATP, and 200nM DNA. B) Representative reaction performed with 5'DNA substrate with 80nt SSO (gray) is shown. This trace was fit to a single exponential formula.

Table 5-1. DNA concentration dependence of clamp loading on 3'DNA substrates.

| DNA Substrate | SSB present | Clamp Loader | $k_{max}$, fast ($s^{-1}$) | $K_{0.5}$, fast (nM) | $k_{max}$, slow ($s^{-1}$) | $K_{0.5}$, slow (nM) |
|---|---|---|---|---|---|---|
| Symmetrical 30nt SSO | None | WT | 16 | 86 | 4.8 | 170 |
| Symmetrical 30nt SSO | WT | WT | 18 | 24 | 3.2 | 16 |
| Symmetrical 5nt SSO | None | WT | 17 | 92 | 3.3 | 115 |
| Symmetrical 30nt SSO | WT | χ-less | 7.1 | 260 | N/A | N/A |
| Symmetrical 30nt SSO | SSBΔC8 | WT | 1.1 | 225 | N/A | N/A |

N/A means no slow rate was calculated for these reactions
$K_{0.5}$ and $k_{max}$ were calculated using Equation 2-6

Table 5-2. Effects of SSB mutations on closing rates with 160 nM symmetrical 30 nt SSO DNA.

| DNA Structure | SSB present | Clamp Loader | $k_{obs}$ ($s^{-1}$) |
|---|---|---|---|
| 3'DNA | WT | WT | 15.4 |
| | WT | χ-less | 2.7 |
| | SSBΔC8 | WT | 0.5 |
| | SSBΔC1 | WT | 0.7 |
| 5'DNA | WT | WT | 0.05 |
| | WT | χ-less | 0.04 |
| | SSBΔC8 | WT | 0.04 |
| | SSBΔC1 | WT | 0.04 |

$k_{obs}$ was calculated using Equation 2-8 or 2-9

Table 5-3. Rates of clamp loading on 160nM 5'DNA substrate.

| DNA Structure | SSB present | Clamp Loader | $k_{obs}$ ($s^{-1}$) |
|---|---|---|---|
| Symmetrical 30nt SSO | None | WT | 1.03 |
| Symmetrical 30nt SSO | WT | WT | 0.05 |
| Asymmetrical 30nt SSO with one blunt end | WT | WT | 0.3 |
| Symmetrical blunt ends | None | WT | 0.8 |
| Symmetrical 30nt SSO | None | χ-less | 0.2 |
| Symmetrical 30nt SSO | WT | χ-less | 0.04 |
| Symmetrical 30nt SSO | SSBΔC8 | WT | 0.04 |
| Symmetrical 30nt SSO | SSBΔC1 | WT | 0.04 |

$k_{obs}$ was calculated using Equation 2-8 or 2-9

Table 5-4. Rates of clamp loading on internal 14 nt oligonucleotide substrate.

| DNA Structure | SSB present | Clamp Loader | $k_{obs}$ ($s^{-1}$) |
|---|---|---|---|
| Internal 14 nt primer with one 3' SSO and one 5' SSO | No | WT | 4 |
| Internal 14 nt primer with one 3' SSO and one 5' SSO | Yes | WT | 0.7 |

$k_{obs}$ was calculated using Equation 2-8 or 2-9

Table 5-5. Rates of clamp loading on 30, 50, and 80 nt SSO substrates.

| DNA Structure | SSB present | Clamp Loader | $k_{fast}$ ($s^{-1}$) | amp fast | $k_{slow}$ ($s^{-1}$) | amp slow |
|---|---|---|---|---|---|---|
| 3'DNA, 30nt SSO | WT | WT | 7.6 | 0.78 | 1.47 | 0.22 |
| 3'DNA, 50nt SSO | WT | WT | 11.4 | 0.56 | 0.66 | 0.44 |
| 3'DNA, 80nt SSO | WT | WT | 6.5 | 0.88 | 0.89 | 0.12 |
| 5'DNA, 30nt SSO | WT | WT | 0.5 | N/A | N/A | N/A |
| 5'DNA, 80nt SSO | WT | WT | 0.4 | N/A | N/A | N/A |

$k_{obs}$ and amp (fractional amplitude) were calculated using Equation 2-8 or 2-9

# CHAPTER 6
# CONCLUSIONS AND FUTURE DIRECTIONS

The experiments presented here examined different aspects of the *E. coli* clamp loader reaction and how the reaction is regulated. To be efficient and precise, sliding clamps must be loaded onto the correct DNA substrate at the right time. The lagging strand of replication requires a sliding clamp to be loaded at the beginning of each Okazaki fragment meaning a sliding clamp is loaded every 2-3s. Failure to load clamps at sites where they are needed could jeopardize the genome integrity. While many studies have examined the different parts of the clamp loading reaction, there are still many unanswered questions as to how the clamp loading reaction is regulated. Experiments presented here were implemented to study how the clamp loaders load the sliding clamps and how this reaction is regulated to ensure clamps are loaded where they are required. The roles of the sliding clamp, clamp loader, and clamp loader-SSB interactions in the clamp loading reaction were examined. In Chapter 3, destabilizing electrostatic mutations of the sliding clamp were used to determine if the clamp loader actively opens the clamp or if the clamp transiently opens. Experiments in Chapter 4 examined the biochemical difference between the two *E. coli* clamp loaders, γ- and τ-complex. Finally, in Chapter 5, the mechanism of clamp loading regulation by single-stranded DNA binding protein (SSB) was studied.

## Destabilizing the Sliding Clamp Does Not Affect the Clamp Loading Reaction

In Chapter 3, the effect of destabilizing the interface of the β sliding clamp on the clamp loading reaction was examined to determine if the clamp loader actively opens the clamp. While the clamp loading mechanism has been studied, there is a still a debate in the field as to whether the clamp loaders actively open the clamp or if they

stabilize the clamp once the clamp transiently opens. Electrostatic interactions were disrupted in the sliding clamp through amino acid substitutions or addition of 500 mM NaCl as this has been shown to destabilize the clamp (29). If the sliding clamp transiently opened and the clamp loader stabilized the open form, then it would be expected that destabilizing the clamps interface would increase the rate of clamp opening. Using clamp opening assays, it was determined that the electrostatic mutations did not have any effect on the clamp opening or closing reactions, even though these mutations significantly destabilized the clamp. Additionally, destabilizing the clamp interface did not change the kinetics of the clamp closing reactions. These results suggest that the clamp loader actively opens the sliding clamp.

Previous work has shown that the clamp opening reaction is at least a 2-step reaction in which the clamp loader binds and then opens the sliding clamp. Kinetic modeling of the clamp opening reaction using clamp binding and opening data revealed a minimum 3-step opening model in which the clamp loader binds the sliding clamp then opens the sliding clamp followed by a conformational change of the open clamp-clamp loader complex. It is hypothesized that this confirmation change is stabilization of the open clamp by the clamp loader. Previous studies suggested that the δ subunit is the clamp loader subunit that initially interacts with the sliding clamp after ATP binding and “cracks” open the sliding clamp. This opening by the δ subunit could be the initial open step in our model and the second open confirmation could be when the rest of the clamp loader subunits interact with the sliding clamp, stabilizing the open confirmation. There was not enough data to rule out additional conformational changes in the reaction, but based on the opening and binding data there are at least three steps in the

clamp opening reaction. The model presented here suggests that the clamp loader destabilizes the close clamp to open it and then stabilizes the open confirmation to prevent monomerization of the subunits. The PCNA sliding clamp is quite stable in solution (29), like the bacterial sliding clamp. In addition, it has been hypothesized that the open sliding clamp is stabilized by the clamp loader (149), as proposed for the bacterial clamp loader, suggesting that the mechanisms of sliding clamp opening may be preserved throughout the domains of life.

### DnaX2016 γ and τ Clamp Loader Subunits Aggregate *in Vitro*

In Chapter 4, the effects of the DnaX2016 mutations on the γ and τ clamp loaders were determined to give insight into the different clamp loaders roles within the cell. Cells with the *dnaX2016* gene are defective in template-switching repair and this pathway is restored when WT γ, not τ, is expressed in these cells (170). Studying the effects of these mutations can help determine a role for γ, which is still currently unknown. While the DnaX2016 subunits were able to be purified, the subunits aggregated into large complexes with each other. WT DnaX is known to form tetramers in solution (200), but the molecular weight of the DnaX2016 aggregates were at least 4-fold larger equivalent to sixteen subunits. *In vitro* reconstitution of the clamp loader complex with the DnaX2016 subunits resulted in precipitation of the subunits and no clamp loader complex could be obtained.

To assist with the purification of DnaX2016 clamp loaders and to increase the efficiency of our laboratory's purification protocol, a Duet Vector system was constructed to allow expression of the *E. coli* clamp loaders and Pol III all at once *in vivo*. Chapter 4 gives details on the creation of these vectors. Previously, the clamp loader complexes were isolated by purification of the individual subunits then followed

by an *in vitro* reconstitution. The total time of this method of clamp loader purification would take months to complete. The Duet Vector system allows purification of the entire pol III* complex in a week. This system also allows for easy swapping of genes in the multiple cloning sites to create mutations and variations of the clamp loader for studies. The Duet Vector system of expression and purification results in mg quantities of proteins, giving enough product for biochemical assays.

An *in vivo* expression vector was constructed previously by another laboratory, but this vector only contained the subunits of the clamp loader and could not be expressed with the pol III subunits to create holoenzyme (173). To purify holoenzyme using this system, after purification of the clamp loader complex there would be an *in vitro* reconstitution method performed. It has been suggested that the *in vitro* reconstitution of the holoenzyme differs from *in vivo* reconstitution in that it is hypothesized the pol III subunits interact with the τ subunits before τ interacts with the other clamp loader subunits (164). The Duet Vector system of expression and purification presented here allows for *in vivo* reconstitution which may be required for formation of active clamp loader complex with the DnaX2016 mutations. It will be interesting to perform the expression and purification of the DnaX2016 clamp loaders to determine if clamp loader complex or pol III* can be purified. Cells with the *dnaX2016* mutation are viable at permissive temperatures and since τ-complex is required for cell viability (63), it is hypothesized that at least the pol III* complex will be able to form somewhat active complex *in vivo*. It is possible that the DnaX2016 τ subunit must interact with pol III first, as hypothesized *in vivo* (164), in order to prevent the high oligomerization seen with the DnaX2016 subunits *in vitro* when expressed alone. If

DnaX2016 clamp loader with τ can be formed but clamp loader with γ cannot be formed since it does not interact with the pol III subunits, this could explain the phenomenon seen that expression of WT γ, but not τ, restores the template-switching repair pathway if clamp loader with γ is required for this pathway. Another possibility is that the *in vivo* form of the clamp loader contains two τ subunits and one γ as previously described (60), and that this ratio is important for the template-switching mechanism. Without functional γ in the clamp loader this could disturb the template-switching process. It is currently unknown exactly how the clamp loader plays a role in template-switching.

### γ and τ Clamp Loaders Are Kinetically the Same

In Chapter 4, the kinetics of γ and τ clamp loaders during multiple steps of the clamp loading reaction were measured to determine if there is any kinetic difference between the two clamp loaders. While both clamp loaders have been shown to load clamps equally, it is unknown if the mechanism in which they load the clamps is the same or not. Various fluorescence-based assays were used to probe multiple steps in the clamp loading reaction. The affinity of the different clamp loaders for the sliding clamp was the same, showing that one clamp loader did not have a better interaction with the sliding clamp than the other. Kinetics of clamp opening, ATP hydrolysis, clamp closing, and clamp release were the same for the two clamp loaders showing that indeed the two clamp loaders are kinetically equivalent and the clamp loading reaction does not differ between the two clamp loaders.

If the clamp loading reactions are independent of which clamp loader is used, the reason τ is required for viability, but γ is not, must be due to the ability of τ to assist with DNA replication. The τ subunit assists with DNA replication by giving pol III preferential access to the sliding clamp, interacting with the helicase, and recycle clamps on the

lagging strand, none of which γ can perform (4, 64, 67). Giving pol III direct access to the sliding clamp is important to prevent other enzymes, like error-prone polymerases, from accessing the clamp at the replication fork when these enzymes are not needed in order to help keep the integrity of the genome. Recent studies suggest that one γ subunit is present at the replication fork (60, 201). While the role for γ is unknown, it has been suggested that the presence of γ at the replication fork allows occasional pol IV-dependent mutagenesis important for the production of spontaneous mutations (60). Studies have shown that these types of mutations are important for natural selection and evolutionary fitness (202). It Is interesting to note that the γ and τ subunits are produced at equal quantities. If only one γ subunit is at the replication fork, it raises the question of what the other γ subunits are doing if they have a cellular function. Elg1-RFC clamp loader has been shown to be a clamp unloader (203). Possibly γ functions to unload the sliding clamps, which have been shown to have a long half-life on DNA (30). Mutations found to inhibit γ function *in vivo,* like with the DnaX2016 clamp loaders, could provide evidence of the role of γ through biochemical investigation. The Duet Vectors provide a simple and efficient method of producing large enough quantities of the clamp loaders to make these studies possible.

## SSB Regulation of Clamp Loading

### SSB stimulates clamp loading on the correct polarity DNA through multiple interactions with the clamp loader

In Chapter 5, the mechanism of how SSB stimulates clamp loading on the correct polarity DNA (3'DNA) was investigated. It was shown previously that the presence of SSB stimulated clamp loading on correct polarity DNA (105). This stimulation is important during DNA replication because pol III can only extend off of a 3'OH so the

clamps must be loaded at these sites (3’ recessed ends, 3’DNA). While the phenomenon of SSB stimulation has been well documented, it is still unknown what mechanism SSB uses to cause this stimulation. Fluorescence-based assays were utilized as well as variants of the clamp loader and SSB to give insight into what the mechanism of regulation is.

Clamp closing assays were used as a screen to determine how the presence of SSB stimulated clamp closing on the correct polarity DNA (3’DNA). Rate constants were determined in order to compare reactions without SSB to reactions with SSB. When SSB was present in the reactions, the $K_{0.5,}$ was reduced over 3.5-fold compared to reactions without SSB. This result suggests that SSB stimulates clamp loading by increasing the clamp loader’s affinity for the correct DNA substrate. Previous studies have shown that the clamp loader binds more efficiently to 3’DNA substrates that contained SSB when compared to the 5’DNA (96). SSB could be increasing the contacts between the clamp loader-clamp complex and the primer-template junction. Also, SSB could be reducing the number of nonspecific contacts the clamp loader makes with SSB to lower the $K_{0.5}$.

The SSB C-terminal tail has been shown to interact with the clamp loader through the χ subunit (100, 101). Clamp loaders without the χ do not have a known clamp loading deficiently, but when SSB is present, the rate of clamp loading on the correct polarity DNA decreases by 5-fold indicating that this interaction is required for the stimulation on the correct polarity DNA. The role of the χ-SSB interaction could be to move SSB away from the primer-template to give the clamp loader-clamp complex access. The DNA concentration dependence of the reactions without χ could be due to

the inability to move SSB and the clamp loader waiting for SSB to transiently move before it can gain access to the primer-template junction. It should be noted that there is an excess of the χ subunit at the replication fork (31, 58). The mechanism of remodeling SSB by the interaction with χ could have implications on how other proteins gain access to the replication fork in the presence of SSB.

Interestingly, when a C-terminal truncated form of SSB was used, the rate of clamp loading was even slower than the χ-less clamp loader reactions. This indicates that SSB may be able to interact with a different region of the clamp loader reaction other than χ, which would be a novel interaction. A previous study has suggested there was an additional interaction between the clamp loader and SSB (183) . Another study also found that when the hydrophobic pocket of the sliding clamp was mutated, it reduced the specificity of clamp loading of 3'DNA-SSB compared to 5'DNA-SSB (96). It is possible that SSB not only interacts with the clamp loader, but also the sliding clamp. Additionally, in Chapter 4, it was shown that the stimulation of clamp loading on correct polarity DNA by SSB was also present in reactions with τ-complex and the holoenzyme complex, the forms of the clamp loader present at the replication fork.

Based on the results presented, the direct protein-protein interaction between SSB and the clamp loader on the correct polarity DNA increases the contacts between the clamp loader-clamp complex and the primer-template junction. There seems to be a minimum of two interactions between the clamp loader-clamp and SSB that is responsible for this stimulation of DNA binding. The clamp loader-clamp complex could use this interaction to physically move SSB out of the way, gaining access to the primer-template junction. This could also involve a SSB-DNA remodeling step where the

interaction of the clamp loader-clamp complex with SSB could induce a change of the SSB-DNA binding mode. SSB could also direct the clamp loader-clamp complex to the primer-template junction by reducing the number of non-productive DNA binding events. Additionally, clamp loading on naked DNA was strongly dependent on the DNA concentration, whereas loading on SSB-coated DNA was not very dependent on the DNA concentration. Possibly, DNA binding is the rate-determining step of the reaction without SSB, but with SSB DNA binding is no longer rate limiting. Another step, like SSB remodeling, could be the rate determining step of clamp closing when SSB is present.

To determine if the clamp loader remodels SSB at the primer-template junction, a FRET-based assay is currently being developed in our laboratory. The primers of 3'DNA and 5'DNA will be labeled with a fluorescence donor and the N-terminal end of SSB will be labeled with a non-fluorescent donor. When SSB is directly next to the primer-template junction, there will be little fluorescence. If SSB is displaced there will be an increase in fluorescence. The changes in fluorescence can be measured using a stopped-flow machine to measure the rates of movement in real-time. Combining this experiment with DNA binding, ATP hydrolysis, and clamp closing assays can help determine the timing of events of clamp loading on 3'DNA. This would help determine whether or not the clamp loader changes the position of SSB by moving it away from the 3'DNA primer-template junction to allow the clamp loader-clamp complex to bind.

### SSB inhibits clamp loading on the incorrect polarity DNA through SSB-DNA interactions

In Chapter 5, the mechanism by which SSB inhibits clamp loading on the incorrect polarity DNA (5'DNA) was investigated. Previously, our laboratory

demonstrated that the presence of SSB inhibits clamp loading onto the incorrect polarity DNA to levels of reactions without DNA. To determine the mechanism of inhibition, fluorescence-based assays were used to measure the rate of clamp loading in the presence and absence of WT SSB or truncated SSB. Unlike reactions with the correct polarity DNA (3'DNA), inhibition of clamp loading reactions on the incorrect polarity (5'DNA) was not dependent on clamp loader-SSB interactions. Clamp loading with WT and χ-less clamp loader both occurred at 0.05 $s^{-1}$, which is equivalent to reactions with no DNA. In addition, clamp loading reactions with C-terminal truncated SSB variants occurred at the same rate.

The results of the presented experiments suggest that the inhibition of clamp loading is not dependent on known clamp loader-SSB interactions, but possibly due to SSB-DNA interactions preventing the clamp loader from loading clamps on 5'DNA. Additionally, in Chapter 4, it was shown that the inhibition of clamp loading on the incorrect polarity DNA by SSB was also present in reactions with τ-complex and the holoenzyme complex, the forms of the clamp loader present at the replication fork. Interestingly, the rate of clamp loading on the incorrect polarity DNA is similar to the rate of dissociation of the clamp from the clamp loader (Table 3-2). Measuring clamp loading reactions for a longer time period (500s) as in the dissociation assays would give a better estimate of the reaction rates and to determine if there are biphasic kinetics as seen with the dissociation reactions. This result is in agreement with a previous study which demonstrated that ATP hydrolysis was very low when using a 5'DNA substrate (96). This study also used pull-down assays that showed DNA binding of the clamp loader was reduced, but did occur at 5'DNA-SSB structures. If the clamp loader does

bind DNA, but does not perform ATP hydrolysis, then this would suggest that the SSB-DNA interaction traps the open clamp-clamp loader in a complex in which the clamp cannot close and the only way the clamp loader can release itself is to dissociate from the clamp. Alternatively, SSB could be blocking DNA binding all together and the clamp loaders seen on 5'DNA in the 2009 study could be an artifact of nonspecific binding. If this was the case, it would be expected to little-to-none ATP hydrolysis would occur and that the closing rates would match dissociation rates, which was seen in the clamp closing assays using 5'DNA.

To determine if the clamp loader is binding 5'DNA or not, a FRET-based assay could be used to measure the rate of DNA binding. By labeling the primer-template junction of a DNA substrate with a fluorescent donor and the sliding clamp with a non-fluorescent quencher, rates of DNA binding could be measured. As the clamp loader-clamp complex binds the DNA, the fluorescence will decrease which can be measured by a stopped-flow apparatus in order to determine DNA binding rates. These experiments would confirm whether or not the clamp loader can gain access to the primer-template junction when SSB is present.

**Model for SSB regulation of clamp loading**

Combining the results of SSB regulation of clamp loading on the incorrect and correct polarity DNA suggests that the C-terminal tail of SSB can recruit enzymes to DNA, but does not define DNA specificity. The DNA specificity of the clamp loading reaction conferred by SSB seems to stem from a SSB-DNA interaction. SSB may sterically block the primer-template junction and must repositioned in order to gain access. Another possibility, and more likely, is that there is a difference of the dynamics of the 3'DNA-SSB and 5'DNA-SSB when the clamp loader-clamp complex binds. It may

be that on the 3'DNA the clamp loader can move SSB away from the primer-template junction, but on 5'DNA the clamp loader can only move SSB towards the primer-template junction. This matches clamp closing results on a 14 nt internal primer in which SSB on the 5'DNA had to move in order for the clamp loader to load the sliding clamp. It has previously been hypothesized that the clamp loader must reposition SSB not only to load the clamp, but to also to give DNA polymerase access to the primer (183). SSB and the clamp loader could be in competition for the primer-template junction and that remodeling of SSB must occur before the clamp loader can gain access. This dynamic remodeling of 3'DNA-SSB requires χ-SSB interactions and possibly another clamp loader-clamp interaction with SSB. Based on the results presented here, on the correct polarity DNA, χ interacts with SSB to remodel the SSB-DNA complex, either by moving the SSB molecule away from the primer-template junction, changing the SSB DNA-binding mode, or possibly by reducing the amount of nonproductive binding events, which allows the clamp loader to load the sliding clamp. This interaction seems to increase the binding of the clamp loader-clamp to 3'DNA.

One possibility for inhibition of the clamp loading on 5'DNA-SSB is that on the incorrect polarity DNA, the SSB-DNA complex cannot be remodeled by the clamp loader, preventing clamp loading. The structure of SSB-DNA could be different on a 3' recessed primer-template junction compared to a 5' primer-template junction. If this was the case then it would be expected that DNA binding is inhibited, which seems unlikely because SSB moves dynamically along DNA and previous studies have shown the clamp loader binds to 5'DNA-SSB (96). Another case could be that interaction of the clamp loader-clamp with 5'DNA-SSB could cause remodeling or an interaction that

traps the clamp loader-clamp in an unproductive complex that cannot undergo ATP hydrolysis. There could also be an effect of the direction that the clamp loader-clamp complex approaches the DNA-SSB complex. Possibly on 3'DNA-SSB the clamp loader can push SSB away from the primer-template junction, but on 5'DNA-SSB the clamp loader pushes the SSB towards the primer-template junction inhibiting clamp loading. Since the inhibition of clamp loading on the incorrect polarity DNA was independent of protein-protein interactions, this suggests that the DNA binding domain of SSB is important in the regulation. Novel interactions between the DNA-SSB and clamp loader-clamp complex may exist that play a role in this inhibition.

To further investigate this mechanism of clamp loading regulation by SSB, the exact step that is being regulated by SSB should be determined. The clamp closing assays used in Chapter 5 was completed to study the effect of SSB on clamp loading, but before clamp closing, DNA binding and ATP hydrolysis occur, either of which could be effected by SSB. Our laboratory already has an ATP hydrolysis assay that could be used and a FRET-based DNA binding assay is currently being developed. Determining the exact step in which SSB is inhibiting the clamp loading reaction would help to determine the mechanism of regulation. Another interesting experiment would be to determine if SSB binds the incorrect polarity DNA with the same affinity as the correct polarity DNA. DNA binding can be measured through anisotropy assays as performed in Chapter 5. If SSB has a higher affinity for the incorrect polarity DNA, this may explain the inhibition of clamp loading. These experiments should also be performed with the eukaryotic clamp and clamp loader to determine if the eukaryotic SSB, RPA, regulates clamp loading through the same mechanism.

LIST OF REFERENCES

1. Chandler,M., Bird,R.E. and Caro,L. (1975) The replication time of the Escherichia coli K12 chromosome as a function of cell doubling time. *Journal of Molecular Biology*, **94**, 127–132.

2. Schaaper,R.M. (1993) Base selection, proofreading, and mismatch repair during DNA replication in Escherichia coli. *Journal of Biological Chemistry*, **268**, 23762–23765.

3. Drake,J.W. (1969) Comparative rates of spontaneous mutation. *Nature*, **221**, 1132.

4. Kim,S., Dallmann,H.G., McHenry,C.S. and Marians,K.J. (1996) Coupling of a replicative polymerase and helicase: a tau-DnaB interaction mediates rapid replication fork movement. *Cell*, **84**, 643–650.

5. Stukenberg,P.T., Studwell-Vaughan,P.S. and O'Donnell,M. (1991) Mechanism of the sliding beta-clamp of DNA polymerase III holoenzyme. *Journal of Biological Chemistry*, **266**, 11328–11334.

6. Kelman,Z. and O'Donnell,M. (1995) Structural and functional similarities of prokaryotic and eukaryotic DNA polymerase sliding clamps. *Nucleic Acids Res*, **23**, 3613–3620.

7. Ogawa,T. and Okazaki,T. (1980) Discontinuous DNA replication. *Annu. Rev. Biochem.*, **49**, 421–457.

8. Benkovic,S.J., Valentine,A.M. and Salinas,F. (2001) Replisome-mediated DNA replication. *Annu. Rev. Biochem.*, **70**, 181–208.

9. Maki,H., Maki,S. and Kornberg,A. (1988) DNA Polymerase III holoenzyme of Escherichia coli. IV. The holoenzyme is an asymmetric dimer with twin active sites. *Journal of Biological Chemistry*, **263**, 6570–6578.

10. Friedberg,E.C. (2006) The eureka enzyme: the discovery of DNA polymerase.

11. Gefter,M.L., Hirota,Y., Kornberg,T., Wechsler,J.A. and Barnoux,C. (1971) Analysis of DNA polymerases II and 3 in mutants of Escherichia coli thermosensitive for DNA synthesis. *Proc. Natl. Acad. Sci. U.S.A.*, **68**, 3150–3153.

12. Studwell-Vaughan,P.S. and O'Donnell,M. (1993) DNA polymerase III accessory proteins. V. Theta encoded by holE. *Journal of Biological Chemistry*, **268**, 11785–11791.

13. Welch,M.M. and McHenry,C.S. (1982) Cloning and identification of the product of the dnaE gene of Escherichia coli. *J. Bacteriol.*, **152**, 351–356.

14. Scheuermann,R.H. and Echols,H. (1984) A separate editing exonuclease for DNA replication: the epsilon subunit of Escherichia coli DNA polymerase III holoenzyme. *Proc. Natl. Acad. Sci. U.S.A.*, **81**, 7747–7751.

15. Fijalkowska,I.J. and Schaaper,R.M. (1996) Mutants in the Exo I motif of Escherichia coli dnaQ: defective proofreading and inviability due to error catastrophe. *Proc. Natl. Acad. Sci. U.S.A.*, **93**, 2856–2861.

16. Slater,S.C., Lifsics,M.R., O'Donnell,M. and Maurer,R. (1994) holE, the gene coding for the theta subunit of DNA polymerase III of Escherichia coli: characterization of a holE mutant and comparison with a dnaQ (epsilon-subunit) mutant. *J. Bacteriol.*, **176**, 815–821.

17. Conte,E., Vincelli,G., Schaaper,R.M., Bressanin,D., Stefan,A., Dal Piaz,F. and Hochkoeppler,A. (2012) Stabilization of the Escherichia coli DNA polymerase III ε subunit by the θ subunit favors in vivo assembly of the Pol III catalytic core. *Arch. Biochem. Biophys.*, **523**, 135–143.

18. Hamdan,S., Bulloch,E.M., Thompson,P.R., Beck,J.L., Yang,J.Y., Crowther,J.A., Lilley,P.E., Carr,P.D., Ollis,D.L., Brown,S.E., *et al.* (2002) Hydrolysis of the 5'-p-nitrophenyl ester of TMP by the proofreading exonuclease (epsilon) subunit of Escherichia coli DNA polymerase III. *Biochemistry*, **41**, 5266–5275.

19. Taft-Benz,S.A. and Schaaper,R.M. (1999) The C-terminal domain of dnaQ contains the polymerase binding site. *J. Bacteriol.*, **181**, 2963–2965.

20. Fay,P.J., Johanson,K.O., McHenry,C.S. and Bambara,R.A. (1981) Size classes of products synthesized processively by DNA polymerase III and DNA polymerase III holoenzyme of Escherichia coli. *Journal of Biological Chemistry*, **256**, 976–983.

21. Bloom,L.B., Chen,X., Fygenson,D.K., Turner,J., O'Donnell,M. and Goodman,M.F. (1997) Fidelity of Escherichia coli DNA polymerase III holoenzyme. The effects of beta, gamma complex processivity proteins and epsilon proofreading exonuclease on nucleotide misincorporation efficiencies. *Journal of Biological Chemistry*, **272**, 27919–27930.

22. Georgescu,R.E., Kurth,I. and O'Donnell,M.E. (2011) Single-molecule studies reveal the function of a third polymerase in the replisome. *Nat. Struct. Mol. Biol.*, **19**, 113–116.

23. Maki,S. and Kornberg,A. (1988) DNA polymerase III holoenzyme of Escherichia coli. III. Distinctive processive polymerases reconstituted from purified subunits. *Journal of Biological Chemistry*, **263**, 6561–6569.

24. LaDuca,R.J., Crute,J.J., McHenry,C.S. and Bambara,R.A. (1986) The beta subunit of the Escherichia coli DNA polymerase III holoenzyme interacts functionally with the catalytic core in the absence of other subunits. *Journal of Biological Chemistry*, **261**, 7550–7557.

25. Scouten Ponticelli,S.K., Duzen,J.M. and Sutton,M.D. (2009) Contributions of the individual hydrophobic clefts of the Escherichia coli beta sliding clamp to clamp loading, DNA replication and clamp recycling. *Nucleic Acids Res*, **37**, 2796–2809.

26. Duzen,J.M., Walker,G.C. and Sutton,M.D. (2004) Identification of specific amino acid residues in the E. coli beta processivity clamp involved in interactions with DNA polymerase III, UmuD and UmuD'. *DNA Repair (Amst.)*, **3**, 301–312.

27. Kim,D.R. and McHenry,C.S. (1996) Identification of the beta-binding domain of the alpha subunit of Escherichia coli polymerase III holoenzyme. *Journal of Biological Chemistry*, **271**, 20699–20704.

28. Kong,X.P., Onrust,R., O'Donnell,M. and Kuriyan,J. (1992) Three-dimensional structure of the beta subunit of E. coli DNA polymerase III holoenzyme: a sliding DNA clamp. *Cell*, **69**, 425–437.

29. Binder,J.K., Binder,J.K., Douma,L.G., Ranjit,S., Ranjit,S., Kanno,D.M., Kanno,D.M., Chakraborty,M., Bloom,L.B. and Levitus,M. (2014) Intrinsic stability and oligomerization dynamics of DNA processivity clamps. *Nucleic Acids Res*, **42**, 6476–6486.

30. Yao,N., Turner,J., Kelman,Z., Stukenberg,P.T., Dean,F., Shechter,D., Pan,Z.Q., Hurwitz,J. and O'Donnell,M. (1996) Clamp loading, unloading and intrinsic stability of the PCNA, beta and gp45 sliding clamps of human, E. coli and T4 replicases. *Genes Cells*, **1**, 101–113.

31. Leu,F.P., Hingorani,M.M., Turner,J. and O'Donnell,M. (2000) The delta subunit of DNA polymerase III holoenzyme serves as a sliding clamp unloader in Escherichia coli. *Journal of Biological Chemistry*, **275**, 34609–34618.

32. Georgescu,R.E., Kim,S.-S., Yurieva,O., Kuriyan,J., Kong,X.-P. and O'Donnell,M. (2008) Structure of a sliding clamp on DNA. *Cell*, **132**, 43–54.

33. Oakley,A.J., Prosselkov,P., Wijffels,G., Beck,J.L., Wilce,M.C.J. and Dixon,N.E. (2003) Flexibility revealed by the 1.85 A crystal structure of the beta sliding-clamp subunit of Escherichia coli DNA polymerase III. *Acta Crystallogr. D Biol. Crystallogr.*, **59**, 1192–1199.

34. Georgescu,R.E., Yurieva,O., Kim,S.-S., Kuriyan,J., Kong,X.-P. and O'Donnell,M. (2008) Structure of a small-molecule inhibitor of a DNA polymerase sliding clamp. *Proc. Natl. Acad. Sci. U.S.A.*, **105**, 11116–11121.

35. Naktinis,V., Onrust,R., Fang,L. and O'Donnell,M. (1995) Assembly of a chromosomal replication machine: two DNA polymerases, a clamp loader, and sliding clamps in one holoenzyme particle. II. Intermediate complex between the clamp loader and its clamp. *Journal of Biological Chemistry*, **270**, 13358–13365.

36. Naktinis,V., Turner,J. and O'Donnell,M. (1996) A molecular switch in a replication machine defined by an internal competition for protein rings. *Cell*, **84**, 137–145.

37. Yao,N.Y., Georgescu,R.E., Finkelstein,J. and O'Donnell,M.E. (2009) Single-molecule analysis reveals that the lagging strand increases replisome processivity but slows replication fork progression. *Proc. Natl. Acad. Sci. U.S.A.*, **106**, 13236–13241.

38. Maki,S. and Kornberg,A. (1988) DNA polymerase III holoenzyme of Escherichia coli. II. A novel complex including the gamma subunit essential for processive synthesis. *Journal of Biological Chemistry*, **263**, 6555–6560.

39. O'Donnell,M.E. and Kornberg,A. (1985) Dynamics of DNA polymerase III holoenzyme of Escherichia coli in replication of a multiprimed template. *Journal of Biological Chemistry*, **260**, 12875–12883.

40. López de Saro,F.J., Georgescu,R.E., Goodman,M.F. and O'Donnell,M. (2003) Competitive processivity-clamp usage by DNA polymerases during DNA replication and repair. *EMBO J*, **22**, 6408–6418.

41. López de Saro,F.J. and O'Donnell,M. (2001) Interaction of the beta sliding clamp with MutS, ligase, and DNA polymerase I. *Proc. Natl. Acad. Sci. U.S.A.*, **98**, 8376–8380.

42. López de Saro,F.J., Marinus,M.G., Modrich,P. and O'Donnell,M. (2006) The beta sliding clamp binds to multiple sites within MutL and MutS. *Journal of Biological Chemistry*, **281**, 14340–14349.

43. Pluciennik,A., Burdett,V., Lukianova,O., O'Donnell,M. and Modrich,P. (2009) Involvement of the beta clamp in methyl-directed mismatch repair in vitro. *J. Biol. Chem.*, **284**, 32782–32791.

44. Kunkel,T.A. and Erie,D.A. (2005) DNA mismatch repair. *Annu. Rev. Biochem.*, **74**, 681–710.

45. Pillon,M.C., Miller,J.H. and Guarné,A. (2011) The endonuclease domain of MutL interacts with the β sliding clamp. *DNA Repair (Amst.)*, **10**, 87–93.

46. Lenne-Samuel,N., Wagner,J., Etienne,H. and Fuchs,R.P.P. (2002) The processivity factor beta controls DNA polymerase IV traffic during spontaneous mutagenesis and translesion synthesis in vivo. *EMBO Rep.*, **3**, 45–49.

47. Dalrymple,B.P., Kongsuwan,K., Wijffels,G., Dixon,N.E. and Jennings,P.A. (2001) A universal protein-protein interaction motif in the eubacterial DNA replication and repair systems. *Proc. Natl. Acad. Sci. U.S.A.*, **98**, 11627–11632.

48. Stewart,J., Hingorani,M.M., Kelman,Z. and O'Donnell,M. (2001) Mechanism of beta clamp opening by the delta subunit of Escherichia coli DNA polymerase III holoenzyme. *Journal of Biological Chemistry*, **276**, 19182–19189.

49. Bloom,L.B. (2009) Loading clamps for DNA replication and repair. *DNA Repair (Amst.)*, **8**, 570–578.

50. Park,A.Y., Jergic,S., Politis,A., Ruotolo,B.T., Hirshberg,D., Jessop,L.L., Beck,J.L., Barsky,D., O'Donnell,M., Dixon,N.E., *et al.* (2010) A single subunit directs the assembly of the Escherichia coli DNA sliding clamp loader. *Structure*, **18**, 285–292.

51. O'Donnell,M., Jeruzalmi,D. and Kuriyan,J. (2001) Clamp loader structure predicts the architecture of DNA polymerase III holoenzyme and RFC. *Curr. Biol.*, **11**, R935–46.

52. Jeruzalmi,D., O'Donnell,M. and Kuriyan,J. (2001) Crystal structure of the processivity clamp loader gamma (gamma) complex of E. coli DNA polymerase III. *Cell*, **106**, 429–441.

53. Davey,M.J., Jeruzalmi,D., Kuriyan,J. and O'Donnell,M. (2002) Motors and switches: AAA+ machines within the replisome. *Nat. Rev. Mol. Cell Biol.*, **3**, 826–835.

54. Neuwald,A.F., Aravind,L., Spouge,J.L. and Koonin,E.V. (1999) AAA+: A class of chaperone-like ATPases associated with the assembly, operation, and disassembly of protein complexes. *Genome Res.*, **9**, 27–43.

55. Tsuchihashi,Z. and Kornberg,A. (1990) Translational frameshifting generates the gamma subunit of DNA polymerase III holoenzyme. *Proc. Natl. Acad. Sci. U.S.A.*, **87**, 2516–2520.

56. Blinkowa,A.L. and Walker,J.R. (1990) Programmed ribosomal frameshifting generates the Escherichia coli DNA polymerase III gamma subunit from within the tau subunit reading frame. *Nucleic Acids Res*, **18**, 1725–1729.

57. Flower,A.M. and McHenry,C.S. (1990) The gamma subunit of DNA polymerase III holoenzyme of Escherichia coli is produced by ribosomal frameshifting. *Proc. Natl. Acad. Sci. U.S.A.*, **87**, 3713–3717.

58. Reyes-Lamothe,R., Sherratt,D.J. and Leake,M.C. (2010) Stoichiometry and architecture of active DNA replication machinery in Escherichia coli. *Science*, **328**, 498–501.

59. McInerney,P., Johnson,A., Katz,F. and O'Donnell,M. (2007) Characterization of a triple DNA polymerase replisome. *Mol. Cell*, **27**, 527–538.

60. Dohrmann,P.R., Correa,R., Frisch,R.L., Rosenberg,S.M. and McHenry,C.S. (2016) The DNA polymerase III holoenzyme contains γ and is not a trimeric polymerase. *Nucleic Acids Res*, **44**, gkv1510–1297.

61. Glover,B.P. and McHenry,C.S. (2000) The DnaX-binding subunits delta' and psi are bound to gamma and not tau in the DNA polymerase III holoenzyme. *Journal of Biological Chemistry*, **275**, 3017–3020.

62. Onrust,R., Finkelstein,J., Turner,J., Naktinis,V. and O'Donnell,M. (1995) Assembly of a chromosomal replication machine: two DNA polymerases, a clamp loader, and sliding clamps in one holoenzyme particle. III. Interface between two polymerases and the clamp loader. *Journal of Biological Chemistry*, **270**, 13366–13377.

63. Blinkova,A., Hervas,C., Stukenberg,P.T., Onrust,R., O'Donnell,M.E. and Walker,J.R. (1993) The Escherichia coli DNA polymerase III holoenzyme contains both products of the dnaX gene, tau and gamma, but only tau is essential. *J. Bacteriol.*, **175**, 6018–6027.

64. Gao,D. and McHenry,C.S. (2001) Tau binds and organizes Escherichia coli replication proteins through distinct domains. Domain III, shared by gamma and tau, binds delta delta ' and chi psi. *Journal of Biological Chemistry*, **276**, 4447–4453.

65. Gao,D. and McHenry,C.S. (2001) tau binds and organizes Escherichia coli replication through distinct domains. Partial proteolysis of terminally tagged tau to determine candidate domains and to assign domain V as the alpha binding domain. *Journal of Biological Chemistry*, **276**, 4433–4440.

66. Dallmann,H.G., Kim,S., Pritchard,A.E., Marians,K.J. and McHenry,C.S. (2000) Characterization of the unique C terminus of the Escherichia coli tau DnaX protein. Monomeric C-tau binds alpha AND DnaB and can partially replace tau in reconstituted replication forks. *Journal of Biological Chemistry*, **275**, 15512–15519.

67. Glover,B.P., Pritchard,A.E. and McHenry,C.S. (2001) tau binds and organizes Escherichia coli replication proteins through distinct domains: domain III, shared by gamma and tau, oligomerizes DnaX. *Journal of Biological Chemistry*, **276**, 35842–35846.

68. Naue,N., Beerbaum,M., Bogutzki,A., Schmieder,P. and Curth,U. (2013) The helicase-binding domain of Escherichia coli DnaG primase interacts with the highly conserved C-terminal region of single-stranded DNA-binding protein. *Nucleic Acids Res*, **41**, 4507–4517.

69. Bailey,S., Eliason,W.K. and Steitz,T.A. (2007) Structure of hexameric DnaB helicase and its complex with a domain of DnaG primase. *Science*, **318**, 459–463.

70. Wang,G., Klein,M.G., Tokonzaba,E., Zhang,Y., Holden,L.G. and Chen,X.S. (2008) The structure of a DnaB-family replicative helicase and its interactions with primase. *Nat. Struct. Mol. Biol.*, **15**, 94–100.

71. Chintakayala,K., Machón,C., Haroniti,A., Larson,M.A., Hinrichs,S.H., Griep,M.A. and Soultanas,P. (2009) Allosteric regulation of the primase (DnaG) activity by the clamp-loader (tau) in vitro. *Molecular Microbiology*, **72**, 537–549.

72. Blaauwen,den,T., Aarsman,M.E.G., Wheeler,L.J. and Nanninga,N. (2006) Pre-replication assembly of E. coli replisome components. *Molecular Microbiology*, **62**, 695–708.

73. Studwell-Vaughan,P.S. and O'Donnell,M. (1991) Constitution of the twin polymerase of DNA polymerase III holoenzyme. *Journal of Biological Chemistry*, **266**, 19833–19841.

74. Gao,D. and McHenry,C.S. (2001) tau binds and organizes Escherichia coli replication proteins through distinct domains. Domain IV, located within the unique C terminus of tau, binds the replication fork, helicase, DnaB. *Journal of Biological Chemistry*, **276**, 4441–4446.

75. Liu,B., Lin,J. and Steitz,T.A. (2013) Structure of the PolIIIα-τc-DNA complex suggests an atomic model of the replisome. *Structure*, **21**, 658–664.

76. Kim,S., Dallmann,H.G., McHenry,C.S. and Marians,K.J. (1996) Tau protects beta in the leading-strand polymerase complex at the replication fork. *Journal of Biological Chemistry*, **271**, 4315–4318.

77. Wu,C.A., Zechner,E.L., Hughes,A.J., Franden,M.A., McHenry,C.S. and Marians,K.J. (1992) Coordinated leading- and lagging-strand synthesis at the Escherichia coli DNA replication fork. IV. Reconstitution of an asymmetric, dimeric DNA polymerase III holoenzyme. *Journal of Biological Chemistry*, **267**, 4064–4073.

78. Goldfless,S.J., Morag,A.S., Belisle,K.A., Sutera,V.A. and Lovett,S.T. (2006) DNA repeat rearrangements mediated by DnaK-dependent replication fork repair. *Mol. Cell*, **21**, 595–604.

79. Hingorani,M.M. and O'Donnell,M. (1998) ATP binding to the Escherichia coli clamp loader powers opening of the ring-shaped clamp of DNA polymerase III holoenzyme. *Journal of Biological Chemistry*, **273**, 24550–24563.

80. Turner,J., Hingorani,M.M., Kelman,Z. and O'Donnell,M. (1999) The internal workings of a DNA polymerase clamp-loading machine. *EMBO J*, **18**, 771–783.

81. Stewart,J., Hingorani,M.M., Kelman,Z. and O'Donnell,M. (2001) Mechanism of beta clamp opening by the delta subunit of Escherichia coli DNA polymerase III holoenzyme. *Journal of Biological Chemistry*, **276**, 19182–19189.

82. Indiani,C. and O'Donnell,M. (2003) Mechanism of the delta wrench in opening the beta sliding clamp. *Journal of Biological Chemistry*, **278**, 40272–40281.

83. Jeruzalmi,D., Yurieva,O., Zhao,Y., Young,M., Stewart,J., Hingorani,M., O'Donnell,M. and Kuriyan,J. (2001) Mechanism of processivity clamp opening by the delta subunit wrench of the clamp loader complex of E. coli DNA polymerase III. *Cell*, **106**, 417–428.

84. Bertram,J.G., Bloom,L.B., Hingorani,M.M., Beechem,J.M., O'Donnell,M. and Goodman,M.F. (2000) Molecular mechanism and energetics of clamp assembly in Escherichia coli. The role of ATP hydrolysis when gamma complex loads beta on DNA. *Journal of Biological Chemistry*, **275**, 28413–28420.

85. Anderson,S.G., Thompson,J.A., Paschall,C.O., O'Donnell,M. and Bloom,L.B. (2009) Temporal correlation of DNA binding, ATP hydrolysis, and clamp release in the clamp loading reaction catalyzed by the Escherichia coli gamma complex. *Biochemistry*, **48**, 8516–8527.

86. Ason,B., Bertram,J.G., Hingorani,M.M., Beechem,J.M., O'Donnell,M., Goodman,M.F. and Bloom,L.B. (2000) A model for Escherichia coli DNA polymerase III holoenzyme assembly at primer/template ends. DNA triggers a change in binding specificity of the gamma complex clamp loader. *Journal of Biological Chemistry*, **275**, 3006–3015.

87. Onrust,R., Stukenberg,P.T. and O'Donnell,M. (1991) Analysis of the ATPase subassembly which initiates processive DNA synthesis by DNA polymerase III holoenzyme. *Journal of Biological Chemistry*, **266**, 21681–21686.

88. Simonetta,K.R., Kazmirski,S.L., Goedken,E.R., Cantor,A.J., Kelch,B.A., McNally,R., Seyedin,S.N., Makino,D.L., O'Donnell,M. and Kuriyan,J. (2009) The mechanism of ATP-dependent primer-template recognition by a clamp loader complex. *Cell*, **137**, 659–671.

89. Hingorani,M.M., Bloom,L.B., Goodman,M.F. and O'Donnell,M. (1999) Division of labor--sequential ATP hydrolysis drives assembly of a DNA polymerase sliding clamp around DNA. *EMBO J*, **18**, 5131–5144.

90. Bertram,J.G., Bloom,L.B., Turner,J., O'Donnell,M., Beechem,J.M. and Goodman,M.F. (1998) Pre-steady state analysis of the assembly of wild type and mutant circular clamps of Escherichia coli DNA polymerase III onto DNA. *Journal of Biological Chemistry*, **273**, 24564–24574.

91. Williams,C.R., Snyder,A.K., Kuzmic,P., O'Donnell,M. and Bloom,L.B. (2004) Mechanism of loading the Escherichia coli DNA polymerase III sliding clamp: I. Two distinct activities for individual ATP sites in the gamma complex. *Journal of Biological Chemistry*, **279**, 4376–4385.

92. Hayner,J.N. and Bloom,L.B. (2012) The β-Sliding Clamp Closes Around DNA Prior to Release by the Escherichia coli Clamp Loader γ complex. *J. Biol. Chem.*, 10.1074/jbc.M112.406231.

93. Kelch,B.A., Makino,D.L., O'Donnell,M. and Kuriyan,J. (2011) How a DNA polymerase clamp loader opens a sliding clamp. *Science*, **334**, 1675–1680.

94. Goedken,E.R., Kazmirski,S.L., Bowman,G.D., O'Donnell,M. and Kuriyan,J. (2005) Mapping the interaction of DNA with the Escherichia coli DNA polymerase clamp loader complex. *Nat. Struct. Mol. Biol.*, **12**, 183–190.

95. Yao,N., Leu,F.P., Anjelkovic,J., Turner,J. and O'Donnell,M. (2000) DNA structure requirements for the Escherichia coli gamma complex clamp loader and DNA polymerase III holoenzyme. *Journal of Biological Chemistry*, **275**, 11440–11450.

96. Park,M.S. and O'Donnell,M. (2009) The clamp loader assembles the beta clamp onto either a 3' or 5“ primer terminus: the underlying basis favoring 3” loading. *J. Biol. Chem.*, **284**, 31473–31483.

97. Anderson,S.G., Williams,C.R., O'Donnell,M. and Bloom,L.B. (2007) A function for the psi subunit in loading the Escherichia coli DNA polymerase sliding clamp. *Journal of Biological Chemistry*, **282**, 7035–7045.

98. Olson,M.W., Dallmann,H.G. and McHenry,C.S. (1995) DnaX complex of Escherichia coli DNA polymerase III holoenzyme. The chi psi complex functions by increasing the affinity of tau and gamma for delta.delta' to a physiologically relevant range. *Journal of Biological Chemistry*, **270**, 29570–29577.

99. Xiao,H., Dong,Z. and O'Donnell,M. (1993) DNA polymerase III accessory proteins. IV. Characterization of chi and psi. *Journal of Biological Chemistry*, **268**, 11779–11784.

100. Glover,B.P. and McHenry,C.S. (1998) The chi psi subunits of DNA polymerase III holoenzyme bind to single-stranded DNA-binding protein (SSB) and facilitate replication of an SSB-coated template. *Journal of Biological Chemistry*, **273**, 23476–23484.

101. Kelman,Z., Yuzhakov,A., Andjelkovic,J. and O'Donnell,M. (1998) Devoted to the lagging strand-the subunit of DNA polymerase III holoenzyme contacts SSB to promote processive elongation and sliding clamp assembly. *EMBO J*, **17**, 2436–2449.

102. Yuzhakov,A., Kelman,Z. and O'Donnell,M. (1999) Trading places on DNA--a three-point switch underlies primer handoff from primase to the replicative DNA polymerase. *Cell*, **96**, 153–163.

103. Lohman,T.M. and Ferrari,M.E. (1994) Escherichia coli single-stranded DNA-binding protein: multiple DNA-binding modes and cooperativities. *Annu. Rev. Biochem.*, **63**, 527–570.

104. Roy,R., Kozlov,A.G., Lohman,T.M. and Ha,T. (2007) Dynamic structural rearrangements between DNA binding modes of E. coli SSB protein. *Journal of Molecular Biology*, **369**, 1244–1257.

105. Hayner,J.N., Douma,L.G. and Bloom,L.B. (2014) The interplay of primer-template DNA phosphorylation status and single-stranded DNA binding proteins in directing clamp loaders to the appropriate polarity of DNA. *Nucleic Acids Res*, 10.1093/nar/gku774.

106. Indiani,C. and O'Donnell,M. (2006) The replication clamp-loading machine at work in the three domains of life. *Nat. Rev. Mol. Cell Biol.*, **7**, 751–761.

107. Bowman,G.D., O'Donnell,M. and Kuriyan,J. (2004) Structural analysis of a eukaryotic sliding DNA clamp-clamp loader complex. *Nature*, **429**, 724–730.

108. Krishna,T.S., Kong,X.P., Gary,S., Burgers,P.M. and Kuriyan,J. (1994) Crystal structure of the eukaryotic DNA polymerase processivity factor PCNA. *Cell*, **79**, 1233–1243.

109. Ayyagari,R., Impellizzeri,K.J., Yoder,B.L., Gary,S.L. and Burgers,P.M. (1995) A mutational analysis of the yeast proliferating cell nuclear antigen indicates distinct roles in DNA replication and DNA repair. *Mol. Cell. Biol.*, **15**, 4420–4429.

110. Chen,S., Levin,M.K., Sakato,M., Zhou,Y. and Hingorani,M.M. (2009) Mechanism of ATP-driven PCNA clamp loading by S. cerevisiae RFC. *Journal of Molecular Biology*, **388**, 431–442.

111. Uhlmann,F., Cai,J., Gibbs,E., O'Donnell,M. and Hurwitz,J. (1997) Deletion analysis of the large subunit p140 in human replication factor C reveals regions required for complex formation and replication activities. *Journal of Biological Chemistry*, **272**, 10058–10064.

112. Gomes,X.V. and Burgers,P.M. (2001) ATP utilization by yeast replication factor C. I. ATP-mediated interaction with DNA and with proliferating cell nuclear antigen. *Journal of Biological Chemistry*, **276**, 34768–34775.

113. Majka,J., Binz,S.K., Wold,M.S. and Burgers,P.M.J. (2006) Replication protein A directs loading of the DNA damage checkpoint clamp to 5'-DNA junctions. *Journal of Biological Chemistry*, **281**, 27855–27861.

114. Kubota,T., Nishimura,K., Kanemaki,M.T. and Donaldson,A.D. (2013) The Elg1 replication factor C-like complex functions in PCNA unloading during DNA replication. *Mol. Cell*, **50**, 273–280.

115. Green,C.M., Erdjument-Bromage,H., Tempst,P. and Lowndes,N.F. (2000) A novel Rad24 checkpoint protein complex closely related to replication factor C. *Curr. Biol.*, **10**, 39–42.

116. Bylund,G.O. and Burgers,P.M.J. (2005) Replication protein A-directed unloading of PCNA by the Ctf18 cohesion establishment complex. *Mol. Cell. Biol.*, **25**, 5445–5455.

117. Tang,H., Hilton,B., Musich,P.R., Fang,D.Z. and Zou,Y. (2012) Replication factor C1, the large subunit of replication factor C, is proteolytically truncated in Hutchinson-Gilford progeria syndrome. *Aging Cell*, **11**, 363–365.

118. Kim,Y.R., Song,S.Y., Kim,S.S., An,C.H., Lee,S.H. and Yoo,N.J. (2010) Mutational and expressional analysis of RFC3, a clamp loader in DNA replication, in gastric and colorectal cancers. *Hum. Pathol.*, **41**, 1431–1437.

119. Xiang,J., Fang,L., Luo,Y., Yang,Z., Liao,Y., Cui,J., Huang,M., Yang,Z., Huang,Y., Fan,X., *et al.* (2014) Levels of human replication factor C4, a clamp loader, correlate with tumor progression and predict the prognosis for colorectal cancer. *J Transl Med*, **12**, 320.

120. Arai,M., Kondoh,N., Imazeki,N., Hada,A., Hatsuse,K., Matsubara,O. and Yamamoto,M. (2009) The knockdown of endogenous replication factor C4 decreases the growth and enhances the chemosensitivity of hepatocellular carcinoma cells. *Liver Int.*, **29**, 55–62.

121. Xiong,S., Wang,Q., Zheng,L., Gao,F. and Li,J. (2011) Identification of candidate molecular markers of nasopharyngeal carcinoma by tissue microarray and in situ hybridization. *Med. Oncol.*, **28 Suppl 1**, S341–8.

122. Lockwood,W.W., Thu,K.L., Lin,L., Pikor,L.A., Chari,R., Lam,W.L. and Beer,D.G. (2012) Integrative genomics identified RFC3 as an amplified candidate oncogene in esophageal adenocarcinoma. *Clin. Cancer Res.*, **18**, 1936–1946.

123. Yin,Z., Whittell,L.R., Wang,Y., Jergic,S., Ma,C., Lewis,P.J., Dixon,N.E., Beck,J.L., Kelso,M.J. and Oakley,A.J. (2015) Bacterial Sliding Clamp Inhibitors that Mimic the Sequential Binding Mechanism of Endogenous Linear Motifs. *J. Med. Chem.*, **58**, 4693–4702.

124. Bradford,M.M. (1976) A rapid and sensitive method for the quantitation of microgram quantities of protein utilizing the principle of protein-dye binding. *Anal. Biochem.*, **72**, 248–254.

125. Gill,S.C. and Hippel,von,P.H. (1989) Calculation of protein extinction coefficients from amino acid sequence data. *Anal. Biochem.*, **182**, 319–326.

126. Yao,N., Hurwitz,J. and O'Donnell,M. (2000) Dynamics of beta and proliferating cell nuclear antigen sliding clamps in traversing DNA secondary structure. *Journal of Biological Chemistry*, **275**, 1421–1432.

127. Johanson,K.O., Haynes,T.E. and McHenry,C.S. (1986) Chemical characterization and purification of the beta subunit of the DNA polymerase III holoenzyme from an overproducing strain. *Journal of Biological Chemistry*, **261**, 11460–11465.

128. Paschall,C.O., Thompson,J.A., Marzahn,M.R., Chiraniya,A., Hayner,J.N., O'Donnell,M., Robbins,A.H., McKenna,R. and Bloom,L.B. (2011) The Escherichia coli clamp loader can actively pry open the β-sliding clamp. *J. Biol. Chem.*, **286**, 42704–42714.

129. Brune,M., Hunter,J.L., Corrie,J.E. and Webb,M.R. (1994) Direct, real-time measurement of rapid inorganic phosphate release using a novel fluorescent probe and its application to actomyosin subfragment 1 ATPase. *Biochemistry*, **33**, 8262–8271.

130. Johnson,K.A. (2009) Fitting enzyme kinetic data with KinTek Global Kinetic Explorer. *Meth. Enzymol.*, **467**, 601–626.

131. Johnson,K.A., Simpson,Z.B. and Blom,T. (2009) Global kinetic explorer: a new computer program for dynamic simulation and fitting of kinetic data. *Anal. Biochem.*, **387**, 20–29.

132. Wickner,W., Schekman,R., Geider,K. and Kornberg,A. (1973) A new form of DNA polymerase 3 and a copolymerase replicate a long, single-stranded primer-template. *Proc. Natl. Acad. Sci. U.S.A.*, **70**, 1764–1767.

133. Hurwitz,J. and Wickner,S. (1974) Involvement of two protein factors and ATP in in vitro DNA synthesis catalyzed by DNA polymerase 3 of Escherichia coli. *Proc. Natl. Acad. Sci. U.S.A.*, **71**, 6–10.

134. Piperno,J.R. and Alberts,B.M. (1978) An ATP stimulation of T4 DNA polymerase mediated via T4 gene 44/62 and 45 proteins. The requirement for ATP hydrolysis. *Journal of Biological Chemistry*, **253**, 5174–5179.

135. Fay,P.J., Johanson,K.O., McHenry,C.S. and Bambara,R.A. (1982) Size classes of products synthesized processively by two subassemblies of Escherichia coli DNA polymerase III holoenzyme. *Journal of Biological Chemistry*, **257**, 5692–5699.

136. Vivona,J.B. and Kelman,Z. (2003) The diverse spectrum of sliding clamp interacting proteins. *FEBS Lett.*, **546**, 167–172.

137. Maga,G. and Hubscher,U. (2003) Proliferating cell nuclear antigen (PCNA): a dancer with many partners. *J. Cell. Sci.*, **116**, 3051–3060.

138. Moldovan,G.-L., Pfander,B. and Jentsch,S. (2007) PCNA, the maestro of the replication fork. *Cell*, **129**, 665–679.

139. Hedglin,M., Kumar,R. and Benkovic,S.J. (2013) Replication clamps and clamp loaders. *Cold Spring Harb Perspect Biol*, **5**, a010165.

140. Georgescu,R., Langston,L. and O'Donnell,M. (2015) A proposal: Evolution of PCNA's role as a marker of newly replicated DNA. *DNA Repair (Amst.)*, 10.1016/j.dnarep.2015.01.015.

141. Kelch,B.A. (2016) Review: The lord of the rings: Structure and mechanism of the sliding clamp loader. *Biopolymers*, **105**, 532–546.

142. Alley,S.C., Shier,V.K., Abel-Santos,E., Sexton,D.J., Soumillion,P. and Benkovic,S.J. (1999) Sliding clamp of the bacteriophage T4 polymerase has open and closed subunit interfaces in solution. *Biochemistry*, **38**, 7696–7709.

143. Alley,S.C., Abel-Santos,E. and Benkovic,S.J. (2000) Tracking sliding clamp opening and closing during bacteriophage T4 DNA polymerase holoenzyme assembly. *Biochemistry*, **39**, 3076–3090.

144. Liu,C., McKinney,M.C., Chen,Y.-H., Earnest,T.M., Shi,X., Lin,L.-J., Ishino,Y., Dahmen,K., Cann,I.K.O. and Ha,T. (2011) Reverse-chaperoning activity of an AAA+ protein. *Biophys. J.*, **100**, 1344–1352.

145. Koonin,E.V. (1993) A superfamily of ATPases with diverse functions containing either classical or deviant ATP-binding motif. *Journal of Molecular Biology*, **229**, 1165–1174.

146. Erzberger,J.P. and Berger,J.M. (2006) Evolutionary relationships and structural mechanisms of AAA+ proteins. *Annu Rev Biophys Biomol Struct*, **35**, 93–114.

147. Berdis,A.J. and Benkovic,S.J. (1996) Role of adenosine 5'-triphosphate hydrolysis in the assembly of the bacteriophage T4 DNA replication holoenzyme complex. *Biochemistry*, **35**, 9253–9265.

148. Gomes,X.V., Schmidt,S.L. and Burgers,P.M. (2001) ATP utilization by yeast replication factor C. II. Multiple stepwise ATP binding events are required to load proliferating cell nuclear antigen onto primed DNA. *Journal of Biological Chemistry*, **276**, 34776–34783.

149. Tainer,J.A., McCammon,J.A. and Ivanov,I. (2010) Recognition of the ring-opened state of proliferating cell nuclear antigen by replication factor C promotes eukaryotic clamp-loading. *J. Am. Chem. Soc.*, **132**, 7372–7378.

150. Fang,J., Engen,J.R. and Beuning,P.J. (2011) Escherichia coli processivity clamp β from DNA polymerase III is dynamic in solution. *Biochemistry*, **50**, 5958–5968.

151. Thompson,J.A., Paschall,C.O., O'Donnell,M. and Bloom,L.B. (2009) A slow ATP-induced conformational change limits the rate of DNA binding but not the rate of beta clamp binding by the escherichia coli gamma complex clamp loader. *J. Biol. Chem.*, **284**, 32147–32157.

152. Zhuang,Z., Yoder,B.L., Burgers,P.M.J. and Benkovic,S.J. (2006) The structure of a ring-opened proliferating cell nuclear antigen-replication factor C complex revealed by fluorescence energy transfer. *Proc. Natl. Acad. Sci. U.S.A.*, **103**, 2546–2551.

153. Thompson,J.A., Marzahn,M.R., O'Donnell,M. and Bloom,L.B. (2012) Replication Factor C Is a More Effective Proliferating Cell Nuclear Antigen (PCNA) Opener than the Checkpoint Clamp Loader, Rad24-RFC. *J. Biol. Chem.*, **287**, 2203–2209.

154. Snyder,A.K., Williams,C.R., Johnson,A., O'Donnell,M. and Bloom,L.B. (2004) Mechanism of loading the Escherichia coli DNA polymerase III sliding clamp: II. Uncoupling the beta and DNA binding activities of the gamma complex. *Journal of Biological Chemistry*, **279**, 4386–4393.

155. Sakato,M., O'Donnell,M. and Hingorani,M.M. (2012) A central swivel point in the RFC clamp loader controls PCNA opening and loading on DNA. *Journal of Molecular Biology*, **416**, 163–175.

156. Miyata,T., Oyama,T., Mayanagi,K., Ishino,S., Ishino,Y. and Morikawa,K. (2004) The clamp-loading complex for processive DNA replication. *Nat. Struct. Mol. Biol.*, **11**, 632–636.

157. Miyata,T., Suzuki,H., Oyama,T., Mayanagi,K., Ishino,Y. and Morikawa,K. (2005) Open clamp structure in the clamp-loading complex visualized by electron microscopic image analysis. *Proc. Natl. Acad. Sci. U.S.A.*, **102**, 13795–13800.

158. Singh,M.I., Ganesh,B. and Jain,V. (2016) On the domains of T4 phage sliding clamp gp45: An intermolecular crosstalk governs structural stability and biological activity. *Biochim. Biophys. Acta*, 10.1016/j.bbagen.2016.08.012.

159. Dallmann,H.G., Thimmig,R.L. and McHenry,C.S. (1995) DnaX complex of Escherichia coli DNA polymerase III holoenzyme. Central role of tau in initiation complex assembly and in determining the functional asymmetry of holoenzyme. *Journal of Biological Chemistry*, **270**, 29555–29562.

160. Lee,S.H., Kanda,P., Kennedy,R.C. and Walker,J.R. (1987) Relation of the Escherichia coli dnaX gene to its two products--the tau and gamma subunits of DNA polymerase III holoenzyme. *Nucleic Acids Res*, **15**, 7663–7675.

161. Yao,N.Y. and O'Donnell,M. (2010) SnapShot: The replisome. *Cell*, **141**, 1088–1088.e1.

162. Kim,S., Dallmann,H.G., McHenry,C.S. and Marians,K.J. (1996) tau couples the leading- and lagging-strand polymerases at the Escherichia coli DNA replication fork. *Journal of Biological Chemistry*, **271**, 21406–21412.

163. Pritchard,A.E., Dallmann,H.G., Glover,B.P. and McHenry,C.S. (2000) A novel assembly mechanism for the DNA polymerase III holoenzyme DnaX complex: association of deltadelta' with DnaX(4) forms DnaX(3)deltadelta'. *EMBO J*, **19**, 6536–6545.

164. Downey,C.D., Crooke,E. and McHenry,C.S. (2011) Polymerase chaperoning and multiple ATPase sites enable the E. coli DNA polymerase III holoenzyme to rapidly form initiation complexes. *Journal of Molecular Biology*, **412**, 340–353.

165. Larsen,B., Wills,N.M., Nelson,C., Atkins,J.F. and Gesteland,R.F. (2000) Nonlinearity in genetic decoding: homologous DNA replicase genes use alternatives of transcriptional slippage or translational frameshifting. *Proc. Natl. Acad. Sci. U.S.A.*, **97**, 1683–1688.

166. Vass,R.H. and Chien,P. (2013) Critical clamp loader processing by an essential AAA+ protease in Caulobacter crescentus. *Proc. Natl. Acad. Sci. U.S.A.*, 10.1073/pnas.1311302110.

167. Yeung,T., Mullin,D.A., Chen,K.S., Craig,E.A., Bardwell,J.C. and Walker,J.R. (1990) Sequence and expression of the Escherichia coli recR locus. *J. Bacteriol.*, **172**, 6042–6047.

168. Filip,C.C., Allen,J.S., Gustafson,R.A., Allen,R.G. and Walker,J.R. (1974) Bacterial cell division regulation: characterization of the dnaH locus of Escherichia coli. *J. Bacteriol.*, **119**, 443–449.

169. Chu,H., Malone,M.M., Haldenwang,W.G. and Walker,J.R. (1977) Physiological effects of growth of an Escherichia coli temperature-sensitive dnaZ mutant at nonpermissive temperatures. *J. Bacteriol.*, **132**, 151–158.

170. Seier,T. (2010) Studies of Template Switching at the Replication Fork. *Brandeis University*.

171. Seier,T., Zilberberg,G., Zeiger,D.M. and Lovett,S.T. (2012) Azidothymidine and other chain terminators are mutagenic for template-switch-generated genetic mutations. *Proc. Natl. Acad. Sci. U.S.A.*, **109**, 6171–6174.

172. Hwang,C., Venkatakrishnan,B., Paschall,C.O. and Bloom,L.B. Biochemical Characterization of a Mutant Clamp Loader Defective in Template Switching Department of Biochemistry and Molecular Biology, College of Medicine, University of Florida.

173. Pritchard,A.E., Dallmann,H.G. and McHenry,C.S. (1996) In vivo assembly of the tau-complex of the DNA polymerase III holoenzyme expressed from a five-gene artificial operon. Cleavage of the tau-complex to form a mixed gamma-tau-complex by the OmpT protease. *Journal of Biological Chemistry*, **271**, 10291–10298.

174. Tsuchihashi,Z. and Kornberg,A. (1989) ATP interactions of the tau and gamma subunits of DNA polymerase III holoenzyme of Escherichia coli. *Journal of Biological Chemistry*, **264**, 17790–17795.

175. Flower,A.M. and McHenry,C.S. (1986) The adjacent dnaZ and dnaX genes of Escherichia coli are contained within one continuous open reading frame. *Nucleic Acids Res*, **14**, 8091–8101.

176. Haroniti,A., Anderson,C., Doddridge,Z., Gardiner,L., Roberts,C.J., Allen,S. and Soultanas,P. (2004) The clamp-loader-helicase interaction in Bacillus. Atomic force microscopy reveals the structural organisation of the DnaB-tau complex in Bacillus. *Journal of Molecular Biology*, **336**, 381–393.

177. Wieczorek,A., Downey,C.D., Dallmann,H.G. and McHenry,C.S. (2010) Only one ATP-binding DnaX subunit is required for initiation complex formation by the Escherichia coli DNA polymerase III holoenzyme. *J. Biol. Chem.*, **285**, 29049–29053.

178. Tondnevis,F., Gillilan,R.E., Bloom,L.B. and McKenna,R. (2015) Solution study of the Escherichia coli DNA polymerase III clamp loader reveals the location of the dynamic ψχ heterodimer. *Struct Dyn*, **2**, 054701.

179. Lee,S.H. and Walker,J.R. (1987) Escherichia coli DnaX product, the tau subunit of DNA polymerase III, is a multifunctional protein with single-stranded DNA-dependent ATPase activity. *Proc. Natl. Acad. Sci. U.S.A.*, **84**, 2713–2717.

180. McHenry,C.S. (1982) Purification and characterization of DNA polymerase III'. Identification of tau as a subunit of the DNA polymerase III holoenzyme. *Journal of Biological Chemistry*, **257**, 2657–2663.

181. McHenry,C.S. (2003) Chromosomal replicases as asymmetric dimers: studies of subunit arrangement and functional consequences. *Molecular Microbiology*, **49**, 1157–1165.

182. Bloom,L.B., Turner,J., Kelman,Z., Beechem,J.M., O'Donnell,M. and Goodman,M.F. (1996) Dynamics of loading the beta sliding clamp of DNA polymerase III onto DNA. *Journal of Biological Chemistry*, **271**, 30699–30708.

183. Downey,C.D. and McHenry,C.S. (2010) Chaperoning of a replicative polymerase onto a newly assembled DNA-bound sliding clamp by the clamp loader. *Mol. Cell*, **37**, 481–491.

184. Shereda,R.D., Kozlov,A.G., Lohman,T.M., Cox,M.M. and Keck,J.L. (2008) SSB as an organizer/mobilizer of genome maintenance complexes. *Crit. Rev. Biochem. Mol. Biol.*, **43**, 289–318.

185. Ason,B., Handayani,R., Williams,C.R., Bertram,J.G., Hingorani,M.M., O'Donnell,M., Goodman,M.F. and Bloom,L.B. (2003) Mechanism of loading the Escherichia coli DNA polymerase III beta sliding clamp on DNA. Bona fide primer/templates preferentially trigger the gamma complex to hydrolyze ATP and load the clamp. *Journal of Biological Chemistry*, **278**, 10033–10040.

186. Tsurimoto,T. and Stillman,B. (1991) Replication factors required for SV40 DNA replication in vitro. I. DNA structure-specific recognition of a primer-template junction by eukaryotic DNA polymerases and their accessory proteins. *Journal of Biological Chemistry*, **266**, 1950–1960.

187. Marceau,A.H., Bahng,S., Massoni,S.C., George,N.P., Sandler,S.J., Marians,K.J. and Keck,J.L. (2011) Structure of the SSB-DNA polymerase III interface and its role in DNA replication. *EMBO J*, **30**, 4236–4247.

188. Curth,U., Genschel,J., Urbanke,C. and Greipel,J. (1996) In vitro and in vivo function of the C-terminus of Escherichia coli single-stranded DNA binding protein. *Nucleic Acids Res*, **24**, 2706–2711.

189. Hobbs,M.D., Sakai,A. and Cox,M.M. (2007) SSB protein limits RecOR binding onto single-stranded DNA. *Journal of Biological Chemistry*, **282**, 11058–11067.

190. Naue,N., Fedorov,R., Pich,A., Manstein,D.J. and Curth,U. (2011) Site-directed mutagenesis of the χ subunit of DNA polymerase III and single-stranded DNA-binding protein of E. coli reveals key residues for their interaction. *Nucleic Acids Res*, **39**, 1398–1407.

191. Hayner,J. (2013) Comparing the mechanism of the E. coli and S. cerevisiae clamp loaders.

192. Reems,J.A. and McHenry,C.S. (1994) Escherichia coli DNA polymerase III holoenzyme footprints three helical turns of its primer. *Journal of Biological Chemistry*, **269**, 33091–33096.

193. Zhou,R., Kozlov,A.G., Roy,R., Zhang,J., Korolev,S., Lohman,T.M. and Ha,T. (2011) SSB functions as a sliding platform that migrates on DNA via reptation. *Cell*, **146**, 222–232.

194. Cadman,C.J. and McGlynn,P. (2004) PriA helicase and SSB interact physically and functionally. *Nucleic Acids Res*, **32**, 6378–6387.

195. Bhattacharyya,B., George,N.P., Thurmes,T.M., Zhou,R., Jani,N., Wessel,S.R., Sandler,S.J., Ha,T. and Keck,J.L. (2014) Structural mechanisms of PriA-mediated DNA replication restart. *Proc. Natl. Acad. Sci. U.S.A.*, **111**, 1373–1378.

196. Chen,S., Coman,M.M., Sakato,M., O'Donnell,M. and Hingorani,M.M. (2008) Conserved residues in the delta subunit help the E. coli clamp loader, gamma complex, target primer-template DNA for clamp assembly. *Nucleic Acids Res*, **36**, 3274–3286.

197. Roy,R., Kozlov,A.G., Lohman,T.M. and Ha,T. (2009) SSB protein diffusion on single-stranded DNA stimulates RecA filament formation. *Nature*, **461**, 1092–1097.

198. Hill,T.M., Henson,J.M. and Kuempel,P.L. (1987) The terminus region of the Escherichia coli chromosome contains two separate loci that exhibit polar inhibition of replication. *Proc. Natl. Acad. Sci. U.S.A.*, **84**, 1754–1758.

199. Mulcair,M.D., Schaeffer,P.M., Oakley,A.J., Cross,H.F., Neylon,C., Hill,T.M. and Dixon,N.E. (2006) A molecular mousetrap determines polarity of termination of DNA replication in E. coli. *Cell*, **125**, 1309–1319.

200. Dallmann,H.G. and McHenry,C.S. (1995) DnaX complex of Escherichia coli DNA polymerase III holoenzyme. Physical characterization of the DnaX subunits and complexes. *Journal of Biological Chemistry*, **270**, 29563–29569.

201. Yuan,Q., Dohrmann,P.R., Sutton,M.D. and McHenry,C.S. (2016) DNA Polymerase III, but Not Polymerase IV, Must Be Bound to a τ-Containing DnaX Complex to Enable Exchange into Replication Forks. *J. Biol. Chem.*, **291**, 11727–11735.

202. Yeiser,B., Pepper,E.D., Goodman,M.F. and Finkel,S.E. (2002) SOS-induced DNA polymerases enhance long-term survival and evolutionary fitness. *Proc. Natl. Acad. Sci. U.S.A.*, **99**, 8737–8741.

203. Kubota,T., Myung,K. and Donaldson,A.D. (2013) Is PCNA unloading the central function of the Elg1/ATAD5 replication factor C-like complex? *Cell Cycle*, **12**, 2570–2579.

# BIOGRAPHICAL SKETCH

Lauren Douma was born in Plantation, Florida. Lauren attended Nova Southeastern University where she received a Bachelor of Science in biology with minors in chemistry and psychology. During her time at NSU, she was a research assistant for Dr. Aurelien Tartar where she studied the roles of genes in the infection of mosquitoes by *Laginudium giagantium*. Lauren also received a research grant from NSU to complete an undergraduate thesis under the mentorship of Dr. Emily Schmitt and Dr. Joshua Loomis. For her thesis, she researched her families' ancestry using NSU's ancestry library and through genomic analysis of her family's DNA. Lauren's love for research brought her to the Genetics and Genomics PhD program at the University of Florida. Lauren began working with Dr. Linda Bloom in 2011 studying the regulation of clamp loading during DNA replication by the *E. coli* clamp loader complexes. She graduated in December of 2016 with a Ph.D. in genetics and genomics. During her graduate career, Lauren had the opportunity to assist with the undergraduate biochemistry course and developed a passion for teaching. Lauren plans to explore this further by pursuing a post-doctoral position and eventually pursing a professor or lecturer position at a small liberal arts college.